THE UNIVERSITY OF QUEENSLAND

AUSTRALIA

Reducing Disinfection Byproduct Formation Potential

Using Ozonation and Biological Drinking Water Treatment

Glen Andrew D. de Vera

MSc Chemistry

A thesis submitted for the degree of Doctor of Philosophy at

The University of Queensland in 2017

School of Chemical Engineering

Advanced Water Management Centre

Abstract

The occurrence of natural organic matter (NOM) in source waters presents a concern in water treatment plants due to formation of toxic disinfection byproducts (DBPs). In this doctoral thesis, the fate of NOM during ozonation, biofiltration, and chlorination was investigated to identify important aspects in these processes that can be manipulated for better DBP control. Specifically, this thesis studied (1) reaction mechanisms of ozone with dissolved organic nitrogen (DON), an important fraction of NOM that forms nitrogenous DBPs, (2) role of ozone and $^{\bullet}OH$-mediated attack on NOM and DBP formation during chlorination, and (3) impact of ozonation on biodegradability of DBP precursors.

The reaction of ozone with DON (Chapter 4) was observed to produce various transformation products including nitrate (NO_3^-) and ammonium (NH_4^+). This observation was shown in batch ozonation experiments involving NOM standards, surface water and wastewater effluent samples. A strong correlation was found between NO_3^- formation and O_3 exposure ($R^2 > 0.82$) during ozonation of both model DON solutions and real water samples. High NO_3^- yields were obtained for solutions containing primary amines such as glycine. Experiments with glycine showed that NO_3^- was formed via an intermediate with a second-order rate constant of 7.7 ± 0.1 $M^{-1}s^{-1}$ while NH_4^+ was formed by an electron-transfer mechanism with O_3 as confirmed from a $^{\bullet}OH$ yield of $24.7 \pm 1.9\%$. The NH_4^+ concentrations, however, were lower than the $^{\bullet}OH$ yield (0.03 mol NH_4^+/mol $^{\bullet}OH$) suggesting other $^{\bullet}OH$-producing reactions that compete with NH_4^+ formation. This study showed evidence that NO_3^- formation during ozonation of DON is induced by an oxygen-transfer to nitrogen forming hydroxylamine and oxime, while NH_4^+ formation is induced by electron-transfer reactions involving C-centered radicals and imine intermediates.

These reactions of ozone and other generated reactive oxygen species with NOM also affect NOM's reactivity during post-chlorination, consequently affecting formation potentials of nitrogen-containing and carbon-based DBPs. Chapter 5 presents the effects of varying exposures of O_3 and $^{\bullet}OH$ on the resulting DBP concentrations and their associated toxicity generated after subsequent chlorination. DBP formation potential tests (target Cl_2 residual after 24 h = 1 – 2 mg/L) and *in vitro* bioassays were conducted after ozonation of coagulated surface water at O_3- and $^{\bullet}OH$-dominated conditions. Although ozonation led to a 24 – 37% decrease in formation of total trihalomethanes (THM4), haloacetic acids (HAA8), haloacetonitriles (HAN4), and trihaloacetamides (THAM), an increase in formation of total trihalonitromethanes (THNM2), chloral hydrate (CH), and haloketones (HK2) was observed. This effect however was less pronounced for samples ozonated at conditions favoring ozone (e.g., pH 6 and in the presence of t-BuOH) over $^{\bullet}OH$ reactions (e.g., pH 8 and in the

presence of H_2O_2). Compared to ozonation only, addition of H_2O_2 consistently enhanced formation of all DBP groups (20 – 61%) except trihalonitromethanes. This proves that $^{\bullet}OH$-transformed NOM is more susceptible to halogen incorporation. Analogously, adsorbable organic halogen (AOX) concentrations increased under conditions that favor $^{\bullet}OH$ reactions. The ratio of unknown to known AOX, however, was greater at conditions that promote O_3 reactions. Although significant correlation was found between AOX and genotoxicity with p53 bioassay, toxicity tests using 4 *in vitro* bioassays showed relatively small differences between various ozonation conditions.

Following ozonation, the biodegradability of DBP precursors was investigated in Chapter 6, with emphasis on two operational factors: ozone exposure and empty bed contact time (EBCT). Ozone exposure was varied through addition of H_2O_2 during ozonation at 1 mgO_3/mgDOC followed by biological filtration using either activated carbon (BAC) or anthracite. Ozonation led to a 10% decrease in dissolved organic carbon (DOC), without further improvement from H_2O_2 addition. Compared to ozonation without H_2O_2, raising H_2O_2 concentrations to 2 mmol/mmolO_3 resulted in increased DBP formation potentials during post-chlorination of the ozonated water (target Cl_2 residual after 24 h = 1 – 2 mg/L) as follows: THM4 (37%), HAA8 (44%), CH (107%), HK2 (97%), HAN4 (33%), trichloroacetamide (TCAM, 43%), and AOX (27%), but a decrease in concentrations of THNM2 (43%). Coupling ozonation with biofiltration prior to chlorination effectively lowered the formation potentials of all DBPs including CH, HK2, and THNM2, all of which increased after ozonation. The dynamics of DBP formation potentials during BAC filtration at different EBCTs followed first-order reaction kinetics. Minimum steady-state concentrations were attained at an EBCT of 10 – 20 min, depending on the DBP species. The rate of reduction in DBP formation potentials varied among individual species before reaching their minimum concentrations. CH, HK2, and THNM2 had the highest rate constants of between 0.5 and 0.6 min^{-1} followed by HAN4 (0.4 min^{-1}), THM4 (0.3 min^{-1}), HAA8 (0.2 min^{-1}), and AOX (0.1 min^{-1}). Relative to concentrations after ozonation, the reduction in formation potential for most DBPs (e.g., at 15 min EBCT) was less than 50% but was higher than 70% for CH, HK2, and THNM2. The formation of bromine-containing DBPs increased with increasing EBCT likely due to an increase in Br^-/DOC ratio.

Declaration by author

This thesis is composed of my original work, and contains no material previously published or written by another person except where due reference has been made in the text. I have clearly stated the contribution by others to jointly-authored works that I have included in my thesis.

I have clearly stated the contribution of others to my thesis as a whole, including statistical assistance, survey design, data analysis, significant technical procedures, professional editorial advice, and any other original research work used or reported in my thesis. The content of my thesis is the result of work I have carried out since the commencement of my research higher degree candidature and does not include a substantial part of work that has been submitted to qualify for the award of any other degree or diploma in any university or other tertiary institution. I have clearly stated which parts of my thesis, if any, have been submitted to qualify for another award.

I acknowledge that an electronic copy of my thesis must be lodged with the University Library and, subject to the policy and procedures of The University of Queensland, the thesis be made available for research and study in accordance with the Copyright Act 1968 unless a period of embargo has been approved by the Dean of the Graduate School.

I acknowledge that copyright of all material contained in my thesis resides with the copyright holder(s) of that material. Where appropriate I have obtained copyright permission from the copyright holder to reproduce material in this thesis.

Publications during candidature

Peer-reviewed publications

de Vera, G.A., Gernjak, W., Weinberg, H.S., Farré, M.J., Keller, J., and von Gunten, U. (2017) Kinetics and mechanisms of nitrate and ammonium formation during ozonation of dissolved organic nitrogen. *Water Research* 108, 451-461.

de Vera, G.A., Gernjak, W., and Radjenovic, J. (2017) Predicting reactivity of model DOM compounds towards chlorine with mediated electrochemical oxidation. *Water Research* 114, 113-121.

de Vera, G.A., Keller, J., Gernjak, W., Weinberg, H.S., and Farré, M.J. (2016) Biodegradability of DBP precursors after drinking water ozonation. *Water Research* 106, 550-561.

de Vera, G.A., Stalter, D., Gernjak, W., Weinberg, H.S., Keller, J., and Farré, M.J. (2015) Towards reducing DBP formation potential of drinking water by favouring direct ozone over hydroxyl radical reactions during ozonation. *Water Research* 87, 49-58.

Farré, M.J., Lyon, B., **de Vera, G.A.**, Stalter, D., and Gernjak, W. (2016) Assessing adsorbable organic halogen formation and precursor removal during drinking water production. *Journal of Environmental Engineering*, 10.1061/(ASCE)EE.1943-7870.0001022, 04015087.

Lyon, B.A., Farré, M.J., **de Vera, G.A.**, Keller, J., Roux, A., Weinberg, H.S., and Gernjak,W. (2014) Organic matter removal and disinfection byproduct management in South East Queensland's drinking water. *Water Science & Technology: Water Supply* 14 (4), 681–689**.**

Conference paper

de Vera, G.A., Farré, M.J., Gernjak, W., and Keller, J. (2015) Changes in inorganic nitrogen ratio during ozonation of drinking water and its application for micropollutant removal prediction. Disinfection By-products in Drinking Water, Ch. 27, 228-235. DOI**:**10.1039/9781782622710-00228.

Technical report

Farré, M.J., **de Vera, G.A.,** Lyon, B.A., Doederer, K., Weinberg, H.S., Gernjak, W., and Keller, J. (2016) Engineering solutions to minimize nitrogen-containing DBPs. 2016, Water Research Foundation, CO, USA. Available at http://www.waterrf.org/Pages/Projects.aspx?PID=4484 .

Conference Presentations

de Vera, G.A., Stalter, D., Gernjak, W., Weinberg, H.S., Keller, J., and Farré, M.J. (2015) Towards reducing DBP formation potential of drinking water by favouring direct ozone over hydroxyl radical reactions during ozonation. Gordon Research Conference on Disinfection Byproducts, MA, USA. Poster presentation.

de Vera, G.A., Gernjak, W., Weinberg, H.S., Keller, J., and Farré, M.J. (2015) Ozone-enhanced biofiltration for control of drinking water chlorination byproducts. The University of Queensland Engineering Postgraduate Conference, Brisbane, Australia. Oral presentation. *Awarded as best oral presentation.*

de Vera, G.A., Keller, J., Farré, M.J., and Gernjak, W. (2014) NH_4^+-N/NO_3^--N ratio: a surrogate measure for organic matter oxidation by hydroxyl radicals and ozone. Disinfection By-products in Drinking Water Conference, Mulheim an der Ruhr, Germany. Oral presentation.

de Vera, G.A., Farré, M.J., and Gernjak, W. (2014) Effect of varying ozone and $^{\bullet}OH$ radical exposures on disinfection by-product formation potential. The University of Queensland Engineering Postgraduate Conference, Brisbane, Australia. Oral presentation. *Awarded as best oral presentation.*

de Vera, G.A., Lyon, B.A., Gernjak, W., and Farré, M.J. (2013) Variations in natural organic matter properties during ozonation. 5th IWA Specialist Conference on Natural Organic Matter Research, Perth, Australia. Poster presentation. *Awarded as best poster presentation.*

de Vera, G.A., Gernjak, W., and Farré, M.J. (2013) Impacts of climate change on formation of disinfection byproducts. The University of Queensland Engineering Postgraduate Conference, Brisbane, Australia. Oral presentation. *Awarded as best oral presentation (first-year category).*

Publications included in this thesis

de Vera, G.A., Gernjak, W., Weinberg, H.S., Farré, M.J., Keller, J., and von Gunten, U. (2017) Kinetics and mechanisms of nitrate and ammonium formation during ozonation of dissolved organic nitrogen. *Water Research* 108, 451-461.

- Incorporated as Chapter 4

Contributors	Statement of contribution
de Vera, G.A. (candidate)	Idea conception and study design (50%) Experimentation (100%) Data analysis and interpretation (50%) Writing and review of manuscript (45%)
Farré, M.J.	Writing and review of manuscript (5%)
Weinberg, H.S.,	Writing and review of manuscript (5%)
Gernjak, W.	Data analysis and interpretation (10%) Writing and review of manuscript (5%)
Keller, J.	Idea conception and study design (10%)
von Gunten, U.	Idea conception and study design (40%) Data analysis and interpretation (40%) Writing and review of manuscript (40%)

de Vera, G.A., Stalter, D., Gernjak, W., Weinberg, H.S., Keller, J., and Farré, M.J. (2015) Towards reducing DBP formation potential of drinking water by favouring direct ozone over hydroxyl radical reactions during ozonation. *Water Research* 87, 49-58.

- Incorporated as Chapter 5

Contributors	Statement of contribution
de Vera, G.A. (candidate)	Idea conception and study design (60%) Experimentation (80%) Data analysis and interpretation (40%) Writing and review of manuscript (35%)
Stalter, D.	Idea conception and study design (10%) Experimentation (20%) Data analysis and interpretation (10%) Writing and review of manuscript (10%)
Gernjak, W.	Idea conception and study design (20%) Data analysis and interpretation (15%) Writing and review of manuscript (20%)
Weinberg, H.S.	Data analysis and interpretation (15%) Writing and review of manuscript (20%)
Keller, J.	Data analysis and interpretation (5%) Writing and review of manuscript (5%)
Farré, M.J.	Idea conception and study design (10%) Data analysis and interpretation (15%) Writing and review of manuscript (20%)

de Vera, G.A., Keller, J., Gernjak, W., Weinberg, H.S., and Farré, M.J. (2016) Biodegradability of DBP precursors after drinking water ozonation. *Water Research* 106, 550-561.

- Incorporated as Chapter 6

Contributors	Statement of contribution
de Vera, G.A. (candidate)	Idea conception and study design (70%) Experimentation (100%) Data analysis and interpretation (45%) Writing and review of manuscript (35%)
Keller, J.	Idea conception and study design (15%) Data analysis and interpretation (10%) Writing and review of manuscript (5%)
Gernjak, W.	Idea conception and study design (10%) Data analysis and interpretation (15%) Writing and review of manuscript (15%)
Weinberg, H.S.	Data analysis and interpretation (15%) Writing and review of manuscript (15%)
Farré, M.J.	Idea conception and study design (5%) Data analysis and interpretation (15%) Writing and review of manuscript (15%)

Contributions by others to the thesis

The following collaborators are acknowledged for their significant and substantial contributions to this thesis:

Prof. Jurg Keller, who became my principal advisor in 2014, provided useful inputs in the planning, conduct of the research study, and possible industry applications of the research outcomes. He also made substantial effort in ensuring that I receive all possible opportunities needed to improve this thesis.

Dr. Wolfgang Gernjak co-advised me during my PhD candidature and played an integral part in all the chapters of this thesis. He was involved in the initial conceptual thinking, to developing research ideas, identifying appropriate experimental design, and interpreting research data. He also provided critical reviews in all the manuscripts.

Dr. Maria José Farré, who was my principal advisor in 2013, is recognized for sharing her expertise in disinfection byproduct research (i.e., from laboratory techniques, instrumentation, and theory). Our regular exchange of viewpoints were essential in the conception of research ideas and approaches related to DBPs. She was also highly involved in the writing and review of manuscripts.

Prof. Urs von Gunten, who is a world-leading expert in application of ozone for water treatment, was my host professor during my research visit at École Polytechnique Fédérale de Lausanne (EPFL) where I performed the bulk of the experiments reported in Chapter 4. He provided the research direction and experimental needs to better understand the reaction of ozone with dissolved organic nitrogen. Apart from delivering timely detailed reviews of the manuscript, he also imparted his expertise on ozone chemistry which helped in understanding our results in Chapter 4.

Prof. Howard Weinberg highly contributed in the analysis and interpretation of experimental data. He also provided detailed reviews that remarkably improved all manuscripts (Chapters 4-6). He was also part of the project (Water Research Foundation #4484) where the thesis was framed.

Dr. Bonnie Lyon is acknowledged for providing me the necessary training for DBP research (e.g., sample collection, preparation, DBP extraction, and GC analyses) and water characterization.

Dr. Daniel Stalter performed the bioassays used to evaluate the relative toxicity of ozonated/chlorinated water samples in Chapter 5. He also assisted in operating the combustion ion chromatograph system for analysis of adsorbable organic halogens (AOX).

Dr. Deb Gale coordinated all the sampling events for water samples and bioactive filter media with all the other Seqwater staff.

Dr. Kalinda Watson provided her assistance in concentrating the natural organic matter of the coagulated water samples. She also helped in the analysis of AOX.

Dr. Florian Breider, Mr. Sylvain Coudret, and Ms. Caroline Gatchet provided laboratory assistance during my research stay at EPFL.

Mr. Peng Liu assisted in the set-up of the biofiltration columns.

Dr. Beatrice Keller-Lehmann, Mr. Nathan Clayton, and Mrs. Jianghuang Li operated the organic carbon and nitrogen analyzers for total carbon and nitrogen measurements as well as the flow injection analyzers for inorganic nitrogen measurements at the University of Queensland.

Statement of parts of the thesis submitted to qualify for the award of another degree

None.

Acknowledgements

Studying for a PhD degree is tough. It entails commitment, continued motivation, personal sacrifices (e.g., time away from family and friends) and the list goes on. It could be discouraging at times, but because of the support of the people around me, this journey became bearable and enjoyable. For these, I give my sincerest thanks to everyone who made this academic venture a great experience.

First, I would like to thank the institutions who supported my studies by awarding grants. I am grateful for the funding support by the Australia Awards (PhD scholarship), University of Queensland (UQ), Seqwater, Water Research Foundation (WRF #4484), and École Polytechnique Fédérale de Lausanne (EPFL; Water Quality and Treatment Laboratory) which allowed me to conduct my research and use the facilities needed for this thesis. My deepest thanks also to the Philippine-Australia Human Resource and Organisational Development Facility and UQ Global Engagement Office (Regional coordinator: Ms. Catherine Fitzgerald) for an efficient management of the scholarship program. I also acknowledge the UQ International scholarship (RQ3 and RQ4 of 2015) and UQ Graduate School International Travel Award (2015) for their contribution during my research visit at EPFL, Switzerland.

Words are powerless to express my gratitude to my supervisors. I am thankful to my principal supervisor, Prof. Jurg Keller, for putting so much trust on me throughout my candidature. He constantly supported my research ideas while at the same time leading me to the right direction that is both scientifically interesting and valuable to the industry. He made sure that I am exposed to all possible opportunities (e.g., research visit at EPFL, collaboration with water operators, graduate lecture, research assistantship, and others) that will be essential for my candidature and professional development. He showed a good example on how to become a true water professional who can successfully link research with industry application. More than anything, he is always willing to help and provide useful advice about my candidature and my post-PhD plans. Of course, I cannot thank enough the first ones who believed in me: Dr. Wolfgang Gernjak and Dr. Maria José Farré. If not for them, I will not have this great opportunity to pursue my PhD at AWMC. They supported me all the way, from my initial applications in 2012, to research idea conception, methods development, data interpretation, manuscript writing and all other matters. I really enjoyed our brainstorming sessions to discuss my results and bottlenecks in my experiments. They also had the patience of listening to me whenever I practice for my conference presentations. I learned a great deal about DBPs from Dr. Farré, and oxidative processes, chemistry, and other engineering approaches from Dr. Gernjak. These are on top of their helpful friendly advice, creative academic analogies, (and even 'driving' tips). They never disappoint in providing substantial insights about my PhD, future plans, and life in

general. I feel extremely fortunate and happy to have worked with a perfect mix of supervisors as they prepared me well to take on a scientific career.

I would also like to thank my milestone assessors, Prof. Howard Weinberg and Prof. Jochen Mueller, for their patience and time to read and critic my work every year. Prof. Weinberg always gives timely detailed feedback which constantly resulted in significant improvement of our manuscripts. Other than his useful inputs on my thesis, he also provided valuable support for my plans after PhD studies. It was also great to discuss with Prof. Mueller about new ideas and making significant research contributions (e.g., in the field of microplastics and perfluorinated compounds).

During my time at AWMC, I also had the pleasure of working with a number of great students and postdocs. When I arrived in AWMC, I was immediately exposed to a big sampling event to survey DBP concentrations in South East Queensland led by Dr. Bonnie Lyon with the assistance of Ms. Marion Revalor. I could have not mastered the skill of DBP formation potential tests and extraction (volatile DBPs, HAAs, etc.) if not because for Dr. Lyon. She also taught me other laboratory methods for NOM characterization (fluorescence EEM, UV, chlorine demand test, SEC-UVD, up to glassware cleaning and efficient vial labelling). She made sure that I am equipped with all the techniques needed to do my own DBP research. I also greatly appreciated Dr. Peng Liu for being my laboratory buddy throughout my PhD, and for helping me ensure that the SEC-UVD-OCD instrument and the biofiltration columns operated well.

It has always been exciting to work with the other members of the Drinking and Recycled Water Research Group: Dr. Jelena Radjenovic, Dr. Katrin Doederer, Dr. Marie-Laure Pype, Dr. Emma Filloux, Ms. Jingshi Wang, Mr. Jeff Black, Ms. Elisabet Garcia, and Mr. Ali Farhat. I will also not forget Mrs. Vivienne Clayton, the admin team, and all other PhD students in AWMC for their assistance and support. Special thanks to Dr. Radjenovic for patiently mentoring me in electrochemistry (e.g., mediated electrochemical oxidation). I had a better appreciation of electrochemistry because of her and the members of the Environmental Electrochemistry group (Dr. Stefano Freguia and others). I would also like to sincerely thank Dr. Doederer and Dr. Pype for all the fun experiments and valuable discussions about laboratory-related matters, possible grant proposals, industry partnerships, or anything under the sun. Collaborating with them on other research projects (e.g., DBPs/taste and odor compound removal in BAC, DBP formation during chlorine boosting in distribution network, oxidation of DON by ferrate(VI), and others) was also a truly worthwhile learning experience. I also enjoyed all post-PhD project meetings about ferrate and microplastics with Dr. Doederer, Dr. Pype, Dr. Apra Boyle-Gotla, Dr. Bogdan Donose, and Ms. Ludwika Nieradzik as these discussions made me more aware and prepared for the challenges

normally faced by early career researchers (e.g., proposal writing, grant applications, project management, among others).

Dr. Deb Gale of Seqwater is also acknowledged for organizing all our sampling events with water treatment operators, whenever we needed water samples and biofilter media. In addition, I would not have my stock solutions of water samples without the help of Dr. Kalinda Watson who willingly helped me during extended hours of organic matter concentration using her custom-built reverse osmosis system (and not to forget the week-long ion exchange resin wash). She also assisted me in analyzing AOX of some samples at Entox. Through Entox, I also had the pleasure of working with Dr. Daniel Stalter whom I collaborated with to perform *in vitro* bioassays to my ozonated/chlorinated samples. He patiently taught me how to prepare my samples for the bioassays and also assisted in some AOX analyses. Thanks also to Elissa O'Malley for her contributions on the bioanalytical analysis of the water samples.

At the latter part of my PhD, I had the great privilege of working with Prof. Urs von Gunten at EPFL. Long before I started my PhD, his research had already made a significant impact in my desire to study water chemistry. Prof. von Gunten accepted me as a visiting PhD student for 6 months and taught me a great deal about ozone chemistry, which led to a significant portion in this thesis. I will never forget all the good times and discussions (academic and non-academic) during our meetings, lunches, water treatment plant tour, and group retreat in Leysin. My Switzerland stay became even more memorable because of the amazing members of LTQE: Dr. Florian Breider, Dr. Minju Lee, Dr. Michele Heeb, Dr. Ioannis Katsoyiannis, Dr. Ina Kristiana, Mr. Yang Song, Ms. Caroline Gachet, and Ms. Alina Tomaniak. Mr. Sylvain Coudret of ENAC is also acknowledged for his assistance in ion chromatography and flow injection analysis. Thanks also to Dr. Breider for all the fun discussions about chemistry and life over morning, noon, and late afternoon coffee.

I also had the chance to work as a research assistant at the Analytical Services Laboratory of AWMC together with Dr. Beatrice Keller-Lehmann, Mr. Nathan Clayton, and Ms. Jianguang Li. I thank them for an enjoyable experience as I learned different sample preparation and analytical techniques (e.g., TKN digestion, FIA analysis, GC/FID, TOC/TN, IC, ICP/OES, etc.). It was during those times that I appreciated more all their hard work in making sure that AWMC researchers receive timely high quality data.

I will also be forever grateful to my undergraduate professors at the University of the Philippines, Diliman especially my master's advisors, Prof. Pythias Espino and Prof. Yunho Lee, who inspired me to pursue research and further studies more than they know. Continuous collaboration with Prof. Lee and Mr. Jaedon Shin (GIST, Korea) on a study of oxidation by ferrate and N-DBP formation has been a truly rewarding learning experience.

Thanks as well to the Filipino community in Brisbane and Geneva for their overwhelming kindness and generosity. I really appreciated the Alvaran and Samson family for making me their 'adopted' son in Australia. I am also thankful to FilOz-UQ (especially to the 2014 officers and the other Pinoy postgrads) and the Maskipaps band for all the fun-filled events and gigs that helped provide a worthwhile break from research.

Of course, all my love and thanks to my family and relatives for their constant support in all my adventures from beginning to present, even if it always entails leaving home. Words cannot describe how thankful I am to my parents for all their hard work for me, Kuya Wilson, Paolo, and Red. Many thanks to my Mom for all her guidance up there.

Most importantly, I offer this work to my wife, Dr. Erlyn Rachelle Macarayan, who always served as my inspiration, motivation, and my endless source of happiness (no matter how hard my day has been). None of these would have been possible without her support and encouragement (and of course her perfectly cooked meals). We had so many unforgettable exciting experiences together that made my PhD life a wonderful experience. I look forward to our next journey.

Maraming salamat!

Keywords

drinking water treatment, ozonation, biofiltration, chlorination, disinfection byproducts, natural organic matter

Australian and New Zealand Standard Research Classifications (ANZSRC)

ANZSRC code: 090410 Water Treatment Processes, 60%

ANZSRC code: 039901 Environmental Chemistry, 40%

Fields of Research (FoR) Classification

FoR code: 0904 Chemical Engineering, 60%

FoR code: 0907 Environmental Engineering, 40%

Table of Contents

List of Figures

List of Tables

List of Abbreviations

ADWG	Australian Drinking Water Guidelines
AN	Anthracite
AOBr	Adsorbable organic bromine
AOC	Assimilable organic carbon
AOCl	Adsorbable organic chlorine
AOI	Adsorbable organic iodine
AOP	Advanced oxidation process
AOX	Adsorbable organic halogen
BAC	Biological activated carbon
BCAM	Bromochloroacetamide
BCAN	Bromochloroacetonitrile
BCIM	Bromochloroiodomethane
BDCAM	Bromodichloroacetamide
BDCM	Bromodichloromethane
BDIM	Bromodiiodomethane
BDOC	Biodegradable dissolved organic carbon
BIAM	Bromoiodoacetamide
Br-DBP	Bromo-organic DBPs
BSF	Bromine substitution factor
Bt	Biotransformation rule
CDIM	Chlorodiiodomethane
CH	Chloral hydrate
CIAM	Chloroiodoacetamide
Cl-DBP	chloro-organic DBPs
CT	Concentration × time (oxidant exposure)
DAFF	dissolved air flotation and sand filtration
DBAA	Dibromoacetic acid
DBAM	Dibromoacetamide
DBAN	Dibromoacetonitrile
DBCAA	Dibromochloroacetic acid
DBCAM	Dibromochloroacetamide
DBCM	Dibromochloromethane
DBIM	Dibromoiodomethane
DBP	Disinfection byproduct
DCAM	Dichloroacetamide
DCBAA	Dichlorobromoacetic acid
DCAA	Dichloroacetic acid
DCAN	Dichloroacetonitrile
DCIM	Dichloroiodomethane
DCP	1,1-Dichloropropanone
DHAA	Dihaloacetic acids
DHAN	Dihalogenated acetonitrile
DIAM	Diiodoacetamide

DMSO	Dimethylsulfoxide
DNA	Deoxyribonucleic acid
DO	Dissolved oxygen
DOC	Dissolved organic carbon
DOM	Dissolved organic matter
DON	Dissolved organic nitrogen
DPD	*N,N*-diethyl-*p*-phenylenediamine
EBCT	Empty bed contact time
EC	Effective concentration
EDC	Electron-donating capacity
EEM	Excitation-emission matrix
EPFL	École Polytechnique Fédérale de Lausanne
EU	European Union
FA	Fulvic acid-like fluorescence region
FP	Formation potential
GAC	Granular activated carbon
GC/ECD	Gas chromatography with electron capture detection
Gly	Glycine
HA	Humic acid-like fluorescence region
HAA	Haloacetic acid
HAA5	Sum of chloro-, dichloro-, trichloro-, bromo- and dibromo-acetic acid
HAA8	Sum of 8 chlorine- and bromine-containing haloacetic acid
HAM	Haloacetamide
HAN	Haloacetonitrile
HAN4	Sum of dichloro-, trichloro-, dibromo- and bromochloro-acetonitrile
HK	Haloketone
HK2	Sum of 1,1,1-trichloro- and 1,1-dichloropropanone
HNM	Halonitromethane
HOBr	Hypobromous acid
HOCl	Hypochlorous acid
HOI	Hypoiodous acid
HPLC	High performance liquid chromatography
HPSEC	High performance size exclusion chromatography
H_2O_2	Hydrogen peroxide
IC	Inorganic carbon
IT	Light intensity × time
I-DBP	Iodo-organic DBPs
IHSS	International Humic Substances Society
I-THM	Iodine-containing trihalomethane
IR	Induction ratio
k	rate constant
k_{obs}	pseudo-first-order rate constant of ozone decay
k_{app}	apparent second-order rate constant
MCAA	Monochloroacetic acid
MBAA	Monobromoacetic acid

MDL	Method detection limit
MeOH	Methanol
MEO	Mediated electrochemical oxidation
MRL	Method reporting level
MSIA	Methanesulfinic acid
MSOA	Methanesulfonic acid
MtBE	methyl tert-butyl ether
MW	Molecular weight
MWCO	Molecular weight cut-off
NA	Not available
N-DBP	Nitrogen-containing disinfection byproduct
NH_2Cl	Monochloramine
NH_4^+	Ammonium
NA	Not available
NOM	Natural organic matter
NO_2^-	Nitrite
NO_3^-	Nitrate
NO_x	Sum of nitrate and nitrite
O_3	Ozone; $\int[O_3]dt$ refers to ozone exposure
$^1O_2$	Singlet oxygen
$O_2^{\bullet-}$	Superoxide radical
$O_3^{\bullet-}$	Ozonide radical
OCD	Organic carbon detector
$^{\bullet}OH$	Hydroxyl radical; $\int[^{\bullet}OH]dt$ refers to hydroxyl radical exposure
P_{biodeg}	Biodegradable concentration of the contaminant
P_f	Minimum contaminant concentration
P_t	Contaminant concentration at time t
pCBA	*para*-Chlorobenzoic acid
PLFA	Pony Lake fulvic acid
P1	Aromatic protein (tyrosine-like) fluorescence EEM region
P2	Aromatic protein (tryptophan-like) fluorescence EEM region
QHFSS	Queensland Health Forensic and Scientific Services
R_{ct}	Ratio of $^{\bullet}OH$ and O_3 exposures
REF	Relative enrichment factor
RO	Reverse osmosis
RS	Reactions
RU	Raman units
SEC	Size exclusion chromatography
SEQ	South East Queensland
SMP	Soluble microbial products
SPE	Solid phase extraction
SRHA	Suwanee River humic acid
SUVA	Specific UV absorbance at 254 nm
S_{yx}	Standard error of estimate

TA	Tannic acid
TBAA	Tribromoacetic acid
TBAM	Tribromoacetamide
TBM	Tribromomethane
TBNM	Tribromonitromethane
t-BuOH	Tertiary butanol
TCAA	Trichloroacetic acid
TCAM	Trichloroacetamide
TCAN	Trichloroacetonitrile
TCM	Trichloromethane
TCNM	Trichloronitromethane
TCP	1,1,1-Trichloropropanone
TEMPO	2,2,6,6-Tetramethyl-1-piperidinyloxy
THAA	Trihaloacetic acids
THAM	Trihaloacetamides
THM	Trihalomethane
THNM	Trihalonitromethane
THNM2	Sum of trichloronitromethane and tribromonitromethane
THM4	Sum of trichloro-, dichlorobromo-, dibromochloro-, and tribromomethane
TIM	Triiodomethane
TN	Total nitrogen
TOC	Total organic carbon
TON	Total organic nitrogen
UAOX	Unknown adsorbable organic halogen
US	United States
US EPA	United States Environmental Protection Agency
UV	Ultraviolet
UVD	Ultraviolet detector
UQ	University of Queensland
WHO	World Health Organization
WTP	Water treatment plant

Chapter 1

General Introduction

1.1. Background

Drinking water treatment plants aim to have an efficient removal of dissolved natural organic matter (NOM). NOM may not only cause undesirable color, taste and odor, biological instability, but also formation of disinfection byproducts (DBPs) (Rook 1977, Sedlak and von Gunten 2011). DBPs may occur in different forms at varying concentrations and toxicity, depending on the precursor characteristics during disinfection. For example, source waters may form low concentrations of nitrogen-containing DBPs (N-DBPs) compared to carbon-based DBPs (C-DBPs) during chlorination. But unlike their occurrence levels, N-DBPs are more cytotoxic and genotoxic than C-DBPs (Plewa et al. 2008, Richardson et al. 2007). As a result of the possible health implications of these compounds, strict water quality regulations or guidelines were implemented to guarantee that the resulting DBPs after water treatment are at/below the levels considered safe for human consumption.

The standard water treatment systems for NOM removal are comprised of coagulation followed by sedimentation and filtration (Matilainen et al. 2010). This conventional approach can remove hydrophobic NOM fractions by 64 – 84% but can be inefficient for hydrophilic fractions (e.g., 14% – 17%) (Bond et al. 2011a). With subsequent chlorination, the post-coagulated NOM is still amenable for halogenation, leading to products such as N-DBPs from the hydrophilic NOM fraction. Succeeding post-coagulation processes are therefore significant in removing the remaining NOM. As shown in our previous study with full-scale plants in South East Queensland (SEQ), effective NOM removal may be achieved for water utilities including ozonation and biofiltration in their treatment scheme (Lyon et al. 2014a). With ozonation, NOM can be broken down into compounds with low molecular weight and high biodegradability (e.g., aldehydes, ketones, and carboxylic acids) (von Sonntag and von Gunten 2012). During this process, reactions of hydroxyl radicals ($^{\bullet}OH$) can also take place, especially at conditions that promote ozone decay (e.g., at high ozonation pH, presence of H_2O_2) (von Sonntag and von Gunten 2012). These $^{\bullet}OH$ radicals are non-selective oxidants that may contribute in the further transformation of NOM and other ozone recalcitrant compounds (von Sonntag and von Gunten 2012). Ozonation is followed by biological filtration to remove various products formed during oxidation by ozone and/or $^{\bullet}OH$. As a final step, chlorination is performed to provide residual disinfection in the distribution network. The addition of chlorine however raises concerns about DBP formation. In this context, optimal processes for removal of DBP precursors are necessary.

This PhD thesis therefore evaluates ozonation and biofiltration as an effective combined process for NOM removal and DBP control. Understanding the factors affecting their treatment performance is critical particularly for the SEQ region because of its relatively high levels of source water DON (0.35

mg N/L) and DOC (9.2 mg C/L) compared to other studies in the literature (e.g., North America) (Lyon et al. 2014a). These concentrations can potentially lead to elevated levels of DBPs during chlorination. A few studies on ozonation/biofiltration are also available in the literature, however, most of them concentrated mainly on the removal of DOC, biodegradable compounds, and DBPs such as trihalomethanes and haloacetic acids (Chaiket et al. 2002, Speitel et al. 1993, Wobma et al. 2000). Very little is known about the impact of these processes on the precursors of other emerging organic pollutants like the N-DBPs.

This work focuses on understanding the relationships among water quality and NOM, ozonation kinetics, oxidation products, biodegradability, and formation of DBPs. The DBPs investigated include trihalomethanes, haloacetic acids, chloral hydrate, haloketones, and the less studied nitrogenous haloacetonitriles, halonitromethanes, and haloacetamides. In particular, the thesis explored the effect of stepwise ozonation-biofiltration-chlorination processes to understand the mechanisms involved in the reaction of ozone with NOM. The influence of ozone and $^{\bullet}OH$ reactions on NOM removal and DBP formation was also studied. Lastly, the impact of coupled ozonation and biofiltration on the abatement of DBP precursors was assessed. The specific objectives addressed in this work are presented below. This is followed by the thesis outline explaining the contents of each chapter.

1.2. Objectives of the thesis

This thesis explored the fundamental processes involved in the reaction of NOM across a treatment scheme which uses ozonation, biodegradation, and chlorination. It aims to understand the impact of ozonation and biological treatment on formation of oxidation products, and ultimately determine suitable treatment conditions for better DBP control.

The specific objectives of the doctoral thesis include:

- Investigate the effect of ozone on organic nitrogen moieties of NOM and the subsequent formation of oxidation products (e.g., inorganic nitrogen) during ozonation at varying conditions.
- Understand the effect of NOM transformations induced by ozone and $^{\bullet}OH$ radicals on DBP formation.
- Determine the impact of biological treatment on further transformation of pre-ozonated NOM and DBP precursors.

1.3. Thesis outline

This doctoral thesis was carried out through collaborations with Water Research Foundation, Seqwater, University of Queensland, Swiss Federal Institute of Technology, Lausanne (EPFL), and Australia Awards. The study was within the framework of the following research projects: (1) "Engineering solutions to minimize nitrogen-containing DBPs" (Water Research Foundation, Project 4484), (2) "Advanced characterization of raw water and minimizing disinfection byproducts (DOM/DBP)" (Seqwater, Project 4), and (3) "Optimization of DBP formation control" (Seqwater, Project 5). These projects focused on assessment of formation of N-DBPs and other DBP species in SEQ drinking waters. Their scope also include improvements of ozonation procedures as well as other treatment processes that can lead to optimal removal of NOM in the product water.

The joint partnerships have a broader aim of identifying preventive management of known health hazards and other aspects that impact the quality of SEQ drinking water. Under this aim, the current study was included to particularly investigate the key reactions of NOM that affect subsequent formation of DBPs during ozonation, biofiltration, and chlorination. The thesis results are presented in the form of papers (3) published in Water Research.

Chapter 1 provides the context of the study, the main objectives, and organization of the thesis.

Chapter 2 introduces the issue of DBPs in drinking water, with some emphasis on DBP formation in the SEQ region. The properties of NOM which affects DBP formation are first described together with the characterization methods employed in the study. This is followed by a review of known DBP reaction pathways with chlorine. Strategies for DBP control (i.e., conventional versus advanced water treatment using ozone) are also discussed along with some important aspects of ozone chemistry and biological filtration. This chapter highlights the combined ozonation and biofiltration processes as a promising approach for DBP control. The literature review also identifies some key areas that need further investigation.

Chapter 3 provides a summary of the knowledge gaps on ozonation and biofiltration identified in the previous chapter. This chapter includes discussions of the addressed research questions, hypotheses, as well as the general approaches used in the study.

Chapter 4 presents a new concept for ozonation characterization by utilizing the effect of ozone reactions with dissolved organic nitrogen (DON). Particularly, this chapter investigated the formation of DON-derived inorganic nitrogen products (e.g., nitrate and ammonium) during ozonation of different water samples including model solutions (amines), surface water, and wastewater effluent.

Based on the results, reaction mechanisms were proposed and their application for ozone exposure assessment was also explored.

The findings of this chapter were published at: **de Vera, G.A.**, Gernjak, W., Weinberg, H.S., Farré, M.J., Keller, J., and von Gunten, U. (2017) Kinetics and mechanisms of nitrate and ammonium formation during ozonation of dissolved organic nitrogen. *Water Research* 108, 451-461.

Chapter 5 focuses on the effects of ozone and •OH on the formation of C-DBPs and N-DBPs during post-chlorination. Such effects were investigated as both oxidants could play significant roles in DBP precursor transformations. Conditions that favor ozone and •OH reactions were achieved by changing the water quality and addition of radical chain promoters and inhibitors. The effects of these reactions on DBP formation are presented together with bioassay toxicity data to assess the effect of ozonation on the overall quality of the treated water.

The results of this chapter were published at: **de Vera, G.A.**, Stalter, D., Gernjak, W., Weinberg, H.S., Keller, J., and Farré, M.J. (2015) Towards reducing DBP formation potential of drinking water by favouring direct ozone over hydroxyl radical reactions during ozonation. *Water Research*, 87, 49-58.

Chapter 6 investigates the effectiveness of combined ozonation and biodegradation processes in controlling DBP formation. In this chapter, the importance of operational factors such as ozone exposure during ozonation and empty bed contact time (EBCT) during biofiltration was evaluated. This chapter highlights the differences of biodegradability of each DBP precursor and demonstrates the significance of biofiltration in preventing formation of chloral hydrate, haloketones, and halonitromethanes, all of which increased after ozonation.

The results of this chapter were published at: **de Vera, G.A.**, Keller, J., Gernjak, W., Weinberg, H.S., and Farré, M.J. (2016) Biodegradability of DBP precursors after drinking water ozonation. *Water Research* 106, 550-561.

Chapter 7 presents the conclusions and overall research findings of this thesis in connection with the research hypotheses specified in Chapter 3. From the conclusions drawn, practical applications of the results, recommendations for water treatment operators, and opportunities for future research were identified.

Chapter 2

Literature Review

This chapter aims to provide a general understanding of the concepts needed for the succeeding chapters on ozonation, biofiltration, and disinfection byproduct (DBP) formation. The properties of natural organic matter (NOM), characterization methods, and fate through conventional and advanced water treatment plants (WTPs) were first described. These were followed by sections on formation of DBPs and the effect of ozone on removal of their precursors. To better understand ozone chemistry, discussions on reaction mechanisms and kinetics were also included. As ozonation leads to more biodegradable NOM, biological treatment and its effect on DBP formation were also explored. Many examples used in this chapter involved results obtained from the following studies on South East Queensland (SEQ) drinking waters:

- Lyon, B.A., Farré, M.J., **de Vera, G.A.**, Keller, J., Roux, A., Weinberg, H.S., and Gernjak,W. (2014) Organic matter removal and disinfection byproduct management in South East Queensland's drinking water. *Water Science & Technology: Water Supply* 14 (4), 681–689.
- Farré, M.J., Lyon, B., **de Vera, G.A.**, Stalter, D., and Gernjak, W. (2016) Assessing adsorbable organic halogen formation and precursor removal during drinking water production. *Journal of Environmental Engineering*, 10.1061/(ASCE)EE.1943-7870.0001022, 04015087.
- Farré, M.J., **de Vera, G.A.,** Lyon, B.A., Doederer, K., Weinberg, H.S., Gernjak, W., and Keller, J. (2016) Engineering solutions to minimize nitrogen-containing DBPs. 2016, Water Research Foundation, CO, USA. Available at http://www.waterrf.org/Pages/Projects.aspx?PID=4484 .

2.1. Natural organic matter (NOM)

Dissolved NOM is present in all water sources and comprises a complex mixture of organic compounds with different size, structure, and functionalities (Aslam et al. 2013, Leenheer and Croué 2003). It is derived from degradation products of plants surrounding the water source (allochthonous) or of microorganisms within the water source (autochthonous) (Matilainen et al. 2011). In drinking water treatment, the efficient removal of NOM is a priority because of its negative impacts including DBP formation and biological instability in distribution network.

Allochthonous organic matter, commonly characterized by a high carbon (50–75% dissolved organic carbon) to nitrogen content, is dominated by humic substances (McDonald et al. 2004). Meanwhile, autochthonous organic matter is mainly composed of more hydrophilic phenolic and carboxylic moieties in amino acids, carbohydrate, and low molecular weight acids (Croué et al. 2000). Unlike allochthonous organic matter, this type of NOM has higher nitrogen content because of the presence

of more aliphatic nitrogen groups (Boyer et al. 2008). To represent these types of NOM, many laboratory studies used NOM standards isolated from Suwannee River and Pony Lake corresponding to those with allochthonous and autochthonous origin, respectively (Aeschbacher et al. 2012, IHSS 2016, Wenk et al. 2013).

NOM can also be classified into its component fractions like hydrophobic and hydrophilic chemical fractions using XAD resins (Croué et al. 2000, Leenheer and Croué 2003, Thurman and Malcolm 1981). Hydrophobic fractions consist of high molecular weight fulvic and humic acids containing aromatic, phenolic, and carboxylic groups which causes yellowish color in water (Kim and Yu 2005). In contrast, hydrophilic NOM fraction is composed of smaller and more biodegradable carboxylic acids, carbohydrates, amino acids and sugars, and proteins (Nkambule et al. 2009, Yu et al. 2002). Compared to the hydrophobic NOM, this fraction is harder to remove via conventional processes of flocculation, sedimentation, and filtration (White et al. 1997).

The character of NOM depends on catchment characteristics, hydrological pathways, biological predominance, seasonality and climate conditions (Aslam et al. 2013, Delpla et al. 2009, Teixeira and Nunes 2011). For example, the hydrophilic NOM fraction could contain increasing concentrations of dissolved organic nitrogen (DON) as a result of shorter water cycles through indirect or direct potable reuse (Krasner et al. 2009, Leverenz et al. 2011, Rodriguez et al. 2009). In addition, climate-related eutrophication and run-off events in upstream agricultural systems have also been identified to impact NOM concentrations (Delpla et al. 2009, Graeber et al. 2015, Westerhoff and Mash 2002).

2.2. Drinking water treatment

NOM removal during water treatment can be achieved using the processes summarized in Table 2.1 (Bond et al. 2011a). Each treatment step is combined with other processes to comprise a multi-barrier system not only against NOM but also against other micropollutants and pathogens (NHMRC and NRMMC 2011). The success of the overall treatment depends on the effectiveness of each of the processes. For the case of SEQ, conventional WTPs mainly involve coagulation, filtration, and disinfection while advanced WTPs have additional ozonation and biological activated carbon (BAC) filtration steps (Figure 2.1). In some WTPs, pre-oxidation by addition of permanganate, chlorine, or ozone is also performed before coagulation to control taste, odor, iron, and manganese.

Table 2.1. NOM removal mechanisms in different water treatment process (adapted from Bond et al. (2011a), with permission)

Process	Mechanism	Selectivity	Least treatable
Coagulation	Adsorption onto flocs and charge neutralization/ colloid destabilization. Sweep flocculation	Large, anionic molecules	Neutral molecules
Anion exchange	Ion exchange (electrostatic), adsorption (hydrophobic) and H-bonding	Small, anionic molecules	Neutral molecules
Membranes	Size exclusion, differing diffusion rates across membranes. Electrostatics for charged membranes	Species>MWCO	Species < MWCO
Ozone	Electrophilic addition (oxidation and bond cleavage). Also $^{\bullet}$OH reactions	Activated aromatic compounds and amines	Saturated compounds
AOP	$^{\bullet}$OH reactions: electron transfer, H-abstraction, OH addition	Relatively unselective	
Activated carbon	Reversible physical adsorption by non-specific forces	Small, neutral, hydrophobic molecules	Hydrophilic charged molecules
Biotreatment	Enzyme-controlled microbial degradation and adsorption	Low MW polar molecules (e.g., amino acids, aldehydes)	Large and hydrophobic molecules

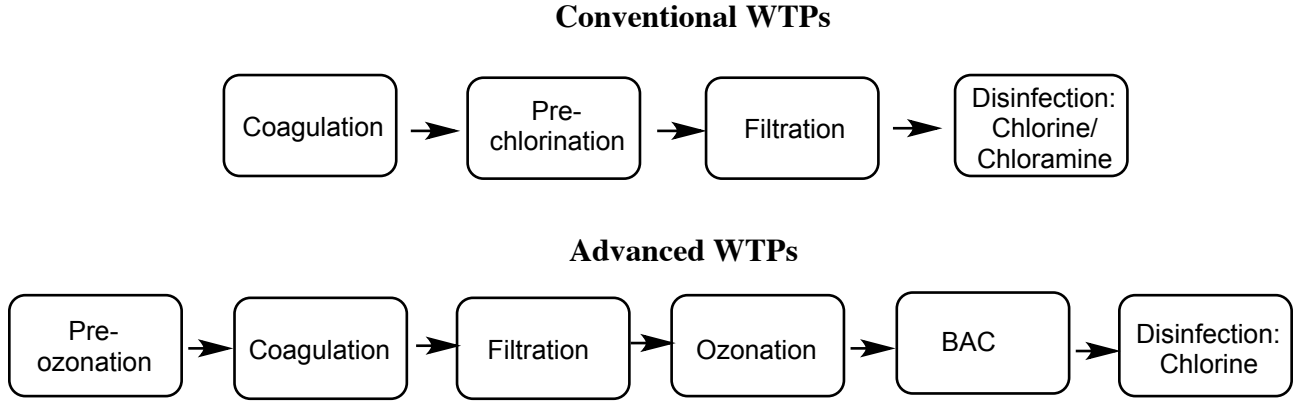

Figure 2.1. Treatment processes employed in conventional and advanced water treatment plants in SEQ (Lyon et al. 2014a)

During coagulation, the suspended and colloidal NOM particles of the source water are neutralized typically using aluminum or iron salts (Edzwald 2010, Matilainen et al. 2010, Xie 2004). These coagulants are hydrolyzed forming soluble positively-charged complexes adsorbing to negatively-charged surfaces of NOM. As reviewed by Matilainen et al. (2010), the aggregation of NOM occurs through a combination of charge neutralization, entrapment, adsorption, and complexation with coagulant metal ions into insoluble particle aggregates that could settle in the following sedimentation basins. Bridging or sweep flocculation is also possible with polymer-based coagulants. Among the different NOM components, coagulation was shown to be effective for removal of hydrophobic fractions (84%: humic acid; 64%: fulvic acid) than the hydrophilic NOM fractions (<20%) (Sharp et al. 2006). Coagulation can be further enhanced and optimized for better removal of NOM and microorganisms by adjusting the coagulant dose and type, pH, coagulation aids, mixing speed and time (Bell et al. 1998, White et al. 1997). Pre-treatment with anion exchange resins (e.g., magnetic ion exchange resin (MIEX®)) is also another option to improve removal of NOM (Singer and Bilyk 2002), particularly the transphilic fraction which has high carboxylic acid content (Bond et al. 2011a).

Following sedimentation is rapid filtration using sand and/or anthracite as media to separate the non-settlable particles from the process water (Edzwald 2010). At this step, large particles are removed by physical straining, while the smaller particles are removed by adsorption and flocculation (Xie 2004). In addition to these filters, some treatment plants also employ membranes where particles with higher molecular weight than the molecular weight cut-off (MWCO) are retained. Using this process, Nilson and DiGiano (1996) found that nanofiltration using a polysulfone hollow fiber membrane (1000 Da MWCO) can be very effective in removing hydrophobic NOM. In that study, NOM rejection decreased as follows: hydrophobic (~95%) > unfractionated (77–82%) > hydrophilic (42–66%). This approach, however, requires high capital and operation costs and is prone to fouling which is influenced by hydrodynamics, electrolyte concentration, pH, and presence of divalent cations (Ca^{2+}) (Hong and Elimelech 1997, Seidel and Elimelech 2002).

For advanced WTPs, ozone can be applied to oxidize many inorganic and organic compounds containing phenolic and amino groups of NOM (von Sonntag and von Gunten 2012). Its decomposition is also known to generate $^{\bullet}OH$ which can oxidize other recalcitrant compounds (von Sonntag and von Gunten 2012). During ozonation, the hydrophobic and aromatic structures of NOM are transformed to lower molecular weight, hydrophilic, and biodegradable compounds (Hammes et al. 2006, van der Kooij et al. 1989). These oxidation products make a subsequent biofiltration step necessary which is commonly performed using activated carbon as the filter media. During initial operation, physical adsorption to the carbon acts as the main NOM removal mechanism. However, this removal would diminish as adsorption sites become exhausted with continuous operation (Simpson 2008). After such

period, NOM concentrations are decreased due to biodegradation of low molecular weight oxidation products.

Prior to distribution, disinfection is performed to inactivate pathogens such as bacteria, viruses, and protozoa, while also oxidizing compounds that may not be removed by the prior treatment steps (Edzwald 2010). Disinfection can be attained by application of chlorine-based disinfectants such as chlorine, chloramine, and chlorine dioxide or by ozone and ultraviolet (UV) irradiation. Disinfection is commonly assessed in terms of the required CT (disinfectant concentration × contact time; mg·min/L) or IT (light intensity × contact time; mJ/cm^2) to attain the desired level of pathogen inactivation. For *E. coli* (pH 7.1, 20ºC), 1 log inactivation (90% removal) can be easily achieved with ozone (0.0021 mg·min/L) followed by chlorine dioxide (0.030 mg·min/L), and free chlorine (0.085 mg·min/L), while for UV, same inactivation corresponds to 3.5 mJ/cm^2 IT (Cho et al. 2010). Microbial inactivation may involve attack to cell surface or damage to intracellular components, with the former mechanism being more dominant for ozone (i.e., stronger oxidant) and the latter for chlorine (i.e., weaker oxidant) (Cho et al. 2010). For UV, disinfection is known to occur via direct photochemical damage to intracellular DNA (Linden et al. 2002). Sequential schemes, such as those described in advanced WTP (Figure 2.1), could therefore enhance disinfection. Ozone can damage the cell wall making chlorine's attack to the inner cell components more amenable. The synergistic effect of ozone and chlorine has been demonstrated for *Cryptosporidium parvum* and *Bacillus subtilis* spores in previous studies (Cho et al. 2006, Rennecker et al. 2000). The combined ozone-chlorine treatment is also beneficial for residual disinfection, especially for WTPs using ozone as the main disinfectant due to ozone's inability to provide residuals during distribution. In Australia, a residual chlorine of >0.5 mg/L is required (NHMRC and NRMMC 2011) to avoid bacterial regrowth. Alongside final chlorination, however, is the formation of DBPs (Krasner et al. 2006, Rook 1977) from the reaction of chlorine with the remaining NOM (see below for further discussion).

2.2.1. Common NOM characterization methods

The water treatment processes discussed in the previous section affect the resulting NOM characteristics. Monitoring these properties could help evaluate the overall effectiveness of the process scheme and evaluate the treatability of the water under the applied treatment conditions. Not having sufficient NOM removal, for example, would require process optimization (e.g., adjusting the pH, coagulant and oxidant dose, filtration contact time, and other operational parameters). Routinely, dissolved organic carbon (DOC) and nitrogen (DON) are measured for quantitative assessment of NOM concentrations in WTPs. In the SEQ region, better NOM removal (i.e., in terms of DOC and DON) was achieved for advanced WTPs compared to conventional systems (Figure 2.2). Among the

treatment processes used, coagulation largely removed DOC (53%), with some additional removal during O_3/BAC (57%) process. Relative to DOC, removal of DON was somewhat lower (45% from coagulation, and 54% from raw to final) (Lyon et al. 2014a). These removals were within the values observed in surveyed WTPs in the US employing a combination of coagulation or lime softening, ozonation, and filtration. In that study, DOC removal ranged from 39–76% and DON from 29–61% (Mitch et al. 2009).

The DOC and DON values could also be used to indicate the origin of NOM in the source waters (Westerhoff and Mash 2002). Waters with high DOC/DON ratios (e.g., C/N of Suwannee River humic acid = 44.9 (IHSS 2016)) represent allochthonous NOM while those with low DOC/DON ratios represent an autochthonous, microbial-derived NOM (e.g., C/N of Pony Lake fulvic acid = 8.1 (IHSS 2016)). For the case of SEQ, source waters had an average of 26 mg C/mg N suggesting that these waters contain more allocthonous, plant- and soil-derived NOM (Lyon et al. 2014a).

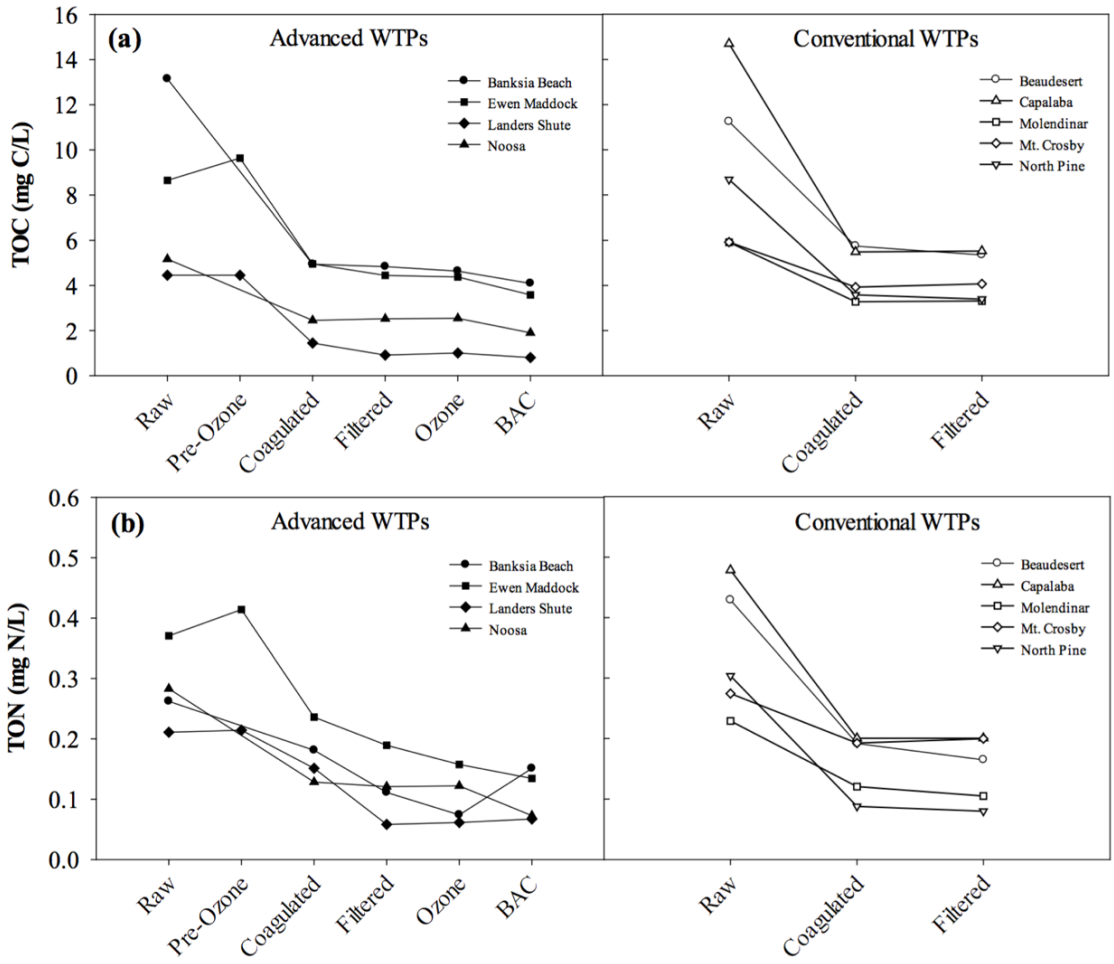

Figure 2.2. Removal of (a) TOC and (b) TON across advanced and conventional water treatment plants in SEQ (Lyon et al. 2014a).

Other than DOC and DON measurements, parameters such as specific UV absorbance (SUVA), fluorescence, and molecular weight also provide complementary information on the transformations of NOM during water treatment. Among these, SUVA can be considered as the most widely used parameter for NOM characterization.

2.2.1.1. UV spectroscopy

SUVA refers to the ratio of absorbance at 254 nm to DOC and represents the the average absorptivity at 254 nm of all compounds comprising NOM (expressed as DOC) (Edzwald et al. 1985, Hua et al. 2015). This parameter provides information about the aromaticity and degree of hydrophobicity of NOM, as well as NOM's amenability for coagulation and DBP formation (Edzwald 1993, Weishaar et al. 2003). A SUVA>4 L/mgC·m indicates a NOM composed mostly of hydrophobic fractions whereas SUVA<3 L/mgC·m indicates a more hydrophilic NOM (Matilainen et al. 2011). Figure 2.3 shows the changes in SUVA values across each treatment step in conventional and advanced WTPs in SEQ (Farré et al. 2016a). As shown, majority of the SUVA of all the raw water was removed by coagulation with further reductions by ozone, demonstrating its selectivity towards aromatic compounds leading to ring-opening reactions and less UV absorbing units.

SUVA can also be applied to evaluate the reactivity of oxidants towards activated aromatic compounds of the source waters. For example, waters with high SUVA values would make ozone more unstable and decay faster. Figure 2.4a shows a linear relationship of the first-order rate constant of ozone decay in water samples from SEQ in relation to those investigated by Westerhoff et al. (1999).

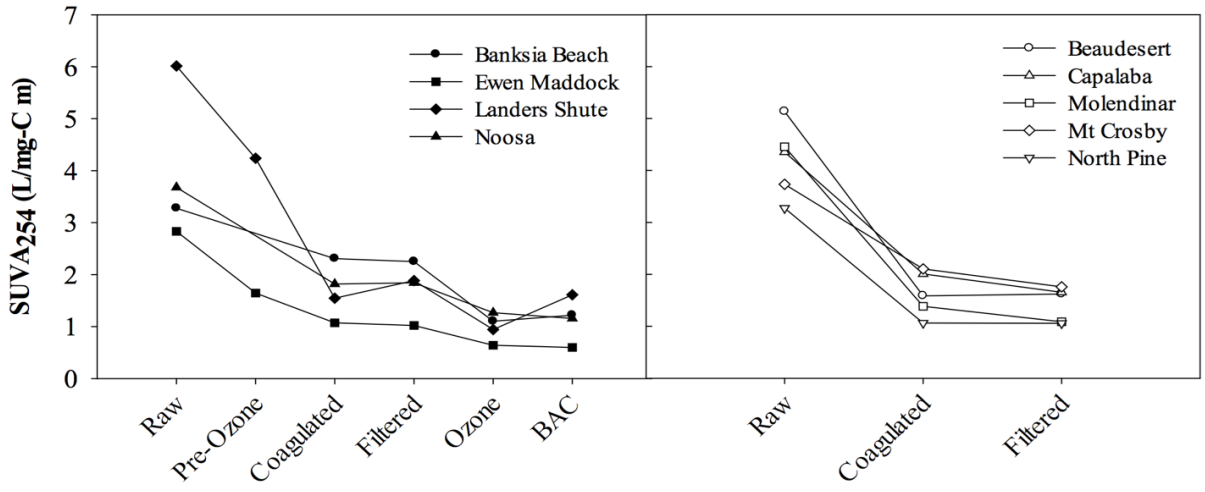

Figure 2.3. SUVA across advanced and conventional water treatment plants in SEQ (Farré et al. 2016a)

While SUVA can provide useful insights about NOM's general characteristics, its use as a surrogate parameter for reactivity with chlorine applies only to highly hydrophobic waters (SUVA >3 L/mgC·m) (Edzwald et al. 1985, Kitis et al. 2001). This limitation is due to SUVA not being able to account for compositional differences and other reactive sites responsible for DBP formation (Weishaar et al. 2003). For example, Figure 2.4b shows that SUVA has poor correlation with formation potentials of adsorbable organic halogen (AOX) in SEQ source waters (Farré et al. 2016b). Other studies also showed that SUVA of various NOM fractions had weak correlation with the formation of trihalomethanes and haloacetic acids (Ates et al. 2007, Hua et al. 2015).

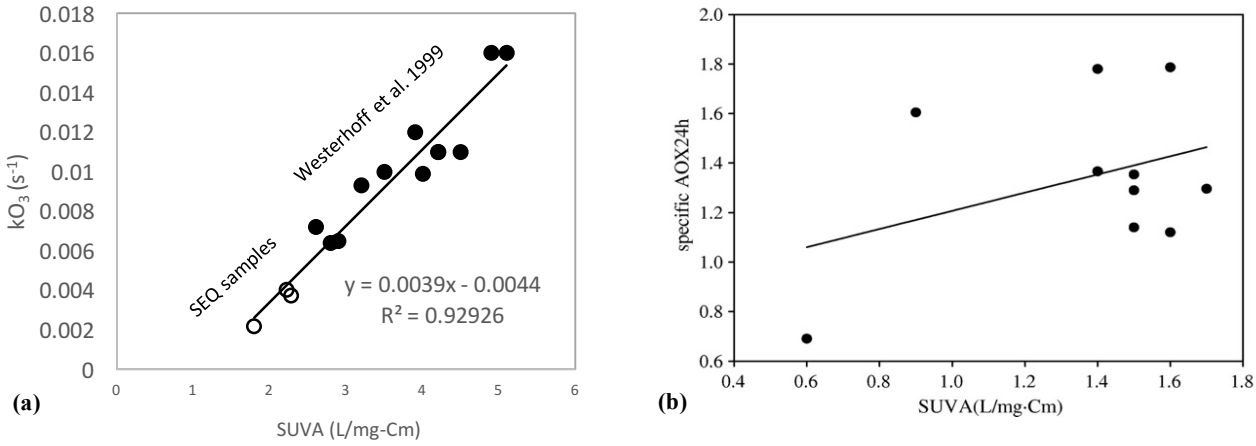

Figure 2.4. (a) Linear relationship of ozone decay constant (slow decay phase) with SUVA obtained from SEQ, Australia and Westerhoff et al. (1999); (b) plot of specific adsorbable organic halogen (AOX) formation potentials versus SUVA (Farré et al. 2016b).

2.2.1.2. Fluorescence spectroscopy

Fluorescence methods are based on the excitation of a molecule by absorbing a high energy photon and emission of a lower energy photon at a longer wavelength (Chen et al. 2003, Matilainen et al. 2011). Compared to absorbance, fluorescence spectroscopy is a more sensitive and selective characterization method. This technique has evolved from measurements of simple selected excitation or emission wavelengths to simultaneous collection of fluorescence measurements in a wide range of excitation and emission wavelengths (Bieroza et al. 2010). It is widely applied to get spectral signatures or optical maps of water samples through a three-dimensional plot of excitation energy, emission wavelength and fluorescence intensity, known as excitation-emission matrix (EEM) (Chen et al. 2003, Hudson et al. 2007, Markechova et al. 2013). The spectra generated at 200-500 nm can be used to

identify NOM components like humic and fulvic acids, soluble microbial products, and aromatic proteins (Chen et al. 2003). Figure 2.5a shows an example fluorescence EEM spectra of a drinking water source in SEQ using fluorescence regional integration of Chen et al. (2003). With this method, transformations of NOM during treatment can be monitored by inspecting changes in intensities of the different regions. In Figure 2.5b, coagulation was demonstrated to effectively decrease the fluorescence of all NOM components, with the largest decrease in the fulvic acid-like region (Farré et al. 2016a). This is in agreement with other previous studies where DOC removal by coagulation showed linear relationship with the decrease of fluorescence in the humic and fulvic acid regions (Bieroza et al. 2010, Gone et al. 2009). Lowest fluorescence was observed after ozonation and BAC filtration (Figure 2.5b), suggesting the effectiveness of oxidation in transforming aromatic compounds. The application of fluorescence EEM as a monitoring tool for NOM removal was also evaluated in our previous study (Farré et al. 2016a) where we showed that fluorescence intensities in the fulvic-acid and humic-acid region correlate very well with TOC, TON, as well as demand for chlorine and chloramine (R^2>0.82) (Figure 2.6). A similar correlation between these fluorescence regions and DOC was also observed in other studies (Baghoth et al. 2011).

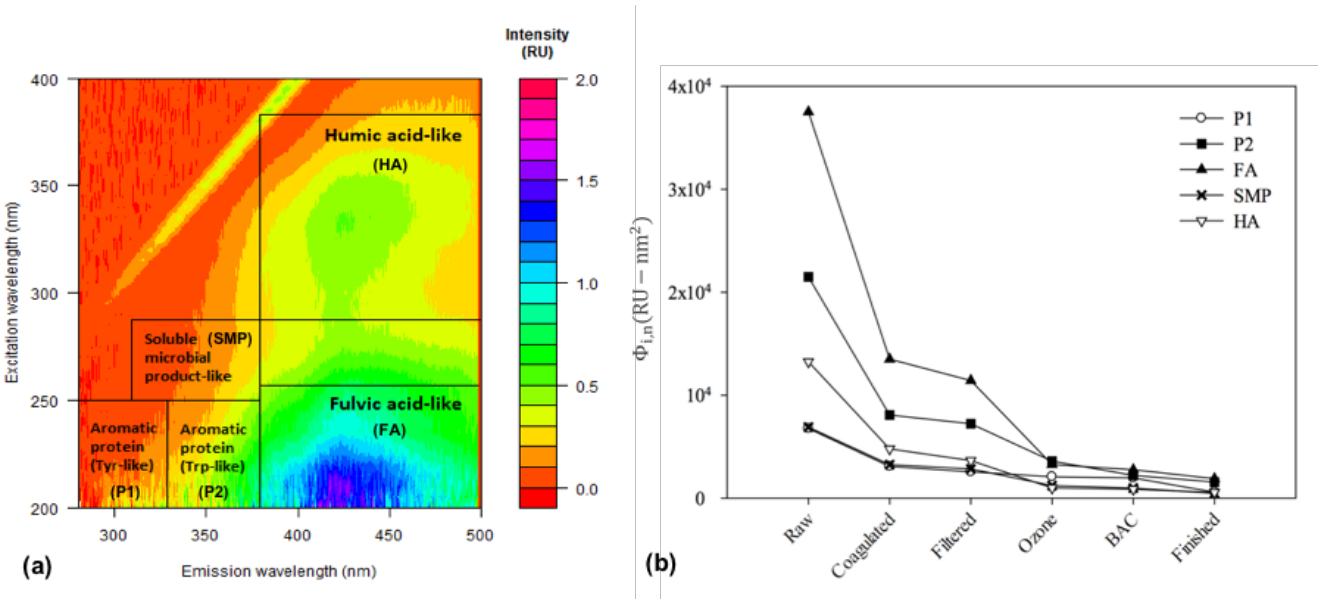

Figure 2.5. (a) Fluorescence EEM spectra of a settled water in SEQ; (b) Change in fluorescence across an advanced wastewater treatment plant (Farré et al. 2016a)

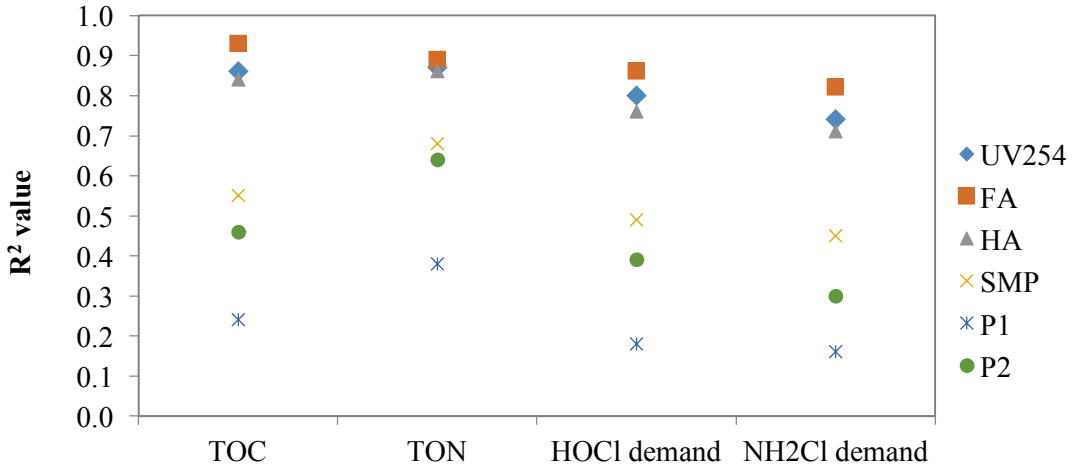

Figure 2.6. Correlations between SEQ water characteristics and UV_{254} or fluorescence (Farré et al. 2016a). Fluorescence EEM regions: FA: fulvic acid, HA: humic acid, SMP: soluble microbial product, P1: aromatic protein (tyrosine-like), P2: aromatic protein (tryptophan-like).

2.2.1.3. Size exclusion chromatography (SEC)

The molecular weight (MW) and size of NOM strongly influence NOM's treatability. To determine the size and apparent MW profile of NOM, high pressure size exclusion chromatography (HPSEC) can be used. In this method, NOM is fractionated based on their molecular size (i.e., bigger molecules elute out of the column first while smaller molecules elute last). MW of fractions can be evaluated using polystyrene sulphonate and polyethylene glycol standards (Her et al. 2002).

HPSEC can be combined with online UV and organic carbon detectors (UV-OCD) (Huber et al. 2011). These detectors allow for characterization of both UV-absorbing (aromatic and double bond compounds) and all other non-UV-absorbing NOM fractions. Specifically, NOM can be fractionated into biopolymers, building blocks, low molecular weight acids and neutrals as well as hydrophobic organic carbon (Chon et al. 2013, Huber et al. 2011). An example chromatogram showing each fraction is shown in Figure 2.7. From the measured fractions, HPSEC can provide information about the origin and relative removal of NOM fractions during water treatment. For example, microbially impacted waters would lead to higher biopolymer fractions, and oxidized NOM can result in decreased humic fractions. Using this method, Sohn et al. (2007) demonstrated that coagulation preferentially removed large-MW NOM (>1500 Da; humic acids) compared to small-MW NOM (<1500 Da) fractions. This is consistent with the results of other studies, with a much better removal across all MW fractions using coagulation with MIEX pretreatment (Allpike et al. 2005, Matilainen et al. 2002). Ozonation also showed reduction of larger-MW NOM (>3000 Da), while the subsequent biofiltration process removes the small- and intermediate-MW NOM (Sohn et al. 2007).

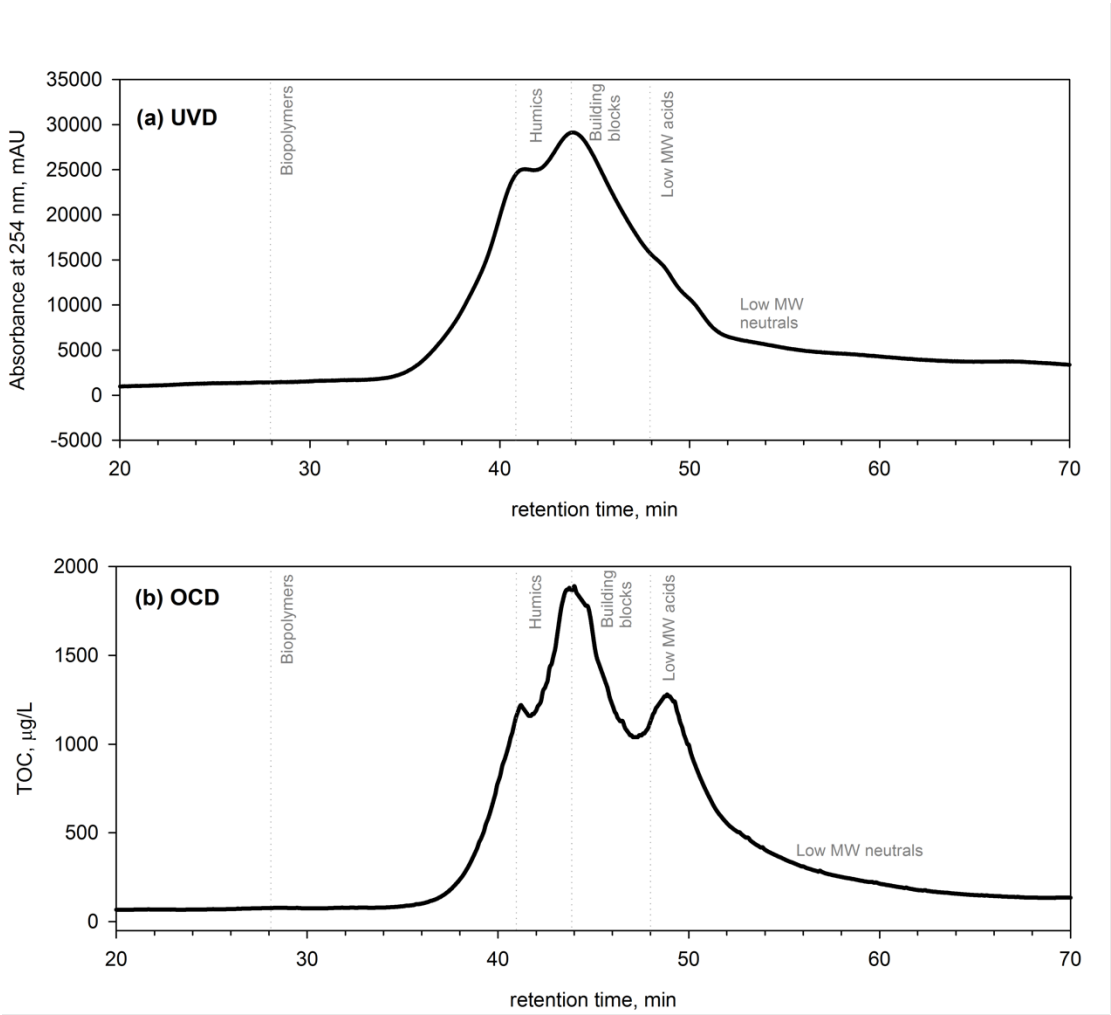

Figure 2.7. HPSEC-UV-OCD chromatogram of a settled water in SEQ

2.3. Disinfection byproducts (DBPs)

The reaction of NOM with disinfectants like chlorine could result in formation of disinfection byproducts (DBPs) (Rook 1974). DBPs became a concern to water utilities because many epidemiological studies associate lifetime exposure to these compounds with hazardous human health outcomes (Hrudey and Fawell 2015, Plewa and Wagner 2015, Richardson et al. 2007). Researchers worldwide have consistently found increased risk of bladder cancer to populations exposed to DBPs mainly through drinking water supplies (Cantor 2010, Hrudey 2009, Michaud et al. 2007, Villanueva et al. 2007). The said association was confirmed using case-control (measure of disease occurrence and reconstruction of exposure histories) (Bove et al. 2007b), cohort (measure of disease development after DBP exposure) (Doyle et al. 1997), and pooled analyses (combination of data from other studies) (Villanueva et al. 2004), among others. The statistically significant association of bladder cancer with human exposure to DBPs (mainly THMs) (e.g., odds ratio > 1) was confirmed in critical reviews of several case-control and cohort studies by Hrudey (2009) and Hrudey et al. (2015). In the US, such

relationship could mean that annually, 2–17% of new bladder cancer cases (Odom et al. 1999) can be attributed to THM exposure (i.e., 1580 – 13440 cases per year based on the 2017 estimate (ACS 2017)). Exposure to DBPs could occur not only via ingestion of drinking water but also through inhalation and dermal absorption during showering, bathing, and swimming in pools (Villanueva et al. 2007). Some studies also suggested that genetic factors play an important role in the susceptibility to bladder cancer with DBP exposure (Cantor et al. 2006). Evidence for other types of DBP-related cancers and human health effects (i.e., reproductive toxicity and developmental effects) remained inconclusive because of varying findings in the literature, mostly showing only marginal significant relationship (Hrudey 2009). For example, previous studies found associations between THM exposure and increased risk of adverse reproductive and developmental outcomes such as low birth weight, birth defects, spontaneous abortion, and stillbirth (Dodds et al. 2004, Grazuleviciene et al. 2013, Levallois et al. 2012). This association, however, did not apply for HAAs (after adjustment for THMs) and stillbirth risks in a case-control study by King et al. (2005). Further, by using a multigenerational reproductive toxicity rat bioassay, Narotsky et al. (2015) showed that a mixture of regulated THMs and HAAs (i.e., at levels of up to 2000 times their maximum contaminant levels) had no adverse effects on fertility, pregnancy maintenance, pre- and postnatal survival, or birth weights. There were also studies on DBPs and colorectal cancers. King et al. (2000) found that men exposed to chlorinated surface waters for 35–40 years had increased risk of colon cancer compared with those exposed for <10 years. This was also in agreement with the study of Rahman et al. (2014) which, in addition to a positive association, showed higher colon cancer risk in men exposed to bromoform in waters from New South Wales, Australia. Hildesheim et al. (1998), on the other hand, reported no important increase in colon cancer risk associated with THM exposure. For rectal cancer, some researchers found that exposure to DBPs is likely related with the disease (Bove et al. 2007a, Hildesheim et al. 1998), with a higher risk at higher bromoform levels in water (Bove et al. 2007a). In contrast, King et al. (2000) observed no relationship between rectal cancer risk and THMs in Canadian public water supplies.

The possible link between DBPs and human health effects, as mentioned above, resulted in establishment of regulations or guidelines (Table 2.2). These regulations led the water treatment industry to consider using alternative disinfectants other than chlorine (e.g., chloramine, chlorine dioxide, ozone). These alternative chemicals, however, were also reported to form their own suite of DBPs such as those shown in Table 2.3 (von Gunten and Ramseier 2010). To complement the shift to alternative chemicals, water operators utilize physical (filtration) and/or chemical (oxidation) barriers to remove or minimize precursors of DBPs prior to final disinfection. In this way, lower DBP formation can be expected. An example application of such approach is the use of combined ozonation and biofiltration to efficiently remove NOM and inactivate its oxidation sites before chlorine is added for

residual purposes during distribution (Figure 2.1). To better understand how to control DBP formation, particularly trihalomethanes, haloacetic acids and other nitrogen-containing DBPs (for the structures, see Table 2.4), mechanisms of their formation from known precursor compounds are presented in the following sections. Knowing such mechanisms could be important in developing removal strategies for DBP precursors. Since chlorine remains the most commonly used disinfectant, especially in SEQ, DBP formation discussed in the succeeding parts focuses on chlorination DBPs.

Table 2.2. DBP regulations or guideline values for Australia, the United States, World Health Organization and European Union (Farré and Knight 2012)

	Current regulation or guideline value (µg/L)			
DBP	ADWG	U.S. EPA	WHO	EU
Bromate	20	10	10	10
Bromoacetic acid		60 as HAA5[b]		
Bromodichloromethane	250 as THM4[a]	80 as THM4	60	100 as THM4
Bromoform	250 as THM4	80 as THM4	100	100 as THM4
Chlorate			700	
Chloroform	250 as THM4	80 as THM4	300	100 as THM4
Chlorite	800	1000	700	
Chloroacetic acid	150	60 as HAA5		
Dibromochloromethane	250 as THM4	80 as THM4	100	100 as THM4
Dichloroacetic acid	100	60 as HAA5	50[c]	
Trichloroacetic acid	100	60 as HAA5		
Dichloroacetonitrile			20[d]	
Dibromoacetic acid		60 as HAA5		
Dibromoacetonitrile			70	
N-nitrosodimethylamine	0.1		0.1	
Chloral hydrate (trichloroacetaldehyde)	20		10	
Cyanogen chloride (as cyanide)	80		[e]	
Formaldehyde	500			

[a]THM4 = sum of chloroform, bromodichloromethane, dibromochloromethane and bromoform
[b]HAA5 = sum of chloro-, dichloro-, trichloro-, bromo- and dibromo-acetic acid
[c]Provisional guideline value, based on technical achievability
[d]Provisional guideline value, due to limitations of toxicological database
[e]Guideline value for cyanogen chloride in 3rd edition was 70 µg/L (WHO 2006), no guideline value set in 4th edition because its occurrence in drinking water determined to be below levels of health concern.

Table 2.3. Example DBPs formed with different oxidants (obtained from von Gunten and Ramseier (2010))

Oxidant	DBPs
Chlorine	Trihalomethanes, haloacetic acids, haloacetonitriles, haloketones, haloaldehydes, trihalonitromethanes
Chloramine	Nitrosamines, cyanogen halides, iodinated THMs, haloacetaldehyde
Chlorine dioxide	Chlorite, chlorate, organic acids
Ozone	Bromate, bromoform, aldehydes, aldoketoacids, carboxylic acids, *N*-nitrosodimethylamine

Table 2.4. DBPs considered in this PhD thesis

DBP group	Structure	Example species
Trihalomethanes (THMs)	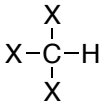	Trichloromethane (TCM) Bromodichloromethane (BDCM) Dibromochloromethane (DBCM) Tribromomethane (TBM)
Haloacetic acids (HAAs)	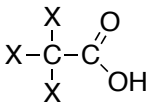	Monochloroacetic acid (MCAA) Dichloroacetic acid (DCAA) Trichloroacetic acid (TCAA) Monobromoacetic acid (MBAA) Dibromoacetic acid (DBAA)
Haloaldehydes (HAs)	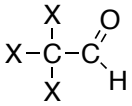	Chloral hydrate (CH)
Haloketones (HKs)	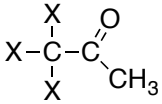	1,1-Dichloropropanone (DCP) 1,1,1-Trichloropropanone (TCP)
Haloacetonitriles (HANs)	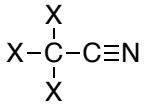	Trichloroacetonitrile (TCAN) Dichloroacetonitrile (DCAN) Bromochloroacetonitrile (BCAN) Dibromoacetonitrile (DBAN)
Halonitromethanes (HNMs)	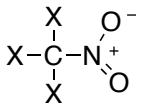	Trichloronitromethane (TCNM) Tribromonitromethane (TBNM)
Haloacetamides (HAMs)	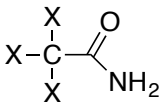	Trichloroacetamide (TCAM) Bromodichloroacetamide (BDCAM) Dibromochloroacetamide (DBCAM)

X = Cl, Br, I, or H. These compounds could be measured using liquid-liquid extraction followed by gas chromatography and via other analytical methods (Weinberg 1999, 2009).

2.3.1. DBP formation mechanisms

As shown in Figure 2.8, halogenated DBPs can be formed from the reaction of chlorine (e.g., HOCl) with NOM and halides (e.g., bromide and iodide). In this process, HOCl can transform bromide and iodide to hypobromous (HOBr) and hypoiodous acids (HOI), which in the presence of NOM induce substitution reactions for formation of brominated and iodinated DBPs in addition to the chlorinated species (Allard et al. 2015, Hua et al. 2006). Once formed, HOBr plays an important role in DBP speciation because of competition reactions with HOCl. It has been reported that compared to HOCl, HOBr generally reacts faster with NOM (Westerhoff et al. 2004), with the hydrophilic NOM fraction being more amenable to HOBr reactions (Hua and Reckhow 2013). For phenolic moieties, second-order rate constants with bromine were found to be about 3 orders of magnitude higher than that of chlorine (Heeb et al. 2014).

NOM concentrations also affect the contribution of HOCl, HOBr, and HOI in DBP speciation. For example, at low NOM concentrations (or low SUVA), HOBr and HOI reactions would dominate, forming brominated NOM moieties and Br-/I-THMs (Allard et al. 2015). For waters with high NOM concentrations (or high SUVA), formation of Cl-/I-THMs are more favored because HOCl reactions with NOM is preferred over HOCl reactions with bromide to HOBr (Allard et al. 2015).

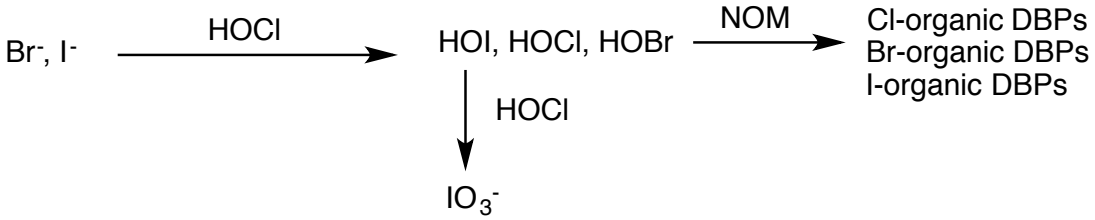

Figure 2.8. General scheme of the reaction of inorganic and organic DBP precursors with chlorine (Gruchlik et al. 2014).

Other than the presence of halide ions, water quality and reaction conditions such as chlorine dose and contact time, pH, temperature, ammonia concentration, type and concentration of NOM are also significant factors in DBP formation (Bond et al. 2012, Bond et al. 2011b, Hua and Reckhow 2008, Xie 2004). When chlorine dose is increased, the formation of THMs, HAAs, and several other chlorinated DBPs also increased (Hua and Reckhow 2008). Extending the chlorine contact time could also increase the formation of DBPs considered as end-products (e.g., THMs and HAAs) while decreasing the formation of DBPs serving as intermediates of other compounds (e.g., DCAN) (Glezer et al. 1999, Hua and Reckhow 2008). DBP formation (e.g., THMs, HAAs) was also found to increase with increasing temperature due to faster reaction rates, although some DBPs (e.g., HKs) may also degrade faster at higher temperature (Hua and Reckhow 2008). In addition, a higher pH promotes

hydrolysis reactions (i.e., to form more THMs), increases the fraction of chlorine as OCl^- ($pK_{HOCl,\ 25^oC}$ = 7.54), and makes NOM moieties (e.g., phenols, amines) more reactive towards oxidants (Deborde and von Gunten 2008). Ammonia could also affect DBP formation due to its reaction with chlorine to chloramine (Diehl et al. 2000, Hua and Reckhow 2008) which is a less reactive oxidant. More importantly, increasing NOM levels increases the chlorine demand (i.e., Cl_2 dose minus Cl_2 residual) and DBP concentrations due to high precursor levels (Krasner et al. 1994). Different NOM fractions also result in different DBP yields, with the hydrophobic fraction causing higher total DBP concentrations (Bond et al. 2009b, Kitis et al. 2002, Reckhow et al. 1990).

Key functional groups in NOM were found to be responsible for the high yields of DBPs. These include *m*-dihydroxybenzenes (e.g., orcinol), β-diketone (e.g., acetylacetone), β-diketoacid (e.g., 3-oxopropanoic acid), and amino acids (e.g., aspartic acid). The reactions of chlorine with these moieties are discussed in the following sections. Note that these reactions are presented with HOCl as the oxidant. If bromide and iodide are present during chlorination, a mix of Cl-/Br-/I-DBPs can be expected.

2.3.1.1. Trihalomethane (THM) formation

Fast-reacting THM precursors include compounds containing β-diketone and β-diketoacid moieties (Gallard and von Gunten 2002). The reaction of chlorine with these carbonyl-containing compounds occurs via substitution reactions on the α-carbon to the carbonyl group, consequently producing chloroform (i.e., haloform reaction) (Deborde and von Gunten 2008). Electron-withdrawing moieties at the acetyl's carbonyl group make the hydrogen atoms of the α-carbon more acidic, further promoting chlorine substitution. This was well observed for β-diketones like acetylacetone (Figure 2.9a).

m-Dihydroxybenzene structures (e.g., resorcinol) have also been considered as fast-reacting THM precursors (Gallard and von Gunten 2002). For the case of orcinol (Figure 2.9b), the doubly activated carbon atom (i.e., carbon ortho to both hydroxyl substituents) is considered to be the main site of attack for chlorine followed by a series of hydrolysis and decarboxylation reactions, eventually leading to chloroform formation. In addition, slow reacting THM precursors, in the form of phenolic compounds, were also observed (Gallard and von Gunten 2002). The different rates of THM formation are hypothesized to be caused by the varying reactivity of intermediates formed during chlorination. While monohydroxy benzenes lead to chlorinated keto-intermediates, polyhydroxy aromatic precursors can generate polyketones and keto-carboxylic acids which have high reactivity with chlorine, resulting in higher THM yields (Deborde and von Gunten 2008).

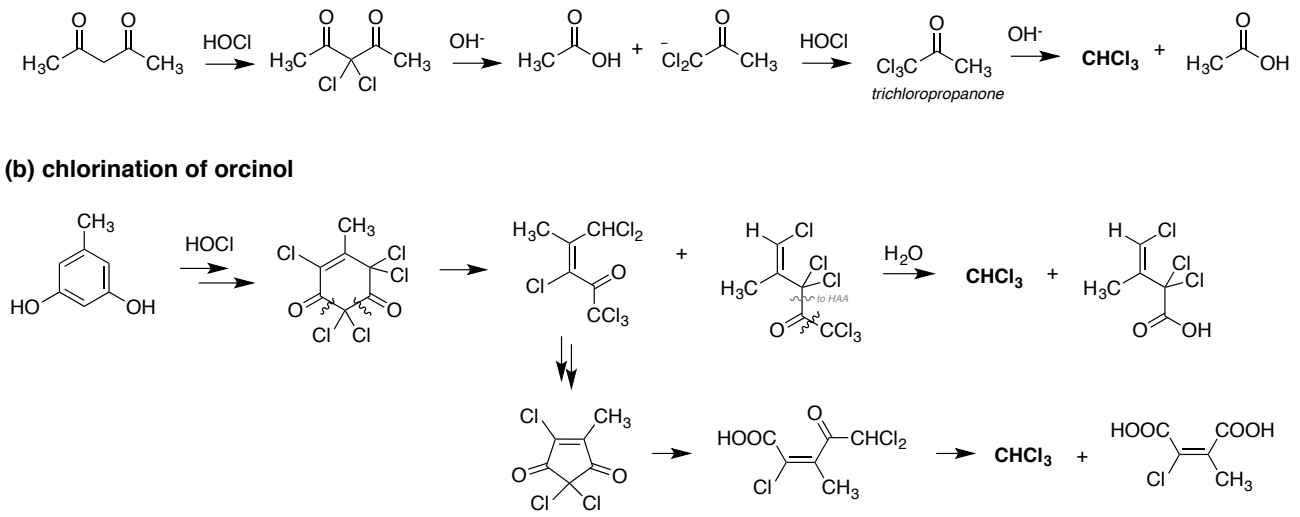

Figure 2.9. Chloroform formation: reaction of chlorine with (a) acetylacetone (Deborde and von Gunten 2008) and (b) orcinol (Tretyakova et al. 1994)

Other DBPs such as haloketones and haloaldehydes can also form through the presented mechanisms. Aldehydes and ketones, which are commonly formed from oxidation of NOM, can react with HOCl at the α-carbon to the carbonyl group, subsequently forming haloaldehydes (e.g., chloral hydrate) and haloketones (e.g., trichloropropanone in Figure 2.9a).

2.3.1.2. Haloacetic acid (HAA) formation

The formation of haloacetic acids (HAAs) proceeds through initial chlorine substitution at the α-carbon to a carbonyl group. High HAA yields were reported for chlorination of β-dicarbonyl species (e.g., β-diketoacids) (Bond et al. 2012, Dickenson et al. 2008). Similar to THM formation, the electron-withdrawing effect of the carbonyl group makes the hydrogen atoms of the α-carbon more acidic, and hence more reactive towards chlorine. As an example, Figure 2.10 shows the formation of dichloroacetic acid (DCAA) from chlorination of 3-oxopropanoic acid.

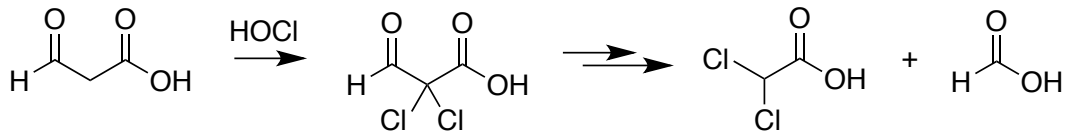

Figure 2.10. Dichloroacetic acid formation: reaction of chlorine with 3-oxopropanoic acid (Bond et al. 2012)

Trihaloacetic and dihaloacetic acids were also proposed to come from NOM with different properties. Comparing various NOM isolates, Hua and Reckhow (2007a) showed that trihaloacetic acids had higher yields with hydrophobic NOM fractions, while dihaloacetic acids had higher yields with hydrophilic NOM fractions (<0.5 kDa).

2.3.1.3. Nitrogenous DBP formation

Due to the oxidant demand of DON in water (e.g., algal and wastewater-impacted waters), nitrogenous DBPs (N-DBPs) could also be formed apart from the carbon-based DBPs (C-DBPs) like THMs and HAAs. Although N-DBP concentrations are lower than C-DBPs, increasing concerns on N-DBP formation arise because of its higher toxicity compared to C-DBPs (Plewa et al. 2008, Stalter et al. 2016a). Halonitromethanes (HNMs), haloacetonitriles (HANs), and haloacetamides (HAMs) are among the most frequently detected N-DBPs in drinking water. These can be formed from chlorination of amines and amino acid moieties of NOM, as shown below.

2.3.1.3.1. Halonitromethane (HNM)

Trichloronitromethane (also known as chloropicrin) is a commonly measured halonitromethane in disinfected waters. Using monomethylamine as a model compound (Figure 2.11), Joo and Mitch (2007) proposed that trichloronitromethanes can be formed via oxidation of dichlorinated amines and sequential chlorination of the nitronate anion. With increasing chlorine substitution, faster addition of chlorine occurs due to the increased acidity of halonitroalkanes, as a result of the electron-withdrawing chlorines.

Trichloronitromethane is also a main concern with treatment plants utilizing O_3/HOCl (Hoigné and Bader 1988). With ozone, halogen reactive nitroalkyl intermediates (e.g., nitroethanol, nitromethane) can be formed resulting in high yields of trichloronitromethane during chlorination (McCurry et al. 2016). For example, glycine was shown to have 22.5% trichloronitromethane yield with O_3/HOCl treatment (McCurry et al. 2016).

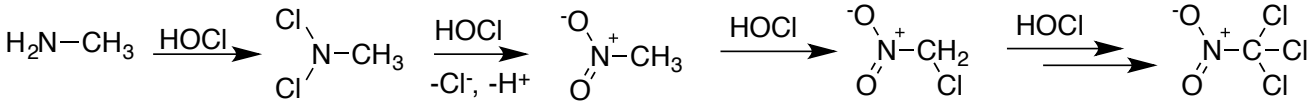

Figure 2.11. Trichloronitromethane formation: reaction of chlorine with monomethylamine (Joo and Mitch 2007)

2.3.1.3.2. Haloacetonitrile (HAN) and haloacetamide (HAM)

Haloacetamides were reported as hydrolysis products of haloacetonitriles. Using aspartic acid as an example precursor (Figure 2.12), chlorine quickly reacts with the amine-*N* (especially at Cl:N >2) to initially form *N*-haloamino acid (Deborde and von Gunten 2008) which undergoes decarboxylation leading to 2-cyanoethanoic acid (Shah and Mitch 2012). The presence of the electron-withdrawing cyano and carboxylic moieties promote successive chlorination of the central carbon atom. Decarboxylation follows forming dichloroacetonitrile (DCAN) and trichloroacetonitrile (TCAN), with further chlorination. Hydrolysis of haloacetonitriles forms their corresponding haloacetamides (e.g., dichloroacetamide (DCAM) and trichloroacetamide (TCAM)) which can further hydrolyze into haloacetic acids (Reckhow et al. 2001). Other than being hydrolysis products of HANs, HAMs can also be formed independently from specific precursors. This was demonstrated in a previous study where chlorination of wastewater effluents and algal extracellular polymeric substances produced more DCAN, while chlorination of humic materials produced more DCAM (Huang et al. 2012).

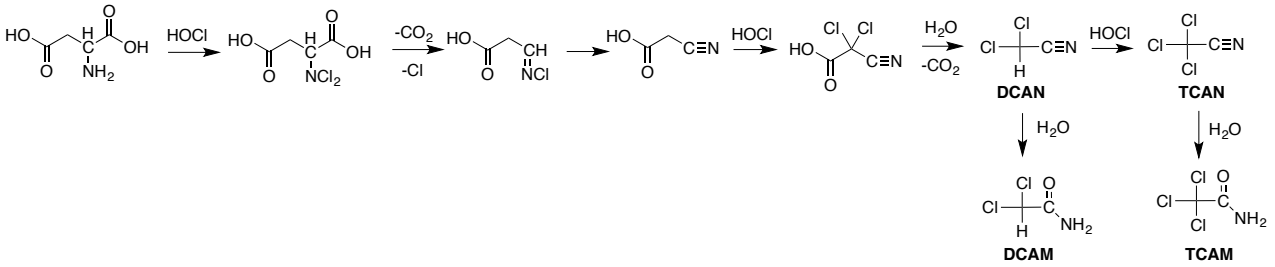

Figure 2.12. Haloacetonitrile and haloacetamide formation: reaction of chlorine with aspartic acid (Shah and Mitch 2012)

2.3.1.4. Adsorbable organic halogen (AOX)

Measurement of adsorbable organic halogens (AOX), also known as total organic halogens (TOX), can provide an estimate of the level of DBP formation in chlorinated waters. This is useful since current analytical and extraction methods for DBPs are somewhat limited to thermally and chemically stable, volatile or semi-volatile, neutral organic halogens (e.g., DBPs mentioned in previous section) (Weinberg 1999). Current AOX determination involves adsorption of DBPs on activated carbon, followed by combustion, and subsequent halide measurement by ion chromatography (Hua 2006). The resulting chloride, bromide, and iodide ions correspond to the adsorbable organic chlorine (AOCl), adsorbable organic bromine (AOBr), and adsorbable organic iodine (AOI), respectively. Although this method does not capture all volatile DBPs and other non-halogenated DBPs, it can provide a general idea on the levels of DBPs produced from chlorine-based disinfectants. A mass balance of the halogen component of the identified DBPs compared with the AOX revealed that a large fraction of the

halogenated DBPs remains uncharacterized (i.e, unknown AOX = measured AOX minus the sum of known individual DBPs) (Krasner et al. 2006, Richardson 2003, Weinberg 1999). These unknown compounds, which could have toxicological relevance, are thought to be non-volatile and/or polar and are therefore unextractable using traditional liquid-liquid extraction and GC methods (Weinberg 1999). In a study of 12 WTPs in the U.S., unknown AOX ranged from 10 – 66% with THMs and HAAs accounting for the majority of the known AOX (Krasner et al. 2006). To investigate the source of the unknown AOX, Hua and Reckhow (2007b) evaluated AOX formation from NOM fractions isolated using XAD resins and ultrafiltration membranes. The authors found that unknown AOX from chlorination are predominantly attributed to hydrophobic and/or high MW NOM (e.g., >0.5 kDa). In that study, unknown AOX yields of hydrophilic NOM were only at 1–20% of those from hydrophobic NOM. The ratio of unknown to known AOX of chlorinated hydrophobic and high MW fractions ranged from 40–60%, which further increased when chloramination was used instead of chlorination (Hua and Reckhow 2007b). For SEQ waters, the levels of unknown DBPs were comparable to these previous studies. Unknown AOX of 14.5 – 62% (Figure 2.13a) were found in a survey of 10 water samples, with THMs and HAAs also comprising most of the known DBPs (Figure 2.13b) (Farré et al. 2016b). In this study, chlorine contact time was found to be a key factor in the resulting AOX concentrations. Compared to AOX measured at WTP outlets (AOX_o), AOX concentrations could increase by up to 170% after 24 h of contact time (AOX_{24h}), which was also confirmed using water samples (i.e., non-chlorinated) subjected to lab-scale 24 h AOX formation potential tests (AOX_{FP}) (Figure 2.13a). In terms of treatment, coagulation was found to effectively remove 67% of the AOX_{FP} across the WTPs (Farré et al. 2016b).

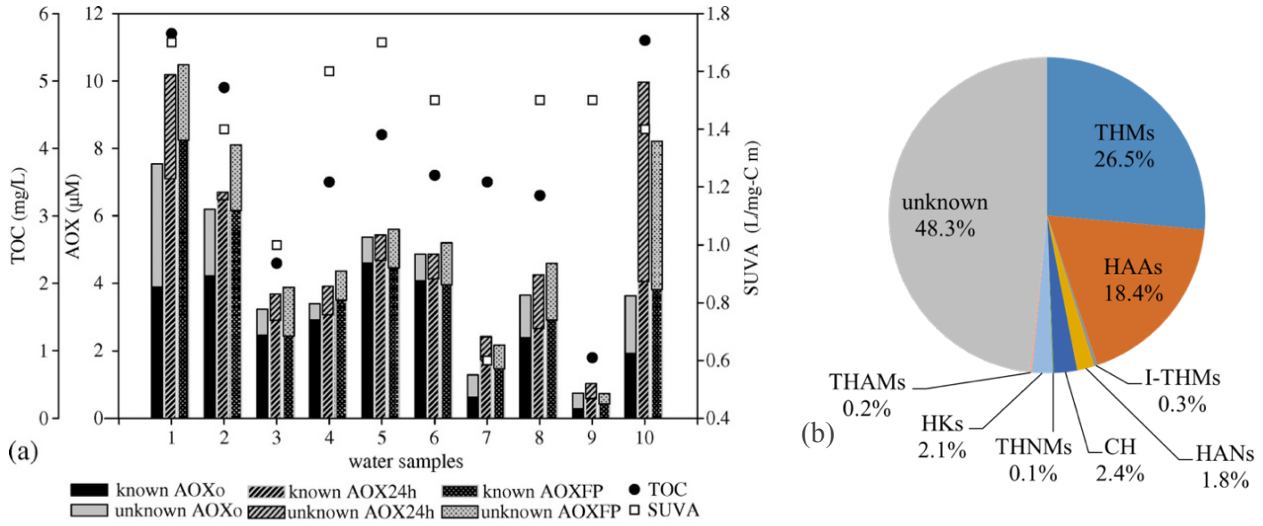

Figure 2.13. (a) Known versus unknown AOX in SEQ water samples, (b) Example %AOX accounted for by individually measured DBPs (Farré et al. 2016b).

2.4. Bioassays for DBP studies

Previous studies on the biological effects of DBPs have indicated some general trends (Figure 2.14). By examining genomic DNA damage in Chinese hamster ovary cells, Plewa et al. (2008) showed that the relative genotoxic activities of different DBP classes decreased as follows: HNMs>HAMs>HANs>HAAs >THMs. From the results of 18 DBPs with matched halogen analogues, it was further observed that the order of toxicity relative to type of halogen atom is iodinated >> brominated >> chlorinated DBPs. That study also compared 26 carbon-based DBPs and 29 nitrogenous DBPs (N-DBPs) and found that N-DBPs are the most toxic among all DBPs investigated. These trends were also consistent with the recent study by Stalter et al. (2016a) wherein a set of cell-based *in vitro* bioassays was used to assess molecular mechanisms of reactive toxicity of 50 different DBP species. These bioassays were based on the specific modes of actions in presence of DBPs including various molecular events (e.g., interactions with DNA, proteins/peptides, and membrane lipids) initiating a series of effects like gene damage, disruption of redox balance, and enzyme inhibition (Stalter et al. 2016a). These effects can then activate a multitude of subsequent adaptive stress responses such as oxidative stress response, p53-mediated response (DNA repair), and inflammation, among others (Stalter et al. 2016a). The results of these effect-driven bioassays suggest that the genotoxic effect of DBPs could occur indirectly through oxidative stress induction and/or enzyme inhibition than direct DNA damage. Some of the bioassays used in that study are shown in Table 2.5.

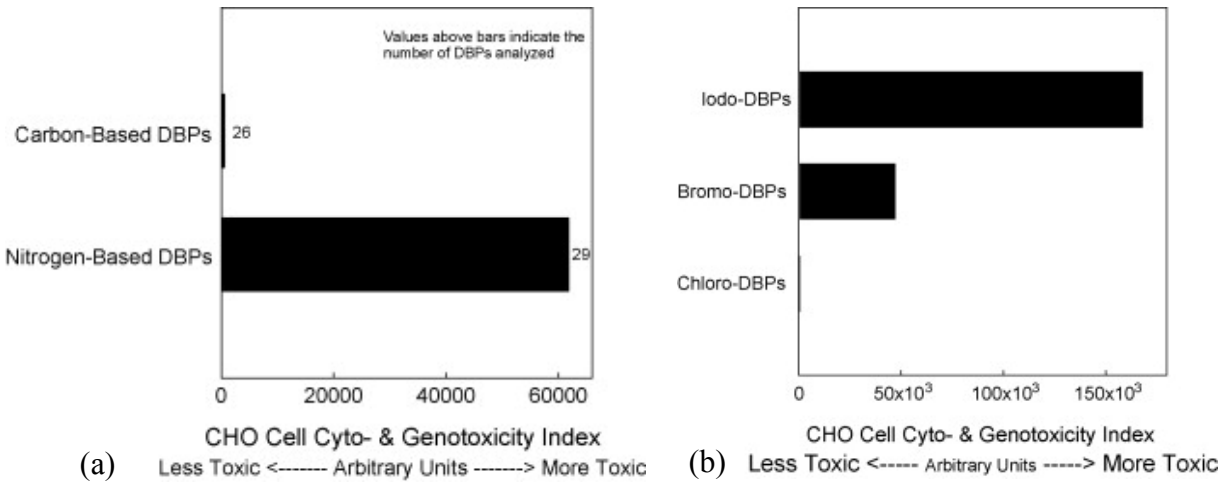

Figure 2.14. Combined toxicity index values for (a) carbonaceous DBPs (C-DBPs) and nitrogenous DBPs (N-DBPs), and (b) iodo-, bromo-, and chloro-DBPs (reprinted from Richardson et al. (2007), with permission)

Table 2.5. Example bioassays for the effect fingerprinting of DBPs (adapted from Stalter et al. (2016a), with permission)

Bioassay	Test species (strain/cell line)	Endpoint	Signal
Microtox	*Aliivibrio fischeri*	Cytotoxicity	Bioluminescence as indicator for cell viability
umuC assay	*Salmonella typhimurium* (TA1535/pSK1002)	Activation of SOS-response	Optical density at 420 nm as marker for conversion of substrate by the reporter enzyme
AREc32	AREc32 cell line, based on human breast cancer cell line MCF7	Activation of the oxidative stress response pathway NRf2-ARE	Bioluminescence as indicator of the reporter enzyme luciferase
p53-bla	p53RE-bla HCT-116 cell line, based on human colon carcinoma cell line HCT-116	Activation of the tumor suppressor protein p53	Ratio of blue (450 nm) to green fluorescence emission (520 nm) at 405 nm excitation as indicator of the reporter enzyme β-lactamase

2.5. Reduction of DBP formation potentials in water treatment

The most practical approach in minimizing DBP formation involves reduction of DBP precursors prior to chlorination. Precursor removal can be achieved using the treatment processes discussed earlier (Section 2.2) which mainly involves coagulation, filtration, and oxidation. The performance of these processes could be variable depending on the water quality and treatment conditions. As reviewed by Bond et al. (2011a), coagulation could be an effective process to remove humic components of NOM, and consequently the DBPs coming from this fraction. These DBPs include HAAs whose precursors were shown to be more amenable to coagulation due to their higher aromatic content (Liang and Singer 2003). The remaining humics (i.e., hydrophobic) can be removed by activated carbon via adsorption which is supported by a moderate correlation between $\log K_{ow}$ (octanol-water partition coefficient; measure of hydrophobicity) and Freundlich parameters (measure of adsorbability) (Bond et al. 2011a). Anion exchange resins can also be used to remove DBP precursors originating from transphilic fractions with high carboxylic acid functionality and charge density (Boyer et al. 2008). Ozonation and AOPs can also be utilized to oxidize DBP precursors, although specific DBPs can still increase due to DBP-forming oxidation products (e.g., aldehydes, ketones) (Kleiser and Frimmel 2000). Hydrophilic DBP precursors like amino acids were found to be reduced well during biological treatment and nanofiltration (Bond et al. 2011a).

In our earlier work, we compared the performance of conventional and advanced WTPs in SEQ (Figure 2.2, Section 2.2). It was shown that WTPs using combined ozonation and BAC filtration results in better DOC reductions. As a result, it is expected that the overall DBP formation potentials in the product water of advanced WTPs would be lower than those obtained from conventional WTPs as shown in Table 2.6. The higher reductions in TOC, TON, and DBP formation potentials were a result of more efficient oxidation and breakdown of NOM by ozone followed by consumption of biodegradable compounds by BAC. To gain a better understanding of these processes, the fundamentals of ozonation and biofiltration are discussed in the following sections.

Table 2.6. Comparison of average TOC (mg C/L) and TON (mg N/L) in final waters and DBP concentrations (µg/L) in finished waters at advanced versus conventional in SEQ (Farré et al. 2016a)

Parameter	Conventional (n=13)	Advanced (n=8)
TOC	4.6	2.3
TON	0.19	0.09
Trihalomethanes	105.9	65.1
Haloacetic acids	71.8	13.5
Iodinated THMs	3.2	0.4
Haloacetonitriles	8.0	2.2
Chloral hydrate	6.5	1.4
Trichloronitromethane	0.3	0.1
Tribromonitromethane	0.2	0.1
1,1-Dichloropropanone	0.8	0.3
1,1,1-Trichloropropanone	4.2	1.3
Haloacetamides	1.3	0.1
AOCl	175	67
AOBr	50	27
AOI	2.3	0.7

2.6. Ozonation

Ozone (O_3) is a strong oxidant and disinfectant. In water treatment plants, it is generated on-site (von Gunten 2007) from air or pure oxygen electrochemically or by corona discharge and introduced into the water through diffusers, Venturi systems, or by static mixers (von Gunten 2007). It is commonly applied for pre-oxidation (before coagulation) and intermediate oxidation (after sedimentation).

Compared to chlorine, ozone can inactivate microorganisms at lower exposures (CT value or the time-integrated concentration of the oxidant). For example, in order to obtain a 99% inactivation of *G. lamblia* cysts (pH 6–7), a chlorine exposure of 47 – 150 mg·min/L is needed, whereas same inactivation can be attained by ozone at an exposure of 0.5 – 0.6 mg·min/L (Langlais et al. 1991). It also reacts quickly with various inorganic (e.g., Mn(II), Fe(II), cyanide) compounds via oxygen-transfer reactions. For organic compounds (e.g., taste and odor pollutants, pharmaceuticals, fuel additives, pesticides, algal products), ozone selectively oxidizes the double bonds, activated aromatic systems, and deprotonated amines (von Sonntag and von Gunten 2012) consequently forming various transformation products (for reaction mechanisms, see below).

Unlike other oxidants in aqueous solutions, ozone can also decompose into hydroxyl radicals (•OH) via a series of chain reactions. This •OH yield could be useful in transforming ozone-recalcitrant compounds through non-selective reactions with second-order rate constants of $>10^9$ $M^{-1}s^{-1}$ (Buxton et al. 1988). However, deliberate production of •OH radicals (i.e., by promoting ozone decay) can minimize disinfection efficiency which is more influenced by ozone (von Gunten 2003a). Hence, characterization of the ozonation process is essential in determining optimum treatment conditions.

2.6.1. Characterization of the ozonation process

The stability of ozone during water treatment is affected by various factors. Waters with high NOM concentrations cause a faster ozone decay due to NOM's abundant reaction sites. The degree of •OH scavenging of the water matrix is also an important consideration (von Sonntag and von Gunten 2012). In the presence of •OH inhibitors (e.g., carbonate/bicarbonate), ozone exposure would be higher (i.e., slow ozone decay) while in the presence of •OH promoters like OH^- (i.e., at high pH) and H_2O_2, ozone exposure would be lower (i.e., fast ozone decay). In surface waters and wastewaters, ozone decomposition involves 2 phases: (1) instantaneous decay phase (<20 sec), and (2) slow decay phase which occurs in minutes range, following an empirical first-order rate law (Buffle et al. 2006).

During oxidation, the contribution of ozone and •OH radicals can be described using equation 2.1 (Elovitz and von Gunten 1999):

$$-\frac{d[P]}{dt} = k_{P,O_3}[O_3][P] + k_{P,\bullet OH}[\bullet\,OH][P] \qquad \text{(eq. 2.1)}$$

where k_{P,O_3} and $k_{P,\bullet OH}$ correspond to second-order rate constants for the reaction of pollutant, P, with ozone and •OH, respectively. [O_3] and [•OH] are ozone and •OH concentrations. Integration of equation 2.1 gives the following form:

$$-ln\frac{[P]}{[P]_0} = k_{P,O_3}\int[O_3]dt + k_{P,\bullet OH}\int[\bullet\,OH]\,dt \qquad \text{(eq. 2.2)}$$

The terms $\int[O_3]dt$ and $\int[\bullet\,OH]\,dt$ are the exposures of ozone and ˙OH, respectively. To account for the relative contribution of ˙OH radicals and ozone on the oxidation process, the R_{ct} parameter (Elovitz and von Gunten 1999) was introduced. From equation 2.3, high R_{ct} would correspond to the conditions favoring fast ozone decay (i.e., low O_3 exposure). R_{ct}s in natural waters commonly range from 10^{-10} – 10^{-8} (von Sonntag and von Gunten 2012).

$$R_{ct} = \frac{\int[\bullet OH]dt}{\int[O_3]dt} \qquad \text{(eq. 2.3)}$$

The O_3 exposure can be calculated from the area under the O_3 decay curve (von Gunten and Hoigné 1994). Concentrations of ozone can be measured using the spectrophotometric indigo method (Bader and Hoigné 1981), which uses indigotrisulfonate, a compound that rapidly reacts with ozone (k_{app} = 9.4×10^7 $M^{-1}s^{-1}$). The decrease in absorbance at 600 nm (ε= 20,000 $M^{-1}cm^{-1}$) of the indigo solution is directly proportional to the ozone concentration (Elovitz and von Gunten 1999).

Unlike ozone, ˙OH concentrations cannot be directly measured due to its low transient concentration (<10^{-12} M). Thus, to measure ˙OH concentrations, a probe compound like *para*-chlorobenzoic acid (pCBA) can be used (Elovitz and von Gunten 1999). pCBA is unreactive with ozone but very reactive with ˙OH ($k_{pCBA,\bullet OH}$ = 5×10^9 $M^{-1}s^{-1}$). The ˙OH exposure can then be determined from the relative decrease of pCBA concentration, [pCBA].

$$ln\frac{[pCBA]}{[pCBA]_0} = -k_{pCBA,\bullet OH}\int[\bullet\,OH]dt \qquad \text{(eq. 2.4)}$$

Substituting equation 2.3 to 2.4 provides a means to experimentally determine the R_{ct} using measurements of ozone exposure and relative pCBA decrease.

$$ln\frac{[pCBA]}{[pCBA]_0} = -k_{pCBA,\bullet OH}R_{ct}\int[O_3]dt \qquad \text{(eq. 2.5)}$$

The plot of ln[pCBA]/$[pCBA]_0$ versus O_3 exposure provides a slope equals to $-k_{pCBA,\bullet OH}R_{ct}$.

2.6.2. Reactions of ozone with organic compounds

The reaction kinetics of ozone with NOM is governed by the presence of electron-rich moieties like activated aromatic systems, olefins, and amines. The known mechanisms of ozone reactions with these compounds are summarized in the following sections. The reactions presented here are based on previous extensive studies on ozone chemistry (von Sonntag and von Gunten 2012). Note that the

ozonation products could be formed along with the products of •OH reactions since typical treatment conditions do not scavenge for these radicals. Addition reactions to C-C and C-N bonds of NOM are common with •OH (von Sonntag and von Gunten 2012).

The reactions of O_3 and •OH can also be pH-dependent since electron density in a given molecule decreases during protonation (von Sonntag and von Gunten 2012). Figure 2.15 shows the second-order rate constants of O_3 and •OH with phenol, butenol (olefin), and glycine at different pH (Lee and von Gunten 2010). It can be observed that pH effects are important especially for phenols and amines. At lower pH, the high reactivity of glycine drops because the lone pair at the amine-N (i.e., ozone's reaction site) are blocked by protons. Similarly, phenol is less activated at lower pH which results in lower second-order rate constants. Thus, the degree of dissociation of compounds should be taken into account when assessing kinetics of ozonation reactions.

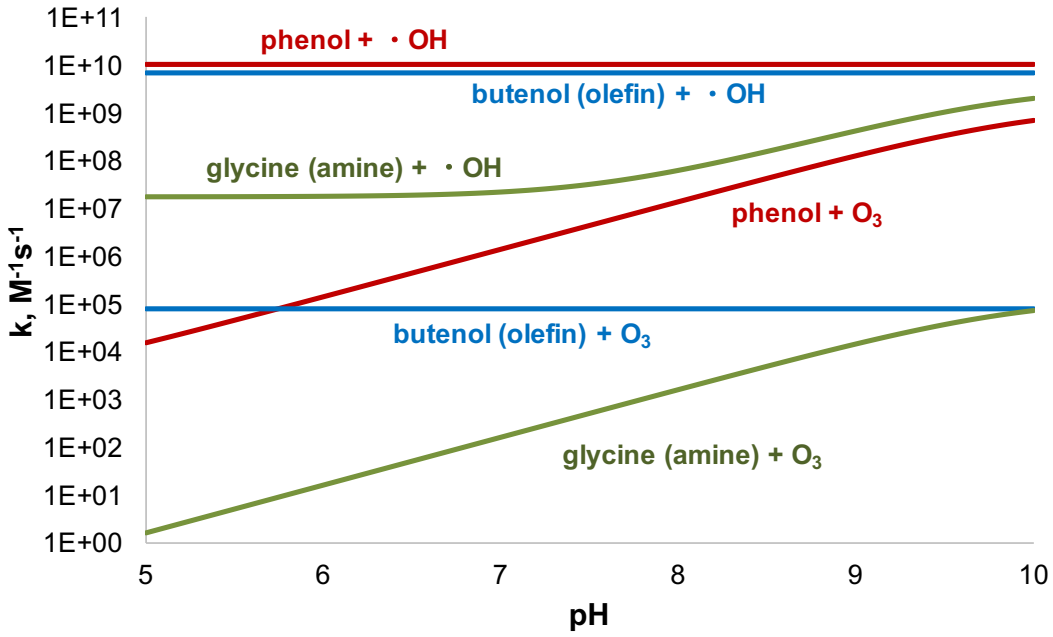

Figure 2.15. pH dependent second-order rate constants (k) for the reaction of O_3 and •OH with phenol, butenol, and glycine (adapted from Lee and von Gunten (2010))

2.6.2.1. Activated aromatics

Ozone reacts with phenols and activated aromatic systems via a transient ozone adduct which can decompose by various pathways (Figure 2.16, reactions 1–4) (von Sonntag and von Gunten 2012). By an oxygen-transfer mechanism (reaction 1), the ozone adduct can release a singlet oxygen ($^1O_2$) and rearrange into a hydroxylated-ring product. Reaction 2 involves ring-opening into muconic type compounds, which can be further oxidized into smaller carbonyl compounds like aldehydes and

carboxylic acids. These reactions can also be in competition with electron-transfer reaction which leads to an ozonide ($O_3^{\bullet-}$) and a radical cation product (reaction 3). It is also possible to form a superoxide ($O_2^{\bullet-}$) and an oxyl radical (reaction 4). Further reactions of the radical cation and phenoxyl radical result in formation of quinones or dimerized products (Lee and von Gunten 2016).

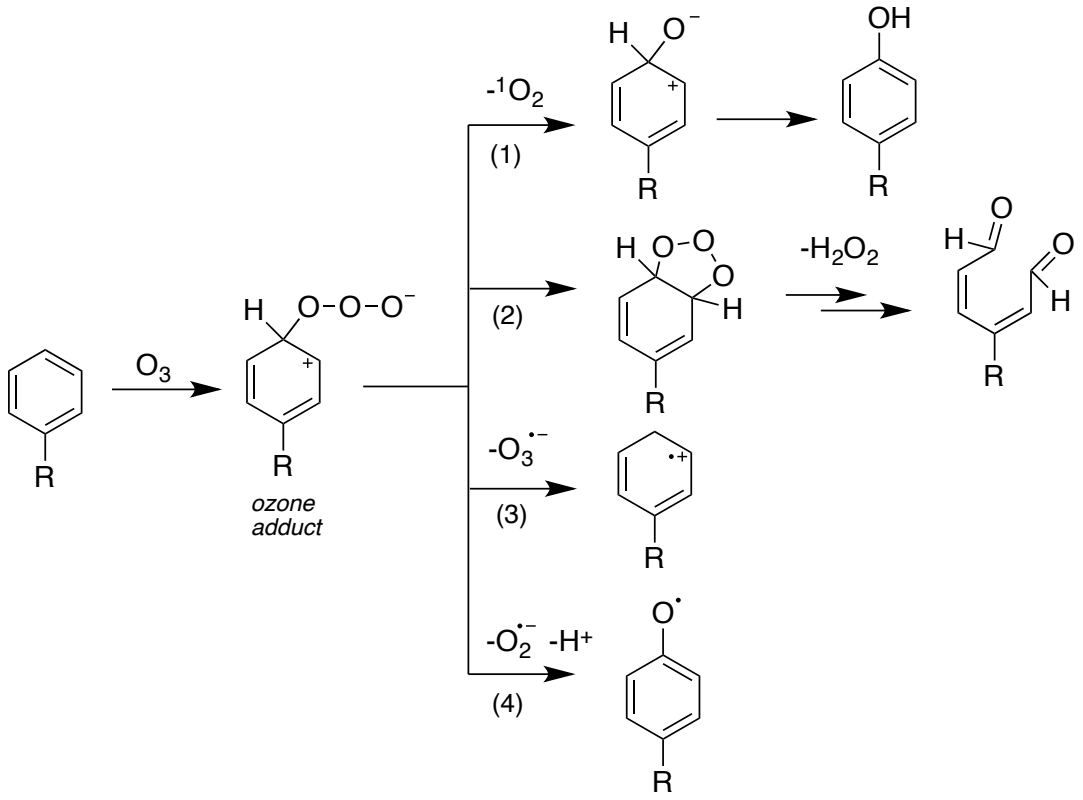

Figure 2.16. Reaction of ozone with activated aromatic compounds (adapted from von Sonntag and von Gunten (2012))

2.6.2.2. Olefins

Ozone reacts with olefins (C=C bonds) through the Criegee mechanism (Figure 2.17) (von Sonntag and von Gunten 2012). This pathway involves the formation of ozonide that decomposes into a carbonyl compound and a hydroxyhydroperoxide leading to formation of another carbonyl compound and H_2O_2. This reaction is expected to happen for ozonation of the muconic-type compounds formed from ring-opening of phenols.

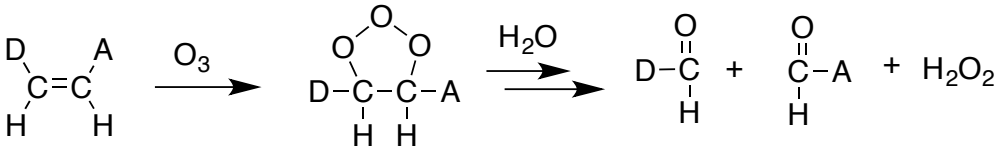

Figure 2.17. Reaction of ozone with olefins (adapted from von Sonntag and von Gunten (2012))

2.6.2.3. Amines

The reaction of ozone with amines occcur through addition to the deprotonated nitrogen moiety. Ozone reacts with the amine functional group via an adduct, leading to formation of *N*-oxides for tertiary amines (Figure 2.18, reaction 1) and to hydroxylamines for primary and secondary amines (Figure 2.18, reactions 2–3) (von Sonntag and von Gunten 2012). In competition with reaction 3 is an electron-transfer reaction that releases $O_3^{\bullet-}$ and forms *N*-centered radical (reaction 4), which can quickly rearrange to a C-centered radical (von Sonntag and von Gunten 2012). Since ozonated solutions are saturated with O_2, peroxyl radicals (R-COO$^{\bullet}$) can also be produced. This reaction is followed by the decay of peroxyl radicals into an imine after a loss of $O_2^{\bullet-}$, eventually forming a lower substituted amine and carbonyl compounds. Among the possible end-products of this process include nitrate and ammonium, as shown in some studies with amino acids (Berger et al. 1999, Le Lacheur and Glaze 1996).

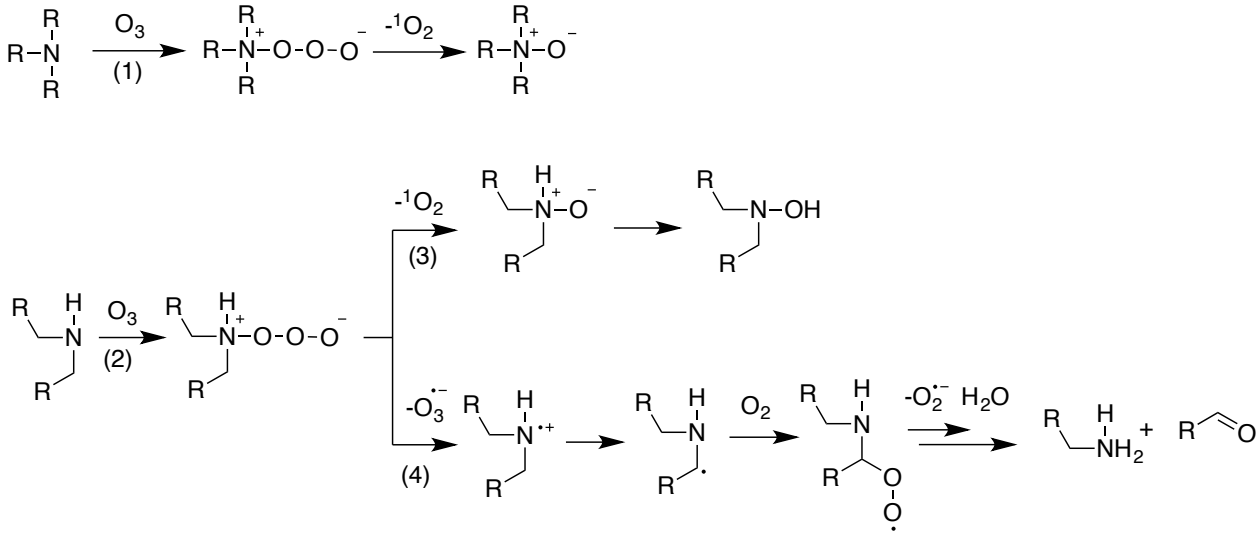

Figure 2.18. Reaction of ozone with amines (adapted from von Sonntag and von Gunten (2012))

2.6.3. Ozonation and DBP formation

In advanced drinking water treatment, ozone is not commonly used as a final disinfectant due to its short lifetime. Instead, chlorination is applied as the final step for residual purposes in the distribution network. In this approach, chlorine can react with the remaining and oxidized NOM, as well as with inorganic ions (e.g., halides) to form DBPs. It could be assumed, however, that less organic DBPs (e.g., THMs and HAAs) would form with pre-ozonation since ozone also attacks the reaction sites of chlorine. This assumption, however, needs to be investigated as oxidation products of ozone as well as $^{\bullet}$OH could also form additional DBP precursors. The effects of O_3 and $^{\bullet}$OH reactions on the overall DBP formation are not clear and are therefore worth exploring.

Table 2.7 summarizes the results of some available studies on DBP formation which used pre-ozonation and post-chlorination. As previously discussed in Section 2.3.1, HOCl can transform bromide and iodide in water to hypobromous and hypoiodous acids, which in the presence of NOM can lead to formation of organic Cl-/Br-/I-DBPs. In the presence of ozone (Figure 2.19), iodinated DBPs can be prevented since HOI can quickly transform to iodate. This would leave a mixture of Cl- and Br-DBPs. To evaluate the extent of Br-DBP formation brought about by HOBr reactions after ozonation, bromine substitution factors (BSF) can be calculated (equation 2.6) (Hua and Reckhow 2013). Apart from organic DBP formation, ozone and $^{\bullet}OH$ can also compete with NOM to form bromate (BrO_3^-) in bromide-containing waters.

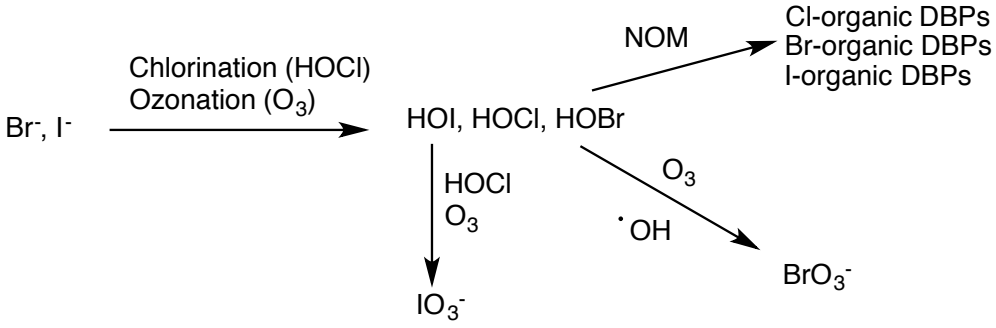

Figure 2.19. Formation of DBPs during chlorination and ozonation (adapted from Gruchlik et al. (2014))

$$BSF = \frac{\sum_{species}(\text{species molar concentration}) \times (\text{species \# Br substituents})}{\text{\#halogen substituents} \times \sum_{species}(\text{species molar concentration})} \quad \text{(eq. 2.6)}$$

Ozone breaks down NOM into smaller and more biodegradable compounds like aldehydes, ketoacids and carboxylic acids (Hammes et al. 2006). With post-chlorination, these carbonyl-containing byproducts may participate in substitution reactions with HOCl forming DBPs such as chloral hydrate and 1,1,1-trichloropropanone (Krasner 2009, von Gunten 2003). Ozonation also alters the characteristics of NOM and cause the hydrophobic fraction to decrease, consequently decreasing the DBPs associated with that fraction (e.g., THMs and trihaloacetic acids (Hua and Reckhow 2007a)). In addition, as a result of the increase in bromine-reactive, carboxylate-rich and hydrophilic NOM, brominated DBPs were observed to increase after ozonation (Hua and Reckhow 2007b, Hua and Reckhow 2013, Liang and Singer 2003). For other DBPs like haloacetonitriles (HANs), the decrease in concentration is caused by the reaction of ozone with the amine moieties of NOM which prevents Cl transfer reactions with further chlorination. Unlike HANs, ozonation favors halonitromethane (HNM) formation through oxidation of amino acids and amino groups of NOM (Hoigné and Bader 1988, McCurry et al. 2016).

Table 2.7. Effect of pre-ozonation on removal of organic DBPs

DBP	General observations and effect of pre-ozonation	References
Trihalomethane (THMs)	▪ Dihydroxybenzenes and readily enolizable compounds (β-diketones and β-diketoacids) are fast-reacting THM precursors; phenolic compounds are slow-reacting THM precursors ▪ Could also be formed from DON (e.g., amino acids algal cells) and HAN hydrolysis ▪ For SUVA > 2, chlorination THMs are reduced by ozone by more than 30% (O_3 dose = 1 mg/mg DOC, pH = 7). For SUVA<2, minimal decrease or sometimes increase in THM were observed. ▪ Shifts of THMs to more brominated DBPs during O_3/HOCl treatment ▪ O_3/NH_2Cl treatment resulted in lower THM concentrations than O_3/HOCl ▪ Pre-ozonation mitigates iodo-THM formation. Iodide is oxidized to iodate.	Gallard and von Gunten (2002); Dickenson et al. (2008);Westerhoff and Mash (2002); Hua and Reckhow (2013); Hua and Reckhow (2007b); Yang et al. (2012a); Allard et al. (2013); Bichsel and von Gunten (2000);
Haloacetic acids (HAAs)	▪ β-dicarbonyl acids are major sources of HAAs ▪ DON (e.g., proteins, amino sugars) are important DHAA precursors ▪ Waters with SUVA>2, trihaloacetic acids (THAA) are decreased by ozone by more than 30% (O_3 dose = 1 mg/mg DOC, pH = 7). ▪ More tribromo- and dibromoacetic acid formed during O_3/HOCl for water with 800 µg/L bromide. ▪ O_3/NH_2Cl is effective in removing THAA. ▪ Increase in dihaloacetic acids (DHAA) for waters with SUVA<2; decrease in DHAA for SUVA>2. ▪ Reduced chloramination DHAAs and increased bromine substitution. ▪ DCAA is most predominantly formed after chlorination. ▪ Preozonation decreased DCAA and bromochloro acetic acid BCAA after chloramination but did not affect dibromoacetic acid (DBAA). ▪ O_3/HOCl enhanced DHAA formation (opposite trend for THAA) ▪ HAAs could be formed from hydrolysis HANs and HAMs	Dickenson et al. (2008); Hua and Reckhow (2007b); Hua and Reckhow (2013); Yang et al. (2012a) Reckhow et al. (2001); Westerhoff and Mash (2002) *(Continued…)*

DBP	General observations and effect of pre-ozonation	References
Haloacetonitriles (HANs)	▪ Amino acids and kynurenine (tryptophan metabolite) are suitable DCAN precursors ▪ Hydrophilic fractions are most reactive in forming HANs ▪ Decreased when HNMs increase. ▪ O_3/HOCl reduced DHAN yields. Reduction of DHAN was higher than for THMs and HAAs (DHANs>THMs and THAAs>DHAAs). Typical DCAN FP removal is 50-70% (O_3 dose = 1 mgO_3/mg DOC, pH = 7). ▪ Formation is suppressed by O_3/NH_2Cl treatment. ▪ O_3/HOCl reduced HAN more than O_3/H_2O_2/HOCl ▪ For High DOC/DON, N comes from chloramine (^{15}N-DCAN). For low DOC/DON, N comes from DOM. Preozonation decreased ^{15}N-DCAN.	Westerhoff and Mash (2002); Hua and Reckhow (2013); Hua and Reckhow (2007b); Yang et al. (2012a); McCurry et al. (2016)
Halonitromethanes (HNMs)	▪ Increased TCNM concentration during O_3/HOCl. High concentrations for water with low humic content (SUVA<2) ▪ Enhanced formation with increasing ozone dose. ▪ Formed from oxidizing amines to nitro compounds. ▪ O_3/HOCl and O_3/NH_2Cl increased TCNM formation by 2-5 and 1-2 times, respectively. Majority of N comes from DOM. ▪ TCNM was undetectable with O_3/H_2O_2/NH_2Cl. ▪ O_3/BAC may remove precursors of TCNM ▪ Higher TCNM yield for dipeptide (e.g., ala-ala) compared to individual amino acid	Yang et al. (2012); Hua and Reckhow (2007b); Krasner (2009); Mitch et al. (2009); Bond et al. (2014); McCurry et al. (2016)
Haloketones (HKs)	▪ 1,1,1-Trichloropropanone (TCP) increased with O_3/HOCl treatment. ▪ Formation enhanced by 3-27% with O_3/H_2O_2 (DOC = 2 mg/L, O_3 dose = 3 mg/L, H_2O_2 = 1.5 mg/L). Undetectable using O_3/H_2O_2/NH_2Cl. ▪ Increased with increasing ozone dose. ▪ 1,1-Dichloropropanone (DCP) increased by preozonation. Highest DCP found with O_3/NH_2Cl treatment.	Yang et al. (2012); Hua and Reckhow (2007b)
Haloaldehydes	▪ Chloral hydrate (CH) increased during O_3/Cl_2 but not detected in O_3/NH_2Cl. Formation was enhanced by 2-10% with O_3/H_2O_2 but undetected using O_3/H_2O_2/NH_2Cl (DOC = 2 mg/L, O_3 dose = 3 mg/L, H_2O_2 = 1.5 mg/L). ▪ Increase with increasing ozone dose. ▪ Acetaldehyde can be removed by BAC which results in decrease in chloral hydrate	Yang et al. (2012) Krasner (2009) *(Continued…)*

DBP	General observations and effect of pre-ozonation	References
Haloacetamides (HAMs)	▪ Known hydrolysis products of HANs, but can be formed independently from chlorination of humic materials ▪ Can be formed from subsequent chlorination/chloramination of ozonation byproducts.	Reckhow et al. (2001); Huang et al. (2012); Weinberg (2001)
Total organic halogen (TOX)	▪ Preozonation led to 36% reduction for TOCl but did not decrease TOBr due to shifts to more brominated DBPs (DOC = 4.2 mg/L, O_3 dose = 1mgO_3/mgDOC, pH = 7). ▪ Unknown TOX (UTOX) generally decreased after O_3/Cl_2 treatment and increase with O_3/NH_2Cl. ▪ UTOX/TOX ratios reached about 85% with O_3/NH_2Cl treatment (O_3 dose = 1mgO_3/mgDOC). ▪ 22% decrease in TOX after ozonation at 0.5 mg O_3/mg DOC. Increased with $^{\bullet}OH$ dominant UV/H_2O_2	Hua and Reckhow (2007b); Kleiser and Frimmel (2000)

2.7. Biological treatment

2.7.1. Basic principles of BAC filtration

Biological treatment is applied mainly to remove biodegradable organic matter and to increase biostability of water in the distribution system by preventing bacterial growth (Rittmann 1990). In ozonation plants, this is often achieved via granular activated carbon (GAC) filtration (Urfer et al. 1997). GAC is used as filter media for optimal adsorption of NOM because of its large surface area (1 g GAC = 600 – 1000 m^2 or higher) brought about by its extremely porous shape acting as sieve for trapping NOM, nutrients, and other contaminants (Figure 2.20a) (Simpson 2008). GAC also has an inherent electro-positive charge that can attract electron donors such as NOM (Simpson 2008). The rich supply of these adsorbed particles results in colonization of heterotrophic bacteria (Servais et al. 1994, Urfer et al. 1997). During early stage of biological colonization, most bacteria hardly adapt to premature attachment as they are first evacuated from GAC instead of building up a fixed biomass (Servais et al. 1994). Gradually, select film-forming bacteria attach and accumulate in the GAC surface, releasing only a few bacteria (e.g., ~0.5×10^5 bacteria/mL) in the effluent upon reaching an equilibrium (Servais et al. 1994). The resulting biofilm then excretes glue-like exopolymeric substances for stronger attachment to the GAC (Simpson 2008). By molecular diffusion and convective transport of contaminants across the biofilm, GAC adsorption sites can become saturated with

continuous operation (Simpson 2008). At this stage, NOM removal by the microbial biofilm (biodegradation) occurs rather than by adsorption; hence the term biological activated carbon (BAC). The shift from adsorption to biodegradation causes a decrease in NOM removal (e.g., from 50% removal of non-biodegradable NOM to less than 10% (Servais et al. 1994)). Despite this, BAC filters remain widely used since they are commonly applied after ozonation where particles are broken down into more biodegradable lower molecular weight compounds. In addition, the use of BAC filters is cost-effective as it can operate for over 10 years, while GAC adsorption sites could already be exhausted in about 3 months (~3000 bed volumes) (Rattier 2013).

The transition from adsorption to biodegradation is illustrated in Figure 2.20b (Simpson 2008). Period A corresponds to the adsorption phase where DOC removal is highest. This is also the acclimation phase of microorganisms in the associated biofilm. Period B happens when GAC adsorption sites become saturated with DOC resulting in an increased biological activity. In Period C, DOC removal reaches a plateau phase due to biodegradation. This process is facilitated by various ezymes (Gao et al. 2010) forming CO_2 and other organic compounds that can be assimilated by other bacteria. Biodegradation at this period is governed by the following processes (Figure 2.21) as described in some mechanistic models (Hozalski and Bouwer 2001, Laurent et al. 1999, Rittmann 1990): mass transport to the biofilm, diffusion within the biofilm, utilization kinetics within the biofilm, and growth yield of the substrate. As the substrate is consumed, new biomass is produced which could also be lost through decay and biofilm detachment by physical means (e.g., fluid shear, backwashing) (Rittmann 1990). At high biodegradation rates, other researchers aslo suggested that desorption from GAC's pores could also occur consequently regenerating carbon (bioregeneration) (Aktas and Cecen 2007). This process is thought to be minimal in BAC systems due to continuous microbial growth (Aktas and Cecen 2007). Microbial growth in BAC, however, should be carefully managed as excessive biomass could clog the filter causing pressure drop across the media and lifting of filter beds (Simpson 2008). Such events are concerns in distribution systems due to possible release of microorganisms (signaled by increased turbidity) that has colonized GAC.

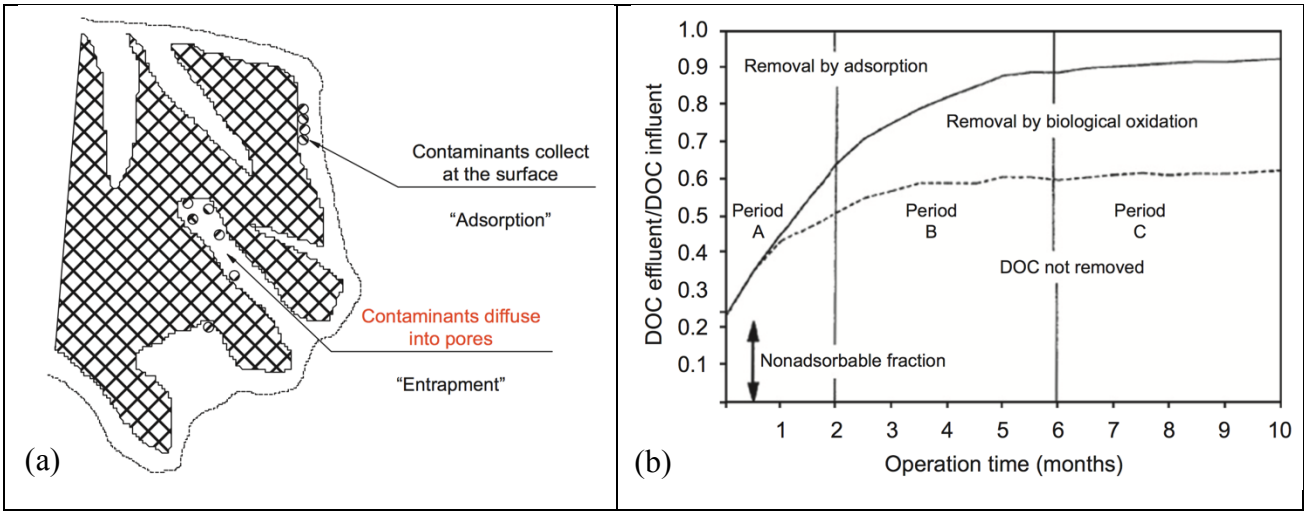

Figure 2.20. (a) Adsorption and pore entrapment in GAC surface; (b) Representation of DOC removal by adsorption and biodegradation as a function of time (reprinted from Simpson (2008), with permission)

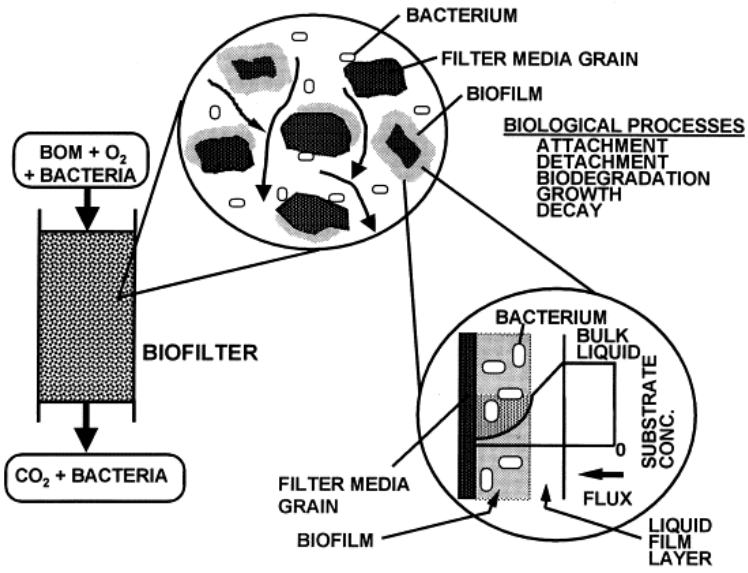

Figure 2.21. Processes occurring in a biofilter (reprinted from Hozalski and Bouwer (2001) with permission)

2.7.2. Biodegradable organic matter

Biodegradable organic matter impacts water treatment in several ways (Laurent et al. 1999). This fraction could support bacterial growth and also consume the added chlorine destabilizing disinfectant residuals in distribution systems. As a consequence, higher chlorine dose would be needed to maintain the target residual, subsequently leading to halogenated DBP formation.

In laboratory settings, the extent of biodegradability of organic matter can be evaluated by determining the assimilable organic carbon (AOC) (van der Kooij et al. 1989), biodegradable organic carbon (BDOC) (Servais et al. 1989), and/or concentrations of readily biodegradable compounds like aldehydes and carboxylic acids (Krasner et al. 1993, Weinberg et al. 1993). In AOC, the growth of test organisms (*Pseudomonas fluorescence* P-17 and *Spirillum* NOX) is measured and correlated with the concentration of biodegradable organic carbon (van der Kooij et al. 1989). The AOC is largely comprised of organic acids after ozonation (Hammes et al. 2006). It typically ranges from 0.1 to 9% of TOC and is considered a subset of BDOC that represents the most readily biodegradable NOM fraction (Escobar and Randall 2001). BDOC, on the other hand, is measured from the difference of the initial DOC and refractory DOC of a water sample exposed to an inoculum of bacteria for a pre-determined time (e.g. 5 days) (Servais et al. 1989). Previous studies have shown that BDOC values are in the range of 10–30% of the TOC of a water sample (Escobar and Randall 2001). Moreover, the formation of biodegradable aldehydes and carboxylic acids after ozonation can also be measured by gas chromatography after derivatization to pentafluorobenzyl oximes (Weinberg et al. 1993).

The biodegradable organic matter can be classified generally into fast, slow, and non-biodegradable fractions to account for DOC degradation kinetics (Yavich et al. 2004). The fast BDOC may contain the small break down products of oxidation. During ozonation, these products (e.g., aldehydes, organic acids, and ketones) are formed extremely rapidly to 60–80% of the AOC and increased continuously at higher ozone exposure but with much slower rate (Hammes et al. 2006). Hammes et al. (2006) suggest that formation of these compounds are directly produced from ozone reactions. In a pilot study of Carlson and Amy (1998), the filter-removable DOC was comprised of aldehydes (formaldehyde, acetaldehyde, glyoxal methyl glyoxal; 3%), ketoacids (glyoxylic acid, puryvic acid, ketomalonic acid; 12%), carboxylic acids (formic acid, acetic acid, oxalic acid; 13–15%), and other unknown oxidation products (70–74%). Many studies also reported comparable values, consistently having >50% of unknown assimilable organic carbon (Richardson 2003). These biodegradable compounds were found to have molecular weights of <0.5 kDa (Zhang et al. 2010). The non-biodegradable organic carbon, on the other hand, is associated to compounds with larger molecular weight and high SUVA (Goel et al. 1995).

The observations of previous studies that DOC removal occurs with initial rapid decrease followed by a period of slow decrease (Yavich et al. 2004) can be modelled using first-order reaction kinetics. Huck et al. (1994) showed good linear relationship between influent concentration and removal rate for DOC, THMs, AOX, and chlorine demand, with a minimum concentration that could not be reduced biologically. The slope of the regression line corresponds to specific removal rate constant of the contaminant which varies with respect to characteristics of the source water and the biofilter. Note that

the removal rate was calculated from the difference of influent and effluent concentrations divided by empty bed contact time (EBCT) (Huck et al. 1994), and EBCT refers to the water detention time in the GAC (i.e., ratio of the filter bed volume to the water flow rate). This first-order dependence of DOC removal on EBCT was also shown in other studies (Black and Berube 2014, DiGiano et al. 2001). In addition, Melin and Odegaard (2000) confirmed the kinetic results using different ozonation by-products (example plot is shown in Figure 2.22). In that study, the removal of formaldehyde, acetaldehyde, acetone, glyoxal, methyl glyoxal, glyoxylic acid, pyruvic acid, and ketomalonic acid followed a single exponential decay to the non-biodegradable DOC (non-linear regression $R^2 > 0.80$).

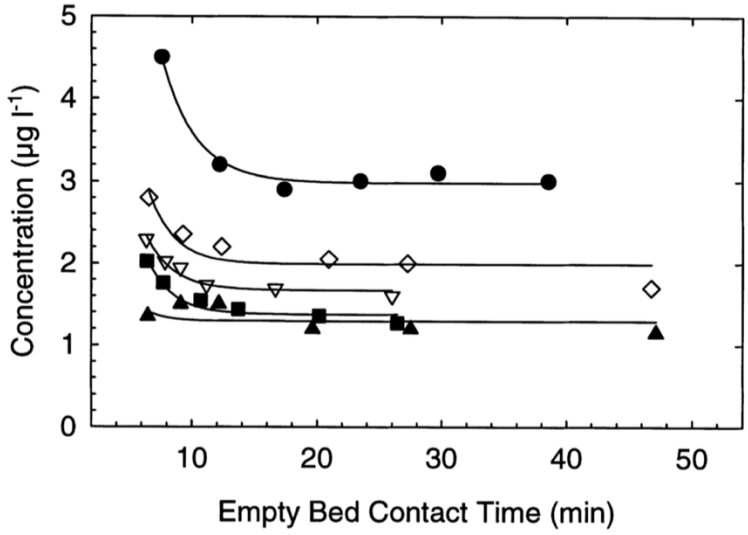

Figure 2.22. Effluent concentration removal efficiency for formaldehyde (reprinted from Melin and Odegaard (2000), with permission)

Having NOM with different biodegradability are expected due to NOM's complex structure and functionality. To be biodegradable, many of the contaminants require oxygenation steps that entail oxygen insertion into the compound's structure (Rittman 1995). Once oxygenated, they can be metabolized by pathways common to bacteria (Rittman 1995). This requirement can be attained during ozonation (e.g., phenolic compounds to aldehydes, carboxylic acids). Recently, Hubner et al. (2015) shows that the probability of biodegradability of ozone transformation products from olefins and ring-opening of aromatic compounds increases relative to the parent compound. Whereas, oxidation products of aromatic compounds that did not undergo ring cleavage were predicted to have no enhancement in biodegradability. For amines, the biodegradability of oxidation products such as hydroxylamines and *N*-oxides was also not expected to improve (Hubner et al. 2015). At present, experimental information on biodegradability of various ozonation transformation products are still lacking.

2.7.3. Factors affecting biofiltration performance

Several factors affect the performance of biofiltration. Some can be controlled quite well by water operators (ozone dose, biofilter media, EBCT, backwashing method) while others are mainly dependent on the influent water quality (e.g., nutrient load, temperature). As discussed earlier, ozone increases the load of biodegradable carbon due to breakdown products of NOM that can be metabolized in the biofilter. Enhancing the load of these biodegradable carbon by ozone or $^{\bullet}OH$ could also affect the biofiltration efficiency, although further studies are needed to determine which ozonation conditions promote better biodegradability. Without intermediate process between ozone and biofiltration, residual ozone can reach the biofilters. This scenario could potentially inhibit biological activity especially at high ozone residuals. With GAC, the presence of ozone seemed not to affect the biological removal of ozonation products like aldehydes (Weinberg et al. 1993) because of ozone's rapid decay in GAC's surface. This could be different in other filters since the reactivity of ozone with the media varies as follows: GAC>anthracite>sand (Urfer and Huck 2000). With peroxone (O_3 + H_2O_2), H_2O_2 residuals of about 1 mg/L in the influent of a lab-scale anthracite-sand filter media were shown to be rapidly destroyed without impairment of biofiltration efficiency (Urfer and Huck 1997, Urfer et al. 1997). Other than residual oxidant reactivity, GAC, anthracite, and sand could also have varying rates for biomass growth. The macroporous structure of GAC offers higher surface area than anthracite and sand for biofilm retention that are less prone to fluid shear stress (Urfer et al. 1997). As a result, GAC filters forms biological activity faster and develop biofilms that are more stable against perturbations (e.g., shutdowns, intermittent chlorination) compared to nonadsorptive media like anthracite (Krasner et al. 1993). In a study by Emelko et al. (2006), higher biomass concentrations were found with GAC (per unit volume of media) compared to anthracite, especially at the top of the filter receiving the influent. Despite differences in biomass concentrations, no significant effect on carboxylic acids removal was observed except at low temperature conditions (Emelko et al. 2006). Similar observation was reported by Krasner et al. (1993) where aldehyde removals remained at 50–75% using GAC/sand and anthracite/sand filters.

EBCT, as discussed earlier, is also a key biofiltration parameter. Removal of the biodegradable fraction increased with increasing contact time (Urfer et al. 1997), although a biorecalcitrant NOM fraction is left at higher EBCTs (Black and Berube 2014, Melin and Odegaard 2000, Yavich et al. 2004) (see previous section). Higher contact times were also required for THM precursors than for the easily biodegradable ozonation byproducts such as aldehydes (Urfer et al. 1997). EBCTs can be changed by either varying the filter depth or hydraulic loading. Servais et al. (1994) demonstrated that at fixed EBCT, biological removal of BDOC in four filters remained relatively the same (40–56%) despite having filters operated with varying depths and filtration velocities (6–18 m/h). This suggest that

external mass transfer plays a minor role in removal of biodegradable organic matter under conditions typical for drinking water treatment (Urfer et al. 1997).

Filter clogging during biofiltration also needs to be controlled. Because of this, water operators perform backwashing on a regular basis (e.g., every week). In this process, bound contaminants and decaying microorganisms are exposed to harsh conditions (e.g., high shear stress by air scour and clean water rinse) and are washed out through the top of the filter. Despite these conditions, biological activity in the filters is retained since biofilms are generally resistant to backwashing conditions (Simpson 2008, Urfer et al. 1997). The use of chlorinated waters for backwashing, however, could damage the biofilter due to biomass oxidation across the filter bed. Ahmad et al. (1998) showed that initial microbial counts in filters backwashed with chlorinated waters were two orders of magnitude lower than those for filters not exposed to chlorine. Another approach for controlling filter clogging would be nutrient supplementation (phosphate-P, ammonium-N). Lauderdale et al. (2012) reported that a C:N:P ratio of 100:10:1 is ideal for the filter biofilm. During coagulation, phosphate could be removed leading to conditions that are nutrient-limited. As a stress response, microorganisms produce excessive amounts of extracellular polymeric substances that clog the filter (Lauderdale et al. 2012). This could also cause release of soluble microbial products (SMPs) like carbohydrates, nucleic acids, proteins, and amino acids, among others (Rittman et al. 1987, Zevin et al. 2015). Thus, to achieve a nutrient-balanced biofilters, phosphate-P, ammonium-N could be dosed based on the BDOC to achieve the ideal C:N:P ratio. Nutrient supplemented biofilters were reported to have better removals for DOC, manganese, and 2-methylisoborneol compared to nutrient-limited filters (Lauderdale et al. 2012).

2.7.4. Coupling ozonation and biofiltration for DBP control

It is clear that oxidation of NOM by ozone increases its biodegradability through formation of low molecular weight byproducts which can be subsequently removed during biofiltration (Krasner et al. 1993, Weinberg et al. 1993). If the oxidation products are significant DBP precursors, biological treatment could decrease the resultant DBP formation potentials with chlorine. For example, aldehydes and ketones formed after ozonation can be consumed by the biofilters, preventing formation of haloaldehydes and haloketones (Krasner 2009). The study by Mitch et al. (2009) showed low removals of chlorination formation potentials of THMs and dihalogenated HANs (~3%) during biofiltration of ozonated waters. In contrast, high removals were achieved for TCNM and chloral hydrate (42–48%) which could be due to biodegradability of precursors formed during ozonation. The low removal of THM formation potentials corroborates with the results of Sohn et al. (2007) where aromatic components of NOM (precursors of THMs and HAAs) were found to be ineffectively removed during sand and BAC filtration. These results were also observed in our study of full scale plants in SEQ. In

that study, it is notable that formation potentials of chloral hydrate and 1,1,1-trichloropropanone both increased with pre-ozonation and intermediate ozonation, but were minimized after BAC filtration (Figure 2.23a – 2.23b) (Lyon et al. 2014a). Moreover, trichloronitromethane decreased but its brominated analogue, tribromonitromethane, increased in some instances.

To date, little is known about the biodegradability of precursors of other emerging DBPs (e.g., nitrogenous DBPs). Table 2.8 shows some of the studies which used biofiltration for DBP removal. In general, the biofiltration process can reduce DBP precursors formed after ozonation, but studies on this process have been limited mostly to THMs and HAAs, thereby requiring further investigations. The behavior of precursor molecules of N-DBPs towards these combined systems has not yet been studied very well. This provides a strong motivation to evaluate the effect of ozone as well as $^{\bullet}OH$ reactions with biofiltration on a wide range of DBPs families.

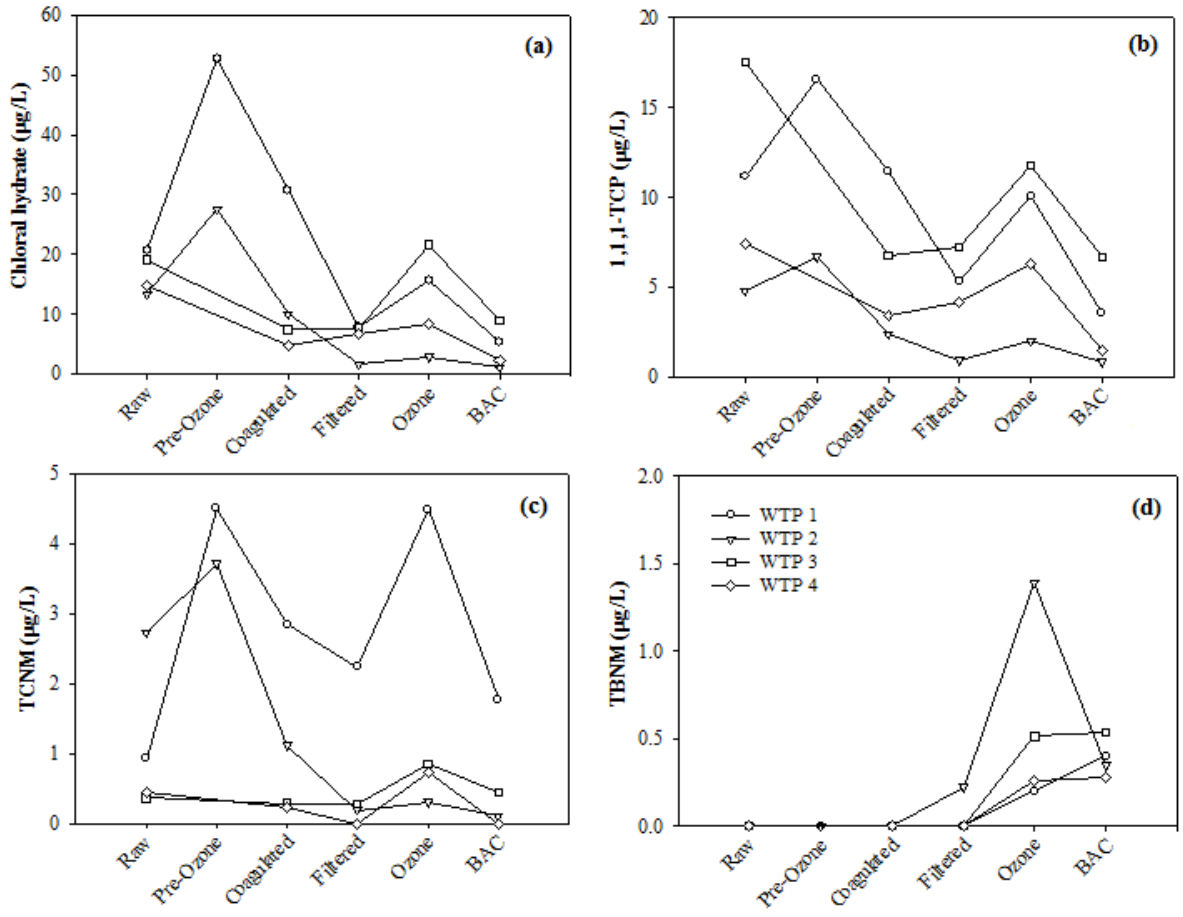

Figure 2.23. Effect of ozonation and BAC filtration in four advanced water treatment plants on (a) choral hydrate, (b) 1,1,1-trichloropropanone (1,1,1-TCP), (c) trichloronitromethane (TCNM) and (d) tribromonitromethane (TBNM) formation potential following chlorination (Lyon et al. 2014a).

Table 2.8. Use of biological treatment for DBP precursor removal

Reference	Conditions	% DBP removal / other findings
Akcay et al. (2015)	Bench-scale filtration (EBCT: 30 min) of raw water. No ozonation	Biofilter efficiency: GAC >sand>zeolite For BAC: DOC = 64%, THMFP = 68%, HAAFP = 64%
Chu et al. (2012)	Pilot plant: coagulation, sedimentation, sand filtration, ozonation (dose = 1.5 – 2 mg/L; contact time = 30 min) and BAC filtration (EBCT = 15 min); HOCl DBP formation potential test	Better removal with O_3/BAC compared to conventional processes. Overall removals with O_3/BAC pilot plant: DOC = 72%; DON = 74% TCM FP= 85%; DCAN FP = 80% TCNM FP = 50%; DCAM FP = 60%
Farré et al. (2011)	Pilot plant wastewater plant: denitrification + pre-O_3 (2 mg/L) + coagulation/ flocculation + dissolved air flotation and sand filtration (DAFF) + main ozonation (5 mg/L) + BAC (18 min contact time) + final ozonation	NDMA FP = 78% THM and HAA: reduced by sand filtration and biodegradation; reduction proportional to DOC removal; brominated species increased TCM FP: 54% (from DAFF to BAC)
Mitch et al. (2009)	Full scale plant: O_3 /BAC + HOCl	Median removals: DOC= 12%; DON = 18% THM and DHAN = 3% Trihaloaldehyde = 42%; TCNM = 48%
Chen et al. (2009)	Catalytic ozonation/fluidized bed reactor (catalyst: TiO_2 on Al_2O_3) + biofiltration column (contact time = 7 days)	DOC = 81.7%, THM FP = 76.1%, HAA FP = 81.3%
Chen et al. (2007)	Pilot plant: Conventional + O_3/BAC O_3 dose = 2.5 mg/L, filter rate in BAC = 4 m/h	Combined conventional + O3/BAC is effective over separate conventional and advanced treatment. TOC = 42%, THMFP = 68%, HAAFP = 23%, AOC = 67%
Chaiket et al. (2002)	Pilot plant: Combination of coagulation, ozonation (O_3 dose: 0.7–3 mg/L), biofiltration (anthracite/sand/GAC; EBCT = 5 min)	TOC = 17% THMFP = 55% HAAFP = 68%

(Continued…)

Reference	Conditions	% DBP removal / other findings
Wobma et al. (2000)	Pilot plant: rapid mix + flocculation + DAF + O_3 + biofiltration Media: GAC, anthracite (AN) Depth: 2.1 m Applied O_3: 0.3–0.6 mg/L Loading rate: 35 m/h	Post-ozone aldehydes: > 90% (GAC) Post-ozone carboxylic and keto acids = 80–100% (GAC) Anthracite filters = 10-40% removal of carbonyl byproducts Background THM: removed when fresh GAC was used (adsorption) Background HAAs: removed by BAC, not by anthracite biofilters
Koffskey and Lykins (1999)	Pilot plant: clarifier + 3 stage ozone + AN/sand; GAC/ sand + chloramine O_3 gas flow: 1.2 L/min EBCT: 3.5–9.2 min	DOC = 37% (ozone/GAC/sand) TOX = ~ 40% (ozone-GAC/sand) THM = 48% (ozone-GAC/sand-NH_2Cl) HAA = 54–63% (ozone-GAC/sand-NH_2Cl) Total aldehyde = 89% after GAC; increased after chloramination HAN = 1.2 ug/L (O_3-BAC) Chloral hydrate/haloketone/cyanogen halide = 0.3–0.5 ug/L (O_3/BAC) TCNM: 0.3 ug/L (O_3/BAC) Cyanogen halide: reduced by biofilters
Siddiqui et al. (1997)	Bench-scale ozonation (2 mg O_3/mg DOC) + sand filtration	DOC = 40 – 50%; aldehydes = 90 – 100% THM FP = 40 – 60% Bromate and dibromoacetic acid: not removed

Chapter 3

Research objectives and approach

3.1. Knowledge gaps

The previous chapter mentioned some key important areas on ozonation of NOM, biological drinking water treatment, and disinfection byproduct (DBP) formation that need further investigation. These research areas are related to the objectives stated in Section 1.2, summarized in Table 3.1, and discussed in more detail in the following sections. The knowledge gaps and research questions presented here were divided into 3 parts representing the reaction series of ozonation-biofiltration-chlorination: (1) reaction of NOM with ozone, (2) reaction of NOM with O_3 and HOCl, and (3) transformation of NOM with O_3 and BAC filtration followed by chlorination.

1. ***NOM + O_3:*** In recent years, higher fractions of dissolved organic nitrogen (DON) end up in drinking water production as a result of direct or indirect potable reuse, agricultural runoffs, and climate related events. DON moieties of NOM also become increasingly more important as they act as precursors of N-DBPs (Section 2.3.1). Although there is already a wealth of knowledge on the reactions of ozone with organic compounds (von Sonntag and von Gunten 2012), **only a few product studies are available to understand the fate of DON during ozonation**. Previous studies showed that DON can be hardly removed by conventional treatment, allowing it to occur across each treatment unit, reaching the ozonation step. This provides a strong motivation to evaluate how ozone transforms DON. During this process, ozone can react with DON via oxygen-transfer and electron-transfer mechanisms (Section 2.6.2) and generate various products including nitrate and ammonium. This was shown in ozonation studies of amino acids (Berger et al. 1999, Le Lacheur and Glaze 1996). It is very likely that such reactions could also take place in the complex structures containing DON moieties. If changes in inorganic nitrogen can be observed during ozonation of DON, nitrate and ammonium concentrations may become important parameters in evaluating the performance of the oxidation process. It is therefore worth exploring to address the following research questions:

   How does ozone react with DON? What transformation products are formed? Can these products be used to characterize the ozonation process (e.g., ozone exposure, contribution by O_3 and $^{\bullet}OH$ during oxidation)?

2. ***NOM + O_3 + HOCl:*** The stability of ozone is affected by the water quality and operational conditions (Section 2.6.1). Conditions that promote ozone decay (e.g. high pH, in presence of H_2O_2) result in possible formation of higher $^{\bullet}OH$ yields. The opposite happens when water samples have $^{\bullet}OH$ scavengers like tertiary butanol and carbonate, or when ozonation is conducted at lower pH. Thus, during ozonation, both ozone and/or $^{\bullet}OH$ can participate in the oxidation reactions

through different mechanisms. Ozone is selective to electron-rich moieties like phenolic groups and deprotonated amines while ˙OH is non-selective and reacts mainly by addition to C-C and C-N bonds (von Sonntag and von Gunten 2012). These reactions can therefore have direct consequences on the resultant reactivity of pre-oxidized NOM/oxidation products towards chlorine, and subsequently on DBP formation. Current ozonation units in water treatment plants were shown to reduce formation of regulated DBPs (e.g., THMs). This is achieved because of the attack of ozone to similar reaction centers of chlorine (Section 2.6.2). During this process, biodegradable compounds such as aldehydes, ketones, and carboxylic acids can be produced, leading to formation of halogenated aldehydes and ketones during chlorination. In bromide-containing waters, hydrophilic products of ozone are also prone to brominated DBP formation. In DON-containing waters, halonitromethanes could also form. **The impact of ozone on other emerging DBPs, however, remains unclear.** To achieve control of both regulated and emerging DBPs, evaluation of factors affecting ozone reactions that influence NOM reactivity with chlorine is necessary. Evidence is therefore needed to determine optimal ozonation conditions for effective DBP control. The following research questions were addressed:

How can the ozonation process be used to control the formation of DBPs? What are the effects of ozone and ˙OH on transformations of precursors of different DBP families (trihalomethanes, haloacetic acids, chloral hydrate, haloketones haloacetonitriles, halonitromethanes, haloacetamides, adsorbable organic halogens)?

3. ***NOM + O_3 + BAC + HOCl:*** Answering the previous research questions led to outcomes related to ozonation conditions that do not promote DBP formation (i.e., ozone versus ˙OH reactions). In advanced water treatment, ozonation is commonly followed by biofiltration due to formation of biodegradable organic matter (Section 2.7). **However, it is uncertain whether the predominance of ozone over ˙OH reactions (or vice versa) would lead to better biofiltration performance.** The resulting oxidized NOM could also have varying degrees of biodegradability due to its different moieties, consequently affecting the formation of DBPs with post-chlorination. **Biodegradable precursors such as aldehydes are expected to be easily removed but information about other precursors are currently lacking.** Therefore, the impact of biofiltration and operational parameters affecting its performance should be investigated on a wide array of disinfection byproducts. These entailed answering the following research questions:

What is the impact of ozone and ˙OH reactions on the biodegradability of DBP precursors? What key parameters can be used to optimize the biodegradation process following ozonation?

Table 3.1. Knowledge gaps identified and addressed in this thesis

Process	Current general knowledge	Knowledge gaps
NOM + O_3	▪ O_3 is reactive to activated aromatic systems, olefins, and deprotonated amines of NOM. ▪ Ozonation reactions also produce ($^{\bullet}$OH); reaction kinetics is affected by $^{\bullet}$OH scavenging. ▪ Reaction produces biodegradable aldehydes, ketones, carboxylic acids. ▪ Reaction with NOM may happen via different mechanisms (e.g., oxygen transfer, electron transfer, etc.)	▪ Studies on oxidation products of amines are limited to few amino acids. ▪ Effects of oxygen transfer and electron transfer reactions on DON are not well understood. ▪ Potential formation of inorganic nitrogen from DON for ozonation characterization (e.g., O_3 exposures) is worth exploring.
NOM + O_3 + HOCl	▪ Ozone can effectively remove hydrophobic NOM fractions. ▪ Ozonation is effective for reducing THM and HAA formation potentials; varying effects at different water quality. ▪ Treatment increases formation of chloral hydrate, haloketones, halonitromethanes. ▪ Brominated DBPs may increase after ozonation in bromide-containing waters; HOBr reacts faster than HOCl.	▪ Few studies are available for N-DBP formation; mostly on THMs and HAAs ▪ Effects of ozone and $^{\bullet}$OH reactions on DBP formation are not clear ▪ Conditions to reduce formation of chloral hydrate, haloketones, and halonitromethanes during ozonation are needed. ▪ Toxicity of mixed DBPs to account for overall effect of ozonation requires further investigation.
NOM + O_3 + BAC + HOCl	▪ BAC is effective for biodegradable compounds (e.g., aldehydes, carboxylic acids); improves biostability of product water ▪ BAC can remove precursors of chloral hydrate and haloketones. ▪ DOC comprises of fast, slow, non-biodegradable fractions. ▪ Empty bed contact time (EBCT) is an important operational parameter for DOC removal ▪ Bromide remains after biofiltration.	▪ Effects of O_3 and $^{\bullet}$OH on biodegradability are not well known. ▪ Limited studies are available for removal of precursors of N-DBPs and other emerging DBPs by biofiltration. ▪ Kinetic studies on DBP precursor removal during BAC are not available; No comparison was made for biodegradability of different DBP precursors. ▪ Optimization of factors affecting biofiltration efficiency (e.g., EBCT) for DBP removal is needed.

3.2. Research hypotheses and corresponding experimental approaches

The research questions in the previous section can be answered by understanding the processes that govern NOM transformation and DBP formation during ozonation and biofiltration. Testing the following hypotheses by means of the general research approaches (stated below) addresses these important fundamental questions. Details of all the experimental procedures are provided in Chapters 4 – 6.

Hypothesis 1: *The transformation products that give rise from the reaction of ozone with DON can be used to evaluate the characteristics of the ozonation process.*

Approach: To understand the effect of ozonation on DON moieties, ozone dosing and kinetics experiments using NOM reference standards, surface water, and wastewater effluent samples were conducted. The changes in nitrate and ammonium concentrations were recorded after treatment at different ozone doses and exposures. In this study, the characteristics of ozonation were mainly described using ozone exposures and R_{ct} (Section 2.6.1). Ozone exposures in the sample solutions were varied by the addition of tertiary butanol, methanol, H_2O_2, as well by changing ozonation pH and inorganic carbon concentrations. Using model DON solutions, yields of nitrate and ammonium were investigated to assess the main drivers of inorganic nitrogen formation during ozonation. The contribution of oxygen-transfer and electron-transfer reactions were also evaluated through kinetics experiments and dimethyl sulfoxide assay (Flyunt et al. 2003, Tekle-Rottering et al. 2016). Nitrate and ammonium formation were evaluated in synthetic waters mimicking realistic water treatment conditions. Lastly, kinetic simulations were performed based on all the observed results to be able to propose a possible reaction mechanism for the reaction of ozone with DON.

Hypothesis 2: *Oxidation of NOM by ozone and/or hydroxyl radicals during ozonation will have different effects on NOM properties and subsequent reactivity with chlorine and DBP formation.*

Approach: In this study, a holistic approach was applied to determine the overall impact of ozone and $^{\bullet}OH$ oxidation on the quality of post-chlorinated water in terms of known DBPs, AOX, and associated biological effects. The following DBPs were analyzed: adsorbable organic halogens, nitrogenous-DBPs such as haloacetonitriles, halonitromethanes, and haloacetamides and the carbon-based DBPs trihalomethanes, haloacetic acids, chloral hydrate, and haloketones. Common ozonation DBPs such as aldehydes and bromate were also investigated. Batch ozonation experiments were performed on samples with and without added tertiary butanol and H_2O_2, varying pH levels, and different specific ozone doses. These conditions were chosen to distinguish the effects of O_3 and $^{\bullet}OH$ reactions on DBP

formation. After all the ozone had reacted, DBP formation potential tests using HOCl and corresponding extraction procedures were conducted. *In vitro* bioassays were also used to assess cytotoxicity, genotoxicity, and induction of oxidative stress of the treated water. Changes in NOM properties such as DOC, SUVA, and fluorescence EEM were also determined to complement DBP formation results.

Hypothesis 3: *Variations in ozone and hydroxyl radical exposure will impact the performance of biological filtration and thereby the final water quality. Provided that a target water quality is defined, it is possible to optimize the oxidation process and biological filtration towards that outcome.*

Approach: This study evaluated the effect of O_3 and $^{\bullet}OH$ reactions on the biodegradability of ozonated waters and the removal rate of formation potentials of different families of DBPs including trihalomethanes, haloacetic acids, chloral hydrate, haloketones, haloacetonitriles, halonitromethanes, and trichloroacetamide. Three sets of experiments were performed to investigate the biodegradability of DBP precursors at different ozonation and biodegradation conditions. The first set involved water samples treated with different O_3 doses and subsequently exposed to bioactive anthracite. The second set involved column experiments using biological activated carbon (BAC) and bioactive anthracite media fed with water ozonated with and without H_2O_2 (to vary ozone exposures). The third set of experiments focused on studying biofiltration performance by varying the empty bed contact time (EBCT) of the BAC columns. Kinetics of precursor removal of each DBP were monitored from 3 – 55 min EBCT to determine the relative biodegradability of the precursors.

Chapter 4

Kinetics and mechanisms of nitrate and ammonium formation during ozonation of dissolved organic nitrogen

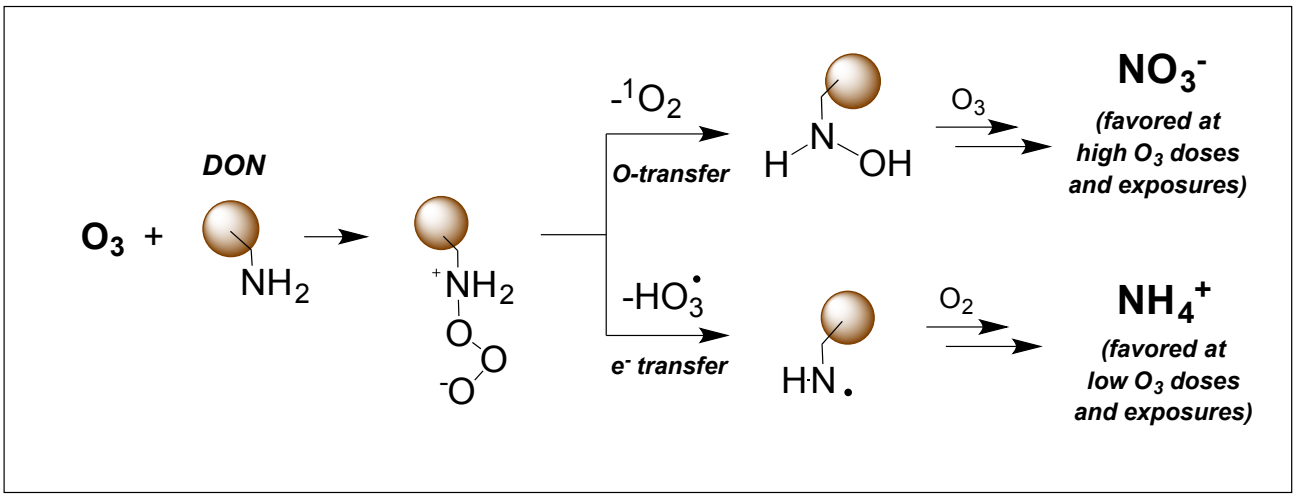

The results of the present chapter are based on the following peer-reviewed publication:

de Vera, G.A., Gernjak, W., Weinberg, H.S., Farré, M.J., Keller, J., and von Gunten, U. (2017) Kinetics and mechanisms of nitrate and ammonium formation during ozonation of dissolved organic nitrogen. *Water Research* 108, 451-461.

http://dx.doi.org/10.1016/j.watres.2016.10.021

4.1. Introduction

Dissolved organic nitrogen (DON) in the aquatic environment commonly occurs as amino acids, peptides and proteins and accounts for 0.5 – 10% (by mass) of the dissolved organic matter (Sharma and Graham 2010, Westerhoff and Mash 2002). Despite these relatively low concentrations, DON is considered an emerging concern for water utilities because it can act as precursor of potentially toxic nitrogenous oxidation/disinfection by-products (e.g., nitrosamines, halonitromethanes, haloacetonitriles) during chlorination and/or chloramination processes (Krasner et al. 2013, Shah and Mitch 2012, Westerhoff and Mash 2002). DON becomes increasingly more important as a result of shorter water cycles through indirect or direct potable reuse leading to higher fractions of wastewaters in source waters used for drinking water production (Krasner et al. 2009, Leverenz et al. 2011, Rodriguez et al. 2009). In addition, climate-related eutrophication and run-off events in upstream agricultural systems have also been identified to impact DON concentrations (Delpla et al. 2009, Graeber et al. 2015, Westerhoff and Mash 2002). Because nitrogen moieties can form hydrogen bonds with the surrounding water molecules, DON moieties can increase the hydrophilic character of NOM (Westerhoff and Mash 2002) making it harder to be removed by conventional treatment processes such as coagulation and filtration. As a result, DON can persist through various non-oxidative treatment schemes and consequently exert oxidant demand and lead to the formation of various measurable nitrogenous oxidation by-products.

Ozone (O_3) can selectively oxidize the electron-rich moieties of DON such as amino acid side chains in polypeptide structures (Sharma and Graham 2010). O_3 reacts with the amine functional groups via adduct formation (Section 2.6.2.3) leading among other products to *N*-oxides for tertiary amines and hydroxylamines for primary and secondary amines (von Sonntag and von Gunten 2012). The adducts can also decay by a series of reaction steps to amine radical cations that subsequently produce dealkylated amines (von Sonntag and von Gunten 2012). Hydroxyl radicals ($^{\bullet}OH$) can also be formed from the reaction of O_3 with DON moieties in addition to other natural or enhanced (e.g., O_3/H_2O_2) O_3 decay processes (von Sonntag and von Gunten 2012).

During ozonation, amino acids play an important role in the reactivity of DON as they can readily react with O_3 through their deprotonated amine nitrogen moiety, with higher second-order rate constants in the presence of methyl, alkyl, or thiol groups (Neta et al. 1988, Sharma and Graham 2010). Glycine, serine, aspartic acid and glutamic acid are the most abundant amino acids in the aquatic environment (Westerhoff and Mash 2002). As reported in a few product studies, amino acids react with O_3 producing nitrate, ammonia, carbonyl and carboxylic acids (Sharma and Graham 2010). Using

serine as a model compound, Le Lacheur and Glaze (1996) reported that nitrate and ammonia were among the major end-products of amine nitrogen oxidation under O_3- and $^{\bullet}OH$-dominated conditions, respectively. A study with glycine also showed that the $^{\bullet}OH$ pathway favors ammonia production while O_3 produces nitrate (Berger et al. 1999, Karpel Vel Leitner et al. 2002). In these studies, nitrate formation is induced from the O_3 attack on the amine-nitrogen before cleavage of the C-N bond (Berger et al. 1999, Le Lacheur and Glaze 1996). In contrast, the reaction of $^{\bullet}OH$ leads to a nitrogen-centered radical which rearranges into a C-centered radical analogous to the 1,2-H shift in reactions of alkoxyl radicals. This is followed by oxygen addition and loss of superoxide and imine formation, which finally induces a deamination and ammonia production (Berger et al. 1999, Karpel Vel Leitner et al. 2002) (Figure 4.1).

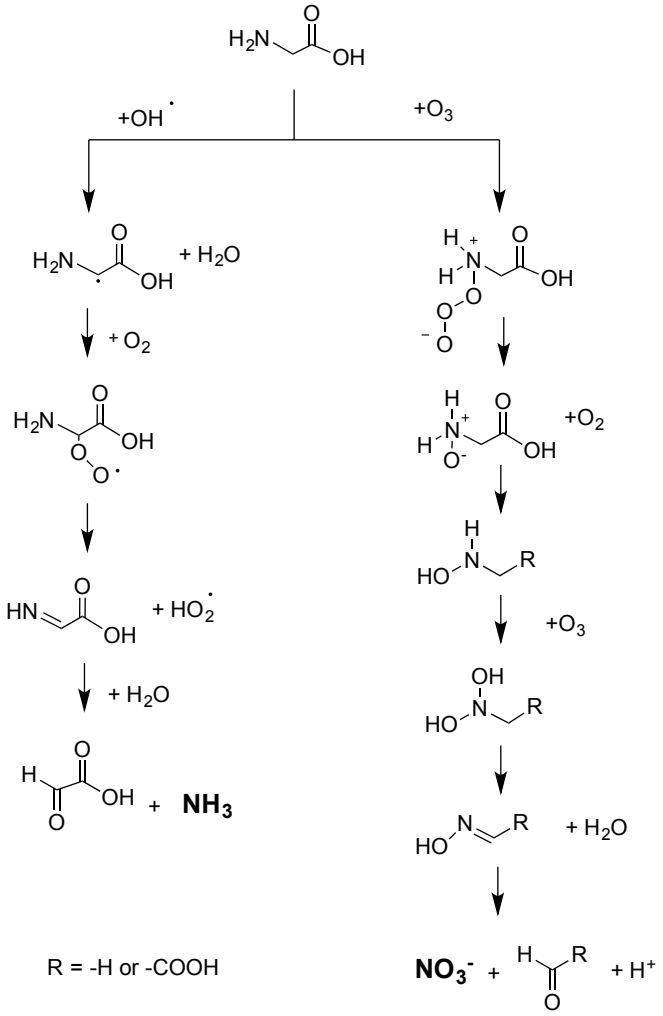

Figure 4.1. Formation of NH_3 and NO_3^- during oxidation of glycine by $^{\bullet}OH$ and O_3 (Adapted from Berger et al. (1999), with permission)

Although the compounds used in these prior studies were smaller molecules than the complex structures of DON moieties, it is worth investigating if the subsequent changes in levels of nitrate and ammonia after ozonation can also occur with differing natural and standard NOM sources. If this is observed, nitrate and ammonia may become important parameters in evaluating the characteristics of an ozonation process such as disinfection efficiency, O_3 exposure (i.e., time integrated concentration of O_3) and contribution of O_3 and $^{\bullet}OH$ to the oxidation. For example, nitrate formed through reactions with O_3 may serve as a surrogate measure for oxidant exposure or disinfection credit (see below for further discussion). Nitrate and ammonia are readily accessible parameters through low cost and low maintenance colorimetric methods (APHA et al. 1999), wherefore, this approach is worth exploring.

This study aims to understand the effect of ozone on DON moieties and the subsequent formation of inorganic nitrogen compounds (NO_3^- and NH_4^+). NOM reference standards, surface water, and wastewater effluent samples were treated under varying ozonation conditions and the changes in nitrate and ammonium concentrations were recorded. Furthermore, the possible major precursors of inorganic nitrogen were identified in experiments using primary, secondary, and tertiary amine model compounds. From the observed results and by using glycine as a model compound, a mechanistic interpretation of the reactions of O_3 with DON was proposed. Lastly, a potential application of the results for characterization of ozonation processes (e.g., estimation of O_3 exposure) was explored.

4.2. Experimental Methods

4.2.1. Reagents and chemical analyses

All stock solutions were prepared using Milli-Q Direct ultrapure water (18.2 MΩ-cm, Millipore). Ozonation experiments were performed at the University of Queensland (UQ), Australia and the École Polytechnique Fédérale de Lausanne (EPFL), Switzerland using ozone generated from pure oxygen (99.995%, Carbagas, Switzerland) with an Anseros COM-AD-04 or an Innovatech Type CMG 3-5 ozone generator, respectively. Ozone stock solutions (1 – 1.3 mM O_3) were prepared by sparging O_3 through 1 L of MilliQ water that was cooled in an ice bath. The stock solutions were standardized spectrophotometrically using the absorbance at 260 nm (ε = 3200 $M^{-1}cm^{-1}$) (Shimadzu UV-1800 Spectrophotometer, Japan) (von Sonntag and von Gunten 2012). Ozone concentrations in samples were determined by the indigo method (Bader and Hoigné 1981) (potassium indigotrisulfonate, Sigma-Aldrich, USA). From these measured concentrations, O_3 exposure was calculated from the area under the O_3 decay curve (von Gunten and Hoigné 1994).

The concentrations of *para*-chlorobenzoic acid (*p*CBA, 99%, Aldrich, USA) during ozone decay kinetics experiments were monitored using high performance liquid chromatography (Dionex Ultimate 3000, USA) equipped with a Nucleosil 100-5 C18 column (Macherey-Nagel, Germany). *p*CBA has a very low reactivity with ozone and is used as a probe compound for $^{\bullet}OH$ ($k_{\cdot OH+pCBA} = 5.0\times10^{9}$ $M^{-1}s^{-1}$ (Elovitz and von Gunten 1999)). *p*CBA was detected at 240 nm using a mobile phase gradient program involving (A) acetonitrile (≥ 99.9%, Carlo Erba, Italy) and (B) 10 mM phosphoric acid (≥ 85%, Merck, Switzerland) (0–2 min: 5% A/ 95% B; 8–13 min: 55% A/ 45% B) at 0.8 mL/min flow rate and a 100 µL injection volume. The method detection limit was 0.01 µM (standard deviation = 2×10^{-4} µM, n = 9 (0.01 µM), measuring range = 0.01 – 2 µM). The $^{\bullet}OH$ exposure was evaluated from the relative decrease of *p*CBA concentrations as a function of reaction time. 1 mM sodium thiosulfate (from 0.1 M, Merck, Germany) was used to quench ozone during kinetic experiments with *p*CBA.

Nitrate was analyzed using a Lachat QuikChem8500 Flow Injection Analyzer (method 31-107-04-1-A, method detection limit = 0.10 µM, standard deviation = 0.03 µM, n = 8 (0.4 µM), measuring range = 0.1 µM – 60 µM) (Hach Company, CO, USA) or an ICS-3000 ion chromatography system (Thermo Scientific, Dionex Products, CA, USA) with an AG11HC pre-column, an AS11HC column, an AERS 500 suppressor, and 30 mM KOH eluent. The analyses were performed at 1 mL/min flow rate, 25 µL injection volume, and 80 mA current. The method detection limit was 0.2 µM (standard deviation = 0.05 µM, n = 7 (1.6 µM), measuring range = 0.2 – 32 µM). Nitrite produced from ozonation of DON is quickly further oxidzed because of its high reactivity with O_3 ($k = 5.83\times10^{5}$ $M^{-1}s^{-1}$) (von Sonntag and von Gunten 2012). Ammonium was measured with a Lachat QuikChem8500 Flow Injection Analyzer (method 31-107-06-1-B, method detection limit = 0.11 µM, standard deviation = 0.03 µM, n = 8 (0.4 µM), measuring range = 0.1 – 64 µM) or with a SEAL analytical autoanalyzer (method no. G-171-96, method detection limit = 0.3 µM, standard deviation = 0.1 µM, n = 18 (0.55 µM), measuring range = 0.3 – 55 µM) equipped with an AA3 colorimeter and a 10 mm flow cell. The standard stock solutions for nitrate (1001 ±5 mg/L), nitrite (1003 ±5 mg/L), and ammonium analyses (1000 ±2 mg/L) were obtained from Merck, Germany.

Details of the flow injection analyses for NO_3^- and NH_4^+ are as follows. In the Lachat QuickChem method, NH_4^+ reacts with hypochlorite (2.5%, Domestos, Australia) which, in the presence of phenol (0.08 g/L, Univar grade, Ajax Finechem, Australia), catalytic amounts of nitroprusside (0.003 g/L, ACS reagent, Merck, Poland) and excess hypochlorite, produces indophenol blue. The absorbance of this product at 630 nm is proportional to the original ammonium concentration. This is similar to the salicylate method using the SEAL analytical autoanalyzer where a blue-green colored complex is

measured at 660 nm. This complex was formed by mixing the NH_4^+-containing sample in a segmented flow system containing the following: (line 1): 300 g/L sodium salicylate (≥ 99.5%, Sigma-Aldrich, China); (line 2): 2 g/L sodium dichloroisocyanurate (≥98%, Aldrich, Japan) + 35 g/L NaOH (≥98%, Aldrich, Japan) and (line 3): 30 g/L ethylenediaminetetraacetic acid (>99%, Sigma-Aldrich, Sweden) + 120 g/L sodium citrate (>99%, Merck, Germany) + 0.5 g/L sodium nitroprusside (ACS reagent, Merck, Poland) + 1.5 mL Brij-35 solution (30%, Merck, Germany). Nitrate, on the other hand, is first reduced to NO_2^- by passage of the sample through a copperized cadmium column. The NO_2^- is determined by diazotization with sulfanilamide (0.04 g/L, GR grade, Merck, Germany) under acidic conditions to form the diazonium ion. The resulting diazonium ion was coupled with *N*-(1-naphthyl)-ethylenediamine dihydrochloride (0.001 g/L, GR grade, Merck, Germany) and the absorbance of the resulting pink dye was measured at 520nm (Lachat) or 550 nm (SEAL). Nitrate concentrations were then obtained by subtracting nitrite that was originally present in the solution from the sum of nitrite and reduced nitrate.

Methanesulfinic (MSIA) and methanesulfonic acids (MSOA) were quantified using the same ion chromatography system used for NO_3^-. The analyses were performed with a flow of 1 mL/min, 40 µL injection volume, 100 mA current, and gradient elution of KOH: 2 mM from 0 – 16 min, 40 mM from 16 – 22 min. The method detection limits for MSIA and MSOA were 6.5 µM (standard deviation = 2 µM, n = 7 (10 µM), measuring range = 10 – 100 µM) and 0.22 µM (standard deviation = 0.07 µM, n = 7 (10 µM), measuring range = 1 – 100 µM), respectively. MSIA (95%) and MSOA (>99.5%) stock solutions were obtained from Alfa Aesar (Germany) and Sigma-Aldrich (France), respectively.

Dissolved organic carbon (DOC) and dissolved organic nitrogen (DON) were measured using a Shimadzu TOC-L total organic carbon analyzer with a TNM-L total nitrogen analyzer and ASI-L autosampler (Shimadzu, Kyoto, Japan). Dissolved organic nitrogen (DON) was calculated as the difference between total nitrogen and the sum of inorganic nitrogen species (ammonium, nitrite and nitrate). To minimize the impact of inorganic nitrogen on the accuracy of DON measurements in the wastewater effluent sample, its DON was measured after a 5-day dialysis using cellulose ester dialysis membranes (Spectra/Por Biotech, 20 mm diameter, 100-500 Da molecular weight cutoff).

pH was measured before and after ozonation using a Metrohm 827 pH meter (Metrohm, Switzerland) calibrated with Certipur buffer solutions (Merck, Germany).

4.2.2. Water samples

Tables 4.1 – 4.2 show the characteristics of the water samples used in this study. The surface water sample was taken after coagulation and sedimentation in a drinking water treatment plant in South East Queensland (SEQ), Australia. A wastewater effluent sample was obtained from the conventional non-nitrifying Vidy plant in Lausanne, Switzerland. This sample was immediately filtered through a 0.45 µm nylon filter (Membrane Solutions, Switzerland) after collection, and stored at 4 °C until use. NOM standard solutions (10 mg C/L) were prepared using Suwannee River humic acid II (SRHA, 2S101H) and Pony Lake fulvic acid (PLFA, 1R109F) obtained from the International Humic Substances Society (IHSS, MN, USA). These samples were chosen to represent NOM with differing properties.

Synthetic DON solutions containing a mixture of glycine (≥98.5%, Sigma-Aldrich, USA), tannic acid (ACS reagent, Sigma-Aldrich, USA), methanol (MeOH, ≥99.9%, Carlo Erba, Italy) and tertiary butanol (t-BuOH, ≥99.7%, Sigma-Aldrich, Germany) were also used (Table 4.3). Solutions with trimethylamine (98%, Sigma-Aldrich, USA) and dimethylamine (40% in water, Sigma-Aldrich, USA) as DON source were also prepared (Table 4.3).

Table 4.1. Water sample characteristics

Source	Type	DOC, mg L^{-1}	UV 254, cm^{-1}	DON, mg/L	NO_2^-, mg/L	NO_3^-, mg/L	NH_4^+, mg/L
South East QLD, Australia	Surface water (after coagulation)	18.7 ± 1.0	0.32 ± 0.02	0.65 ± 0.04	0.0018 ± 0.0002	0.030 ± 0.003	0.015 ± 0.001
Vidy, Lausanne, Switzerland	Wastewater effluent	10.9 ± 0.2	0.129 ± 0.003	0.52*	0.025	0.046 ± 0.002	40.3 ± 0.1

**measured after dialysis; error depicts standard deviation of triplicate measurements.*

Table 4.2. Selected properties of SRHA and PLFA[a]

Properties	SRHA	PLFA
%C	52.63	52.47
%N	1.17	6.51
% Aromaticity	31	12
Phenolic content, meq/g-C	3.72	1.75
Specific UV absorbance,[b] L/mg-C·m	7.0	2.5

[a]*Taken from IHSS (2016) http://www.humicsubstances.org/elements.html);*
[b]*Taken from Wenk et al. (2013)*

4.2.3. Experimental conditions

This study was composed of three parts as summarized in Table 4.3, where the experimental conditions are provided. Further details describing each experiment are provided below.

4.2.3.1. Ammonium and nitrate evolution during ozonation of real water samples

Ozone dosing experiments were conducted with waters containing NOM standards (250 mL), surface water (250 mL), or wastewater effluent (100 mL) to investigate ammonium and nitrate formation during ozonation. The effect of increasing specific ozone doses (0.4 – 1.3 mg O_3/mg DOC) was first studied using SRHA and PLFA at 10 mg/L DOC at pH 7. In addition to the specific ozone dose, the effect of O_3 exposure was also investigated for real water samples by applying ozone destabilizing (e.g., high pH, addition of radical chain initiators (H_2O_2) and promoters (MeOH)) and stabilizing conditions (e.g., low pH, addition of radical scavengers such as t-BuOH or bicarbonate) (Table 4.3, part 1). For the surface water sample, differing ozonation conditions (specific O_3 dose (0.4 – 1.0 mg O_3/mg DOC), pH (6 – 8), inorganic carbon (0.01 – 5 mM HCO_3^-), addition of tBuOH (10 mM) and H_2O_2 (0.4 mM)) were applied. For the wastewater effluent, controlling the O_3 decay by varying the pH was difficult due to precipitation of phosphate salts at buffer concentrations of >1 mM. Thus, to control the O_3 decay for the wastewater effluent (pH 7), concentrations of t-BuOH ($^{\bullet}$OH inhibitor) and MeOH ($^{\bullet}$OH promoter) were instead varied at specific O_3 doses of 0.7 – 2.9 mg O_3/mg DOC. In these experiments, concentrations of t-BuOH and MeOH were changed while maintaining a constant $^{\bullet}$OH scavenging rate. The $^{\bullet}$OH scavenging rate (Elovitz and von Gunten 1999) is defined as the $\sum k_{Si}[S_i]$, where k_{Si} is the individual second-order rate constant for the reaction of $^{\bullet}$OH with a specific scavenger (e.g., DOC, t-BuOH, MeOH) and $[S_i]$ the scavenger concentration. The wastewater effluent, for example, had a total $^{\bullet}$OH scavenging rate of 1.4×10^6 s^{-1} calculated from the sum of the products of: $k_{^{\bullet}OH+DOC}$ (2.5×10^4 $(mg/L)^{-1}s^{-1}$) × [DOC] (6.7 mg/L) + $k_{^{\bullet}OH+tBuOH}$ (6×10^8 $M^{-1}s^{-1}$) × [t-BuOH] (1.87×10^{-3} M) + $k_{^{\bullet}OH+MeOH}$ (1×10^9 $M^{-1}s^{-1}$) × [MeOH] (1.2×10^{-4} M) + $k_{^{\bullet}OH+pCBA}$ (5×10^9 $M^{-1}s^{-1}$) × [*p*CBA] (1×10^{-6} M). More details are shown in Table 4.4.

Aside from dosage experiments, kinetic studies to determine the O_3 exposure were also conducted for the surface water and wastewater effluent samples. O_3 exposure of the surface water sample (250 mL, pH 7) was determined at various specific ozone doses (0.4 – 1.5 mgO_3/mgDOC) and H_2O_2 concentrations (0.04 – 0.17 mM H_2O_2). For the wastewater sample (100 mL, pH 7), O_3 decay was monitored using the same conditions mentioned earlier (specific O_3 dose = 0.7 – 2.9 mgO_3/mgDOC, pH 7, varying t-BuOH/MeOH).

Table 4.3. Summary of experimental conditions

Sample	Baseline conditions	Experimental conditions
1. Nitrate and ammonium evolution during ozonation of NOM standards and real water samples		
SRHA and PLFA (IHSS)	DOC = 10 mg/L pH = 7 (1 mM phosphate)	Specific O_3 doses: 0.4, 0.8, 1, 1.3 $mgO_3/mgDOC$
Surface water (SEQ, Australia)	DOC = 18 mg/L O_3 = 0.75 mg O_3/mgDOC pH = 7 (1 mM phosphate) Inorganic carbon = 0.01 mM HCO_3^-	Specific O_3 doses = 0, 0.4, 0.75, 1 $mgO_3/mgDOC$ pH = 6, 7, 8 Inorganic carbon = 0.01, 5 mM HCO_3^- t-BuOH = 10 mM; H_2O_2 = 0.4 mM
Wastewater effluent (Lausanne, Switzerland)	DOC = 6.7 mg/L (after dilution) pH = 7 (1 mM phosphate) pCBA = 1 µM	Specific O_3 doses = 0.7, 1.4, 1.9, 2.4, 2.9 $mgO_3/mgDOC$; [t-BuOH (µM)]/[MeOH (µM)]= 1870/120, 1250/500, 840/750, 420/1000 Constant $^{\bullet}OH$ scavenging rate = 1.4×10^6 s^{-1}
2. Nitrate yield determination from different amines		
Glycine (primary amine) Dimethylamine (secondary amine) Trimethylamine (tertiary amine)	Amine = 20 µM; O_3 = 400 µM pH 7 (5mM phosphate) tannic acid = 3.3 µM pCBA = 1 µM	[t-BuOH (µM)]/[MeOH (µM)]= 1870/120, 1250/500, 840/750, 420/1000 Constant $^{\bullet}OH$ scavenging rate = 1.33×10^6 s^{-1}
3. Nitrate and ammonium formation using glycine		
Kinetics of NO_3^- formation from glycine	Glycine = 20 µM; O_3 = 400 µM t-BuOH = 2.1 mM pH 7 (10 mM phosphate)	Samples were obtained and quenched with 1 mM thiosulfate at different reaction times (until 50 min).
$^{\bullet}OH$ yield determination (DMSO assay)	Glycine = 100 mM; DMSO = 10 mM; pH 7 (10 mM phosphate)	O_3 doses: 100, 175, 250, 325, 400 µM
Model DON solution (high $^{\bullet}OH$ scavenging)	glycine = 20 µM tannic acid = 3.3 µM pCBA = 0.5 µM pH = 7 (5 mM phosphate)	Constant $^{\bullet}OH$ scavenging rate = 1.3×10^6 s^{-1} [t-BuOH (µM)]/[MeOH (µM)] = 1875/125, 1460/375, 1045/625, 730/815, 417/1000 O_3 doses: 200, 300, 400 µM
Model DON solution (low $^{\bullet}OH$ scavenging)	glycine = 20 µM tannic acid = 3.3 µM pCBA = 1 µM pH = 7 (5 mM phosphate)	Constant $^{\bullet}OH$ scavenging rate = 1.8×10^5 s^{-1} [t-BuOH (µM)]/[MeOH (µM)] = 150/10, 116/30, 84/50, 59/65, 43/74 O_3 doses: 200, 250, 300, 350, 400 µM

**All experiments were performed at 22±1 °C*

Table 4.4. Wastewater effluent sample composition, their respective •OH scavenging rates and the relative contribution of the various components to the overall scavenging.

Contents	Condition 1	Condition 2	Condition 3	Condition 4
tBuOH, µM	1870	1250	840	420
MeOH, µM	120	500	750	1000
DOC[a], mg/L	6.7	6.7	6.7	6.7
pCBA, µM	1	1	1	1
Scavenging rates[b]	Condition 1	Condition 2	Condition 3	Condition 4
tBuOH, s^{-1}	1.1×10^{6}	7.5×10^{5}	5.0×10^{5}	2.5×10^{5}
MeOH, s^{-1}	1.2×10^{5}	5.0×10^{5}	7.5×10^{5}	1.0×10^{6}
DOC, s^{-1}	1.7×10^{5}	1.7×10^{5}	1.7×10^{5}	1.7×10^{5}
pCBA, s^{-1}	5.0×10^{3}	5.0×10^{3}	5.0×10^{3}	5.0×10^{3}
total scavenging rate, s^{-1}	1.4×10^{6}	1.4×10^{6}	1.4×10^{6}	1.4×10^{6}
% OH scavenging[c]	Condition 1	Condition 2	Condition 3	Condition 4
tBuOH	79.3	52.7	35.3	17.7
MeOH	8.5	35.1	52.6	70.2
DOC	11.8	11.8	11.7	11.8
pCBA	0.4	0.4	0.4	0.4
Total scavenging	100	100	100	100

[a] DOC after dilution with O_3; [b] $k_{S+\bullet OH}[S]$; [c] $100\times (k_{S+\bullet OH}[S])/(\text{total scavenging rate})$; pH = 7. The following rate constants were obtained from von Sonntag and von Gunten (2012): $k_{MeOH+\bullet OH} = 1\times10^{9}\ M^{-1}s^{-1}$; $k_{t\text{-}BuOH+\bullet OH} = 6\times10^{8}\ M^{-1}s^{-1}$; $k_{DOC+\bullet OH} = 2.5\times10^{4}\ mg\cdot L^{-1}s^{-1}$; $k_{pCBA+\bullet OH} = 5\times10^{9}\ M^{-1}s^{-1}$.

4.2.3.2. Investigation of the formation of inorganic nitrogen compounds from various amines

The amines (20 µM) glycine, dimethylamine, and trimethylamine were ozonated in excess of ozone (400 µM) to determine the main DON moieties for NO_3^- and NH_4^+ formation (total volume = 100 mL) (Table 4.3, part 2). An excess of O_3 relative to the amines was used to simulate conditions encountered by DON in actual water treatment. The O_3 doses used in these experiments were within the range commonly applied in wastewaters (5 – 20 mg/L O_3) (von Sonntag and von Gunten 2012). Tannic acid (3 mg C/L) was also added to the solutions to mimic the reactivity of phenolic moieties that are present

in NOM and to ensure that the amino groups are not the main consumers of O_3 similar to real water samples. This was demonstrated in the relatively similar O_3 decay kinetics of 3 mg C/L tannic acid solutions with and without glycine (Figure 4.2). O_3 exposure was then controlled by using varying ratios of t-BuOH/MeOH. These experiments were performed to identify the main amine precursors of NO_3^- and NH_4^+.

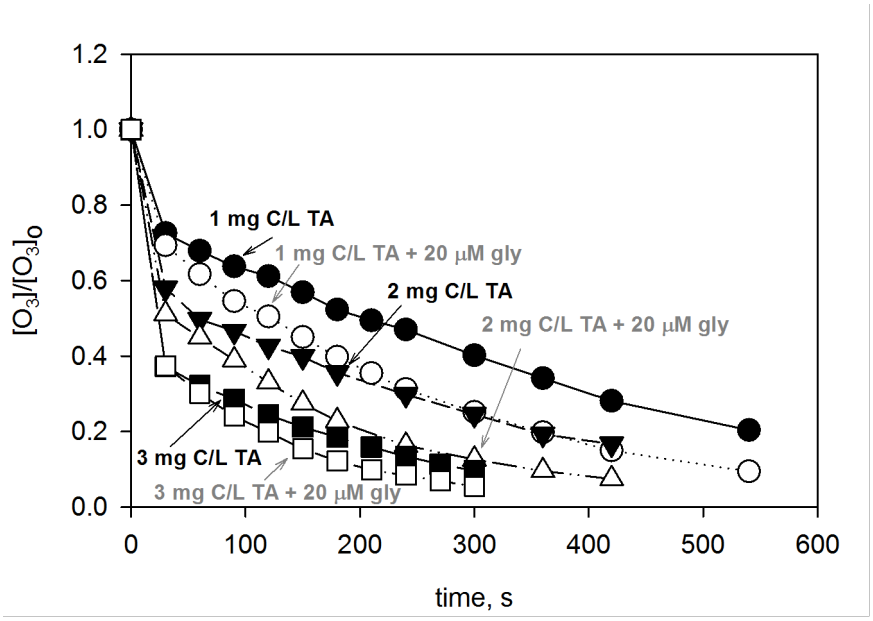

Figure 4.2. Ozone decay in tannic acid solutions with and without glycine. Conditions: O_3 dose = 200 μM, tannic acid = 1 – 3 mgC/L, glycine (only if added, open symbols) = 20 μM, pH = 7 (5 mM phosphate), tBuOH = 1.88 mM, MeOH = 0.13 mM, temperature = 20 ^{0}C.

4.2.3.3. Experiments with glycine as DON model surrogate

This experiment involved 3 components (Table 4.3, part 3): (1) kinetics of NO_3^- formation during ozonation of glycine-containing water, (2) determination of $^{\bullet}OH$ yield from the reaction of ozone with glycine, and (3) NO_3^- and NH_4^+ formation from glycine at differing ozonation conditions.

(1) 100 mL solutions containing 20 μM glycine and 2.1 mM t-BuOH (~100% $^{\bullet}OH$ scavenging) were ozonated with 400 μM O_3 for 50 min. Two 1 mL sample aliquots were obtained (using a bottle-top dispenser, Brand Dispensette III, Germany) at every desired reaction time (0.5, 1, 2, 3, 5, 7, 10, 15, 20, 25, 30, 35, 40, 50 min) in 15 mL centrifuge tubes, one containing indigotrisulfonate for O_3 concentration measurements and the other containing sodium thiosulfate to quench ozone for NO_3^- analyses.

(2) The •OH yield was determined using the dimethylsulfoxide (DMSO) assay (Flyunt et al. 2003, Tekle-Rottering et al. 2016). In this assay, methanesulfinic (MSIA) and methanesulfonic (MSOA) acids were measured to quantify •OH. The •OH yield was calculated from the slope of the plot of the sum of MSIA and MSOA against the O_3 dose. Glycine (100 mM) and DMSO (10 mM, ≥99.9%, Sigma-Aldrich, France) were in large excess over O_3 (0.1 – 0.4 mM) (total volume = 100 mL). For these conditions, glycine consumed 99.5% of O_3 while DMSO scavenged 97.7% of •OH.

(3) The changes in concentrations of NO_3^- and NH_4^+ during ozonation were investigated in 100 mL solutions containing 20 µM glycine, 3 mg C/L as tannic acid, and varying ratios of t-BuOH and MeOH. Two •OH scavenging rates, namely 1.3×10^6 s^{-1} and 1.8×10^5 s^{-1}, were used to test the concept over a wide range of •OH scavenging and R_{ct} (10^{-10} – 10^{-7}). These experiments aimed to mimic •OH scavenging rates representative for natural systems. O_3 dosing experiments were first performed to monitor NO_3^- and NH_4^+ formation at differing O_3 doses (0.2 – 0.4 mM) and •OH scavenging of t-BuOH. Kinetic experiments were also conducted to determine the pseudo-first-order O_3 decay constant (k_{obs}) and R_{ct} (equation 4.1; exposure ratio of •OH and O_3, section 2.6.1) (Elovitz and von Gunten 1999) which are parameters needed for kinetic simulations. The k_{obs} and R_{ct} values from each treatment condition were included in the simulation to account for the effect of O_3 stability (e.g., rate of O_3 decay to •OH, O_2, and other products) on the elementary reactions of glycine oxidation by O_3. Due to experimental limitations, k_{obs} and R_{ct} for the fast initial ozone consumption were excluded.

To determine the O_3 decay constant, the logarithm of the relative decrease of the O_3 concentration was plotted against reaction time. The slope of this plot yields the pseudo-first-order O_3 decay constant. To calculate R_{ct} (equation 4.1), •OH exposure ($\int[^{\bullet}OH]dt$) was first determined by following the kinetics of *p*CBA decay (equation 4.2). By substituting equation 4.1 to equation 4.2, the R_{ct} can be calculated from a plot of $\ln[pCBA]/[pCBA]_0$ versus O_3 exposure ($\int[O_3]dt$). Example plots of O_3 decay and R_{ct} are shown in Figure 4.3.

$$R_{ct} = \frac{\int[\cdot OH]dt}{\int[O_3]dt} \qquad \text{(eq. 4.1)}$$

$$-\ln\left(\frac{[pCBA]}{pCBA_0}\right) = k_{(\cdot OH+pCBA)} \int[\cdot OH]dt \qquad \text{(eq. 4.2)}$$

$$-\ln\left(\frac{[pCBA]}{pCBA_0}\right) = k_{(\cdot OH+pCBA)} R_{ct} \int[O_3]dt \qquad \text{(eq. 4.3)}$$

Kinetic simulations of NO_3^- and NH_4^+ concentrations were performed using the Kintecus software (www.kintecus.com) (Ianni 2003).

All experiments were performed in batch systems by injecting the appropriate volumes of an O_3 stock solution (using a Fortuna Optima glass syringe) into the stirred water samples to reach the desired ozone dose. To maintain a constant pH (± 0.2) during ozonation, the samples were buffered with phosphate (1 – 10 mM) adjusted to the desired pH.

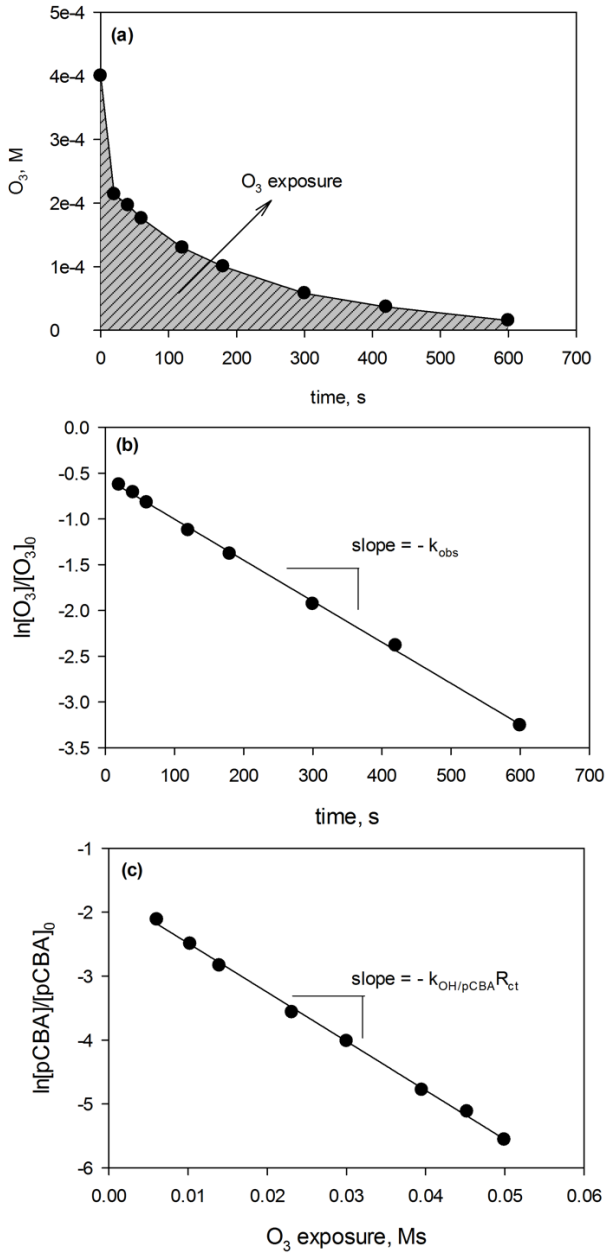

Figure 4.3. O_3 decay kinetics in a synthetic DON water sample. (a) O_3 decomposition as a function of time (shaded area shows the O_3 exposure); (b) determination of pseudo-first-order rate constant (k_{obs}) of O_3 decay; (c) R_{ct} plot for the ozonation experiment. R_{ct} is equal to the slope divided by $-k_{\bullet OH/pCBA}$ = 5×10^9 $M^{-1}s^{-1}$. Conditions: O_3 dose = 400 µM, glycine = 20 µM, tannic acid = 3 mgC/L, pCBA = 2 µM, t-BuOH = 150 µM, MeOH = 10 µM, pH = 7 (5 mM phosphate).

4.3. Results and Discussion

4.3.1. Ozonation of DON and formation of inorganic nitrogen compounds

Figure 4.4 shows the effects of specific ozone doses ($mgO_3/mgDOC$) and various ozonation conditions on NO_3^- and NH_4^+ formation from NOM standards (SRHA and PLFA), surface water, and wastewater effluent samples. Overall, it is apparent that NO_3^- generally increases with increasing specific O_3 doses.

For the NOM standards (Figure 4.4a), NO_3^- from SRHA (C/N = 44.9 (IHSS 2016)) increased from 0.5 – 1.3 μM for an increase of the specific ozone dose from 0.4 – 1.3 $mgO_3/mgDOC$. At the same specific ozone doses, higher yields of NO_3^- were observed for PLFA (1.5 – 4.5 μM) in agreement with the higher relative content of DON (C/N = 8.1 (IHSS 2016)). Figure 4.4a shows that NH_4^+ in the SRHA experiments did not change significantly while for PLFA, NH_4^+ increased by 75% when increasing the specific O_3 doses from 0.4 to 1.3 $mgO_3/mgDOC$. Similar to the results for nitrate, these findings might be explained by the higher nitrogen content of PLFA relative to SRFA.

Previous studies have shown the significance of $^{\bullet}OH$ reactions in driving NH_4^+ formation from amino acids such as glycine (Berger et al. 1999, Karpel Vel Leitner et al. 2002). However, those studies are not comparable to the current study as their $^{\bullet}OH$ transient concentrations were significantly higher because of the use of continuous ozonation (combined with H_2O_2), UV/H_2O_2, or γ-radiolysis. For example, steady-state $^{\bullet}OH$ concentrations of about 5×10^{-12} – 7×10^{-12} M were estimated from a γ-radiolysis study of glycine (i.e., with N_2O or H_2O_2, dose = 2000, 5000, 8000 Gy, average dose rate = 71.6 Gy/min) for reaction times of about 30 – 110 min (Karpel Vel Leitner et al. 2002). In the current study, $^{\bullet}OH$ radicals were only short-lived with expected maximum transient concentrations of about ≤ 10^{-12} M (Elovitz and von Gunten 1999) . Due to these low $^{\bullet}OH$ concentrations, combined with the low reactivity of amines with $^{\bullet}OH$ at neutral pH (e.g., $k_{(^{\bullet}OH+glycine)} = 2.15\times10^7$ $M^{-1}s^{-1}$ at pH 7 (Buxton et al. 1988)), it is unlikely that $^{\bullet}OH$ from O_3 decay significantly contributes to NH_4^+ formation. Without oxidation by $^{\bullet}OH$, NH_4^+ can be possibly formed from the reaction of O_3 via an electron-transfer pathway to produce *N*-centered radicals and an ozonide ($RCH_2\text{-}NH_2 + O_3 \rightarrow RCH_2\text{-}^{\bullet}NH + HO_3^{\bullet}$). The *N*-centered radicals could undergo rearrangement to C-centered radicals ($RCH_2\text{-}^{\bullet}NH \rightarrow R\text{-}^{\bullet}CHNH_2$), which in the presence of oxygen form peroxyl radicals ($R\text{-}^{\bullet}CHNH_2 + O_2 \rightarrow R\text{-}(^{\bullet}OO)CHNH_2$) (von Sonntag and von Gunten 2012). This is followed by a loss of superoxide, formation of imine intermediates ($R\text{-}(^{\bullet}OO)CHNH_2 \rightarrow R\text{-}CH{=}NH_2^+ + O_2^{\bullet-}$), and hydrolysis to NH_4^+ ($R\text{-}CH{=}NH_2^+ + H_2O \rightarrow NH_4^+ + R\text{-}CHO$). For both NOM standards, NO_3^- concentrations were somewhat lower than NH_4^+ possibly due to rapid O_3 decomposition (i.e., no O_3 residual was measured at the first sampling time

of 30 s) leaving insufficient O_3 exposure for oxidation of intermediates to NO_3^-. Because fulvic and humic acid standards may not represent O_3 decomposition kinetics induced by NOM in real waters (Elovitz et al. 2000b), further experiments were performed using surface water and wastewater effluent samples.

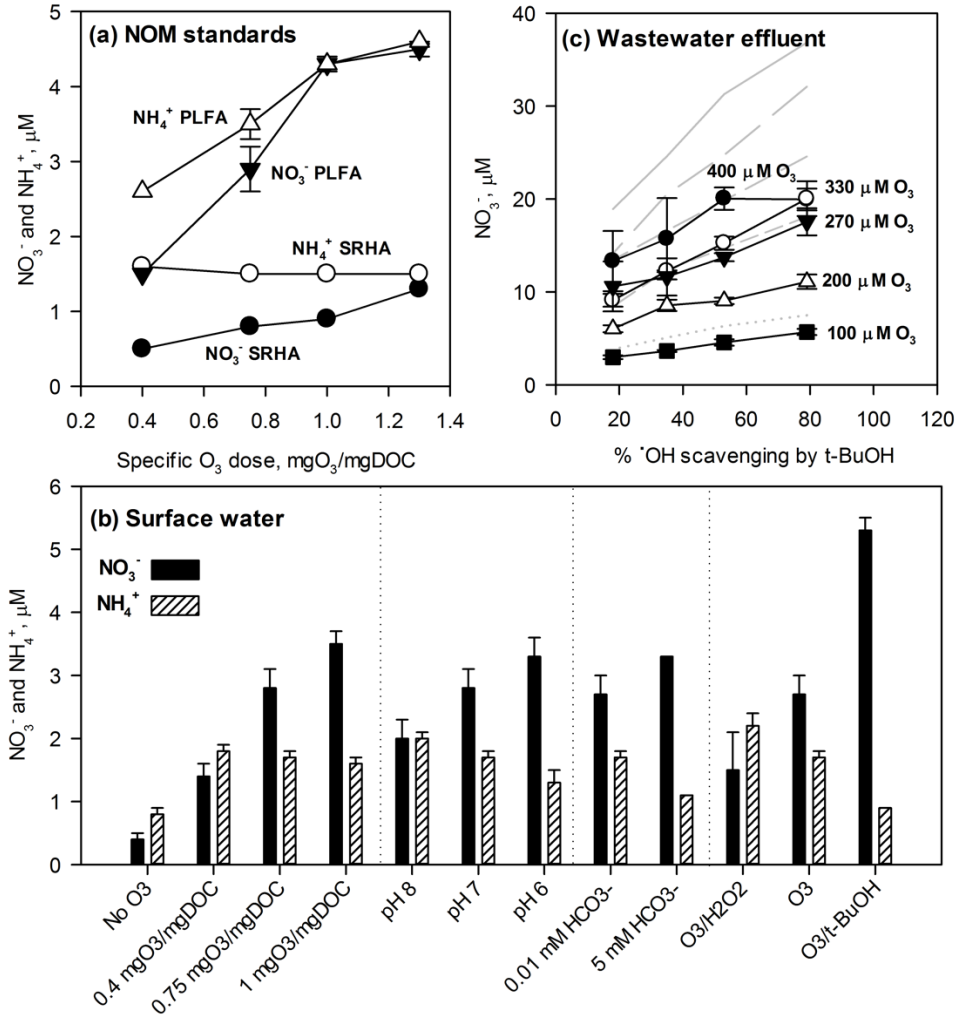

Figure 4.4. NO_3^- and NH_4^+ formation during ozonation of various synthetic and natural waters at differing (a) specific O_3 doses (Suwannee River humic acid (SRHA) or Pony Lake fulvic acid (PLFA)), (b) ozonation conditions (surface water), and (c) % $^{\bullet}$OH scavenging (wastewater effluent). Symbols in (c) are corrected NO_3^- concentrations (i.e., total measured NO_3^- (gray lines) minus predicted NO_3^- from NH_3 oxidation (Table 4.5)). Baseline conditions for NOM standards: DOC = 10 mg/L, DON (SRHA) = 0.26 mg/L, DON (PLFA) = 0.95 mg/L; for surface water: DOC = 18.7 ± 1.0 mg/L, DON = 0.65 ± 0.04 mg/L, specific O_3 dose = 0.75 $mgO_3/mgDOC$, pH = 7, inorganic carbon = 0.01 mM HCO_3^-, NO_3^- = 0.03 mg/L, NH_4^+ = 0.015 mg/L; for wastewater effluent: DOC = 6.7 mg/L, DON = 0.33 mg/L, pH = 7, inorganic carbon = 0.15 mM HCO_3^-, NO_3^- = 0.03 mg/L, NH_4^+ = 25.2 mg/L, $^{\bullet}$OH scavenging rate = 1.4×10^6 s^{-1}. Error bars depict standard deviations from 3 replicate experiments.

For the surface water sample (Figure 4.4b), differing conditions were used to vary the O_3 exposure including changes of the specific O_3 dose, pH, inorganic carbon, and addition of t-BuOH and/or H_2O_2. The results show that when the specific O_3 doses are increased from 0.4 – 1.0 $mgO_3/mgDOC$, the NO_3^- concentrations increase, while NH_4^+ concentrations change only slightly. The oxidation of NH_3/NH_4^+ to NO_3^- does not occur under these conditions because of the low reactivity of O_3 with NH_3/NH_4^+ at pH 7 ($k_{app} = 9.97\times10^{-2}$ $M^{-1}s^{-1}$, $pK_a = 9.3$) (Hoigné and Bader 1983, von Sonntag and von Gunten 2012) and low NH_3/NH_4^+ concentration of 0.8 µM. Thus, the observed changes in concentrations of inorganic nitrogen are assumed to result from the reactions of O_3 with DON moieties and the subsequent reactions. Conditions such as a decrease in pH, increase in alkalinity or addition of t-BuOH, which stabilize O_3, resulted in an increase in NO_3^-. In contrast, addition of H_2O_2 leads to a NO_3^- decrease because O_3 is less stable and transformed more quickly to $^{\bullet}OH$ under these conditions. Overall, these observations strongly suggest that O_3 reactions (and not $^{\bullet}OH$) are controlling NO_3^- formation.

The wastewater effluent sample had a very high background NH_3/NH_4^+ concentration of about 1400 µM and a low NO_3^- concentration of 0.5 µM. As such, after ozonation, changes in concentrations were only measureable for NO_3^- and not for NH_4^+. Because of the effluent's high NH_3/NH_4^+ concentrations, NH_3 oxidation was estimated to contribute 32 ± 7% to the observed NO_3^- concentrations (Table 4.5). The NO_3^- concentrations were then corrected (symbols in Figure 4.4c) to show NO_3^- evolution from the ozone oxidation of DON. Generally, similar trends as for the previous water samples were obtained for the corrected NO_3^- concentrations, i.e., increasing NO_3^- for higher specific O_3 doses and for increasing O_3 exposures, which were achieved by increasing the t-BuOH contribution to the overall $^{\bullet}OH$ scavenging. It should also be noted that the wastewater effluent contained NO_2^- at a concentration of 0.3 µM. However, even for the expected full oxidation of nitrite to nitrate, it has a negligible contribution to the observed NO_3^- levels in the range of 3 – 20 µM. Therefore, the effluent's DON is the major source of NO_3^- during ozonation.

Table 4.5. Predicting nitrate formation from ozonation of background ammonia in the wastewater effluent. Conditions: O_3 dose = 100 – 400 µM, pCBA = 1 µM, pH = 7, µM t-BuOH/ µM MeOH (%$^{\bullet}$OH scavenging by t-BuOH) = 420/1000 (18%), 840/700 (35%), 1250/500 (53%), 1870/120 (79%), total measured NH_3/NH_4^+ = 1397 µM (after dilution).

Note: The oxidation of NH_3/NH_4^+ (or $[NH_4^+]_{total}$) is given by: $\frac{-d[NH_4^+]_{tot}}{dt} = k_{\cdot OH}[\cdot OH][NH_4^+]_{tot} + k_{O_3}[O_3][NH_4^+]_{tot}$

$$= k_{\cdot OH}R_{ct}[O_3][NH_4^+]_{tot} + k_{O_3}[O_3][NH_4^+]_{tot}$$

$$\frac{[NH_4^+]_{tot}}{[NH_4^+]_{tot_0}} = \exp\left\{-\left(\int [O_3]\,dt\right)\left(k_{\cdot OH}R_{ct} + k_{O_3}\right)\right\}$$

where $k_{(O3+NH3)}$ at pH 7 = 9.97×10^{-2} $M^{-1}s^{-1}$ (Neta et al. 1988) and $k_{(\cdot OH+NH3)}$ at pH 7 = 4.49×10^{5} $M^{-1}s^{-1}$ (Buxton et al. 1988). NO_3^- formed from NH_3/NH_4^+ was calculated from the difference of $[NH_4^+]_{tot_0} - [NH_4^+]_{tot}$; $[NH_4^+]_{tot_0}$ = 1397 µM.

(a) 400 µM O_3

% $^{\bullet}$OH scavenging by t-BuOH	R_{ct}	∫[O_3]dt, Ms	$\frac{[NH_4^+]_{tot}}{[NH_4^+]_{tot_0}}$	$[NH_4^+]_{tot}$, µM	NO_3^-, µM (from NH_3)	Measured NO_3^-, µM
79	1.00×10^{-9}	0.121	0.988	1380	16.9	36.9
53	1.84×10^{-9}	0.080	0.992	1386	11.3	31.3
35	2.50×10^{-9}	0.063	0.994	1388	8.9	24.6
18	4.47×10^{-9}	0.040	0.996	1391	5.6	18.9

(b) 330 µM O_3

% $^{\bullet}$OH scavenging by t-BuOH	R_{ct}	∫[O_3]dt, Ms	$\frac{[NH_4^+]_{tot}}{[NH_4^+]_{tot_0}}$	$[NH_4^+]_{tot}$, µM	NO_3^-, µM (from NH_3)	Measured NO_3^-, µM
79	1.23×10^{-9}	0.086	0.991	1385	12.1	32.1
53	1.76×10^{-9}	0.068	0.993	1387	9.5	24.8
35	2.25×10^{-9}	0.059	0.994	1389	8.3	20.5
18	4.27×10^{-9}	0.036	0.996	1392	5.0	14.1

(c) 270 µM O_3

% $^{\bullet}$OH scavenging by t-BuOH	R_{ct}	∫[O_3]dt, Ms	$\frac{[NH_4^+]_{tot}}{[NH_4^+]_{tot_0}}$	$[NH_4^+]_{tot}$, µM	NO_3^-, µM (from NH_3)	Measured NO_3^-, µM
79	1.71×10^{-9}	0.050	0.995	1390	7.0	24.6
53	2.29×10^{-9}	0.044	0.996	1391	6.1	19.9
35	3.38×10^{-9}	0.035	0.996	1392	5.0	16.6
18	6.97×10^{-9}	0.020	0.998	1394	2.8	13.4

(d) 200 µM O_3

% $^{\bullet}$OH scavenging by t-BuOH	R_{ct}	∫[O_3]dt, Ms	$\frac{[NH_4^+]_{tot}}{[NH_4^+]_{tot_0}}$	$[NH_4^+]_{tot}$, µM	NO_3^-, µM (from NH_3)	Measured NO_3^-, µM
79	1.31×10^{-9}	0.050	0.995	1390	7.0	18.1
53	1.78×10^{-9}	0.041	0.996	1391	5.7	14.8
35	3.02×10^{-9}	0.027	0.997	1393	3.9	12.4
18	5.67×10^{-9}	0.017	0.998	1395	2.4	8.4

(e) 100 µM O_3

% $^{\bullet}$OH scavenging by t-BuOH	R_{ct}	∫[O_3]dt, Ms	$\frac{[NH_4^+]_{tot}}{[NH_4^+]_{tot_0}}$	$[NH_4^+]_{tot}$, µM	NO_3^-, µM (from NH_3)	Measured NO_3^-, µM
79	2.23×10^{-9}	0.013	0.999	1395	1.8	7.5
53	3.01×10^{-9}	0.013	0.999	1395	1.8	6.3
35	4.10×10^{-9}	0.010	0.999	1396	1.4	5.1
18	8.48×10^{-9}	0.006	0.999	1396	0.9	3.8

4.3.2. NO_3^- yields from model compounds (amines)

Some potential precursors of NO_3^- and/or NH_4^+ during ozonation of DON were investigated using the model compounds glycine, dimethylamine, and trimethylamine, representing primary, secondary, and tertiary amines, respectively. The ozone-reactive site for amines is the lone electron pair at the nitrogen atom, with a very low reactivity for protonated amines (von Sonntag and von Gunten 2012). At pH 7, the apparent second-order rate constants of the selected compounds with O_3 (Lee and von Gunten 2010, Neta et al. 1988) are as follows: glycine: $k_{app} = 1.63\times10^2$ $M^{-1}s^{-1}$ ($pK_a = 9.3$); dimethylamine: $k_{app} = 3.79\times10^3$ $M^{-1}s^{-1}$ ($pK_a = 10.7$); trimethylamine: $k_{app} = 6.49\times10^3$ $M^{-1}s^{-1}$ ($pK_a = 9.8$). The higher apparent second-order rate constant of trimethylamine over dimethylamine is due to the former's lower pK_a (von Sonntag and von Gunten 2012) leading to a higher reactive amine fraction (trimethylamine = 0.16%; dimethylamine = 0.02%). During ozonation, O_3 can add to the amine nitrogen forming an O_3-adduct ($R_3N + O_3 \rightarrow R_3N^+OOO^-$), followed by a release of singlet oxygen ($^1O_2$) (Muñoz et al. 2001). For tertiary amines, this reaction leads to an *N*-oxide ($R_3\text{-}N^+O^-$) formation with high yield, while for primary and secondary amines (e.g., propranolol), the *N*-oxide rearranges to a hydroxylamine (R-NOH) (Benner and Ternes 2009, von Sonntag and von Gunten 2012). Further oxidation of hydroxylamine can then produce NO_3^-, as observed in the present study.

Figure 4.5 shows the NO_3^- formation for the selected amines as a function of the $^{\bullet}OH$ scavenging rate. Glycine has the highest NO_3^- yield (i.e., mol NO_3^-/mol amine added) followed by trimethylamine and dimethylamine. At 85% $^{\bullet}OH$ scavenging by t-BuOH, the NO_3^- yield was 85% for glycine, 27% for trimethylamine and 24% for dimethylamine. The highest yield for NO_3^- was obtained for glycine despite having the lowest pseudo-first-order rate constant for its reaction with O_3 ($k_{(O3+amine)} \times$ [amine]) and highest R_{ct} (Table 4.6). Dimethylamine and trimethylamine solutions had lower R_{ct} values than glycine possibly due to their faster consumption during ozonation, resulting in higher O_3 residual concentrations and hence higher O_3 exposures. The high NO_3^- yield for glycine is due to the fact, that the reactions of primary amines with O_3 nearly exclusively yield NO_3^- as final product (Berger et al. 1999), while the reaction with higher substituted amines also gives rise to other stable nitrogen-containing products (Elmghari-Tabib et al. 1982, Muñoz and von Sonntag 2000). For secondary amines such as diethylamine, it was reported that the O_3 reaction occurs predominantly via the formation of an amine-oxyl radical ($R_2\text{-}NO^{\bullet}$, 80%) (von Gunten 2003a). From this amine-oxyl radical, nitrone ($R_2{=}N^+O^-$) can be formed which hydrolyzes to ethyl hydroxylamine. This product can be further oxidized to NO_3^- in excess of O_3 (von Gunten 2003a). The slightly higher NO_3^- yield of trimethylamine compared to dimethylamine could be a result of the compound's higher apparent

second-order rate constant and the predominance of oxygen transfer (*N*-oxide formation) over electron-transfer reactions (amine radical cation formation). The predominance of *N*-oxide formation has also been shown in other tertiary amines such as ethylenediamine tetraacetic acid, nitrilotriacetic acid, tramadol, and clarithromycin (Lange et al. 2006, Muñoz and von Sonntag 2000, Zimmermann et al. 2012).

In our experiment, NH_4^+ from electron-transfer reactions was only observed for glycine (0.6 – 1.2 µM, equivalent to yields of 3% – 6% µM NH_4^+/µM glycine added). No NH_4^+ was detected for dimethylamine and trimethylamine because of the higher degree of alkylation. The hydrolysis of the imine intermediate would consequently result in lower substituted amines (e.g., tertiary to secondary amines (Muñoz and von Sonntag 2000)) instead of NH_4^+.

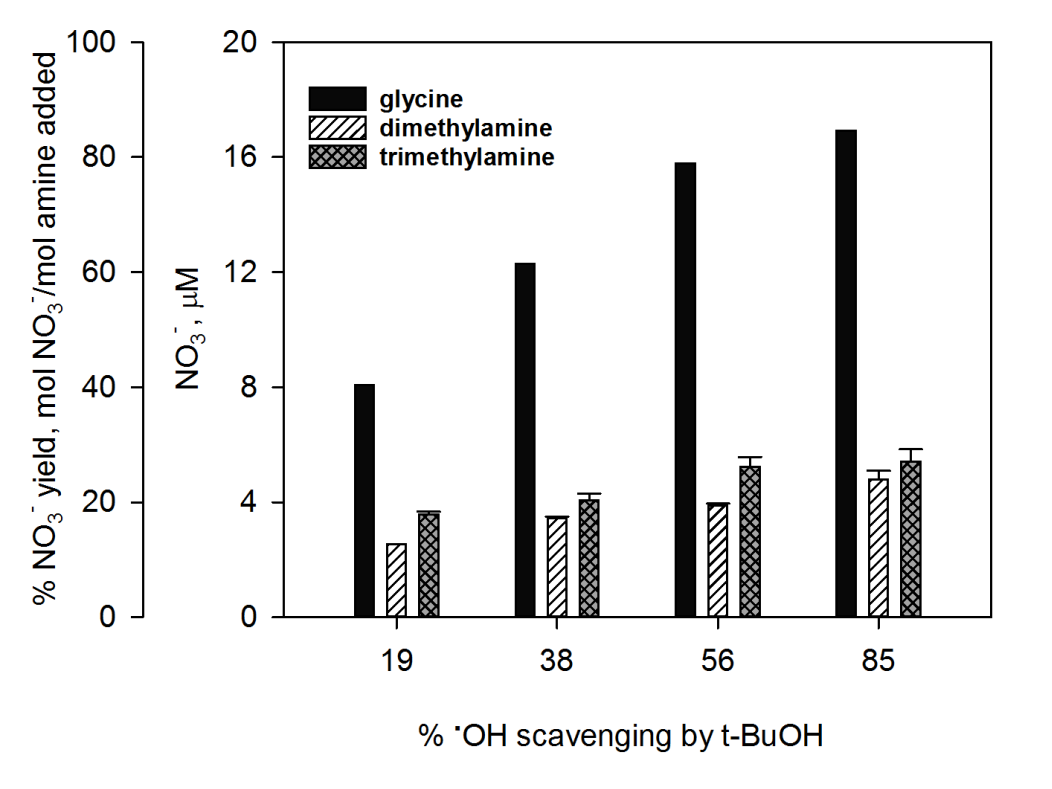

Figure 4.5. NO_3^- formation from the reactions of ozone with glycine, dimethylamine, and trimethylamine as a function of the %•OH scavenging by t-BuOH. Conditions: amine concentration = 20 µM, tannic acid = 3 mg C/L, pH = 7, O_3 dose = 400 µM, •OH scavenging rate = 1.33×10^6 s^{-1}, µM t-BuOH/ µM MeOH (%•OH scavenging by t-BuOH) = 420/1000 (19%), 840/750 (38%), 1250/500 (57%), 1870/120 (85%). Error bars depict the mean absolute deviation (n=2).

Table 4.6. Comparison of R_{ct} and NO_3^- yield during ozonation of glycine, dimethylamine, and trimethylamine. Conditions: amine = 20 μM, O_3 = 400 μM, pH = 7.

% $^{\bullet}$OH scavenging by tBuOH	tBuOH, μM	MeOH, μM	R_{ct} (% nitrate yield (μM NO_3^-/μM amine))		
			Glycine	Dimethylamine	Trimethylamine
85	1870	120	9.70×10^{-10} (85)	6.22×10^{-10} (24)	2.61×10^{-10} (27)
57	1250	500	2.42×10^{-9} (79)	1.08×10^{-9} (19)	5.64×10^{-10} (26)
38	840	750	3.44×10^{-9} (62)	1.90×10^{-9} (17)	8.34×10^{-10} (20)
19	420	1000	7.08×10^{-9} (40)	5.19×10^{-9} (13)	2.10×10^{-10} (18)

4.3.3. NO_3^- formation kinetics from glycine

To further elucidate NO_3^- formation from glycine, ozonation was performed with solutions containing glycine and t-BuOH (complete scavenging of $^{\bullet}$OH). As shown in Figure 4.6a, upon ozonation, the simulated glycine concentration decreases rapidly (pH 7: $k_{gly,O3}$ = 1.63×10^2 $M^{-1}s^{-1,}$ $t_{1/2}$ = $0.69/(k_{gly,O3}\int[O_3]dt)$ = 0.02 s), while NO_3^- increases only slowly. This indicates that NO_3^- is produced from an intermediate species (referred to as X) and not directly from glycine. The rate of NO_3^- formation therefore depends on further oxidation of X. Assuming 100% conversion of glycine to X during ozonation, X_{max} (the maximal yield of X after glycine decomposition) can be estimated equal to $[glycine]_0$. Thus, X at time t (X_t) is equal to $X_{max} - NO_3^-$, and the rate constant for X abatement can be calculated using second-order kinetics. Plotting $\ln[X]_t/[X]_{max}$ versus O_3 exposure yields a linear plot (Figure 4.7) with a slope equal to the second-order rate constant of ozonation of X (k = 7.7 ± 0.1 $M^{-1}s^{-1}$), which corresponds to the formation of NO_3^-. Using this value, the experimentally measured NO_3^- was predicted relatively well (dotted line in Figure 4.6a) using kinetic simulations involving the following reactions: O_3 + glycine → hydroxylamine (k_{app} = 1.63×10^2 $M^{-1}s^{-1}$ (Neta et al. 1988)), hydroxylamine + O_3 → X (k_{app} = 2×10^4 $M^{-1}s^{-1}$ (Hoigné et al. 1985)), X + O_3 → NO_3^- (k_{app} = 7.7 $M^{-1}s^{-1}$), and O_3 → products (experimental first-order O_3 decay = 1.57×10^{-3} s^{-1}). The NO_3^- yield at full O_3 consumption (~50 min) showed a nearly complete mineralization of glycine to NO_3^-. Based on the mechanistic discussion below (Section 4.3.7), the oxime ($HON{=}CHCO_2^-$) formed during further oxidation of hydroxylamine may be a good candidate for X. This hypothesis, however, needs to be validated in future studies.

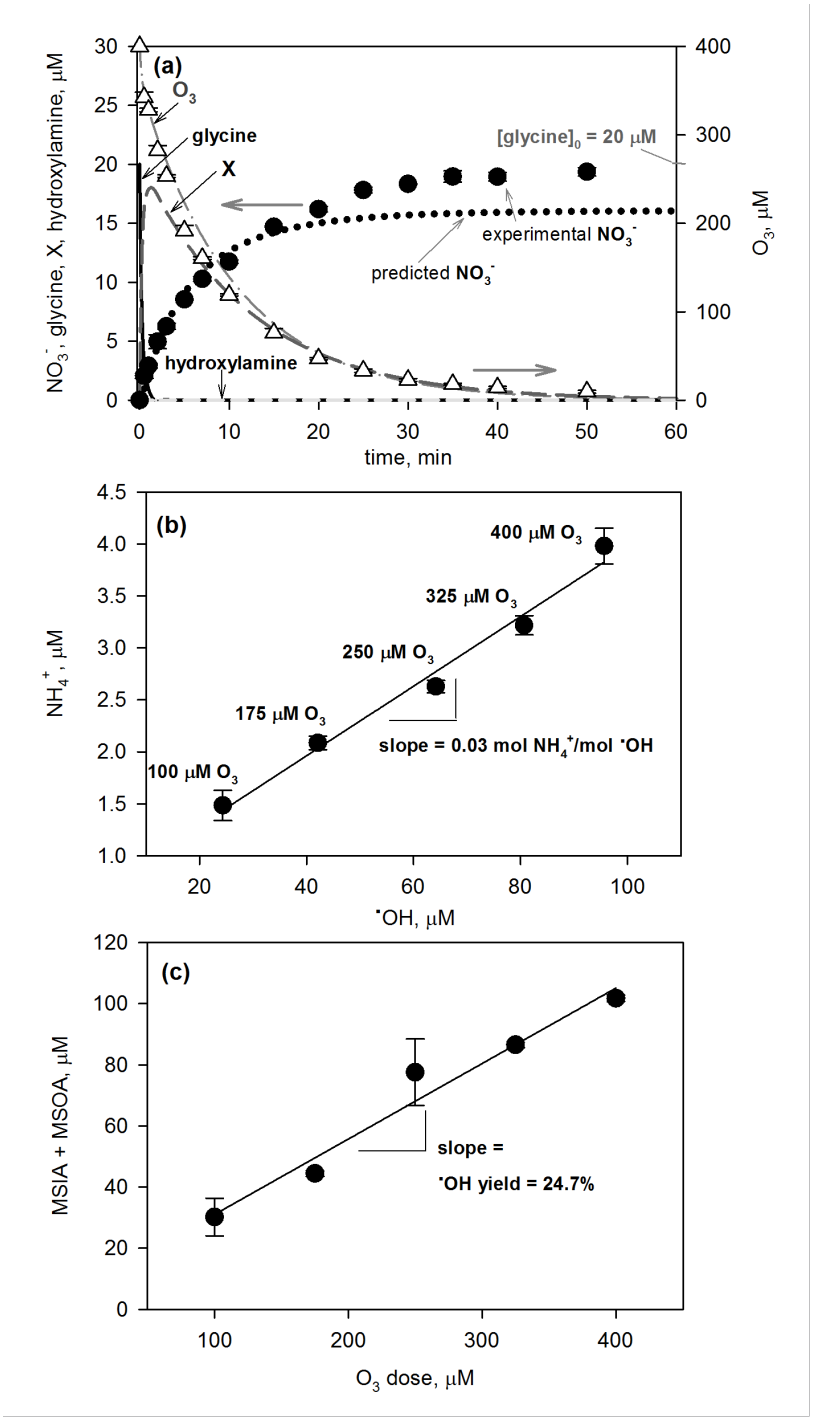

Figure 4.6. Reaction of glycine with ozone. (a) Formation of NO_3^- in excess of O_3 and complete $^{\bullet}OH$ scavenging by t-BuOH. Conditions: glycine = 20 µM, O_3 = 400 µM, pH = 7, t-BuOH = 2.1 mM, n = 2, symbols are the average experimental data and lines are from kinetic simulations (section 4.3.3). (b) Ammonium and $^{\bullet}OH$ concentrations for various ozone doses, correlation of NH_4^+ with $^{\bullet}OH$ formation. (c) Determination of $^{\bullet}OH$ yield by measurement of MSIA and MSOA as a function of the ozone dose. Conditions: glycine = 100 mM, DMSO = 10 mM, pH = 7. Error bars depict standard deviations from 3 replicate experiments.

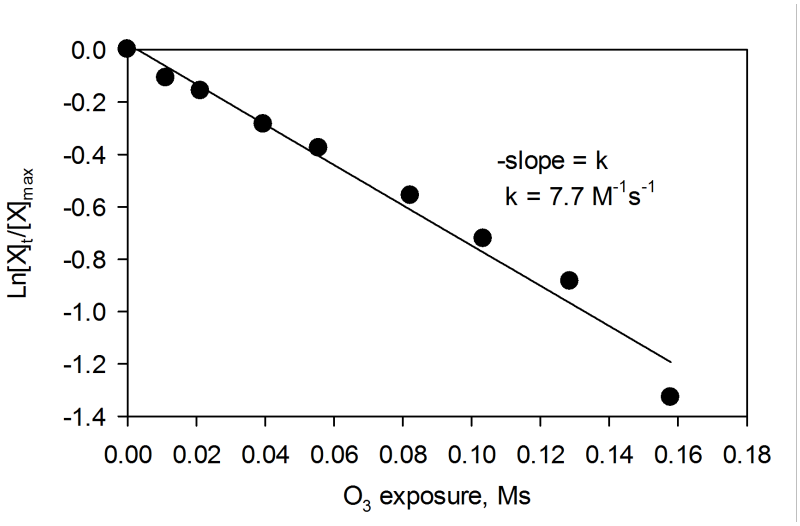

Figure 4.7. Determination of the second-order rate constant for the decrease of intermediate X. Assumption: X_{max} (maximal X after 100% glycine decomposition) = $[glycine]_0$ and X at time t (X_t) = X_{max} – experimental $[NO_3^-]$. NO_3^- was measured for the following reaction conditions: O_3 = 400 µM, glycine = 20 µM, pH = 7, t-BuOH = 2.1 mM (complete $^{\bullet}OH$ scavenging). The slope is the second-order rate constant of the reaction of X with O_3.

4.3.4. $^{\bullet}OH$ yield from the reaction of ozone with glycine

Figure 4.6b shows the NH_4^+ formed when excess of glycine (100 mM) was treated with 0.1 – 0.4 mM O_3. In contrast to previous product studies with glycine (Berger et al. 1999), NH_4^+ in the current study is not formed from the reaction of glycine with $^{\bullet}OH$. This is because at pH 7, the apparent second-order rate constant for the reaction of glycine with $^{\bullet}OH$ is only at 2.15×10^7 $M^{-1}s^{-1}$ (Buxton et al. 1988), which is very low compared to commonly encountered diffusion-controlled second-order rate constants for reactions with $^{\bullet}OH$ (>10^9 $M^{-1}s^{-1}$). Based on this low reactivity and the low steady-state $^{\bullet}OH$ concentrations, NH_4^+ formation by this pathway can be excluded during ozonation. Instead, we propose that NH_4^+ is produced through an electron-transfer pathway involving ozone. This pathway proceeds via an ozone adduct intermediate ($R\text{-}NH_2^+OOO^-$) (von Sonntag and von Gunten 2012), a subsequent *N*-centered radical formation followed by an C-N H-shift, oxygen addition to the C-centered radical, and loss of superoxide ($O_2^{\bullet-}$) (refer to Fig. 4.10, reactions 1,7, 13-15). These reactions would result in an imine intermediate that can hydrolyze to NH_4^+. The $O_3^{\bullet-}$ and $O_2^{\bullet-}$ associated with these reaction steps cause $^{\bullet}OH$ formation. For $O_3^{\bullet-}$, $^{\bullet}OH$ can be formed from the subsequent rapid equilibria of $O_3^{\bullet-} \leftrightarrow O^{\bullet-} + O_2$ and $O^{\bullet-} + H_2O \leftrightarrow {}^{\bullet}OH + OH^-$ (Merényi et al. 2010) whereas for $O_2^{\bullet-}$, $^{\bullet}OH$ can be formed from its reaction with O_3 yielding $O_3^{\bullet-}$ (von Sonntag and von Gunten 2012). Since the

formation of NH_4^+ and $^{\bullet}OH$ occurs simultaneously, a linear correlation between the two parameters is observed (Figure 4.6b).

Furthermore, the $^{\bullet}OH$ yield from ozonation of glycine was determined using the DMSO assay (Figure 4.6c). The $^{\bullet}OH$ yield for glycine was calculated to be 24.7 ± 1.9% (mol $^{\bullet}OH$/mol O_3 consumed), which means that about 25% of the consumed O_3 produces $^{\bullet}OH$ and possibly NH_4^+. The $^{\bullet}OH$ yield is within the range determined for triethylamine (15%) (Flyunt et al. 2003) and piperidine (28%) (Tekle-Rottering et al. 2016). Unfortunately, data for $^{\bullet}OH$ yields for other primary aliphatic amines is lacking in literature limiting the options for comparison with previous studies. The measured $^{\bullet}OH$ formation confirms that an electron-transfer mechanism occurs during ozonation of glycine. A plot of the NH_4^+ against the $^{\bullet}OH$ concentration (Fig. 4.6b) gives a linear correlation with a slope of 0.03 mol NH_4^+/mol $^{\bullet}OH$, which means that the measured NH_4^+ concentrations are much lower than expected from the $^{\bullet}OH$ formed. This is a strong indication that other reactions producing $^{\bullet}OH$ compete with NH_4^+ formation.

4.3.5. NO_3^- and NH_4^+ formation during ozonation of synthetic waters mimicking realistic conditions

Ozonation experiments with synthetic DON solutions (20 µM glycine + 3 mgC/L tannic acid + t-BuOH/MeOH) were performed with two $^{\bullet}OH$ scavenging rates, which are about a factor of 10 apart (high: 1.3×10^6 s^{-1} (Figures 4.8a and 4.8b) and low: 1.8×10^5 s^{-1} (Figures 4.8c and 4.8d)). The first set of experiments was performed using the high $^{\bullet}OH$ scavenging conditions with t-BuOH/MeOH (µM/µM) ratios of 417/1000 – 1875/125. Under these conditions, R_{ct} values of 9.70×10^{-10} – 1.95×10^{-8} were measured for O_3 doses of 200 – 400 µM. To evaluate the formation of inorganic nitrogen compounds over a wider range of R_{ct}s, the concentrations of t-BuOH/MeOH were decreased by 12.5 times resulting in water samples with lower $^{\bullet}OH$ scavenging rates. Therefore, in the second set of experiments, using the same O_3 doses, higher R_{ct} values (2.03×10^{-8} – 1.55×10^{-7}) were obtained. Overall, R_{ct} values (summarized in Tables 4.7 – 4.10) covered a realistic range of 10^{-10} – 10^{-7}, which are within the range of R_{ct}s reported in various types of water samples and for various treatment conditions (Acero and von Gunten 2001, Elovitz et al. 2000b, Shin et al. 2015).

NO_3^- increased with increasing O_3 doses for all experimental conditions (Figures 4.8a and 4.8c). For an 85% $^{\bullet}OH$ scavenging by t-BuOH, NO_3^- increased from 3.6 – 10.6 µM when increasing the O_3 dose from 200 – 400 µM (Figure 4.8a). A similar trend was also observed at 50% $^{\bullet}OH$ scavenging by t-BuOH (Figure 4.8c) where NO_3^- increased from 3.3 – 8.5 µM for the same increase in O_3 doses (200

– 400 µM). Several subsequent O_3 reactions play a major role in the formation of NO_3^-, as demonstrated by an increase in NO_3^- concentrations for increasing %$^{\bullet}$OH scavenging by t-BuOH.

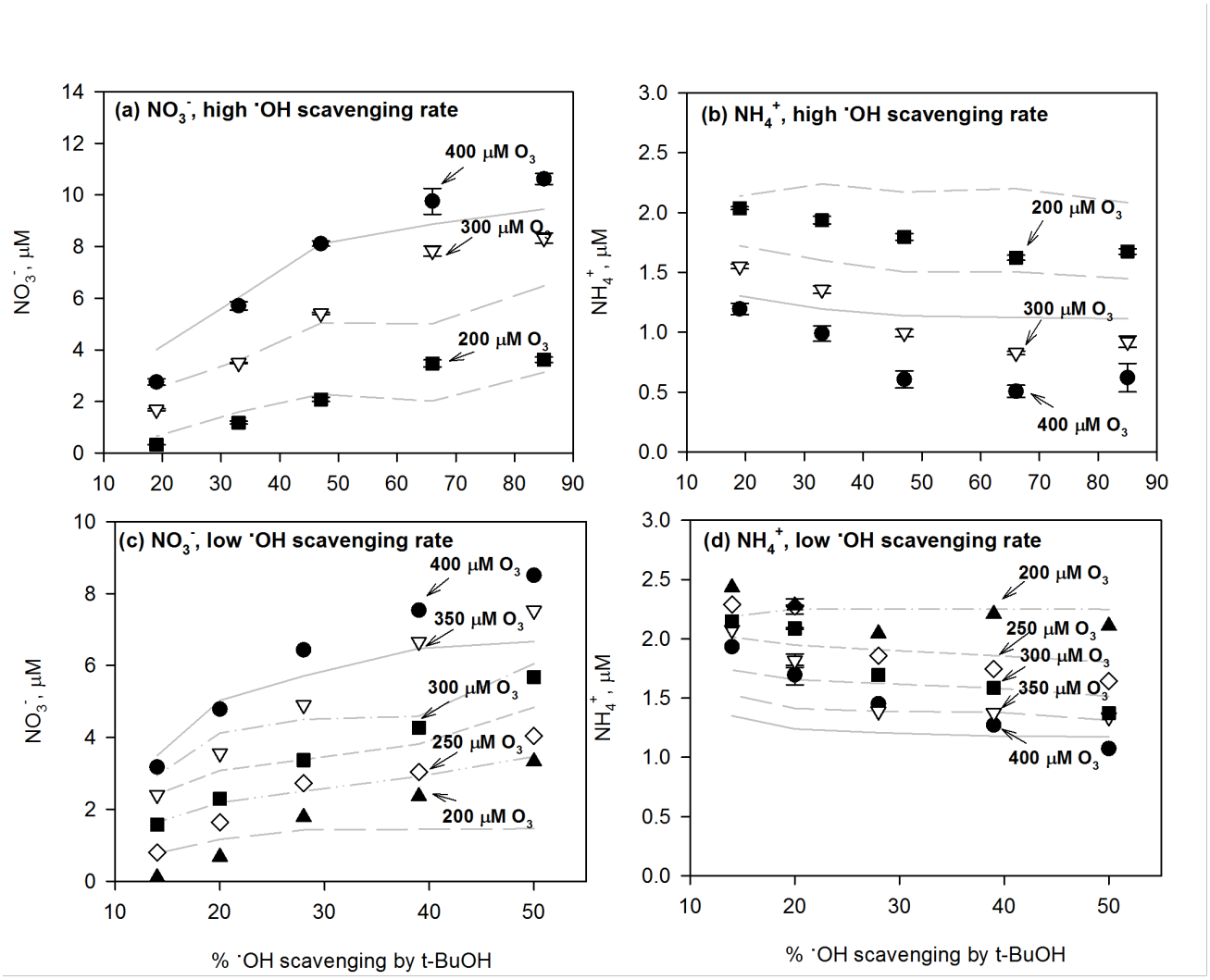

Figure 4.8. NO_3^- and NH_4^+ formation from ozonation of glycine (20 µM) for varying O_3 doses and levels of $^{\bullet}$OH scavenging. Conditions for (a-b): $^{\bullet}$OH scavenging rate = 1.3×10^6 s^{-1}, tannic acid = 3 mg C/L, pCBA = 0.5 µM, µM t-BuOH/ µM MeOH (%$^{\bullet}$OH scavenging by t-BuOH) = 417/1000 (19%), 730/815 (33%), 1045/625 (47%), 1460/375 (66%), 1875/125 (85%), pH = 7, T = 21 ± 1°C, error bars depict standard deviations of 3 replicate experiments; (c-d): $^{\bullet}$OH scavenging rate = 1.8×10^5 s^{-1}, tannic acid = 3 mg C/L, pCBA = 1 µM, µM t-BuOH/ µM MeOH (%$^{\bullet}$OH scavenging by t-BuOH) = 43/74 (14%), 59/65 (20%), 84/50 (28%), 116/30 (39%), 150/10 (50%), pH = 7, T = 21 ± 1 °C. Symbols represent the experimental data; lines represent simulations from the model shown in Table 4.11.

Table 4.7. Pseudo-first-order rate constants (k_{obs}, s^{-1}) of O_3 decay in high $^{\bullet}OH$ scavenging experiments. Conditions: $^{\bullet}OH$ scavenging rate = 1.3×10^{6} s^{-1}, glycine = 20 μM, tannic acid = 3 mgC/L, pH 7, [t-BuOH (μM)]/[MeOH (μM)] = 1875/125, 1460/375, 1045/625, 730/815, 417/1000.

O_3 dose, μM	% $^{\bullet}OH$ scavenging by t-BuOH; k_{obs}, s^{-1}				
	85%	66%	47%	33%	19%
400	2.60×10^{-3}	2.88×10^{-3}	3.29×10^{-3}	4.86×10^{-3}	7.66×10^{-3}
300	3.20×10^{-3}	4.34×10^{-3}	4.31×10^{-3}	6.16×10^{-3}	8.65×10^{-3}
200	4.34×10^{-3}	6.45×10^{-3}	5.81×10^{-3}	7.85×10^{-3}	1.52×10^{-2}

Table 4.8. R_{ct} in high $^{\bullet}OH$ scavenging experiments. Conditions: $^{\bullet}OH$ scavenging rate = 1.3×10^{6} s^{-1}, glycine = 20 μM, tannic acid = 3 mgC/L, pH 7, [t-BuOH (μM)]/[MeOH (μM)] = 1875/125, 1460/375, 1045/625, 730/815, 417/1000.

O_3 dose, μM	% $^{\bullet}OH$ scavenging by t-BuOH; R_{ct}				
	85%	66%	47%	33%	19%
400	9.70×10^{-10}	2.06×10^{-9}	2.77×10^{-9}	4.10×10^{-9}	7.08×10^{-9}
300	1.05×10^{-9}	3.23×10^{-9}	3.86×10^{-9}	5.28×10^{-9}	1.07×10^{-8}
200	1.59×10^{-9}	4.13×10^{-9}	5.96×10^{-9}	9.36×10^{-9}	1.95×10^{-8}

Table 4.9. Pseudo-first-order rate constants (k_{obs}, s^{-1}) of O_3 decay in low $^{\bullet}OH$ scavenging experiments. Conditions: $^{\bullet}OH$ scavenging rate = 1.8×10^{5} s^{-1}, glycine = 20 μM, tannic acid = 3 mgC/L, pH 7, [t-BuOH (μM)]/[MeOH (μM)] = 150/10, 116/30, 84/50, 59/65, 43/74.

O_3 dose, μM	% $^{\bullet}OH$ scavenging by t-BuOH; k_{obs}, s^{-1}				
	50%	39%	28%	20%	14%
400	4.29×10^{-3}	4.45×10^{-3}	5.19×10^{-3}	6.01×10^{-3}	8.79×10^{-3}
350	4.16×10^{-3}	5.71×10^{-3}	5.83×10^{-3}	6.40×10^{-3}	8.92×10^{-3}
300	4.51×10^{-3}	5.81×10^{-3}	6.55×10^{-3}	7.17×10^{-3}	8.94×10^{-3}
250	5.16×10^{-3}	6.10×10^{-3}	7.00×10^{-3}	7.89×10^{-3}	1.01×10^{-2}
200	8.40×10^{-3}	8.50×10^{-3}	8.60×10^{-3}	1.01×10^{-2}	1.36×10^{-2}

Table 4.10. R_{ct} in low $^{\bullet}OH$ scavenging experiments. Conditions: $^{\bullet}OH$ scavenging rate = 1.8×10^{5} s^{-1}, glycine = 20 μM, tannic acid = 3 mgC/L, pH 7, [t-BuOH (μM)]/[MeOH (μM)] = 150/10, 116/30, 84/50, 59/65, 43/74.

O_3 dose, μM	% $^{\bullet}OH$ scavenging by t-BuOH; R_{ct}				
	50%	39%	28%	20%	14%
400	2.03×10^{-8}	2.43×10^{-8}	2.85×10^{-8}	3.61×10^{-8}	5.65×10^{-8}
350	2.24×10^{-8}	3.09×10^{-8}	3.16×10^{-8}	4.19×10^{-8}	7.72×10^{-8}
300	2.24×10^{-8}	2.74×10^{-8}	3.20×10^{-8}	5.10×10^{-8}	8.59×10^{-8}
250	2.45×10^{-8}	2.84×10^{-8}	3.83×10^{-8}	5.60×10^{-8}	1.02×10^{-7}
200	4.13×10^{-8}	5.21×10^{-8}	5.35×10^{-8}	7.78×10^{-8}	1.55×10^{-7}

For NH_4^+, higher concentrations were observed at lower O_3 doses and only slight changes in concentrations were observed at varying t-BuOH concentrations (Figures 4.8b and 4.8d). The latter observation supports our hypothesis that the contribution of $^{\bullet}OH$ reactions to the overall NH_4^+ formation can be neglected. At lower O_3 doses, higher NH_4^+ concentrations were observed because of fast initial O_3 reactions (e.g., electron-transfer and radical chain reactions) forming intermediates that are reactive to the remaining O_3 and O_2 in the solution, consequently producing amides and NH_4^+, respectively (for mechanistic discussion, see below). Briefly, O_3 can also react with C-centered radicals, however, such reactions would lead to an alkoxyl radical (von Sonntag and von Gunten 2012) that will give rise to an amide (not an imine and subsequently NH_4^+). Thus, in the context of NH_4^+ formation, O_3 is only important at the initial electron-transfer step while residual O_3 will compete with O_2 for the C-centered radical. This competition reaction could cause the observed higher NH_4^+ concentration at lower O_3 dose (Figures 4.8b and 4.8d). Because O_2 is high in ozonated solutions, a decrease in available O_3 would promote O_2 reactions with C-centered radicals that eventually lead to NH_4^+ formation (see below).

4.3.6. Relationship between O_3 exposure and NO_3^- formation

So far, it was clearly demonstrated that the NO_3^- formation is sensitive to changes in ozonation conditions for all investigated water samples. For the applied conditions, it was consistently observed that NO_3^- increases with increasing O_3 doses and exposures. A summary of all the related data is presented in Figure 4.9. A similar trend was previously reported, e.g., during continuous ozonation of glycine with decreasing H_2O_2 and increasing bicarbonate concentrations (Berger et al. 1999). However, in the previous study, O_3 exposures were not measured. In the current study, linear relationships ($R^2 \geq 0.82$) were observed between NO_3^- concentrations and O_3 exposures in glycine-containing solutions (both at high and low $^{\bullet}OH$ scavenging), surface water and wastewater samples (Figures 4.9a – 4.9d). This direct relationship applies to a wide range of O_3 exposure (~0 – 0.12 Ms (equivalent to 0 – 96 mg/L·min)), with slopes extending from 51 µM/Ms in surface water to 166 µM/Ms in secondary wastewater effluent. Standard NOM solutions were not included because of the limitation in measuring the fast O_3 decomposition. These results indicate that NO_3^- formation depends on the O_3 exposure, which is a measure for the primary and subsequent O_3 reactions with amine moieties in DON. This also suggests that the conversion of amines to readily oxidizable intermediates and NO_3^- is a relatively straightforward process in the presence of O_3. Intermediates such as hydroxylamines and oximes, as seen in other ozonation studies of amines (Elmghari-Tabib et al. 1982), can be further oxidized to NO_3^- and the corresponding carbonyl compounds (e.g., glyoxylic acid).

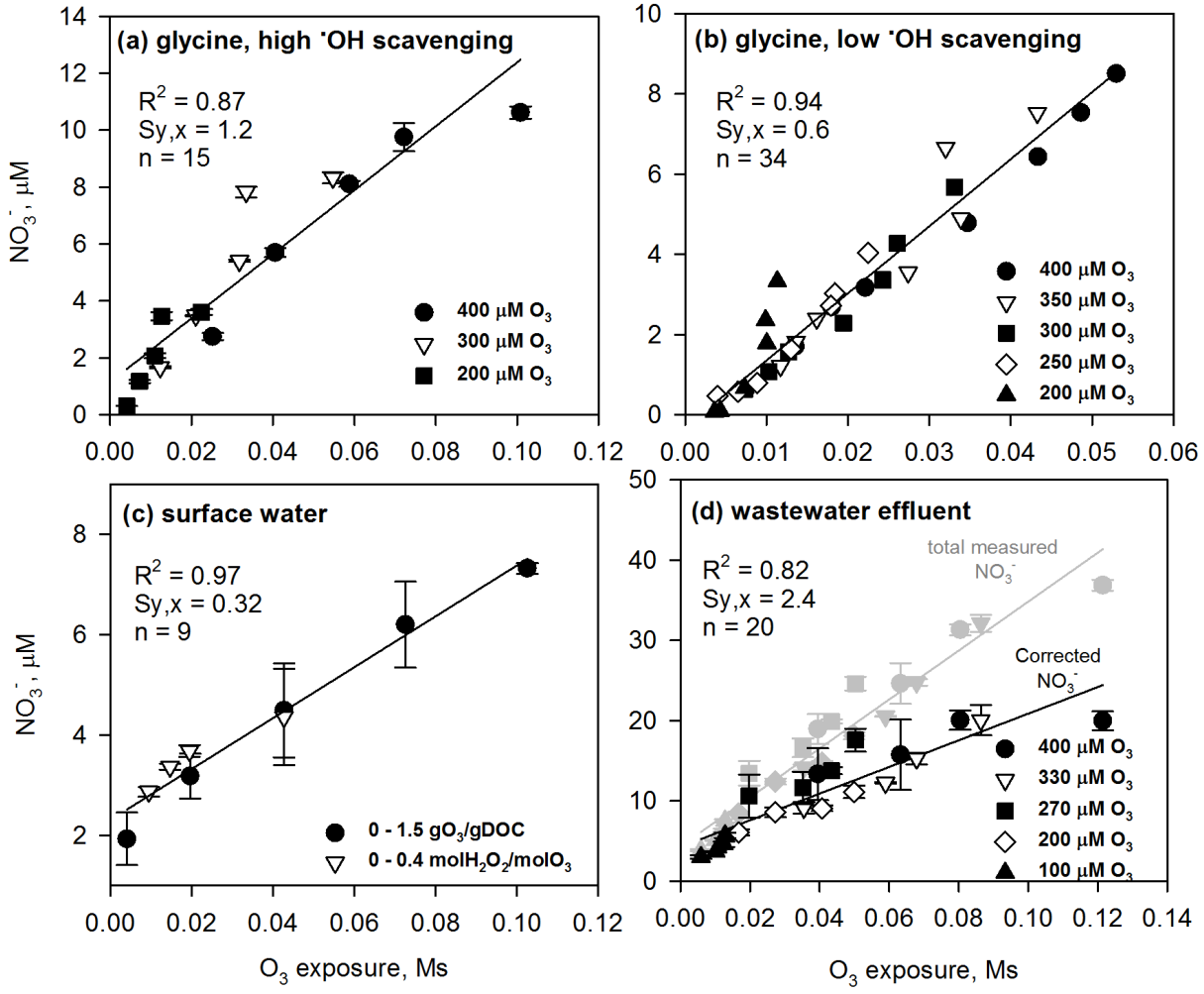

Figure 4.9. NO_3^- formation as a function of the O_3 exposure for (a-b) glycine, (c) surface water, and (d) wastewater effluent (total NO_3^- and corrected for the calculated NO_3^- formation from NH_3/NH_4^+). Conditions: (a) $^{\bullet}OH$ scavenging rate = 1.3×10^6 s^{-1}, glycine = 20 µM, tannic acid = 3 mg C/L, t-BuOH/MeOH (µM/µM) = 417/1000 – 1875/125, pH = 7; (b) $^{\bullet}OH$ scavenging rate = 1.8×10^5 s^{-1}, glycine = 20 µM, tannic acid = 3 mg C/L, t-BuOH/MeOH (µM/µM) = 43/74 – 150/10, pH 7; (c) DOC = 18.7 ± 1.0 mg/L, DON = 0.65 ± 0.04 mg/L; (d): DOC = 6.7 mg/L, DON = 0.33 mg/L, $^{\bullet}OH$ scavenging rate = $1.4\text{x}10^6$ s^{-1}, t-BuOH/MeOH (µM/µM) = 420/1000 – 1870/120.

4.3.7. Mechanistic interpretations

The proposed reactions in the glycine-ozone system are summarized in Figure 4.10. They are based on the following observations from this study: (a) NO_3^- increases with increasing O_3 exposures, (b) NO_3^- is produced from an oxidized glycine intermediate, (c) there is an almost 100% conversion of glycine to NO_3^- in excess of O_3 and for complete $^{\bullet}OH$ scavenging by t-BuOH, (d) NH_4^+ yields were

higher at lower O_3 doses, (e) the O_3 reaction with glycine has a $^{\bullet}OH$ yield of about 25%, and (f) significantly lower NH_4^+ concentrations were observed than expected from the $^{\bullet}OH$ yield.

Ozone reacts with glycine with the formation of an O_3 adduct (reaction 1) which can decompose to an *N*-oxide (reaction 2) and an aminyl radical (reaction 7). The *N*-oxide can then rearrange to monohydroxylamine (reaction 3) (von Sonntag and von Gunten 2012), which leads to dihydroxylamine (reaction 4) upon further oxidation by O_3. Dehydration then forms an oxime (reaction 5) that produces NO_3^- and glyoxylic acid (reaction 6) in the presence of O_3. This series of reactions is based on previously reported pathways by Berger et al. (1999).

Electron-transfer reactions are responsible for the formation of a *N*-centered radical species (reactions 7) (von Sonntag and von Gunten 2012). *N*-centered radicals were reported for similar reactions by Bonifacic et al. (1998) although they used $^{\bullet}OH$ as the oxidant and not O_3. Nevertheless, such types of reactions are plausible for our system as suggested by the measured $^{\bullet}OH$ formation (section 4.3.4).

O_3 can react with the aminyl radical (reaction 8) to form a *N*-oxyl radical after loss of singlet oxygen (reaction 9). The *N*-oxyl radical undergoes a dismutation (reaction 10) (Jayson et al. 1955) to form an oxime and hydroxylamine that can also form NO_3^- upon further oxidation (reaction 11). This reaction is in competition with reaction of O_3 with the *N*-oxyl radical leading to a *N*-centered radical and oxygen (reaction 12). To produce NH_4^+ over the reaction sequence initiated by reaction 7, a C-N H-shift (reaction 13) from the aminyl radical can occur resulting in a C-centered radical (Bonifacic et al. 1998, von Sonntag and von Gunten 2012). Since the reaction occurs in presence of O_2, a peroxyl radical can be produced (reaction 14) (Abramovitch and Rabani 1976, Neta et al. 1990) followed by a release of $O_2^{\bullet-}$ to form an imine intermediate (reaction 15) (von Sonntag and Schuchmann 1991). This product can then hydrolyze to NH_4^+ and glyoxylic acid (reaction 16). Another side reaction can happen through the bimolecular decay of the peroxyl radical forming a tetroxide intermediate (i.e., Bennett- and Russell-type mechanism, reaction 17) (von Sonntag and von Gunten 2012) and eventually oxamic acid (reaction 18) (Berger et al. 1999, Karpel Vel Leitner et al. 2002). Competing with the peroxyl radical formation is the reaction of O_3 with the C-centered radical forming an adduct (reaction 19). This adduct is highly unstable consequently releasing O_2 thereby leading to an oxyl radical (reaction 20) (von Sonntag and von Gunten 2012). This can be followed by 1,2-H shift (Konya et al. 2000) (reaction 21), O_2 addition to form an α-hydroxyperoxyl radical (reaction 22), and loss of $HO_2^{\bullet}$ to also form oxamic acid (reaction 23).

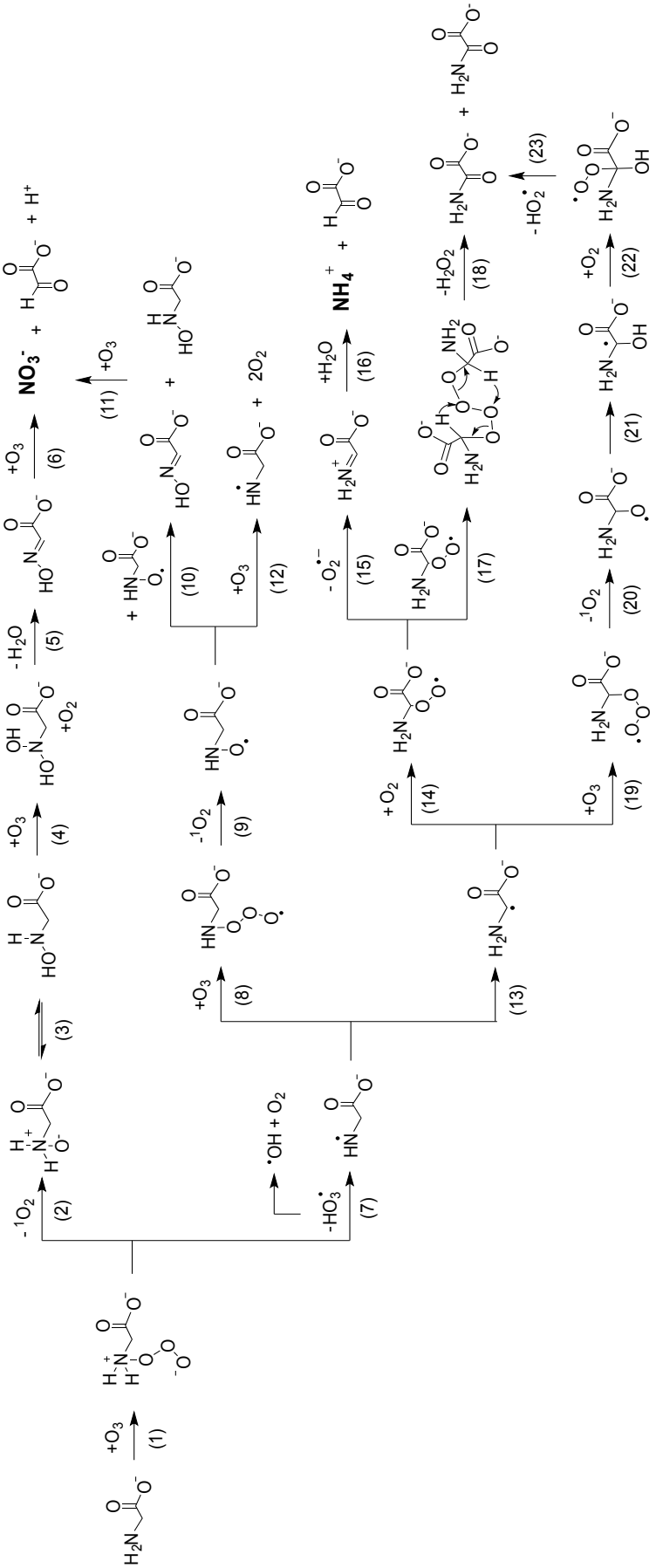

Figure 4.10. Proposed mechanism for the ozone-glycine reaction system: nitrate and ammonium formation

These reactions seem to be quite important in the investigated reaction system because NH_4^+ concentrations were higher at lower O_3 doses suggesting less competition with O_2 for NH_4^+ formation. Based on these reactions, the lower NH_4^+ concentrations compared to the formation of $^{\bullet}OH$ (section 4.3.4) could be caused by: (a) reaction of O_3 with RCH_2-$^{\bullet}NH$ to form NO_3^- (reactions 8 – 11), (b) decay of peroxyl radicals through a tetroxide leading to oxamic acid (reactions 17 – 18), and (c) reaction of O_3 with R-$^{\bullet}CHNH_2$ through an oxyl intermediate that also forms oxamic acid (reactions 19 – 23).

4.3.8. Kinetic simulations of experimental data from model systems

A kinetic model was set up to simulate the experimental data in Figure 4.8. The symbols are experimental results and the lines are derived from kinetic simulations using the reactions (RS) and rate constants listed in Table 4.11. The second column of Table 4.11 shows the corresponding reactions shown in Figure 4.10.

The model accounts for the reaction of glycine with O_3 via oxygen- and electron-transfer. It is mainly composed of 3 components: (1) NO_3^--forming reactions (RS1–RS3, RS5–RS6), (2) NH_4^+-forming reactions and corresponding competing reactions (RS4, RS8–RS14), and (3) O_3 decomposition reactions (RS15–RS17). A reasonable agreement with the experimental results was obtained for NO_3^- both for high and low $^{\bullet}OH$ scavenging rates (Figures 4.8a and 4.8c). This suggests that the rate constants and reactions considered are reasonable to predict NO_3^- formation. Since the model includes measured and estimated rate constants, and measurements of R_{ct} and O_3 decay constants, the observed deviation of the model from the experimental data are not astonishing. Nevertheless, the model was able to show trends which are consistent with the experimentally determined NO_3^- concentrations.

In the model, NO_3^- is formed from an intermediate (assumed to be $HON{=}CHCO_2^-$) by RS3 (Table 4.11; see section 4.3.3) with a second-order rate constant of 7.7 $M^{-1}s^{-1}$ (Figure 4.7). This reaction is preceded by RS1 (O-transfer to N, producing a hydroxylamine) and RS2 (ozonation of hydroxylamine). RS2 was included since hydroxylamines are among the known products of ozonation of primary amines ($k_{RS2} = 2.0\times10^4$ $M^{-1}s^{-1}$) (Hoigné et al. 1985). It can also be seen that RS1 is in competition with RS4, which accounts for electron-transfer reaction. The second-order rate constant used for RS1 was equal to 1.23×10^2 $M^{-1}s^{-1}$, 75% of the known second-order rate constant for the reaction of glycine with O_3 at pH 7 ($k = 1.63\times10^2$ $M^{-1}s^{-1}$) (Lee and von Gunten 2010, Neta et al. 1988). This fraction was used because a 25% $^{\bullet}OH$ yield was measured from the ozone-glycine reaction (section 4.3.4). Considering that $^{\bullet}OH$ can be formed from ozonide in reaction 7, a second-order rate

constant of 41 $M^{-1}s^{-1}$ was assigned for electron-transfer reactions (RS4). The relatively good agreement of the model and the experimental data supports the mechanistic assumptions in this study.

The *N*-centered radical, $HN^{\bullet}\text{-}CH_2CO_2^-$, would react directly with O_3 and indirectly with O_2 after rearrangement to the corresponding C-centered radical. Since we found earlier that glycine can be completely converted to NO_3^- (section 4.3.3), it is highly possible that NO_3^- can also form from reactions involving the *N*-centered radical. O_3 addition to $HN^{\bullet}\text{-}CH_2CO_2^-$ leads to an *N*-oxyl radical (RS5) with subsequent dismutation reaction (RS6). This results in products such as hydroxylamine and oxime that forms NO_3^- by further oxidation. Rate constants for the reaction of aminyl radicals with ozone are still unknown. But for the simulation, a second-order rate constant of 3.0×10^9 $M^{-1}s^{-1}$ (i.e., close to diffusion-controlled reactions) was assumed to fit the experimental data. For the dismutation of the *N*-oxyl radicals (RS6), a rate constant of 1.0×10^9 $M^{-1}s^{-1}$ was assigned which is typical for radical-radical reactions (Buxton et al. 1988). The *N*-oxyl radical can also react with O_3 (RS7) to form another *N*-centered radical, similar to those reported for 2,2,6,6-tetramethyl-1-piperidinyloxy/TEMPO (k = 1.3×10^7 $M^{-1}s^{-1}$) (von Sonntag and von Gunten 2012).

In another pathway, rearrangement of $HN^{\bullet}\text{-}CH_2CO_2^-$ to $H_2N\text{-}^{\bullet}CHCO_2^-$ (RS8; $k = 2.0\times10^6$ s^{-1} based on 1,2-H shift in alkoxyl radicals in RS10) results in reactions with O_3 (to oxamic acid) and O_2 (to NH_4^+) (RS9 – RS14). O_2 addition to $H_2N\text{-}^{\bullet}CHCO_2^-$ results in peroxyl radicals (RS8) that could decay via elimination of $O_2^{\bullet-}$ (RS13) forming an imine that hydrolyzes to NH_4^+, and/or a tetroxide (Bennett mechanism) forming an amide as the final product (RS10). Because of the relatively similar addition reactions of O_3 ($RC\text{-}OOO^{\bullet}$) and O_2 ($RC\text{-}OO^{\bullet}$) for C-centered radicals, second-order rate constants of 1×10^9 – 3×10^9 $M^{-1}s^{-1}$ were assigned for RS9, RS11, and RS12. These rate constants are typical for reactions of C-centered radicals with O_2 and O_3 (Maillard et al. 1983, Neta et al. 1990, von Sonntag and von Gunten 2012). It should be noted that RS9 (reactions 19–20) has a strong influence in NH_4^+ formation. Decreasing its second-order rate constant overestimates the NH_4^+ due to insufficient competition with RS12 (reaction 14). Peroxyl radicals derived from glycine eliminate $O_2^{\bullet-}$ (RS13) with a first-order rate constant of 1.5×10^5 s^{-1} (Neta et al. 1990), whereas their bimolecular decay (RS14) can occur with a second-order rate constant of about 1.0×10^9 $M^{-1}s^{-1}$ which is similar to the decay of most primary peroxyl radicals (Neta et al. 1990, von Sonntag 2006). Although the predicted values for NH_4^+ fall within the range of experimental values, the deviations from the predicted values suggest the possibility of other unknown reactions involving C- and *N*-centered radicals that are not considered in Table 4.11.

Table 4.11. Kinetic modeling of NO_3^- and NH_4^+ formation during ozonation of glycine. Conditions: glycine = 0.02 mM, O_2 = 0.28 mM, O_3 dose = 0.2 – 0.4 mM, pH 7

Reaction No.	Ref. no. for Fig. 4.10	Reactions	Rate constants	Explanation
RS1	1-3	$NH_2CH_2CO_2^- + O_3 \rightarrow HONHCH_2CO_2^- + O_2$	123 $M^{-1}s^{-1}$	75% of $k_{(O3+glycine,\ pH\ 7)}$ = 163 $M^{-1}s^{-1}$ (Lee and von Gunten 2010); O-transfer reaction, only 75% was used due to the measured 25% $^{\bullet}OH$ yield for e^- transfer.
RS2	4	$HONHCH_2CO_2^- + O_3 \rightarrow HONCHCO_2^- + H_2O + O_2$	2.0×10^4 $M^{-1}s^{-1}$	From NH_2OH (Hoigné et al. 1985); intermediate assumed to be the oxime.
RS3	5-6	$HONCHCO_2^- + O_3 \rightarrow NO_3^- + HCOCO_2^- + H^+$	7.7 $M^{-1}s^{-1}$	Rate constant determined in this study (Fig. 4.7)
RS4	1, 7	$NH_2CH_2CO_2^- + O_3 \rightarrow HN^{\bullet}\text{-}CH_2CO_2^- + HO_3^{\bullet}$	41 $M^{-1}s^{-1}$	e^- transfer reactions (25% of $k_{(O3+glycine,\ pH\ 7)}$ = 41 $M^{-1}s^{-1}$), see explanation RS1
RS5	8-9	$HN^{\bullet}\text{-}CH_2CO_2^- + O_3 \rightarrow {}^{\bullet}O\text{-}NHCH_2CO_2^- + O_2$	3.0×10^9 $M^{-1}s^{-1}$	O_3 addition → *N*-oxyl radical (*k* assumed close to diffusion-controlled reactions)
RS6	10	$2\ {}^{\bullet}O\text{-}NHCH_2CO_2^- \rightarrow HONHCH_2CO_2^- + HONCHCO_2^-$	1.0×10^9 $M^{-1}s^{-1}$	Dismutation/termination reaction (Jayson et al. 1955): *N*-oxyl radical → hydroxylamine + oxime (*k* assumed in this study, but common for radical-radical reactions (Buxton et al. 1988))
RS7	12	${}^{\bullet}O\text{-}NHCH_2CO_2^- + O_3 \rightarrow HN^{\bullet}\text{-}CH_2CO_2^- + 2O_2$	1.3×10^7 $M^{-1}s^{-1}$	*k* based on reaction of O_3 with nitroxyl radical of TEMPO (von Sonntag and von Gunten 2012)
RS8	13	$HN^{\bullet}\text{-}CH_2CO_2^- \rightarrow H_2N\text{-}{}^{\bullet}CHCO_2^-$	2.0×10^6 s^{-1}	Aminyl radical rearrangement to C-centered radical (von Sonntag and von Gunten 2012) (*k* assumed in the study)
RS9	19-20	$H_2N\text{-}{}^{\bullet}CHCO_2^- + O_3 \rightarrow NH_2CH(O^{\bullet})CO_2^- + O_2$	3.0×10^9 $M^{-1}s^{-1}$	Ozonation of C-centered radical to C-oxyl radical (*k* assumed close to diffusion-controlled reactions)
RS10	21	$NH_2CH(O^{\bullet})CO_2^- \rightarrow NH_2\text{-}{}^{\bullet}C(OH)CO_2^-$	2.0×10^6 s^{-1}	*k* taken from 1,2-H shift of methoxyl radicals (Naumov and von Sonntag 2011)
RS11	22-23	$NH_2\text{-}{}^{\bullet}C(OH)CO_2^- + O_2 \rightarrow NH_2COCO_2^- + HO_2^{\bullet}$	3.0×10^9 $M^{-1}s^{-1}$	O_2 addition → α-hydroxyalkylperoxyl radicals → oxamic acid (*k* typical for reaction of hydroxyalkyl radicals with O_2 (Maillard et al. 1983)
RS12	14	$H_2N\text{-}{}^{\bullet}CHCO_2^- + O_2 \rightarrow NH_2CH(OO^{\bullet})CO_2^-$	1.0×10^9 $M^{-1}s^{-1}$	Peroxyl radical formation from C-centered radicals with O_2; *k* taken from Neta et al. (1990)
RS13	15-16	$NH_2CH(OO^{\bullet})CO_2^- \rightarrow NH_4^+ + HCOCO_2^- + O_2^{\bullet-}$	1.5×10^5 s^{-1}	Peroxyl radical decay ($O_2^{\bullet-}$ elimination; *k* taken from Neta et al. (1990)) → imine hydrolysis to NH_4^+

Reaction No.	Ref. no. for Fig. 4.10	Reactions	Rate constants	Explanation
RS14	17-18	$2NH_2CH(OO^{\bullet})CO_2^- \rightarrow 2NH_2COCO_2^- + H_2O_2$	1.0×10^9 $M^{-1}s^{-1}$	Bennett mechanism (tetroxide formation is only short-lived) (k common for primary peroxyl radicals (Neta et al. 1990, von Sonntag 2006))
RS15	-	$O_3 \rightarrow {}^{\bullet}OH$	R_{ct}	Measured in this study. If k_{RS15} is set at $1.0x10^9$ s^{-1}, then $k_{RS16} = k_{RS15}/R_{ct}$
RS16	-	${}^{\bullet}OH \rightarrow O_3$		
RS17	-	$O_3 \rightarrow O_2$ + products	k_{obs}, s^{-1}	Measured in this study

The actual O_3 decay characteristics in the synthetic water samples were incorporated using R_{ct} and O_3 decomposition reactions (RS15 – RS17). The elementary reactions for ozone decomposition can lead to formation of ozonide radical that gives rise to ${}^{\bullet}OH$ and O_2 as main products (RS11 and RS13) (Merényi et al. 2010, Pocostales et al. 2010). As can be seen in Figure 4.8, even at differing conditions (O_3 dose and %${}^{\bullet}OH$ scavenging by t-BuOH), the simulation can effectively describe the formation of inorganic nitrogen species provided that R_{ct} and O_3 decay constants are measured for each experimental condition. These constants constitute an integral part of the model because they account for the decay kinetics of O_3 used in reactions RS1–RS5, RS7, and RS9. The experimental first-order O_3 decay constants and R_{ct} values are presented in Tables 4.7 – 4.10. Initial O_2 concentrations of 0.28 mM (9 mg/L O_2) were used to mimic the dissolved O_2 at ambient conditions (20 °C, 1 bar) (USGS 2014).

4.3.9. Practical implications

This study gives evidence that formation of inorganic nitrogen species is greatly influenced by the ozonation conditions of a water sample. One practical application of the results would be in the context of assessment of oxidation/disinfection efficiency during ozonation. Since a strong correlation was found between NO_3^- and O_3 exposure (Figure 4.9), water utilities could continuously monitor NO_3^- concentrations to evaluate if their treatment plant achieves a required O_3 exposure or CT for disinfection or for oxidation of micropollutants. This can be achieved by initial calibrations of the ozonation process with NO_3^- formation, i.e., a measured increase in the NO_3^- level would correspond to a certain O_3 exposure. This approach might be applicable to a wide range of conditions as the direct correlation of NO_3^- concentrations with O_3 exposures applies for different water samples with R_{ct}s ranging from 10^{-10} – 10^{-7}. Hence, the measurement of NO_3^- could be a useful parameter to alert operators that likely a water quality change has occurred in the treatment plant when the detected NO_3^- concentrations deviate from typically observed levels. For example, waters that show a sudden increase

in NO_3^- concentration despite having the same ozonation conditions could indicate that there is a significant change in the quantity and quality of the influent DON. Similarly, an increase in NH_4^+ and decrease in NO_3^- concentrations could suggest having lower O_3 exposures and that higher ozone doses might be needed to achieve the desired disinfection credit. Thus, these results may be useful to complement the monitoring tools currently applied in water treatment to assess O_3 exposures.

However, the new concept that we presented also has limitations. For example, the changes in NO_3^- with O_3 exposure was not very apparent when ozonation pH was varied (Figure 4.11). This is due to the contrasting effects of O_3 exposure and reactivity of amines at differing pH. Despite the increase in O_3 exposure at lower pH, decreasing the pH from 8 to 6 would result in a 100-fold decrease in the rate constant of glycine with O_3. Thus, pH needs to be taken into account, when designing an algorithm based on the present findings to monitor O_3 exposure. In addition, since this approach relies on measuring changes in inorganic nitrogen, the necessary high instrument precision is required. This is problematic in at least two instances. For example, measurement of DON oxidation in a drinking water source in Lausanne (Lake Geneva), Switzerland was not possible due to the low initial NOM concentration (DOC = 0.85 mg/L). Typical C:N ratios in natural water (~15 mgC/mgN) (Westerhoff and Mash 2002) would put the DON at 0.06 mg/L or less which is well below the instrument reporting limit. In contrast, a very high background inorganic nitrogen concentration before ozonation may also pose challenges to the analytical determination of the formation of NO_3^- and/or NH_4^+.

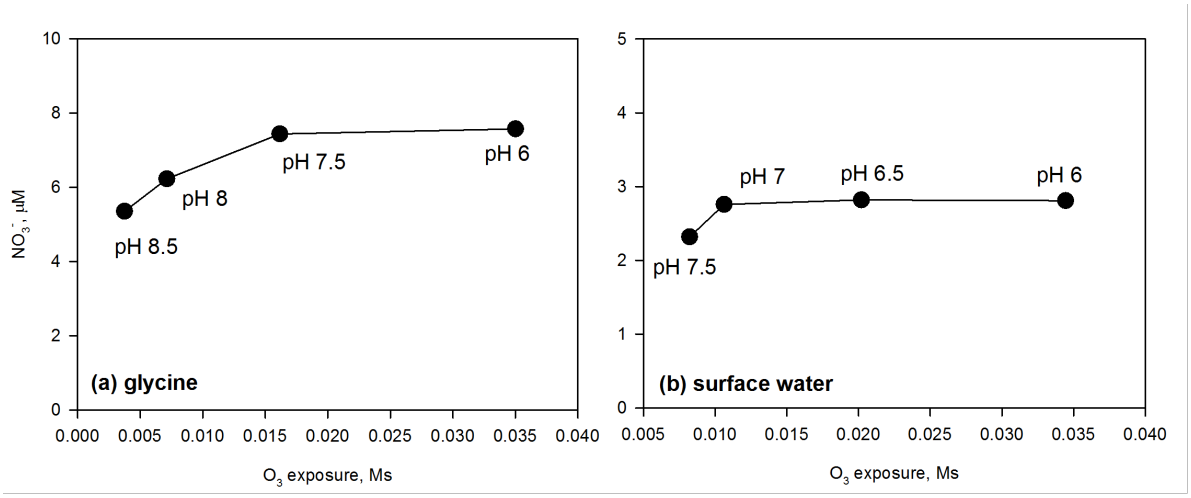

Figure 4.11. Changes in NO_3^- concentrations as a function of O_3 exposure at differing pHs for ozonation. Conditions for (a): glycine = 20 µM, tannic acid = 3 mgC/L, t-BuOH = 84 µM, MeOH = 50 µM, O_3 dose = 400 µM, buffer = 10 mM phosphate; conditions for (b): Specific O_3 dose = 0.75 mgO_3/mg DOC, buffer = 1 mM phosphate, DOC = 20 mg/L, DON = 0.7 mg/L, temperature = 22 °C.

4.4. Conclusions

The reactions between O_3 and DON in real water samples, standard NOM sources, and model DON solutions (e.g., glycine) were investigated. The following conclusions can be drawn from this study:

- NO_3^- and NH_4^+ concentrations vary with changing ozonation conditions in model DON solutions (e.g., glycine) as well as in real water samples (e.g., surface water and wastewater effluent). Increasing NO_3^- concentrations were observed with increasing O_3 doses while the opposite applies for NH_4^+. A direct correlation between NO_3^- and O_3 exposure was apparent for the tested synthetic and natural water samples. Primary amines were found to be a potential precursor for NO_3^- and NH_4^+ formation during ozonation.

- NO_3^- formation during ozonation of glycine occurs via an oxygen-containing intermediate from the oxidation of glycine. To form NO_3^-, an O_3 adduct is formed followed by hydroxylamine formation, which upon further oxidation leads to an oxime and finally NO_3^-.

- For the ozonation conditions in this study, $^{\bullet}OH$ reactions with glycine can be neglected due to the low transient $^{\bullet}OH$ concentrations and the low reactivity of amines at neutral pH. NH_4^+ formation is hypothesized to occur through an electron-transfer reactions involving O_3, which produce $O_3^{\bullet-}$ and C-centered radicals that subsequently react with O_2. The resulting intermediates (e.g., imine compounds) consequently hydrolyze to NH_4^+. This pathway was confirmed from the measured $^{\bullet}OH$ formed from subsequent reactions of $O_3^{\bullet-}$ and $O_2^{\bullet-}$. An $^{\bullet}OH$ yield of 25% was determined from the ozone-glycine reaction.

Chapter 5

Towards reducing DBP formation potential of drinking water by favouring direct ozone over hydroxyl radical reactions during ozonation

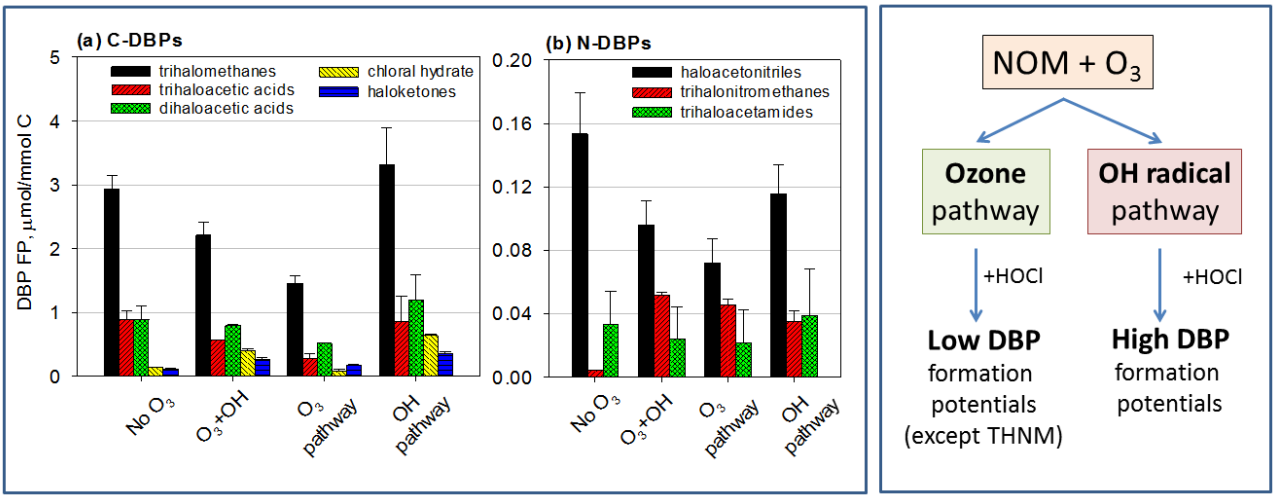

The results of the present chapter are based on the following peer-reviewed publication:

de Vera, G.A., Stalter, D., Gernjak, W., Weinberg, H.S., Keller, J., and Farré, M.J. (2015) Towards reducing DBP formation potential of drinking water by favouring direct ozone over hydroxyl radical reactions during ozonation. *Water Research* 87, 49-58.

http://dx.doi.org/10.1016/j.watres.2015.09.007

5.1. Introduction

Ozonation is used in many drinking water treatment plants because of its efficiency for disinfection as well as oxidation of micropollutants and natural organic matter (NOM) (Lee et al. 2013, von Gunten 2003b, Westerhoff et al. 1999). It has gained additional attention due to its potential to minimize formation of disinfection byproducts (DBPs) from subsequent chlorine disinfection. However, like other oxidants, ozone has its own suite of DBPs including bromate in bromide-containing waters and other organic DBPs from partial oxidation of NOM (von Gunten 2003b). The latter is expected as typical ozonation conditions during drinking water treatment are insufficient for complete NOM mineralization (Nöthe et al. 2009, Ratpukdi et al. 2010, Zhang and Jian 2006). Since ozone is not used as a final disinfectant due to its short lifetime, it is commonly followed by chlorine or chloramine which can react with the remaining and structurally altered NOM to form additional byproducts.

Oxidation during ozonation involves reactions of molecular ozone (O_3) and/or hydroxyl radicals ($^{\bullet}OH$), the latter of which can be formed from ozone decomposition and reaction with NOM (Elovitz and von Gunten 1999). As discussed in Chapter 4, ozone decomposition is affected by promotion and inhibition of $^{\bullet}OH$ chain reactions. Reactions of $^{\bullet}OH$ predominate at conditions that favor ozone decay (e.g., high pH or in presence of H_2O_2). Ozone decay, on the other hand, can be slowed down at low pH or in presence of $^{\bullet}OH$ chain inhibitors such as tertiary butanol (Acero and von Gunten 2001, Elovitz et al. 2000a). To describe the decay kinetics of ozone, the term exposure or its time-integrated concentration is commonly used, i.e., slower ozone decay corresponds to higher exposure and vice versa (see Figure 4.3). Variations in exposures of O_3 and $^{\bullet}OH$ may then result in different transformations of DBP precursors. In the previous chapter, high ozone exposure conditions results in oxygen transfer to amine-N of dissolved organic nitrogen (DON), which upon post-chlorination could influence formation of nitrogenous DBPs (N-DBPs) like halonitromethanes (HNMs). These conditions could also influence transformations of other DBP precursors (e.g., bromide, activated aromatic systems). The formation of bromate, for example, is influenced by both O_3 and $^{\bullet}OH$ during multi-stage oxidation processes involving bromide, hypobromite, and oxybromine intermediates (von Gunten and Hoigné 1994). The presence of bromide can also affect the speciation of organic DBPs.

Apart from bromate, most studies in the literature have investigated the overall impact of the ozonation process on DBP formation without taking into consideration the influence of $^{\bullet}OH$ reactions. Limited studies differentiated the effects of changing O_3 and $^{\bullet}OH$ exposures especially on organic DBP formation. Singer et al. (1999) demonstrated that there was no consistent trend for the effect of

ozonation pH on chlorination DBPs such as trihalomethanes (THMs), haloacetic acids (HAAs), dichloroacetonitrile (DCAN), trichloronitromethane (TCNM), and chloral hydrate (CH). However, Shan et al. (2012) showed an increase in HNMs and THM formation at an ozonation pH of 8 compared to pH 6. Kleiser and Frimmel (2000) showed a less effective removal of THMs and adsorbable organic halogen (AOX) formation potentials in the $^{\bullet}OH$-dominated H_2O_2/UV process compared to ozonation. In addition, when O_3 and O_3/H_2O_2 processes were compared, Yang et al. (2012a) showed only a 5% variation in THM formation and an inconsistent trend in HAA and TCNM formation. The authors also observed an enhanced formation of haloacetonitriles (HANs), CH, and haloketones (HK) with O_3/H_2O_2 treatment followed by chlorination.

Despite these studies, it still remains ambiguous whether ozonation at conditions of higher O_3 or $^{\bullet}OH$ exposures would improve removal of DBP precursors. Additional evidence is needed to confirm which oxidation pathway will assist water treatment plant operators in improving their control over regulated and emerging DBPs. Moreover, there is limited knowledge about the effect of oxidant dynamics during ozonation on formation of N-DBPs even though they are identified to be more toxic than their carbon-based DBP (C-DBPs) analogues (Plewa et al. 2008). Additionally, although ozonation before chlorination has been shown to reduce formation of the regulated THMs and HAAs (Hua and Reckhow 2013), it may potentially transform NOM into forms that render them capable of producing more toxic DBPs (Stalter et al. 2010) after chlorination. These effects may not be easily determined using conventional analytical techniques. For this purpose, recent studies have shown that chemical analysis of DBPs can be complemented with bioanalytical tools such as *in vitro* bioassays to gain a better understanding of the transformations and toxicity that may occur after treatment (Farré et al. 2013, Lyon et al. 2014b, Neale et al. 2012). These tools may also be useful in determining the effects of varying ozonation conditions on the quality of the final disinfected water.

This chapter shows the effects of changing O_3 and $^{\bullet}OH$ exposures prior to chlorination on formation potentials of AOX, N-DBPs such as HANs, HNMs, and haloacetamides (HAMs) and the C-DBPs THMs, HAAs, CH, and HKs. *In vitro* bioassays were used to assess cytotoxicity, genotoxicity, and oxidative stress of the treated water. Thus, a holistic approach was applied to determine the overall impact of ozone and $^{\bullet}OH$ oxidation on the quality of water post-disinfected with chlorine in terms of known DBPs, AOX, and associated biological effects.

5.2. Experimental methods

5.2.1. Water sample

The settled water used in this study was representative of 9 sources with similar character treated at drinking water plants throughout South East Queensland (SEQ), Australia (Lyon et al. 2014a) and was collected after coagulation and sedimentation from one of the plants. The treatment plant's source water originates from a catchment area (88 km^2) which introduces organic matter comprised mostly of allochthonous, plant- and soil-derived material. Across the 9 sources, dissolved organic carbon (DOC) and specific UV absorbance (SUVA) were 3.9 ± 0.5 mg/L and 1.6 ± 0.1 L/mg-C·m, respectively. Differences in DBP formation potentials were also minimal (e.g., THMs and HANs had relative standard deviations of 22 and 30%, respectively) as shown in Figure 5.1. Thus, it is likely that the findings from the study of this water would be applicable across the SEQ region.

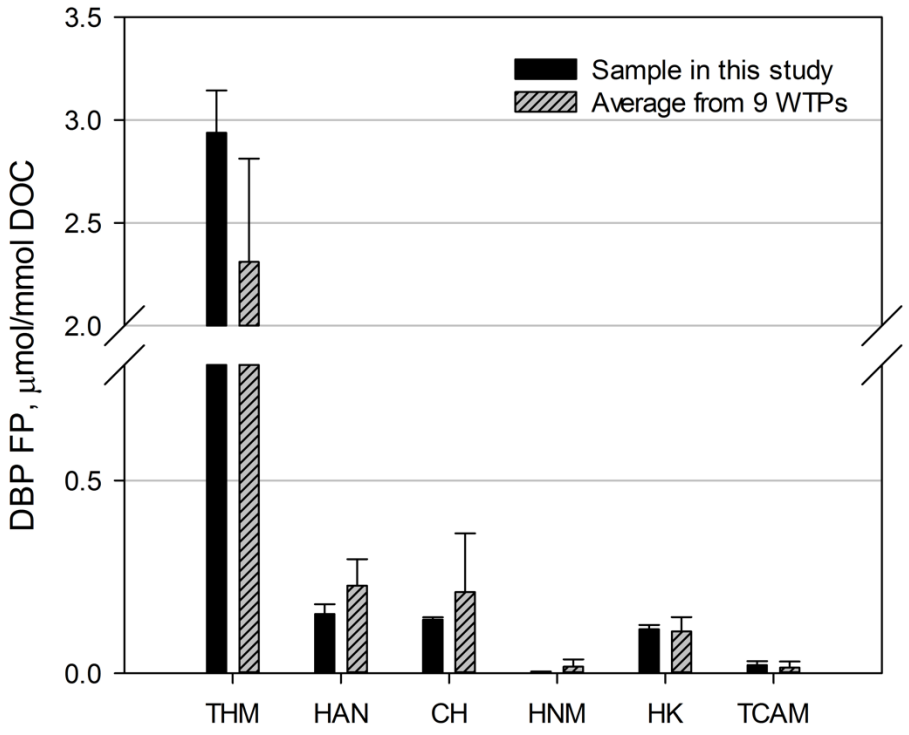

Figure 5.1. Comparison between DBP formation potentials of settled water sample used in this study and of samples taken from 9 different drinking water treatment plants (WTPs) in South East Queensland, Australia.

To obtain a stock solution of organic matter that could be used for a series of ozonation experiments, the settled water was concentrated by reverse osmosis (RO). The RO system (Biopure 962, QLD, Australia) included two polyamide spiral wound membranes (RE-2521BE, Biopure, QLD, Australia), three polyspun sediment filters (0.5, 1, 5 μm) (Hydrotwist, Australia) and two cation exchange resin cartridges containing Tulsion T-42 strong cation exchange resin in Na^+ and H^+ form (Thermax, India). Prior to use of the system, cation exchange resins were rinsed with deionized water for about one week until no impurities were detected in the filtered water by absorbance and fluorescence measurements. The 1000 L settled water was first passed through the sediment filters once and collected in 200 L reservoirs. The RO system was operated until 20 L of concentrate was collected. The concentrate was then stored in high density polyethylene bottles (QHFSS, QLD, Australia) and frozen until use. The characteristics of the source settled water and RO concentrate are shown in Table 5.1. The RO concentrate contained 181 ± 3 mg/L DOC, 6.0 mg/L DON, and 3.2 ± 0.1 mg/L bromide. Iodide was below the reporting limit of 0.1 mg/L. Because of the decrease in pH with use of cation exchange resins in H^+-form, no inorganic carbon was detected in the concentrate. To show that the concentration process did not significantly alter the characteristics of DBP precursors in the source settled water, volatile DBP formation potentials (in μmol/mmol C) of a reconstituted RO concentrate were compared to those in the settled water sample (Table 5.2). It can also be noted that concentration factors of dissolved organic carbon and nitrogen are 37 and 20, respectively. The lower concentration factor for organic nitrogen is possibly due to loss of low molecular-size organics during NOM isolation (Gjessing et al. 1999, Sun et al. 1995). The lost organic nitrogen fractions could also be precursors of HANs as observed in the lower DBP formation potential compared to the actual sample.

Table 5.1. Settled water and RO concentrate characteristics*

Parameter (units)	Original settled water sample (feed water)	RO concentrate
DOC (mg C/L)	4.8±0.1	181±3
DON (mg N/L)	0.3	6.0
SUVA 254 (L/mg-C·m)	1.7	1.9±0.1
Inorganic carbon (mg C/L)	2.5±0.1	<0.5
Bromide (mg/L)	0.1	3.2±0.1
Iodide (mg/L)	<0.1	<0.1

** error bars correspond to mean absolute deviation from duplicate measurements*

Table 5.2. Comparison of volatile DBP formation potentials (μmol/mmol C×10^2) of original settled water (4.8 mg/L DOC) and reconstituted water samples (19.5 mg/L DOC)

DBPs	Original settled water sample	Reconstituted sample
Trihalomethanes (THM4)	295	280
Trichloromethane (TCM)	206	201
Bromodichloromethane (BDCM)	74	68
Dibromochloromethane (DBCM)	15	11
Tribromomethane (TBM)	0.8	0.4
Haloacetonitriles (HAN4)	30	17
Trichloroacetonitrile (TCAN)	0.8	0.3
Dichloroacetonitrile (DCAN)	23	13
Bromochloroacetonitrile (BCAN)	5.0	3.7
Dibromoacetonitrile (DBAN)	1.0	0.5
Chloral hydrate (CH)	16	16
Halonitromethanes (THNM)	1.4	0.7
Trichloronitromethane (TCNM)	0.9	0.5
Tribromonitromethane (TBNM)	<0.02	0.2
Haloketones (HK)	16	11
1,1-dichloropropanone (11DCP)	1.0	0.8
1,1,1,-trichloropropanone (111TCP)	15	11
Trihaloacetamides (THAM)	6.6	7.1
Trichloroacetamide (TCAM)	3.5	3.6
Bromodichloroacetamide (BDCAM)	3.1	2.0
Dibromochloroacetamide (DBCAM)	< 0.1	1.5

5.2.2. Batch ozonation experiments

Experiments were performed as batch experiments mixing 1.2 μm GF/C (Whatman, UK) filtered reconstituted water with ozone stock solutions. Reconstituted water was prepared by mixing deionized water (MilliQ A10 Advantage, Millipore, Australia) with RO concentrate to a DOC concentration of 17 ± 2 mg/L, a level that helped to improve detection of all targeted DBPs. The samples were buffered with 1 mM phosphate to ensure relatively constant pH (± 0.2 pH units) during ozonation. All ozonation experiments were carried out in triplicate and results are reported as mean ± standard deviation. For this study, the following baseline conditions were defined: specific ozone dose = 0.75 mgO_3/mg DOC, inorganic carbon concentration = 0 mg/mg DOC, pH = 7, temperature

= 22°C and bromide concentration = 20 µg Br^-/mg DOC. Details on preparation of ozone stock solutions (1 – 1.3 mM O_3) are discussed previously in Section 4.2.1.

In this study, the first set of experiments used samples with and without added tertiary butanol (t-BuOH; 10 mM; Sigma-Aldrich, 99.6%, St. Louis, MO, USA) and hydrogen peroxide (H_2O_2; 15 mg O_3/L; Merck, 30%, Darmstadt, Germany) to distinguish the effects of O_3 and $^{\bullet}OH$ reactions on DBP formation. To confirm these results, the second set studied the effect of varying pH levels (6, 7, 8) on ozonation using samples buffered with 1 mM phosphate ($NaH_2PO_4 \cdot 2H_2O$ (>99%, Ajax Finechem, NSW, Australia) and $Na_2HPO_4 \cdot 2H_2O$ (≥99.5%, Merck, Darmstadt, Germany)). The third set varied specific ozone dose (0, 0.4, 0.75, 1 mgO_3/mg DOC) to determine the impact of having both O_3 and $^{\bullet}OH$ reactions on DBP formation. Ozone doses were adjusted in each experiment to simulate actual O_3/DOC ratios of water utilities in SEQ. After all the ozone had reacted, samples were stored headspace free at 4°C for no more than 24 hours until conducting DBP formation potential tests.

5.2.3. Characterization of water samples

Dissolved organic carbon (DOC): The DOC was measured with a Shimadzu TOC-L total organic carbon analyser with a TNM-L total nitrogen analyzer unit and ASI-L autosampler (Shimadzu, Kyoto, Japan). The method reporting limit for DOC was 0.3 mg/L (measuring range = 0.3 to 25 mg/L).

UV-Visible absorbance: UV-visible absorbance was measured from 600-200 nm in a quartz cuvette with a Varian Cary 50 Bio UV-Visible spectrophotometer. $SUVA_{254}$ was calculated by multiplying the UV absorbance at 254 nm (cm^{-1}) by 100 and then dividing by the DOC (mg-C/L) to obtain units of L/mg-C·m.

Excitation Emission Matrix (EEM) fluorescence: Fluorescence measurements were performed in a quartz cuvette using a PerkinElmer LS-55 luminescence spectrometer (Perkin Elmer, Australia). EEM measurements were made from 200 – 400 nm excitation wavelengths and 280 – 500 nm emission wavelengths. Regional integration of the fluorescence spectra using R statistical software (R Foundation for Statistical Computing, Vienna, Austria) was used to classify components of NOM according to the regions of Chen et al. (2003).

Aldehyde analysis: Formaldehyde, acetaldehyde, glyoxal and methyl glyoxal were extracted within 1 week after ozonation of the sample. These aldehydes were extracted using EPA Method 556 (Munch et al. 1998). The following standards were used: formaldehyde (36.5 – 38% in water, Sigma-Aldrich, St. Louis, MO, USA), acetaldehyde (≥99.5%, Sigma-Aldrich, Switzerland), glyoxal (40% in water, Sigma-Aldrich, Germany), methylglyoxal (40% in water, Sigma, Germany), 4-fluorobenzaldehyde (surrogate standard, 98%, Aldrich, Hong Kong), and 1,2-dibromopropane

(internal standard, 97%, Aldrich, USA). In this method, the analytes were derivatized in aqueous solution to their corresponding pentafluorobenzyl oximes using *O*-(2,3,4,5,6-pentafluorobenzyl hydroxylamine hydrochloride (≥99.0%, Fluka, Switzerland) and were extracted using hexane (B&J GC^2, Honeywell, Muskegon, MI, USA). The extracts were analyzed by GC/ECD. The method detection limit for the 4 aldehydes was 2 µg/L with recoveries ranging from 80 – 120%.

Inorganic nitrogen: Ammonia, nitrite and total NO_x were measured on a Lachat QuikChem8500 Flow Injection Analyzer (Hach Company, CO, USA) using Lachat QuickChem method 31-107-06-1-A. For further details, refer to Section 4.2.1.

5.2.4. DBP Formation potential tests

Formation potential tests were carried out in 250 mL headspace-free samples buffered at pH 7 with 10 mM phosphate. The buffer was prepared from a mixture of KH_2PO_4 (99%) and NaOH (98%) both purchased from Chem-Supply, SA, Australia. The concentration of sodium hypochlorite (reagent grade, available chlorine 4 − 4.99%, Sigma-Aldrich, St. Louis, MO, USA) added was based on chlorine demand tests with the same water and aimed to have a residual of 1 – 2 mg/L as Cl_2 after 24 h to simulate realistic conditions. Prior to this, residual H_2O_2 for samples treated with O_3/H_2O_2 was quenched using either equimolar concentrations of sodium sulfite (≥98%, Sigma-Aldrich, Japan) or excess sodium hypochlorite (Liu et al. 2003). The latter was used simultaneously for quenching H_2O_2 and the excess for DBP formation potential tests. Chlorine residual in samples was measured using the *N,N*-diethyl-*p*-phenylenediamine (DPD) free chlorine colorimetric method (Hach, Loveland, CO, USA). After one day of contact time, samples were quenched of chlorine depending on the subsequent analytical fraction (i.e., L-ascorbic acid (≥99%, Sigma-Aldrich, China), sodium sulfite (≥98%, Sigma-Aldrich, Japan), and ammonium chloride (99.5%, Sigma-Aldrich, Japan) prior to extraction of neutral-extractable DBPs, AOX, and haloacetic acids, respectively). DBP formation potentials were normalized to the measured DOC of the water samples before ozonation and reported in µmol/mmol DOC to account for possible variability in preparing reconstituted water samples. For bioassays, 500 mL of ozonated samples were also subjected to 24-h formation potential tests with chlorine. The residual chlorine was quenched with equimolar concentrations of sodium thiosulfate ($Na_2S_2O_3 \cdot 5H_2O$; 99.5%, Sigma-Aldrich, USA) (Farré et al. 2013, Yeh et al. 2014).

5.2.5. Analysis of disinfection byproducts

The following volatile DBPs were analyzed in aqueous samples at pH 7 after duplicate extractions with methyl tert-butyl ether (MtBE; 99.9%, Sigma-Aldrich, USA): (a) four trihalomethanes (THM4: trichloromethane (TCM), dibromochloromethane (DBCM), bromodichloromethane (BDCM), tribromomethane (TBM)), four haloacetonitriles (HAN4: trichloroacetonitrile (TCAN), dichloroacetonitrile (DCAN), bromochloroacetonitrile (BCAN), dibromoacetonitrile (DBAN)), two haloketones (HK2: 1,1-dichloropropanone (DCP), 1,1,1-trichloropropanone (TCP)), two trihalonitromethanes (THNM2: trichloronitromethane (TCNM), tribromonitromethane (TBNM)), chloral hydrate (CH), and three trihaloacetamides (THAM; trichloroacetamide (TCAM), bromodichloroacetamide (BDCAM), and dibromochloroacetamide (DBCAM)). Iodinated DBPs (e.g., dichloroiodomethane, bromochloroiodomethane, dibromoiodomethane, chlorodiiodomethane, bromodiiodomethane, triiodomethane, chloroiodoacetamide, bromoiodoacetamide, and diiodoacetamide), and most other haloacetamides (e.g., dichloroacetamide, bromochloroacetamide, dibromoacetamide, and tribromoacetamide) were also measured but not detected in samples chlorinated after ozonation. The standards were purchased from different suppliers: THM4 calibration mix (TCM, DBCM, BDCM, and TBM; 2000 µg/mL each in methanol, Supelco, Bellefonte, PA, USA), EPA 551B halogenated volatiles mix (BCAN, DBAN, DCAN, 1,1-DCP, 1,1,1-TCP, TCAN, and TCNM; 2000 µg/mL each in acetone, Supelco, Bellefonte, PA, USA), CH (>99.5%, Sigma-Aldrich 15307, Belgium), and TCAM (99%, Aldrich 217344, Switzerland). The standards for TBNM and other THAMs were purchased with >99% purity from Orchid Cellmark, Canada. 1,2-dibromopropane (97%, Aldrich, USA) was used as the internal standard.

As described by Farré et al. (2013), MtBE extracts containing the volatile DBPs and the internal standard were injected into an Agilent 7890A gas chromatograph equipped with two independent electron-capture detector (GC/ECD) (Agilent, USA) connected to a separate DB-5 and a DB-1 Agilent column (30 m length × 0.25 mm inner diameter × 1.0 µm film thickness each) and two injectors. Pulsed splitless injection was used at 140 ºC. The oven temperature program started at 35 ºC for 25 min, followed by three ramps to have a total analysis time of 81 min: (1) 100 ºC at 2 ºC/min (2 min holding time), (2) 200 ºC at 5 ºC/min, and (3) 280 ºC at 50 ºC/min. The ECD temperature was set at 300 ºC. The method reporting limit for all volatile DBPs was 0.1 µg/L (measuring range = 0.1 – 200 µg/L) with recoveries normally ranging from 80% to 120%. Table 5.3 provides more details on the DBPs used.

Table 5.3. List of volatile DBPs analyzed in this study

Compound	Abbreviation	Compound class	GC retention time, min*
trichloromethane	TCM	trihalomethane (THM)	9.3
dibromochloromethane	DBCM		17.3
bromodichloromethane	BDCM		32.7
tribromomethane	TBM		44.8
bromochloroiodomethane	BCIM		48.1
dibromoiodomethane	DBIM		57.5
dichloroiodomethane	DCIM		37.0
chlorodiiodomethane	CDIM		60.2
bromodiiodomethane	BDIM		66.8
triiodomethane	TIM		72.4
trichloroacetonitrile	TCAN	haloacetonitrile (HAN)	13.9
dichloroacetonitrile	DCAN		18.8
bromochloroacetonitrile	BCAN		35.6
dibromoacetonitrile	DBAN		47.7
chloral hydrate	CH	haloaldehyde	18.4
1,1-dichloropropanone	DCP	haloketone (HK)	21.3
1,1,1-trichloropropanone	TCP		39.7
trichloronitromethane	TCNM	halonitromethane (HNM)	30.6
tribromonitromethane	TBNM		50.0
dichloroacetamide	DCAM	haloacetamide (HAM)	59.5
bromochloroacetamide	BCAM		65.8
trichloroacetamide	TCAM		67.7
dibromoacetamide	DBAM		69.9
chloroiodoacetamide	CIAM		71.4
bromodichloroacetamide	BDCAM		71.6
bromoiodoacetamide	BIAM		74.6
dibromochloroacetamide	DBCAM		75.0
tribromoacetamide	TBAM		78.0
diiodoacetamide	DIAM		78.7

** from DB-5 column; method reporting limit = 0.1 µg/L*

The haloacetic acids (HAAs) were classified into (i) trihaloacetic acids (THAAs) which included trichloroacetic acid (TCAA), bromodichloroacetic acid (BDCAA), and chlorodibromoacetic acid (CDBAA), and (ii) dihaloacetic acids (DHAAs) which included dichloroacetic acid (DCAA), bromochloroacetic acid (BCAA), and dibromoacetic acid (DBAA). These together with monochloroacetic acid (MCAA) and monobromoacetic acid (MBAA) were measured at Queensland Health Forensic and Scientific Services (QHFSS) based on EPA Method 552.3 (Domino et al. 2003) using an acidic, salted microextraction followed by derivatization with acidic methanol and GC/ECD analysis (Xie et al. 2002). The method reporting limit for all HAA species was 5 µg/L. Tribromoacetic acid was not analyzed because of its low stability during extraction with MtBE.

The analysis of AOX was based on previously reported methodologies (Farré et al. 2013, Stalter et al. 2016b, Yeh et al. 2014). In this method, 10 mL of quenched aqueous sample was first acidified with 10 µL of concentrated HNO_3 (70%, Sigma-Aldrich, Australia). The acidified sample was then passed through two consecutive activated carbon cartridges (50 mg C in 3 mm ID Euroglass, CPI International, USA) using a 10 mL gas-tight Hamilton syringe. The cartridges were washed with 8.2 g/L potassium nitrate (≥99%, Sigma-Aldrich, Australia) at a rate of about 5 mL/min to remove inorganic halides. The activated carbon was next transferred to sample boats for pyrolysis at 1000 ºC (in the presence of oxygen) using a Mitsubishi AQF-2100 Automated Quick Furnace unit connected to a Dionex ICS-2100 Dual Channel Ion Chromatograph system (Thermo Fisher Scientific, Australia). Using argon as a carrier gas, the halogens produced from pyrolysis were then reduced to halide ions in a 10 mL absorption solution (0.003% H_2O_2 with 1 mg/L phosphate). Chloride, bromide, and iodide ions were quantified by ion chromatography with method reporting limits of 12, 6, and 15 µg/L, respectively. The commonly used linear range was up to 800 µg/L for bromide, 2000 µg/L for chloride, and 400 µg/L for iodide. AOX is reported as a Cl equivalent concentration (µM as Cl), which refers to the sum of the equivalent concentrations of adsorbable organic chlorine, bromine, and iodine multiplied by the atomic mass of Cl.

Bromide, iodide, and bromate were measured at QHFSS with a Metrohm 861 Advanced Compact Ion Chromatograph (Metrohm, Switzerland) equipped with a CO_2 suppressor, a Thermo AS23 column, Thermo AG23 guard column and a 50 µL sample loop. The eluent was a carbonate (4.5 mM Na_2CO_3)/bicarbonate (0.8 mM $NaHCO_3$) mixture with a 1 mL/min flow rate and its conductivity suppressed using Metrohm's chemical (100 mM H_2SO_4) and CO_2 suppression modules. The method reporting limit for bromide, iodide, and bromate of QHFSS were 5, 100, and 10 µg/L, respectively.

5.2.6. Sample preparation for bioassays

The quenched chlorinated 500 mL samples were first acidified to pH 1.5 using sulfuric acid (98%, Merck, Darmstadt, Germany) followed by a solid phase extraction (SPE) using TELOS ENV 1g/6ml cartridges (Kinesis, QLD, Australia). It should be noted that samples used here (DOC = 19 mg/L) were already enriched 4 times compared to DOC of actual water samples (4.8 mg/L). The cartridges were conditioned with 20 mL each of MtBE, methanol (≥99.8%, Merck, Darmstadt, Germany), and MilliQ water adjusted to pH 1.5 with sulfuric acid, respectively. After sample loading, cartridges were dried with >99.998% nitrogen gas. The retained compounds were eluted with 20 mL methanol followed by 20 mL MtBE. The eluates were blown down to 200 µL, which generates a 2,500 concentration factor for those DBPs completely recovered through the process. This extraction

procedure enriched only non-volatile DBPs while the more volatile compounds were likely lost during the blow-down step (Neale et al. 2012). With the initial ~4-fold enrichment of DOC, the effects of treatment on the original settled water were highly magnified to the point of making any differences in biological effect more discernible. Extracts were stored at -80 °C and analyzed within 4 weeks.

5.2.7. Bioassays

Four types of *in vitro* bioassays were used to target nonspecific and reactive endpoints. These together with the relevant reference compounds were the bacterial cytotoxicity (Microtox) or bioluminescence inhibition assay with *V. fischeri* using phenol (Tang et al. 2013), the umuC bacterial reporter gene assay for genotoxicity using 4-nitroquinoline-1-oxide (Reifferscheid et al. 1991), the AREc32 MCF7 human cell reporter gene assay for oxidative stress using t-butylhydroquinone (tBHQ) (Escher et al. 2012), and the p53RE-bla HCT-116 human cell reporter gene assay for genotoxicity using benzo(a)pyrene (Yeh et al. 2014). 1% Methanol was used as negative control in the assay medium. Relative enrichment factors (REF) were calculated from the ratio of a 10,000 enrichment factor of sample (representing the combination of 4-fold DOC enrichment and 2,500 concentration factor by SPE) to the bioassay dilution factor (i.e., dilution of SPE extracts with assay medium by factor of 100). Each sample was analyzed in an 8-point serial dilution. For Microtox, the 50% effect concentration (EC_{50}) was derived from a log-logistic concentration-effect curve and corresponds to an REF which induces 50% of the maximum effect. For other bioassays, effect concentration (EC) is defined as induction ratio (IR) of 1.5 ($EC_{IR1.5}$) which corresponds to the REF needed to elicit 1.5 times induction of effect (e.g., production of luciferase for the AREc32 assay) compared to the negative control. Thus, water samples that have lower ECs are more toxic. The contribution of t-BuOH to toxicity was not measured since it is expected to have been lost during SPE. Further details on the bioassays were reported previously (Farré et al. 2013, Neale et al. 2012, Yeh et al. 2014).

5.3. Results and Discussions

5.3.1. Effect of ozonation conditions on formation of known DBPs

Figure 5.2 compares DBP formation potential of samples collected for three replicate experiments with and without previous ozonation at a specific O_3 dose of 0.75 mg O_3/mg DOC and pH 7 (columns labelled as "O_3" and "No O_3"). As expected, ozone increased the formation potentials of CH, HKs, and THNMs (Bond et al. 2011b, Krasner 2009, Singer et al. 1999, Yang et al. 2012a) by 192%, 133%, and 1079%, respectively.

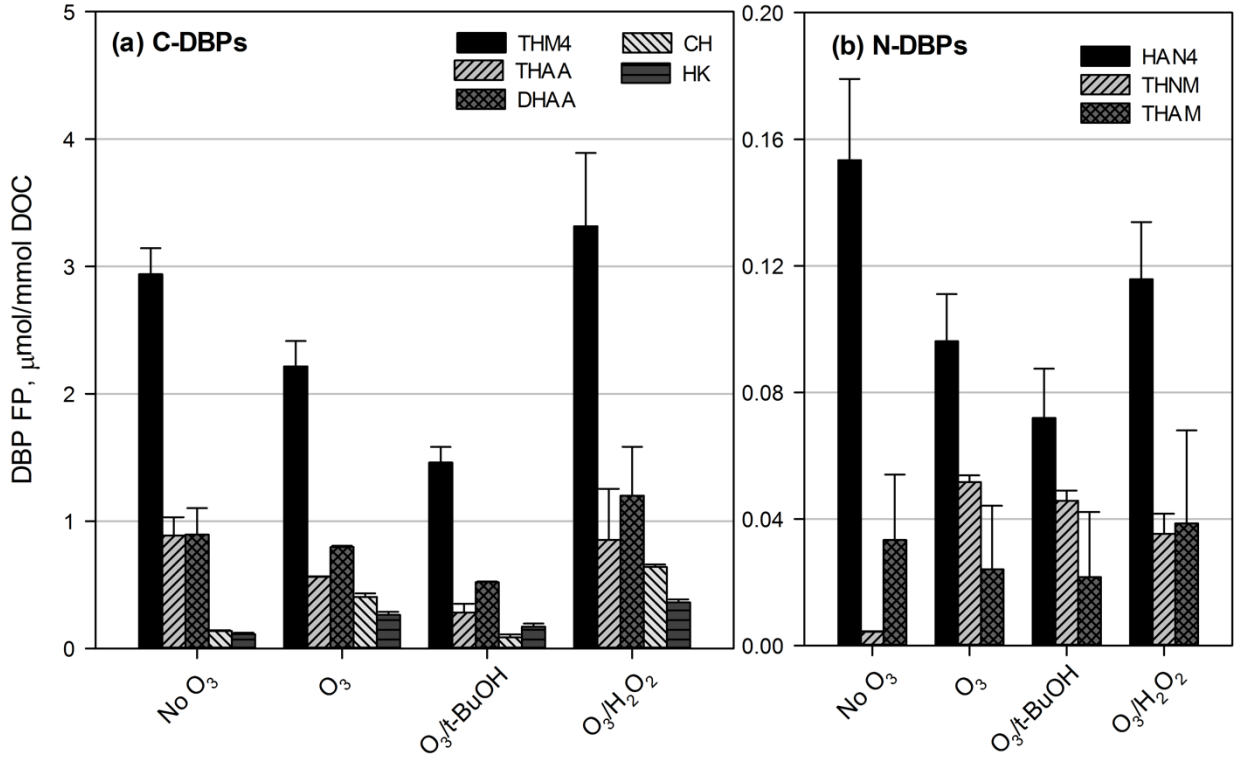

Figure 5.2. Formation potentials (FP) of (a) C-DBPs and (b) N-DBPs in the presence and absence of t-BuOH and H_2O_2. Conditions: DOC = 17.2 ± 2.0 mg/L, specific ozone dose = 0.75 mgO_3/mg DOC, pH = 7 (1 mM phosphate), t-BuOH = 10 mM, H_2O_2 = 1 mg/mg O_3, temperature = 22±1 °C. HOCl DBP 24 h formation potentials tests at pH 7 were targeted to have a 1 – 2 mg/L Cl_2 residual. Error bars depict standard deviation of 3 replicate experiments.

The average concentration of other DBPs decreased in the following order: HAN4 (37%) ≈ THAA (37%) > THAMs (28%) ≈ THM4 (25%) > DHAAs (11%). Iodinated DBPs (I-DBPs) were all below detection limits which is in agreement with the study of (Allard et al. 2013) which showed ozonation of iodide to iodate preventing I-DBP formation.

Differences in DBP formation are dependent on precursor characteristics and their reactivity towards O_3. When ozone reacts with nitrogen-containing moieties such as amines, oxygen transfer intermediates (see Chapter 4) and possibly R-NO_2 (McCurry et al. 2016) are formed which are potential THNM precursors. These remove the nitrogen source for HAN4 and THAM formation explaining the observed trends in these experiments. Moreover, an increase in NO_3^--N concentrations (7.6 – 44.5 µg/L) was observed during ozonation, indicating the attack of ozone on the nitrogen atom of DON yielding a mixture of products including hydroxylamine, and nitrate, among others. This

observation is consistent with what was shown in the previous chapter. Ozonation of C-DBP precursors (e.g., phenol-type entities), on the other hand, occurs via a Criegee-type reaction where aromatic rings are cleaved forming muconic-type and aliphatic products (Wenk et al. 2013) including precursors of CH and HKs (see Section 2.6.2). This is reflected in a measured decrease in SUVA from 1.88 L/mg-C·m in the source water down to 0.88 L/mg-C·m after ozonation at 0.75 mg O_3/mg DOC (Figure 5.3a). At this same specific ozone dose, an 80% decrease in fluorescence intensities of humic and fulvic acid-like peaks was also observed (Figure 5.3b). During this process, electron-rich constituents of NOM are oxidized leading to fewer halogenation sites (Westerhoff et al. 2004) that are necessary for THM and HAA precursors. The oxidized NOM also becomes more hydrophilic resulting in a large decrease in THAAs whose precursors are known to be more hydrophobic compared to those of THMs and DHAAs (Hua and Reckhow 2007a). This increase in hydrophilicity also enhanced formation of bromine-containing DBPs such as DBCM, TBM, DBAA, CDBAA, DBAN, TBNM, and DBCM (Table 5.4) from oxidation by both O_3 and $^{\bullet}OH$. The influence of each oxidant on DBP formation was then distinguished by addition of t-BuOH and H_2O_2 to represent O_3- and $^{\bullet}OH$-dominated conditions, respectively.

5.3.1.1. Addition of tertiary butanol and H_2O_2

Figure 5.2 shows that ozonation of water samples in the presence of t-BuOH decreased the formation potentials of both C- and N-DBPs compared to O_3 with H_2O_2 and O_3 alone, the latter containing a mixture of molecular ozone and $^{\bullet}OH$. The results confirm that reactions of ozone decreased nucleophilic centers of NOM available for chlorine substitution (Westerhoff et al. 2004). They also support the observations of Wenk et al. (2013) that O_3 reactions resulted in NOM with lower electron-donating capacity compared to non-selective oxidation with $^{\bullet}OH$. The average formation potentials of each DBP species are presented in Table 5.4. It should be noted that in the presence of NOM, t-BuOH is less likely to react with ozone ($k = 3\times10^{-3}$ $M^{-1}s^{-1}$) (Reisz et al. 2014). This was apparent from lower DBP formation potentials produced from samples treated with O_3/t-BuOH compared to O_3 only and O_3/H_2O_2. Control experiments using ozonated t-BuOH in pure water were performed to investigate DBP formation related to t-BuOH. In pure water, TCM and AOX concentrations produced from ozonated t-BuOH were only about 15% of the formation potentials observed for water samples treated with O_3/t-BuOH. In the presence of NOM, this percentage is expected to be much lower. Ozonation of t-BuOH alone, however, may form acetone and butan-2-one (Reisz et al. 2014) and $^{\bullet}OH$ scavenging may form formaldehyde (Nöthe et al. 2009). These compounds can possibly act as precursors of HKs including 1,1,1-TCP and 1,1-DCP whose respective concentrations after ozonation

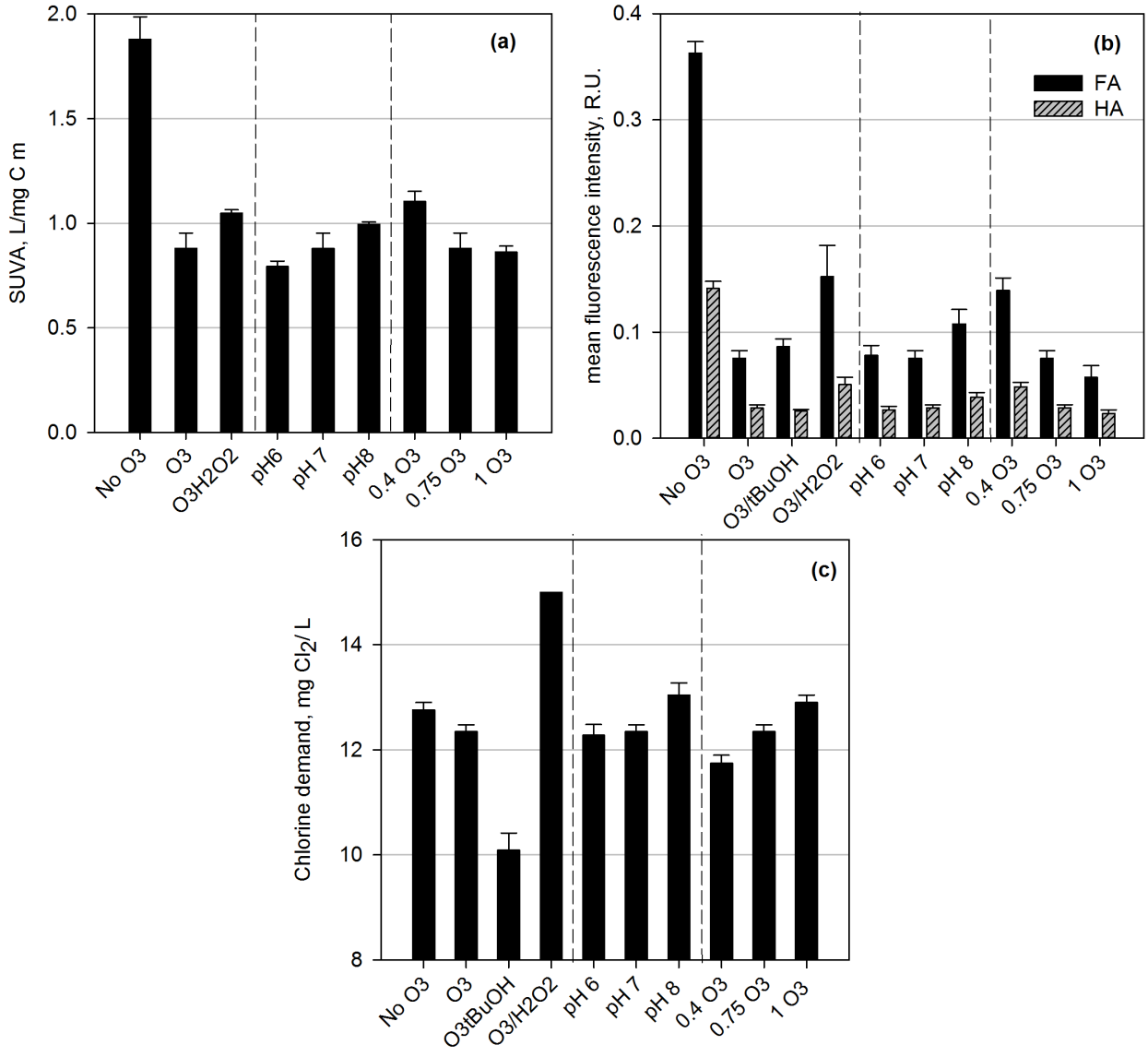

Figure 5.3. Changes in (a) SUVA, (b) fluorescence of fulvic acid- (FA) and humic acid (HA)-like EEM regions, and (c) chlorine demand of samples after ozonation for different oxidant exposures. Error bars depict the standard deviation of 3 replicate experimental results. Reported fluorescence measurements (R.U. = Raman Units) were taken from samples diluted 4-fold.

Table 5.4. Average formation potentials of DBPs (µmol/mmolC×10^2) during ozonation at different conditions*. Numbers in parentheses are the standard deviation (n=3) and mean absolute deviation (n=2).[a]

DBP	No O_3	O_3/pH 7/0.75 O_3	O_3/t-BuOH	O_3/H_2O_2	pH 6	pH 8	0.4 O_3	1 O_3
Trichloromethane (TCM)	225 (13)	156 (23)	77 (8)	256 (56)	128 (19)	163(6)	140 (21)	152 (24)
Bromodichloromethane (BDCM)	59 (8)	52 (3)	54 (3)	63 (3)	49 (2)	52 (6)	50 (3)	51 (2)
Dibromochloromethane (DBCM)	9.0 (2.3)	12 (3)	14 (1)	12 (2)	13 (2)	13 (2)	14 (3)	12 (2)
Tribromomethane (TBM)	0.3 (0.1)	1.0 (0.4)	1.6 (1.0)	0.7 (0.2)	1.0 (0.4)	1.0 (0.3)	1.3 (0.5)	0.9 (0.4)
Monochloroacetic acid (MCAA)[a]	9.2 (6.7)	<3.7	17 (3)	19 (2)	13 (4)	15 (6)	11 (4)	16 (6)
Monobromoacetic acid (MBAA)[a]	<2.5	3.3 (0.8)	4.6 (0.1)	<2.5	5.6 (0.3)	<2.5	<2.5	5.1 (0.2)
Dichloroacetic acid (DCAA)[a]	70 (26)	60 (1)	34 (0)	101 (53)	52 (6)	73 (21)	51 (3)	64 (8)
Trichloroacetic acid (TCAA)[a]	66 (15)	36 (4.)	16 (4)	61 (41)	33 (6)	40 (3)	32 (8)	38 (9)
Bromochloroacetic acid (BCAA)[a]	17 (3)	16 (0.0)	11 (0)	16 (2)	14 (0)	17 (1)	15 (1)	15 (0)
Bromodichloroacetic acid (BDCAA)[a]	19 (4)	16 (1)	8.7 (4.4)	19 (10)	14 (1)	16 (4)	14 (0)	16 (0)
Dibromoacetic acid (DBAA)[a]	2.9 (0.6)	4.3 (0.1)	7.1 (0.4)	3.2 (0.1)	6.2 (0.2)	4.0 (0.7)	4.0 (0.0)	4.9 (0.2)
Chlorodibromoacetic acid (CDBAA)[a]	3.4 (1.7)	4.3 (2.3)	3.5 (2.0)	5.5 (6.0)	3.8 (1.9)	4.7 (3.7)	4.0 (1.6)	4.3 (2.3)
Trichloroacetonitrile (TCAN)	0.2 (0.1)	0.2 (0.0)	0.2 (0.2)	0.2 (0.1)	0.2 (0.0)	0.2 (0.1)	0.2 (0.0)	0.3 (0.0)
Dichloroacetonitrile (DCAN)	12 (2)	6.5 (0.9)	4.2 (1.1)	8.3 (1.2)	6.5 (1.0)	6.5 (1.7)	6.9 (1.0)	6.5 (0.8)
Bromochloroacetonitrile (BCAN)	3.1 (0.9)	2.1 (0.4)	1.8 (0.5)	2.6 (0.7)	2.0 (0.4)	2.3 (0.6)	2.8 (0.8)	1.9 (0.4)
Dibromoacetonitrile (DBAN)	0.4 (0.0)	0.6 (0.1)	0.9 (0.1)	0.6 (0.1)	0.7 (0.1)	0.7 (0.1)	0.8 (0.1)	0.6 (0.1)
Chloral hydrate (CH)	14 (1)	43 (3)	8.7 (2.4)	64 (2)	27 (2)	44 (4)	33 (2)	43 (3)
Trichloronitromethane (TCNM)	0.4 (0.1)	5.1 (0.3)	3.6 (0.2)	3.4 (0.6)	4.6 (0.4)	4.2 (0.6)	3.5 (0.3)	5.5 (0.5)
Tribromonitromethane (TBNM)	0.04 (0.07)	0.3 (0.1)	1.0 (0.2)	0.1 (0.1)	0.4 (0.1)	0.3 (0.1)	0.2 (0.1)	0.3 (0.1)
1,1-dichloropropanone (11DCP)	1.0 (0.6)	1.8 (1.4)	1.8 (0.3)	1.9 (0.5)	1.4 (0.7)	2.2 (1.0)	1.0 (0.4)	1.9 (1.4)
1,1,1,-trichloropropanone (111TCP)	10 (1)	28 (3)	16 (2)	35 (2)	20 (2)	24 (3)	18 (1)	31 (4)
Trichloroacetamide (TCAM)	2.1 (1.0)	1.2 (0.8)	0.5 (0.3)	1.8 (1.0)	0.9 (0.5)	1.3 (0.8)	1.1 (0.6)	1.0 (0.6)
Bromodichloroacetamide (BDCAM)[a]	1.1 (0.1)	0.9 (0.3)	0.9 (0.0)	1.8 (0.8)	0.8 (0.3)	1.0 (0.4)	1.0 (0.2)	0.9 (0.4)
Dibromochloroacetamide (DBCAM)[a]	0.5 (0.2)	1.0 (0.8)	1.6 (1.9)	1.3 (0.7)	1.0 (0.9)	1.1 (0.6)	1.4 (1.2)	1.1 (0.6)
Adsorbable organic halogen (AOX)[a]	2250 (1)	2050 (50)	1210 (234)	2500 (467)	1800 (133)	2140 (89)	1570 (522)	2330 (436)

**average values from experiments (n=3; n=2 for HAAs, BDCAM, DBCAM, and AOX) with two extractions per sample and DOC = 17±2mg/L; Chlorine residuals normally ranged from 1 to 2 mg Cl_2/L.*

of t-BuOH in pure water were 72% and 21% higher than the formation potentials of water samples treated with O_3/t-BuOH. As can be seen from Figure 5.2, this possible increase in DBP formation potentials was not apparent in the actual water sample due to competing reactions with more reactive NOM, producing less HKs compared to O_3 only and O_3/H_2O_2 conditions. This strongly suggests that t-BuOH does not contribute to further DBP formation in our water sample.

In terms of THM4, addition of t-BuOH caused a further 34% decrease in their formation potential compared to ozonation without t-BuOH. This implies that t-BuOH improved the reaction of O_3 towards THM precursors which are often correlated with hydrophobic fractions containing aromatic carbon and this is reflected in decreased fluorescence at the humic and fulvic acid-like regions (Figure 5.4). When O_3/H_2O_2 was used, THM4 formation potentials after subsequent chlorination increased by 50% relative to O_3 only and were almost equal to those in samples without O_3. Such an increase is consistent with the increased SUVA and fluorescence observed in O_3/H_2O_2 treatments compared to ozone alone (Figures 5.3a and 5.3b).

The results for HAAs were similar to those observed for THM4. Relative to ozonated samples without H_2O_2, THAA and DHAA formation potentials were higher by about 50% after O_3/H_2O_2 treatment. On the other hand, addition of t-BuOH during ozonation lowered THAA and DHAA formation potentials by 50% and 35%, respectively. These findings are reflected in the decrease of chlorine demand when O_3 reactions were favored over $^{\bullet}OH$ reactions (Figure 5.3c). For example, ozonated samples without t-BuOH had a chlorine demand of 12.3 mg/L while this value was reduced to 10.1 mg/L in those ozonated samples to which t-BuOH was added.

Although the levels of CH and HKs after chlorination increased with ozonation as a result of increased aldehyde and methyl ketone species, their formation potentials were still lower with O_3/t-BuOH (CH=0.09; HK=0.17 μmol/mmol C) than those treated with O_3/H_2O_2 (CH=0.64; HK=0.36 μmol/mmol C). In the presence of t-BuOH, CH decreased by 79% and HKs by 35% compared to samples ozonated without t-BuOH. These findings suggest that $^{\bullet}OH$ radicals are able to react with O_3-refractory moieties of NOM leading to formation of more CH and HK precursors. This is demonstrated in lower acetaldehyde concentrations measured after ozonation in the presence of t-BuOH than with H_2O_2 (Figure 5.5).

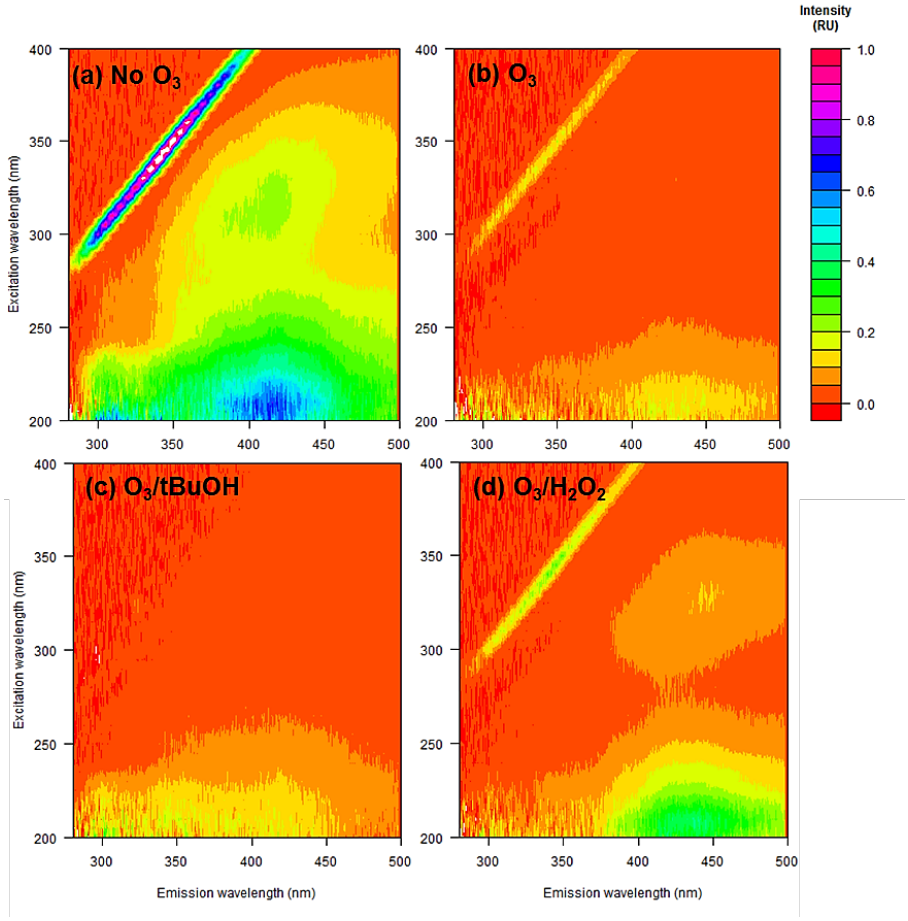

Figure 5.4. Example fluorescence EEM plots showing the influence of O_3 and $^{\bullet}OH$ on NOM characteristics.

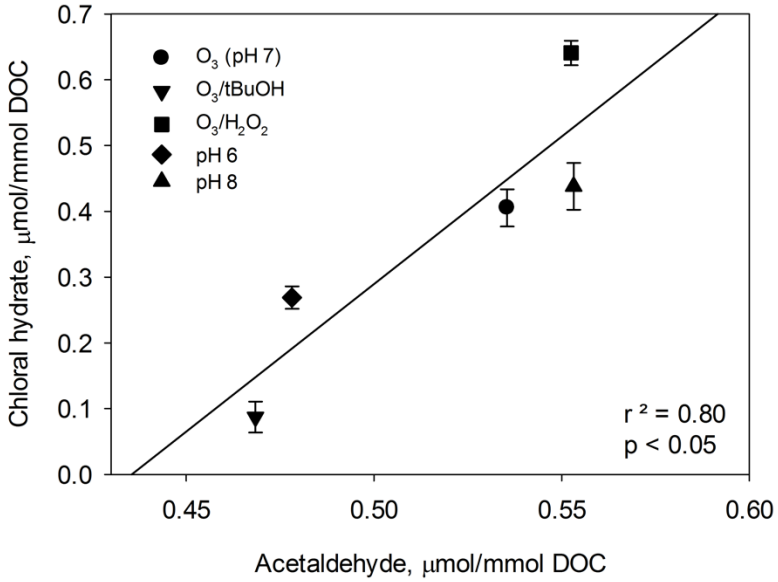

Figure 5.5. Correlation between acetaldehyde formation after ozonation and chloral hydrate formation after subsequent chlorination of the same sample. Conditions: DOC = 18 mg/L; specific ozone dose = 0.75 mg O_3/mg DOC.

The observed trends for THM4, HAAs, CH, and HKs also occurred for N-DBPs pertaining to the groups of HAN4 and THAMs. The formation potentials of HAN4 were reduced by 53% in the presence of t-BuOH while in presence of H_2O_2, the reduction was 29% lower. The results shown here were consistent with the findings of Molnar et al. (2012b) who showed that $^{\bullet}OH$ reactions generated from TiO_2-catalyzed ozonation resulted in an increase in hydrophilic NOM fractions, which are known to contain HAN precursors. In terms of THAMs, which can be formed from hydrolysis of HANs (Glezer et al. 1999) or from other HAN-independent reactions (Huang et al. 2012), addition of t-BuOH tends to improve reduction of THAM formation potentials relative to ozonation without t-BuOH. With O_3/H_2O_2, the formation potentials were even higher compared to samples not treated with ozone. The differences between these treatments, however, showed weak statistical significance due to large deviations arising from relatively low THAM concentrations.

The differences between THNM formation potentials (sum of TCNM and TBNM) in samples treated with and without t-BuOH and H_2O_2 were not markedly significant ($p=0.06$) due to contrasting changes in concentrations of TCNM and TBNM (Table 5.4). TCNM concentrations were lower in ozonated samples with either t-BuOH or H_2O_2. At these conditions, a rupture of the C-N bond to form inorganic nitrogen is likely such that HNM formation is minimized regardless of whether the reaction proceeds via the O_3 or $^{\bullet}OH$ pathways. This mechanism is supported by previous studies where ozonation reactions with organic nitrogen were observed to yield nitrate and ammonia as end products, respectively (Berger et al. 1999, Le Lacheur and Glaze 1996) (see also Chapter 4). The results here also demonstrate that O_3 reactions are mainly responsible for formation of TCNM precursors (e.g., nitroalkanes), mostly coming from primary and secondary amines (McCurry et al. 2016). At high ozone exposures, the nitromethane intermediate can decrease with concomitant production of NO_3^-, resulting in lower TCNM formation potential with O_3/t-BuOH compared to ozonation without t-BuOH. With the addition of H_2O_2, TCNM levels were lower (compared to both O_3 and O_3/t-BuOH) due to the limited O_3 exposure for reaction of primary oxidation intermediates to produce nitromethane. At that condition, TCNM formation was still formed likely due to C-C cleavage from $^{\bullet}OH$ reactions consequently releasing chloropicrin precursors (McCurry et al. 2016) and/or reactions of other oxidizing radical species from O_3 decomposition (e.g., $O^{\bullet-}$) as proposed by Shan et al. (2012). Significant differences were observed for TBNM ($p<0.05$). Compared to ozonation alone and in the presence of H_2O_2, TBNM formation potential was higher for ozonated samples containing t-BuOH. This is a result of an increased $HOBr/OBr^-$ concentration, which enhances bromine substitution into nitroalkane groups. The changes in percent bromine substitution factors after ozonation are illustrated in Figure 5.6. These values were calculated from the ratio of the molar concentration of bromine incorporated in one DBP group to the total molar concentration of chlorine

and bromine in that group (Hua and Reckhow 2013). Less TBNM was found in samples containing H_2O_2 most likely due to the reduction of HOBr/OBr^- to Br^- by H_2O_2 as reported by von Gunten and Oliveras (1998). Similar trends were observed for other bromine-containing DBPs including DBCM, TBM, DBAN, TBNM, DBCAM, DBAA, and CDBAA.

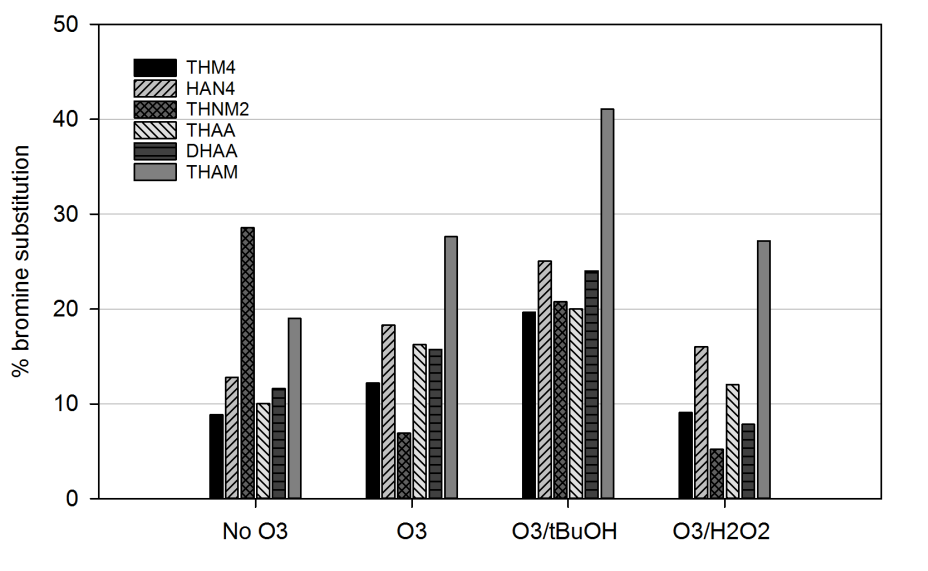

Figure 5.6. Effect of ozone and •OH pathways on percent bromine substitution of C- and N-DBPs following subsequent chlorination. %Bromine substitution (Hua and Reckhow 2013) for each DBP group was calculated as follows:

$$\mathrm{THM4} = \frac{[\mathrm{BDCM}] + 2[\mathrm{DBCM}] + 3[\mathrm{TBM}]}{3 \times ([\mathrm{TCM}] + [\mathrm{BDCM}] + [\mathrm{DBCM}] + [\mathrm{TBM}])} \times 100$$

$$\mathrm{HAN4} = \frac{[\mathrm{BCAN}] + 2[\mathrm{DBAN}]}{3 \times [\mathrm{TCAN}] + 2 \times ([\mathrm{DCAN}] + [\mathrm{BCAN}] + [\mathrm{DBAN}])} \times 100$$

$$\mathrm{THNM2} = \frac{3 \times [\mathrm{TBNM}]}{3 \times ([\mathrm{TCNM}] + [\mathrm{TBNM}])} \times 100$$

$$\mathrm{THAA} = \frac{[\mathrm{BDCAA}] + 2[\mathrm{DBCAA}]}{3 \times ([\mathrm{TCAA}] + [\mathrm{BDCAA}] + [\mathrm{DBCAA}])} \times 100$$

$$\mathrm{DHAA} = \frac{[\mathrm{BCAA}] + 2[\mathrm{DBAA}]}{2 \times ([\mathrm{DCAA}] + [\mathrm{BCAA}] + [\mathrm{DBAA}])} \times 100$$

$$\mathrm{THAM} = \frac{[\mathrm{BDCAM}] + 2[\mathrm{DBCAM}]}{3 \times ([\mathrm{TCAM}] + [\mathrm{BDCAM}] + [\mathrm{DBCAM}])} \times 100$$

5.3.1.2. Ozonation pH

The changes in formation potentials with varying ozone and •OH exposures were confirmed using ozonation conditions at differing pH. Consistent with our earlier results, formation potentials of C-DBPs were found to be lower at pH 6 where O_3 exposures are higher compared to pH 8 (Figure 5.7). Unlike with the addition of t-BuOH and H_2O_2, changes in C-DBP formation potentials as a result of

varying ozonation pH were relatively small. This is due to the opposing effects of O_3 exposure and reactivity of C-DBP precursors (e.g., phenol moieties) with O_3 at differing pH (see Section 2.6.2). It is expected that O_3 would be more reactive with phenolic moieties at higher pH, but such reaction will be limited by the fast hydroxide-initiated O_3 decomposition reactions (von Sonntag and von Gunten 2012).

Compared to chlorination of non-ozonated samples, THM4 formation potentials decreased by 35% when samples ozonated at pH 6 were subsequently chlorinated to achieve the same target residual. When ozonation was carried out at pH 8, THM4 formation potential was 20% higher than at pH 6. This could be the result of having low O_3 exposures, $^{\bullet}OH$ reactions with aromatic structures in NOM ($k_{app(^{\bullet}OH+phenol)} = 1\times10^{10}$ $M^{-1}s^{-1}$ (Buxton et al. 1988)), and transformation products that are more susceptible to halogenation with chlorine (Kleiser and Frimmel 2000, von Gunten 2003b). Kleiser and Frimmel (2000) also proposed that $^{\bullet}OH$ attack on NOM via H-abstraction of aliphatic structures and reactions with oxygen and peroxyl radicals may produce alcohol or keto-groups which react with chlorine to form THMs (Kleiser and Frimmel 2000).

A similar trend was observed for HAAs but with a higher increase at pH 8 for DHAAs (31%) compared to THAAs (21%). This difference could be related to the change in content and structure of HAA precursors. At higher ozonation pH, more hydrophilic NOM fractions could form which are known precursors of DHAA. In a study by Molnar et al. (2012a), ozonation at 3 mg O_3/mg DOC of a raw water sample at pH 10 compared to pH 6 increased the hydrophilic NOM fraction to 90%. This fraction may contain β-dicarbonyl acid species which are important in DHAA formation (Bond et al. 2009a, Dickenson et al. 2008).

The degradation products of $^{\bullet}OH$ reactions with NOM (e.g., saturated compounds like aldehydes and ketones) are also important for formation of CH and HK as shown in the previous section. The formation potentials of these groups increased after ozonation, with this increase being stronger at pH 8 compared to lower pH. This provides further evidence that a shift from O_3 to $^{\bullet}OH$ pathway promotes formation of precursors of halogenated aldehydes (Figure 5.5) and ketones.

After ozonation, HAN4 and THAM formation potentials decreased with concurrent increase in THNM formation potential. However, across the ozonation pH levels used in this study, no significant differences were observed for the N-DBPs analyzed. The results may imply that the change in O_3 and $^{\bullet}OH$ exposures at the pH 6 – 8 may be insufficient to cause dramatic change in precursor concentrations as compared to exposures obtained through addition of t-BuOH and H_2O_2. The results were also an indication of the contrasting effects of O_3 exposure and reactivity of N-DBP precursors (e.g., amines). Lower pH would mean an increase in O_3 exposure but a decrease in rate constant of

amines with ozone (von Sonntag and von Gunten 2012) (Section 2.6.2). The results may also have an implication on the nature of organic nitrogen present in the sample. Shan et al. (2012), for example, showed that most amino acids (except glycine and lysine) and amino sugars did not cause an apparent increase in the yield of HNMs when ozonation pH was increased from pH 6 to 8.

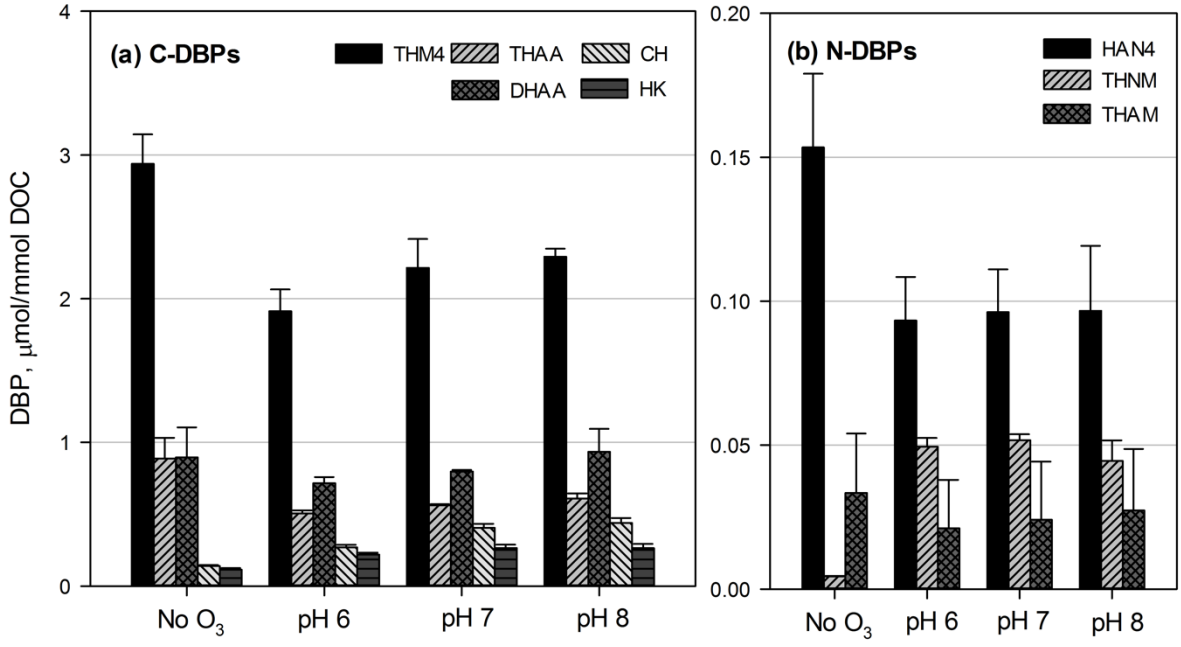

Figure 5.7. Formation potentials of (a) C-DBPs and (b) N-DBPs at different ozonation pH. Conditions: DOC = 17.2 ± 2.0 mg/L, specific ozone dose = 0.75 mgO_3/mg DOC, buffer = 1 mM phosphate, temperature = 22 ± 1 °C. HOCl DBP 24 h formation potentials tests at pH 7 were targeted to have a 1 – 2 mg/L Cl_2 residual. Error bars depict standard deviation of 3 replicate experiments.

5.3.1.3. Transferred ozone dose

Figure 5.8 shows the effect of increasing specific ozone dose on formation potentials of C- and N-DBPs. It should be noted, however, that increasing the ozone dose may not completely differentiate the effects of ozone and $^{\bullet}$OH because, as shown in Figure 5.9, the exposures of both oxidants increase with dose. Thus, this section demonstrates the combined effects of ozone and $^{\bullet}$OH on formation potentials of DBPs.

Ozonation at an initial low specific dose of 0.4 mg O_3/mg DOC led to 20 – 40% lower formation of THM4, THAAs, DHAAs, HAN4, and THAMs after chlorination compared to non-ozonated samples that were chlorinated to achieve the same target residual. When the ozone dose was increased, no statistically significant effect was observed for THM4. This could be a result of complete

consumption of chlorine's reactive sites at the lowest specific O_3 dose as well as the competing effects of O_3 and $^{\bullet}OH$ reactions, (i.e., O_3 reactions minimize THM formation while $^{\bullet}OH$ reactions form more precursors). Although bromine-containing THMs increased after ozonation, only slight variations in their formation potentials were observed when ozone dose was increased (Table 5.4).

HAA precursor concentrations were also reduced during initial low dose ozonation. However, at higher specific ozone doses, THAA and DHAA formation potentials appeared to increase slightly. From 0.4 to 1 mg O_3/mg DOC, concentrations of THAAs increased by 15% while those of DHAAs increased by 22%. Between the two groups and at all specific ozone doses, THAA formation potentials were lower than those of DHAAs because of the more hydrophobic nature of the former (Hua and Reckhow 2007a). The same rationale applies for higher reduction of THAA formation potentials at the same 0.75 mg O_3/mg DOC ozone dose (37%) compared to THM4 (25%).

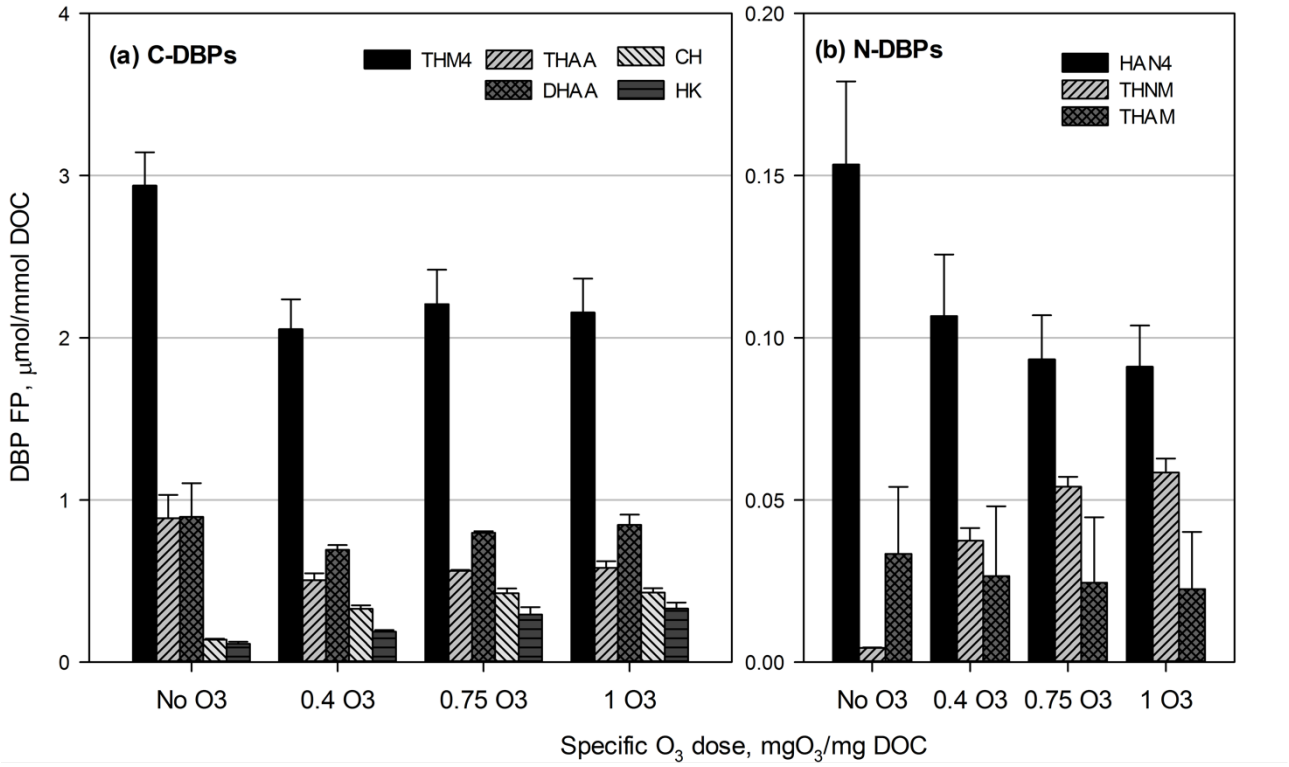

Figure 5.8. Formation potentials of (a) C-DBPs and (b) N-DBPs at different specific ozone doses. Conditions: DOC = 17.2 ± 2.0 mg/L, pH =7 (1 mM phosphate), temperature = 22 ± 1°C. HOCl DBP 24 h formation potentials tests at pH 7 were targeted to have a 1 – 2 mg/L Cl_2 residual. Error bars depict standard deviation of 3 replicate experiments.

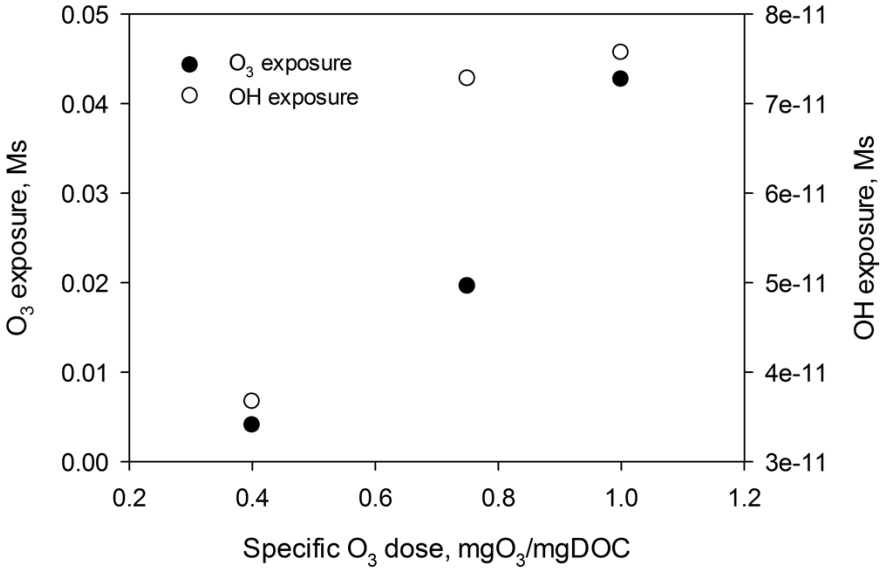

Figure 5.9. Increase in O_3 and $^{\bullet}OH$ exposures during ozonation of reconstituted RO concentrate with increase in specific ozone dose. Conditions: DOC = 20 mg/L, DON = 0.7 mg/L, pH = 7, temperature = 22 ± 1°C; Ozone exposures were measured using the indigo method while $^{\bullet}OH$ exposures were indirectly determined through decay of *para*-chlorobenzoic acid (1 µM) (Elovitz and von Gunten 1999).

The formation potentials of CH and HK were shown to increase at higher ozone doses. Compared to samples without ozone, CH and HK increased by 137 to 209% and 64 to 190% from 0.4 to 1 mg O_3/mg DOC, respectively. These results demonstrate the strong contribution of both O_3 and $^{\bullet}OH$ in the formation of aldehydes and methyl ketone precursors which caused an increase in CH and HK formation. The increases in aldehyde concentrations are presented in Figure 5.10. These results, together with those observed at different ozonation pH, show that ozonation at lower doses and pH may be necessary for better control of C-DBP formation.

Ozonation of dissolved organic nitrogen with increasing dose may result in a mixture of oxidized amines, nitriles, and amides (Chapter 4). The formation potentials of HAN4 and THAMs decreased 30 to 41% and 20 to 32%, respectively, when the specific ozone dose increased from 0.4 to 1 mg O_3/mg DOC. Although the differences in concentrations after ozonation did not reach statistical significance ($p>0.05$), the decreasing trend in formation potentials at higher ozone dose suggests favorable oxidation of HAN4 and THAM precursors to nitroalkane groups which in turn promotes THNM formation (Huang et al. 2012, McCurry et al. 2016, Yang et al. 2012b). These reactions may explain the significant increase in THNM formation potentials from 0.005 to 0.060 µmol/mmol C when ozone dose was increased.

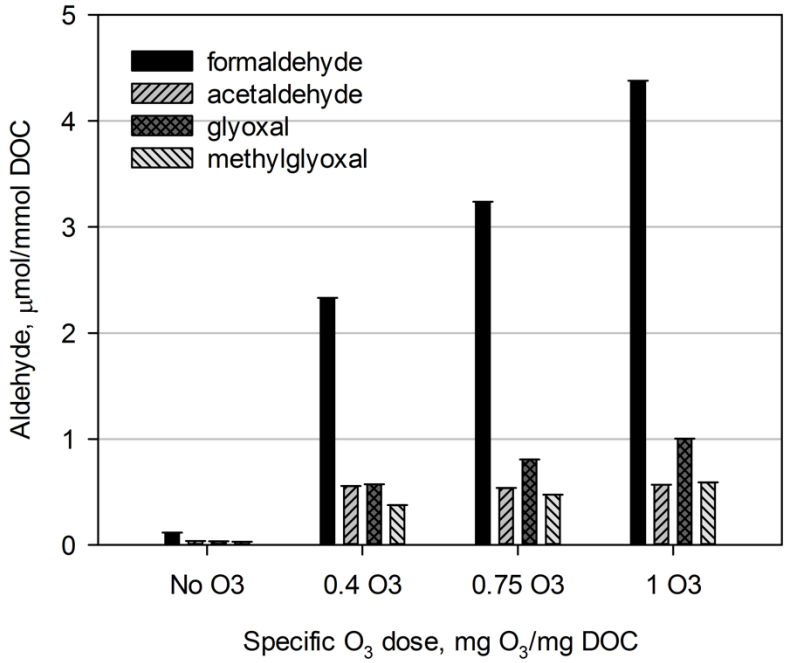

Figure 5.10. Aldehyde formation as a function of specific ozone dose.

Since bromate formed during ozonation is among the DBPs of most interest, it was also measured after ozonation at different conditions. Both O_3 and $^{\bullet}OH$ radical reaction pathways were reported to significantly affect bromate formation through mechanisms involving oxidation of bromide and bromite by molecular O_3 and oxidation of intermediate oxybromine species by $^{\bullet}OH$ (von Gunten and Hoigné 1994). Figure 5.11 shows bromate concentrations during ozonation at various specific ozone doses, bromide and inorganic carbon concentrations, and in the presence of t-BuOH and H_2O_2. Bromate increased with increasing specific ozone dose and bromide concentrations. When inorganic carbon was increased from 0 to 6 mg/mg DOC at the same specific ozone dose (0.75 mg O_3/mg DOC) and bromide concentration (20 µg Br^-/mg DOC), bromate increased from 0.01 to 0.05 mg/L due to reactions of bromide and hypobromite with ozone, $^{\bullet}OH$, and carbonate radicals formed from $^{\bullet}OH$ scavenging by HCO_3^-/CO_3^{2-} (von Gunten and Hoigné 1994). In natural waters, a higher inorganic carbon can elevate pH which might favor bromate formation by the $^{\bullet}OH$ pathway. In the presence of t-BuOH and H_2O_2 at 0.75 mg O_3/mg DOC and the same bromide concentration (20 µg Br^-/mg DOC), no bromate was formed which is similar to the observations of Gillogly et al. (2001). H_2O_2 reduces HOBr to Br^- while t-BuOH can scavenge available $^{\bullet}OH$. Since no bromate was found after ozonation with t-BuOH, the $^{\bullet}OH$ pathway, therefore, played an important role in bromate formation in our water sample. It should be noted that the reported bromate concentrations in our study came from reconstituted water samples (DOC = 18 mg/L) which are about 4 to 10 times more concentrated than

commonly encountered in water treatment plants where the resulting bromate concentrations would typically be much lower.

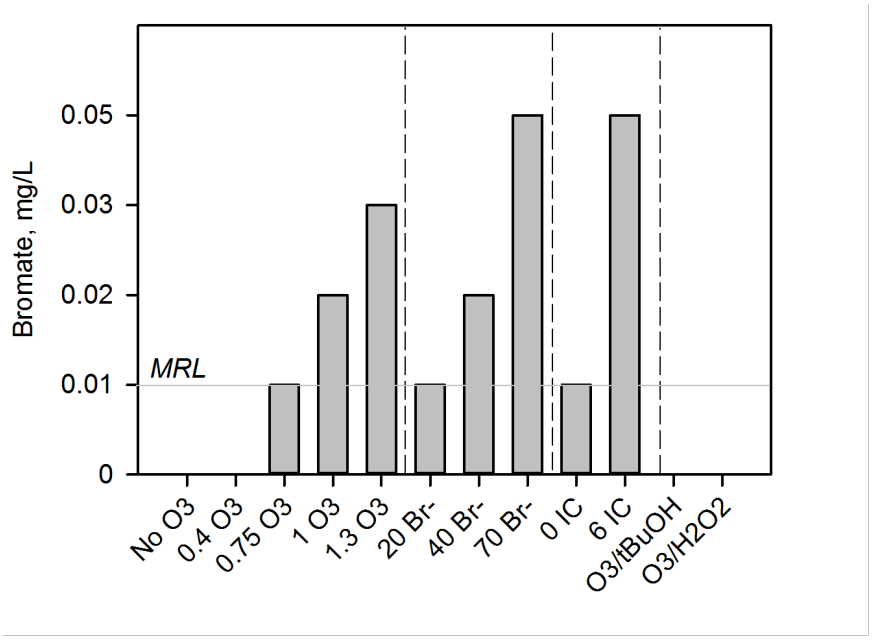

Figure 5.11. Bromate concentrations at different specific ozone dose (0 – 1.3 mgO_3/mg DOC), bromide concentrations (20 – 70 µg Br^-/mg DOC), inorganic carbon (IC) concentrations (0 – 6 mg/mg DOC), and in the presence of t-BuOH (10 mM) and H_2O_2 (1 mg/mg O_3). Baseline conditions: DOC = 18 mg/L as C, pH = 7 (1 mM phosphate), temperature = 22±1 °C, bromide = 20 µg Br^-/mg DOC, IC = 0 mg/mg DOC, specific ozone dose = 0.75 mgO_3/mg DOC. Bromide and IC concentrations were varied by spiking NaBr and $NaHCO_3$, respectively. *MRL* = method reporting limit.

5.3.2. Effect of ozonation conditions on formation of unknown byproducts

One of the concerns during ozonation is the formation of unknown transformation products that may be associated with certain toxic effects. To address this, AOX and *in vitro* bioassays were conducted after the ozonated water had been chlorinated in the formation potential tests.

Figure 5.12a shows the changes in AOX at different ozonation conditions which could be partially attributed to the largest constituents: THM4 at 29 – 42% and total HAAs at 16 – 22% across all experimental conditions in this study. The results were generally consistent with those observed for the sum of the measured DBPs, i.e., conditions that favor ozone over $^{\bullet}OH$ reactions led to lower AOX formation potentials. Figure 5.13 shows examples of changes in AOX distributions as a function of different oxidant exposure. After chlorination of O_3/t-BuOH treated water, the AOX concentration (12.1 µmol/mmol C) was found to be lower than AOX from ozonation at ambient conditions (20.5 µmol/mmol C). Higher AOX was found for O_3/H_2O_2 treatment (25.0 µmol/mmol C) which was 11%

higher than AOX from samples not treated with ozone. AOX at pH 8 (21.4 µmol/mmol C) was also higher than AOX at pH 6 (18.0 µmol/mmol C). AOX formation potentials also had an initial decrease of 30% at 0.4 mg O_3/mg DOC followed by an increase in concentrations in the range of 15.7 – 23.3 µmol/mmol C with increasing specific ozone dose. This supports our hypothesis that the increase in DBP formation potentials with increasing ozone dose is due to $^{\bullet}OH$ induced formation of halogen reactive organic matter fractions. This can be seen from a linear relation of AOX formation potentials with chlorine demand of samples ozonated at different conditions (Figure 5.14).

Another notable outcome of ozonation at different O_3 exposures is the change in unknown to known AOX ratio (UAOX/AOX) (Figure 5.12b). UAOX refers to the difference between the measured AOX and the organic halogen content of the measured DBPs. It was clearly shown that conditions that promote ozone reactions have higher UAOX/AOX values compared to conditions that promote $^{\bullet}OH$ reactions. For example, samples ozonated with t-BuOH had a UAOX/AOX value of 50% while those treated with O_3/H_2O_2 only had 27%. Ozonation at pH 6 resulted in a UAOX/AOX value of 60% while at pH 8, this ratio decreased to 52%. The gap between the total AOX and known AOX became closer when the %AOX accounted for by the measured THMs and HAAs was higher (Figure 5.15).

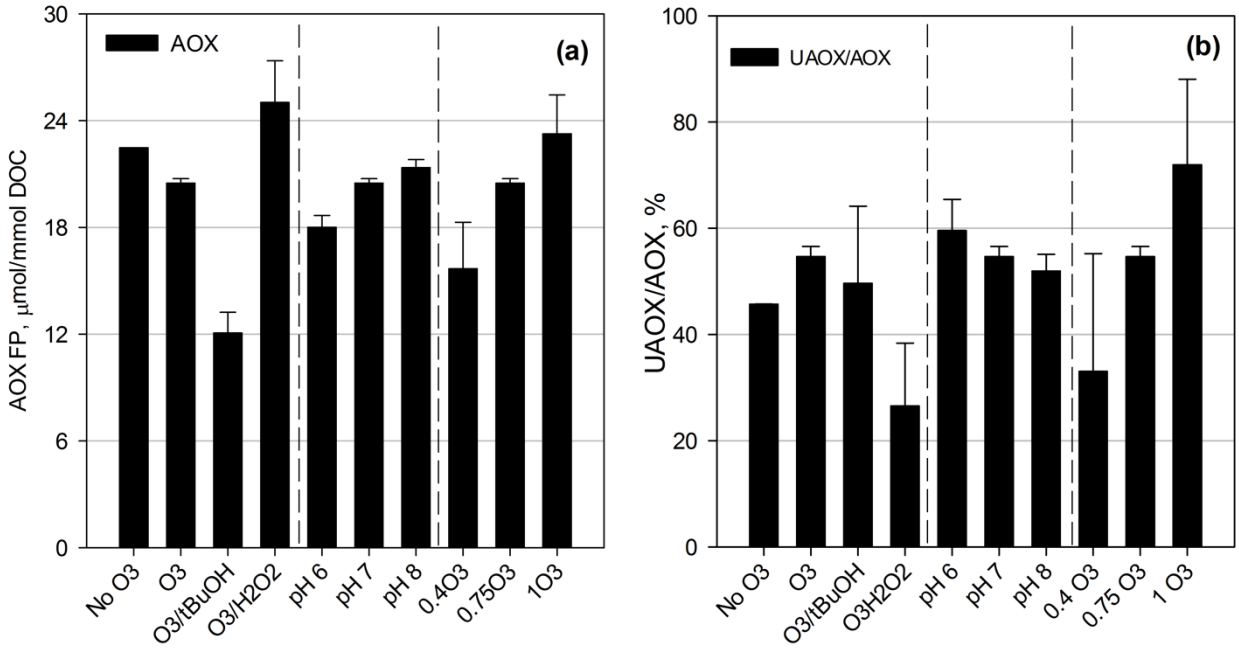

Figure 5.12. Changes in (a) AOX and (b) unknown/known AOX after ozonation and subsequent chlorination (n=2). DOC = 16.4 ± 2.0 mg/L; first set of bars in each plot correspond to samples ozonated with and without t-BuOH and H_2O_2; the second set were treated at different ozonation pH values (buffered with 1 mM phosphate); the third set were ozonated with increasing specific ozone dose (0.4 – 1 mg O_3/mg DOC). Error bars depict the mean absolute deviation.

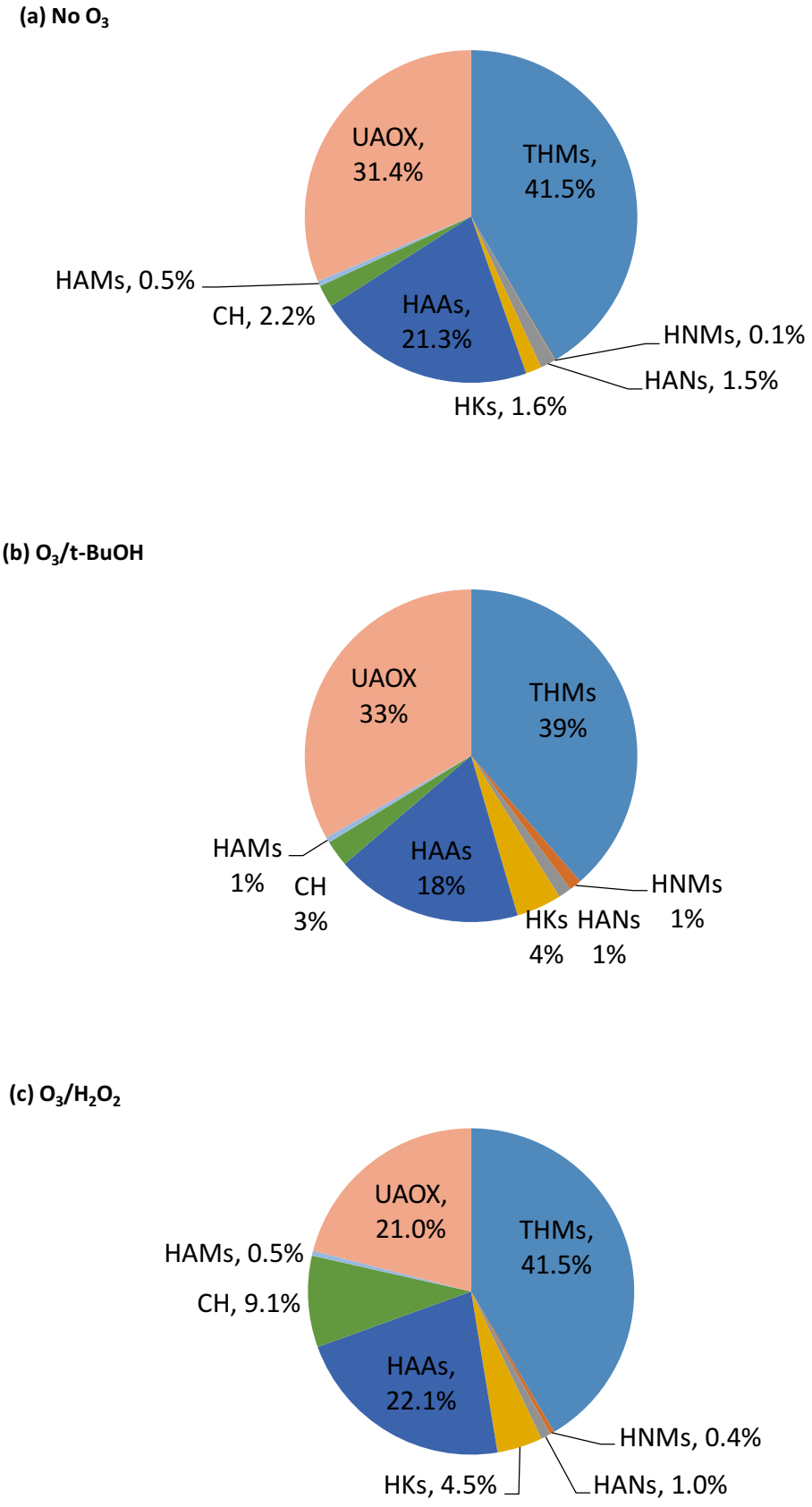

Figure 5.13. Comparison of AOX distribution for samples treated with (a) no O_3, (b) O_3/t-BuOH, and (c) O_3/H_2O_2.

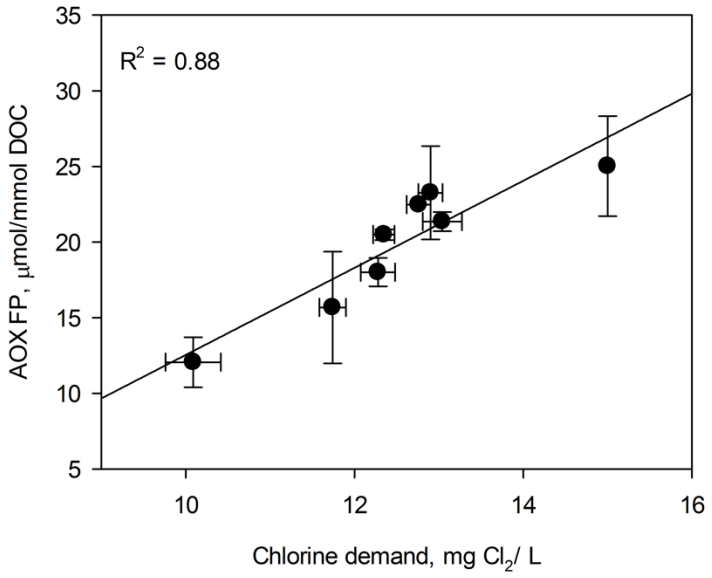

Figure 5.14. Linear relationship of AOX formation potential (AOXFP) with chlorine demand

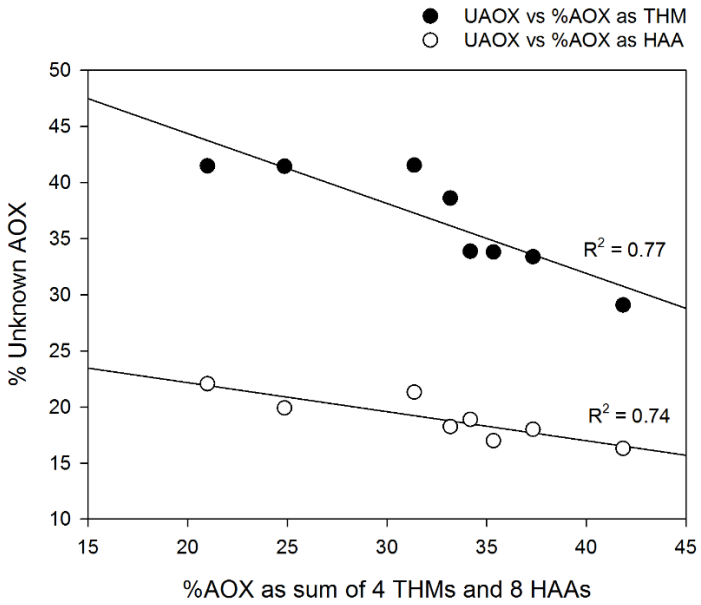

Figure 5.15. Dependence of unknown AOX on %AOX accounted for by THMs and HAAs

The changes in reactivity of the organic matter towards chlorine after ozonation may also influence the overall toxicity of the treated water sample. A summary of the bioassay responses are presented in Figure 5.16. Symbols E1 – E6 correspond to the toxicity and AOX data of 6 ozonation experiments at different pH (6, 7, and 8) and specific ozone dose (0, 0.4, 0.75 and 1 mgO_3/mg DOC). The points for O_3/t-BuOH and O_3/H_2O_2 were not included in the linear regression so as to have responses from water samples with relatively constant characteristics. Among the bioassays, the p53 assay was the only test to show a significant correlation between AOX and genotoxicity ($p = 0.006$; $R^2 = 0.87$), i.e., the higher the AOX, the more genotoxic the water becomes. Since less AOX was produced when conditions favored ozone reactions, it also follows that genotoxicity could be lower at similar conditions. Other than non-volatile DBPs, genotoxicants causing the response may also include other oxidation products such as aldehydes and aldehyde-containing moieties which may potentially damage DNA and enzymes (Magdeburg et al. 2014, Petala et al. 2008).

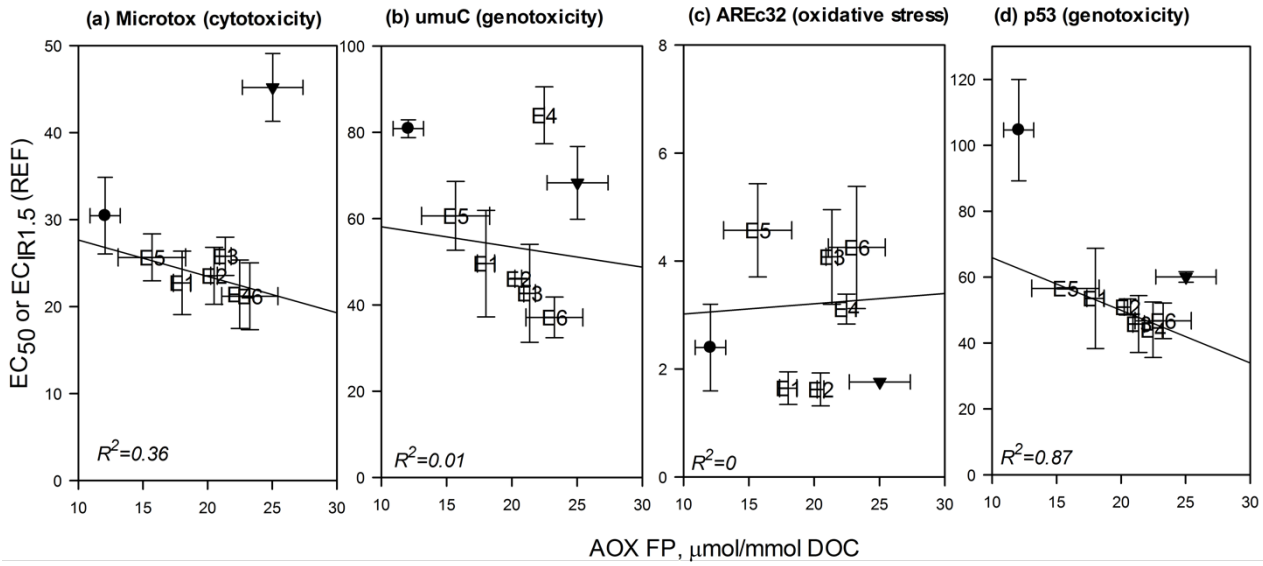

Figure 5.16. Relationship of AOX formation potentials to bioassay results (Microtox, umuC, AREc32, p53) of samples ozonated at different conditions prior to chlorination (n=2). Bioassay results show the range of effect concentrations (EC_{50} and $EC_{IR1.5}$) in units of relative enrichment factor (REF). Numbered symbols (E) correspond to the results of 6 experiments, namely ozonation at different specific O_3 doses (0, 0.4, 0.75 (also for pH 7), 1 mg O_3/mg DOC) and pH (6, 8). Circle and inverted triangle symbols correspond to samples treated with O_3/t-BuOH and O_3/H_2O_2, respectively. Error bars depict the mean absolute deviation.

Despite the correlation found for the p53 assay, the differences in toxic response from the other bioassays were generally less pronounced. The toxicity of all O_3/HOCl treated waters in our study remained relatively constant and within the commonly encountered precision of bioassay responses despite observed changes of AOX concentration with varying oxidant exposures. This suggests that the toxicological impact of AOX generated by a combination of ozone and chlorine compared to chlorine alone is insignificant. This is in contrast to studies evaluating other water treatment combinations (Farré et al. 2013, Reungoat et al. 2010). The study of Farré et al. (2013), for example, showed less variability in toxicity between samples treated with HOCl and NH_2Cl. When source waters with different organic matter characteristics and concentrations were used (e.g., samples from conventional drinking water treatment plant and a desalination plant), large differences in effect concentrations were observed. Hence, neither organic matter changes nor DBP formation brought about by different ozone exposures is sufficient to elicit a statistically significant trend in toxicity or the toxicity assays used in this study are not as sensitive as AOX measurements when it comes to evaluating ozonation effects on organic matter transformation.

5.4. Conclusions

This study evaluated the effects of ozonation conditions on formation potentials of C-DBPs, N-DBPs, AOX, and associated toxicity after chlorine disinfection. From this study, the following conclusions can be drawn:

- Ozonation at conditions favoring ozone over the $^{\bullet}OH$ pathway promotes reduction of halogenated DBP formation potentials with subsequent chlorination. This observation also applies to DBPs that are known to form as a result of pre-ozonation and subsequent chlorination such as CH and HKs. Table 5.5 provides a summary of percent removals of DBP formation potentials during ozonation under ozone- and $^{\bullet}OH$-dominated conditions.
- Increasing ozone dose without changing other conditions (e.g., pH, no addition of t-BuOH or H_2O_2) resulted in a mixture of effects brought about by additional O_3 and $^{\bullet}OH$ reactions. DBP formation potentials first decreased at the initial O_3 dose but increased at higher doses due to the contribution of $^{\bullet}OH$ in organic matter oxidation.
- The results for AOX followed the trend for the known DBPs analyzed. Subjecting samples to conditions favoring ozone reaction pathway resulted in lower AOX formation potentials but a higher percentage of UAOX.

- *In vitro* bioassay results for p53 showed significant correlation with AOX formation. Although the toxic effects were not very prominent in this study, the observed differences imply that the degree of oxidation prior to chlorine disinfection could influence the overall toxicity of the treated water. No significant changes in toxicity were observed using Microtox, umuC and AREc32 bioassays.

Table 5.5. Average percent removal of DBP formation potentials under ozone- and OH-dominated conditions*

DBP	O_3 pathway		Control (ozonated, pH 7, no t-BuOH and H_2O_2)	$^{\bullet}OH$ pathway	
	pH 6	O_3/t-BuOH		pH 8	O_3/H_2O_2
THM4	35	50	25	22	-13
HAN4	39	53	37	37	25
CH	-94	37	-192	-215	-361
THNM	-1028	-945	-1079	-915	-706
HK	-91	-51	-133	-131	-219
THAM	37	35	28	18	-16
THAA	43	68	37	32	4
DHAA	20	42	11	-4	-34
AOX	20	46	9	5	-11

**calculated from DBP formation potentials of non-ozonated water sample*

Chapter 6

Biodegradability of DBP precursors after drinking water ozonation

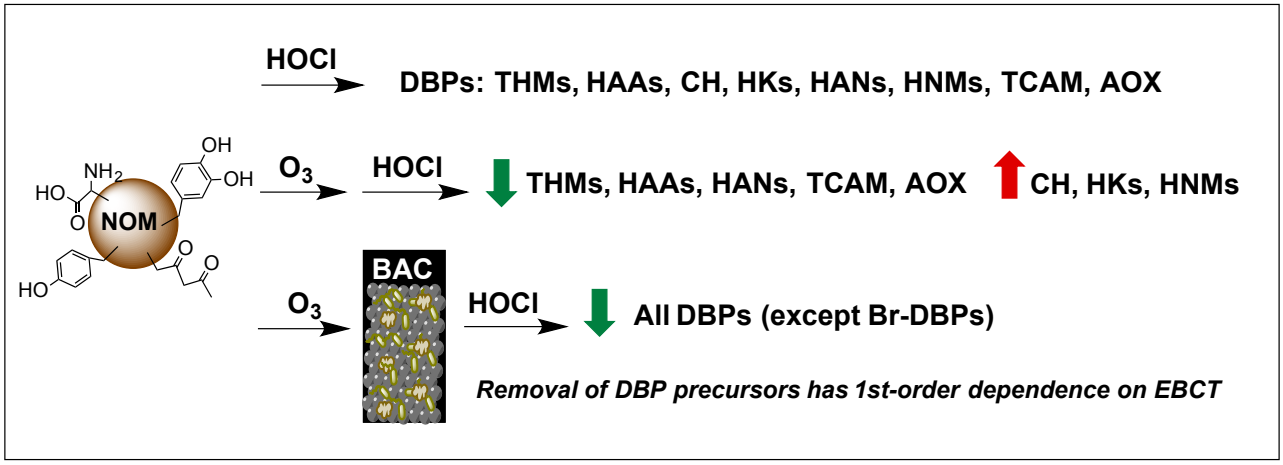

The results of the present chapter are based on the following peer-reviewed publication:

de Vera, G.A., Keller, J., Gernjak, W., Weinberg, H.S., and Farré, M.J. (2016) Biodegradability of DBP precursors after drinking water ozonation. *Water Research* 106, 550-561.

http://dx.doi.org/10.1016/j.watres.2016.10.022

6.1. Introduction

Ozonation can be applied as an intermediate process to reduce organic disinfection byproduct (DBP) formation associated with drinking water chlorination (Hua and Reckhow 2013, Sedlak and von Gunten 2011). In Chapter 5, it was demonstrated that DBP precursor removal can even be enhanced using high ozone exposure conditions. During this oxidative treatment, ozone can significantly alter the structure and reactivity of natural organic matter (NOM) (Wenk et al. 2013) resulting in the formation of a mixture of compounds with lower molecular weight and aromaticity, and higher carboxylic acid functionality (Carlson and Amy 1998, Urfer et al. 1997). This treatment then increases the assimilable organic carbon (AOC) content (Hammes et al. 2006, Ramseier et al. 2011) which is of great concern for water utilities because of increased bacterial regrowth potential in distribution systems. On the other hand, biofiltration can take advantage of this process as a means of removing additional DBP precursors from the water prior to final disinfection, while at the same time reducing AOC.

Several studies have shown that biofiltration can remove some DBP precursors and the associated chlorine demand as well as biodegradable organic carbon which includes products formed by ozonation in water such as aldehydes and carboxylic acids, among others (Chu et al. 2012, Gagnon et al. 1997, Krasner 2009, Speitel et al. 1993, Weinberg et al. 1993). This can be achieved because of the presence of biofilm (i.e., heterotrophic bacteria attached to a media) that utilizes biodegradable NOM as a carbon source for energy production (Urfer et al. 1997). The degree of NOM removal is affected by the characteristics of both the influent ozonated water and the biofilter. As clearly shown in the previous chapter, the ozonated water quality varies depending on whether ozonation conditions promote O_3 over hydroxyl radical ($^{\bullet}OH$) reactions or vice versa. However, information about the effects of these conditions on biofiltration is currently missing in the literature. Moreover, filter media, biomass, and operational parameters such as empty bed contact time (EBCT) can impact the biofilter performance. For example, Melin and Odegaard (2000) evaluated the removal rate of influent ozonation byproducts aldehydes and aldo- and keto-acids as a function of EBCT. Several modelling studies attempted to gain a mechanistic understanding of the biodegradation kinetics of NOM (Gagnon and Huck 2001, Huck and Sozanski 2008). Huck et al. (1994) reported a linear relationship between the removal rate and filter influent concentrations (i.e., a first-order process) of the following: biodegradable and assimilable organic carbon, chlorine demand, and precursors of trihalomethanes (THMs) and adsorbable organic halogen (AOX). There are no published kinetic studies, however, in the literature describing the impact of combined ozone/biofiltration on the formation potentials of chloral hydrate (CH), haloketones (HKs) and the more toxic nitrogen-containing DBPs (Plewa et al. 2008) such as halonitromethanes (HNM) which are the organic DBPs most commonly elevated when

treating ozonated waters with chlorine. If a first-order kinetics would hold true for these DBPs as well, water utilities might be able to predict and set biofiltration conditions that could control DBP formation during drinking water treatment.

This chapter, therefore, evaluated (1) the effect of O_3 and $^{\bullet}OH$ reactions on the biodegradability of ozonated waters and (2) the reduction in formation potentials of different families of DBPs including THMs, haloacetic acids (HAAs), CH, HKs, haloacetonitriles (HANs), HNMs, and trichloroacetamide (TCAM) by ozone-biofiltration treatment with varying EBCT. These objectives were achieved by conducting ozone dosing experiments followed by batch biodegradation and once-through column experiments using anthracite and biological activated carbon (BAC) as media and subsequent chlorination. As little is known about biodegradation of DBP precursors and most biofiltration studies have only focused on removal of biodegradable organic carbon and ozonation by-products, this study provides important novel insights on the impact of ozonation and biofiltration on DBP precursors and subsequent byproduct formation in chlorinated drinking water.

6.2. Materials and methods

6.2.1. Water sample and bioactive media

The water and bioactive media used in this study were obtained from drinking water treatment plants in South East Queensland, Australia (SEQ). The water sample was a reconstituted reverse osmosis (RO) concentrate of coagulated and settled surface water as described in Section 5.2.1. The concentrate was reconstituted to the desired dissolved organic carbon (DOC) for batch ozonation experiments prior to biodegradation. Reconstituted reverse osmosis water was used with the aim of having a more constant water quality throughout all ozonation and biofiltration experiments as water quality changes substantially in the region depending on rainfall events. The water sample showed similar characteristics (e.g., SUVA and specific DBP formation potentials) to other settled water samples taken from other treatment plants in the SEQ region (de Vera et al. 2015). Two types of bioactive media were used: (i) anthracite (AN) with an effective size of about 1.2–1.3 mm and apparent density of 650 kg/m^3 taken from the top layer of a rapid media filter which had been used for more than 5 years and (ii) granular biological activated carbon (BAC) with an effective size of 0.7–0.9 mm and apparent density of 435 kg/m^3 (ACTICARB GA1000N, Activated Carbon Technologies Pty Ltd, Australia) taken from the top layer of the post-O_3 filter that had been in operation for more than two years. Adsorption would not, therefore, be expected to play a major role on NOM removal in either of these media. The filter media was taken from a plant which treats gravity fed water from a reservoir using the following process scheme: pre-ozonation, coagulation,

sedimentation, rapid media filtration, ozonation, BAC filtration, and chlorination. The schematic of the treatment plant is shown in Figure 6.1.

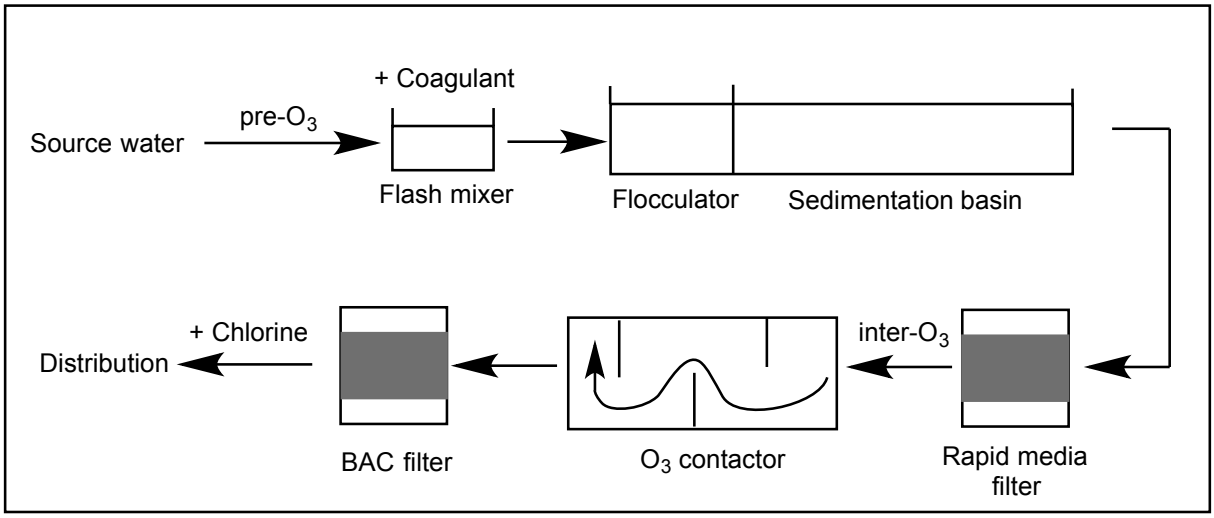

Figure 6.1. Treatment processes employed in the advanced water treatment plant in South East Queensland supplying the biofilter media

6.2.2. Experiments carried out

Three sets of experiments were performed to investigate the biodegradability of DBP precursors at different ozonation and biodegradation conditions. The first set involved water samples treated with different O_3 doses and subsequently exposed to bioactive anthracite. Details on preparation of ozone stock solutions (1 – 1.3 mM O_3) are presented in Section 4.2.1. Appropriate volumes of the ozone stock solution were spiked into the water samples (pH = 7) to obtain the desired specific ozone dose, assuming 100% transfer efficiency. Ozone was allowed to fully decay prior to biological treatment. Bioactivity in these batch biodegradation tests was confirmed by measuring consumption of biodegradable organic carbon. A control experiment with 0.3 mM sodium acetate (DOC = 7.2 mg/L; >99%, Ajax Finechem, Australia) showed an 84% DOC removal after 8 days of exposure with the bioactive anthracite (Figure 6.2a). The second set involved column experiments using BAC and bioactive anthracite media fed with water ozonated with and without H_2O_2. These two sets of experiments evaluated optimization of the ozonation process for better NOM biodegradability. The third set of experiments focused on studying biofiltration performance by varying the EBCT of the BAC columns. For these column experiments, bioactivity was confirmed by constantly monitoring dissolved oxygen consumption by the bioactive media and removal of influent DOC. Similar to other studies (Evans et al. 2013, Liao et al. 2016, Persson et al. 2007, Pipe-Martin 2008, Rattier et al. 2014), DO measurements served as the indicator of oxygen consumed by microorganisms during respiration and an indirect proof of aerobic biological activity in the filters.

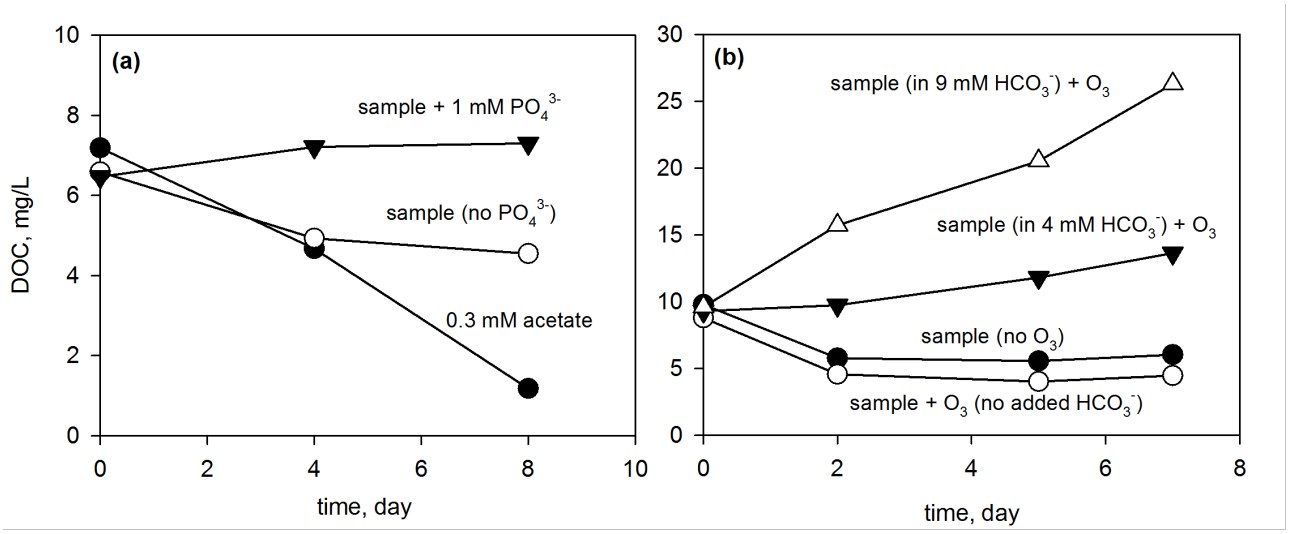

Figure 6.2. Effect of (a) phosphate and (b) bicarbonate addition on DOC removal during batch biodegradation tests. Conditions: specific O_3 dose = 0.75 mgO_3/mgDOC, volume of water sample = 500 mL, mass of bioactive anthracite = 170 g, temperature = 22 ± 1 °C. Solutions were contained in amber-colored glass bottles.

6.2.2.1. Batch biodegradation and column filtration

Prior to biodegradation, ozonation experiments (pH 7) were performed on the water sample by adding ozone to create ozone to DOC ratios (mg/mg) ranging from 0.4 to 1. These samples were not buffered since preliminary results revealed that 1 mM phosphate ($NaH_2PO_4 \cdot 2H_2O$, >99%, Ajax Finechem, Australia and $Na_2HPO_4 \cdot 2H_2O$, ≥99.5%, Merck, Germany) and 4–9 mM $NaHCO_3$ (>99.5%, Sigma-Aldrich, USA) inhibited biodegradation of NOM (Figure 6.2a and 6.2b). Instead, the pH of the ozonated aqueous samples was readjusted to pH 7 using small quantities of 0.5 M HCl (Merck, Germany) prior to contact with the bioactive anthracite in order to mimic the actual influent pH during biofiltration in a full-scale plant. 500 mL of ozonated water sample was mixed with 170 g of bioactive anthracite with contact time of 7 days at ambient temperature.

Column experiments (Figure 6.3) were also performed using bioactive anthracite and BAC. Filtration was carried out upflow to avoid bed compaction, clogging, and to obtain a more uniform distribution of organic matter through the filter media. The biofiltration system was comprised of 4 glass columns (two each for columns of non-ozonated and ozonated feed lines; internal diameter: 1 cm; length: 12 cm; manufactured at University of Queensland Glassblowing Services) containing the bioactive media (bed volume = 6.5 mL), a multi-channel peristaltic pump (Sci-Q 323, Watson Marlow, USA), a dissolved oxygen (DO) probe (WTW, Germany), ozonated water as feed, and effluent collection bottles. The specific ozone dose employed for these experiments was 1.2 mgO_3/mgDOC. Each biofiltration line was connected to the columns using Norprene tubing (Cole-Palmer, USA).

Biofiltration experiments were performed at room temperature (22 ± 1°C), influent water DO of 9.0 ± 0.8 mg/L and an EBCT of 11 minutes. To condition the media and equilibrate influent concentrations through the filter, 100 bed volumes of the ozonated water sample were pumped at a rate of 0.6 mL/min prior to sampling. The effluent for this conditioning step was discarded.

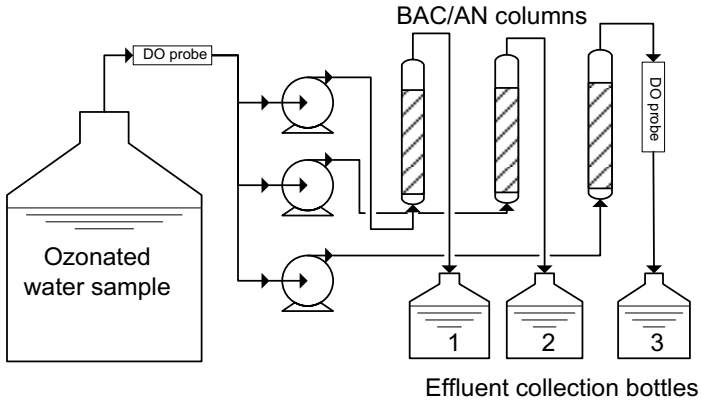

Figure 6.3. Schematic diagram of the bench-scale biofiltration column system. BAC = biological activated carbon, AN = anthracite. Performed under dark conditions (i.e., bottles and columns were completely covered with aluminum foil).

6.2.2.2. Biofiltration of samples treated with O_3/H_2O_2

Ozone decomposition was varied by adding increasing H_2O_2 concentrations. Ozonation was conducted at a specific O_3 dose of 1 mgO_3/mgDOC with H_2O_2 concentrations ranging from 0 to 2 mmol H_2O_2/mmol O_3. Stock solutions of H_2O_2 (30%, Merck, Germany) were previously standardized spectrophotometrically at 240 nm ($\varepsilon = 40\ M^{-1}cm^{-1}$) (Bader et al. 1988) while the H_2O_2 concentration in samples was determined using the method described by Nogueira et al. (2005). Prior to DBP formation potential tests and/or biofiltration, H_2O_2 was quenched by adding 1.4 g of MnO_2 (≥ 99%, Sigma-Aldrich, Australia) to 1 L ozonated sample (Sarathy 2004). MnO_2 was chosen as an adequate H_2O_2 quencher since it has been reported to not affect bacterial growth. For example, MnO_2 quenching of H_2O_2 did not interfere with AOC measurements, unlike other common quenchers such as catalase and sodium thiosulfate (Sarathy 2004). Figure 6.4 illustrates the removal of H_2O_2 after addition of MnO_2. Bioactive anthracite and BAC were used separately as biofiltration media each with a 7 mL bed volume and 11 min EBCT.

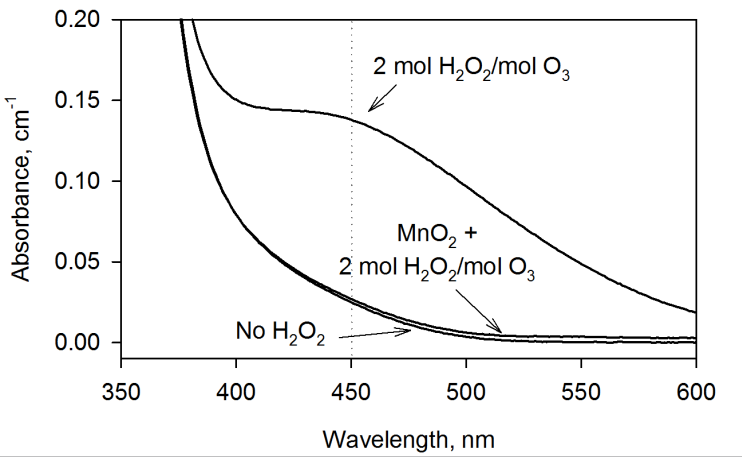

Figure 6.4. Removal of H_2O_2 by addition of MnO_2. Conditions: MnO_2 = 1.4 g to 1 L sample treated with O_3/H_2O_2; mixing time = 90 min; $[H_2O_2]_0$ = 2 mmol H_2O_2/mmolO_3; O_3 dose = 10 mg/L. H_2O_2 concentrations before and after MnO_2 addition were confirmed from the absorbance at 450 nm which indicates the formation of red-orange peroxovanadium cation from the reaction of peroxide and vanadate (Nogueira et al. 2005).

6.2.2.3. Biofiltration at different EBCT values

Each biofiltration line was connected to two BAC columns with a total bed volume of 12 mL. Three parallel lines were used for replicate measurements. Although the biomass concentration in the biofilters was not measured, bioactivity was confirmed through measurements of DO consumption and NO_3^- evolution (Figure 6.5) due to the presence of nitrifiers as observed in a preliminary study. Effluent collection was performed at the lowest flow rate first (0.22 mL/min) and increased successively to the highest flow rate (4.0 mL/min) which corresponds to filtration at decreasing EBCT (ratio of bed volume to influent flow rate). Samples were collected before biological filtration and at the following EBCTs: 3, 5, 8, 11, 15, 19, 30, 39, and 55 min. In between sampling at the different EBCTs, mild backwashing was done using a sample-containing syringe connected online. After this step, at least 3 bed volumes of the ozonated sample were pumped through the columns and discarded. This volume was assumed sufficient to flush the sample used in a previous condition out of the columns. Biofiltered samples (250 mL) were collected in acid-washed amber-colored glass bottles and stored at 4 °C prior to subsequent analyses. Sample collection during column experiments was performed within a week to avoid possible changes in biomass and biofilm characteristics that may be a significant variable on NOM removal. A constant biological activity in the media was desired to be able to compare the reactivity of different precursors with changes in EBCT.

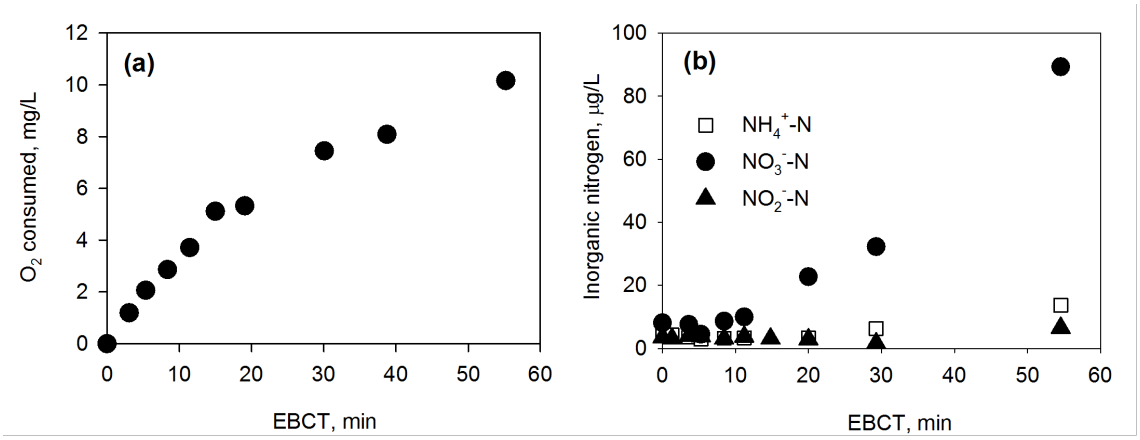

Figure 6.5. Changes in (a) oxygen consumption, and (b) inorganic nitrogen during biofiltration of ozonated water at different EBCTs. Conditions: ozone dose = 15 mg/L; bed volume = 12 mL; media = BAC; pH = 6.9; temperature = 22 ± 1 °C.

6.2.3. DBP formation potential tests and analyses

DBP formation potential tests were as described in previous studies (de Vera et al. 2015, Doederer et al. 2014, Farré et al. 2013) and elaborated in Section 5.2.4. In this test, sodium hypochlorite was added to samples buffered at pH 7 with 10 mM phosphate (target Cl_2 residual after 24 h = 1 – 2 mg/L). After one day of contact time, residual chlorine was quenched with either L-ascorbic acid, ammonium chloride, or sodium sulfite depending on the subsequent extractions for volatile neutral-extractable DBPs, HAAs, or AOX, respectively. Volatile DBPs and HAAs in these aqueous samples were subsequently extracted with methyl tert-butyl ether (i.e., after acidic methanol methylation for HAAs). AOX was solid-phase extracted using activated carbon cartridges. Analyses of THMs and HAAs were done using gas chromatography with electron-capture detector, while analyses of AOX were performed using a combustion ion chromatography system. All procedures described here are presented in more detail in Section 5.2.5. Throughout this chapter, DBP formation potentials are reported as the average, with intervals corresponding to either standard deviation (n=3) or mean absolute deviation (n=2).

6.2.4. Analytical methods

6.2.4.1. Dissolved oxygen and inorganic nitrogen

Influent and effluent DO concentrations were measured on-line in a gas tight flow through cell using a WTW Multi 3420 meter equipped with DO probe FDO 925 (DO measuring range specified by manufacturer = 0 – 20 mg/L, WTW, Germany). Ammonia, nitrite and total NO_x (i.e., sum of NO_2^- and NO_3^-) were measured on samples collected before and after biofiltration by a Lachat QuikChem8500 Flow Injection Analyzer (Hach Company, USA) using Lachat methods 31-107-06-

1-B (NH_4^+), 31-107-04-1-A (NO_x), and 31-107-05-1-A (NO_2^-) (see Section 4.2.1 for more details). The method reporting limits (MRL; 3 × method detection limit (MDL) (NATA 2013); MDL = standard deviation of at least 7 replicate analyses of the lowest laboratory standard in reagent blank × Student's t-statistic for a 99% confidence level and n-1 degrees of freedom (USEPA 2010)) were 4 µg/L for NH_4^+-N (measuring range = 4 – 900 µg/L), 0.6 µg/L for NO_2^--N (measuring range = 0.6 – 72 µg/L), and 4 µg/L for NO_x-N (measuring range = 4 – 900 µg/L).

6.2.4.2. Size exclusion chromatography (SEC)

The molecular weight distribution of NOM in each water sample (untreated, ozonated, and biofiltered) was evaluated using a Shimadzu prominence LC-20AT high performance liquid chromatograph (HPLC, Shimadzu, Japan) equipped with a SIL-20A HT autosampler and a Toyopearl HW-50S SEC column (250 mm × 20 mm packing material; Tosoh, Japan). The unit was connected to a SPD-M20A diode array detector (UVD) and a GE Sievers 900 portable online total organic carbon analyzer (OCD) with an inorganic carbon remover (GE, USA). The retention times of eluted volumes were calibrated against polyethylene glycol standards (Agilent, UK) in order to convert to molecular weight. The analyses used a 25 mM phosphate mobile phase (pH 6.85), 1 mL/min flow rate, 1100 µL injection volume, 35 °C oven temperature, and 100 min analysis time.

Separate measurements of DOC and UV absorbance at 254 nm were also performed with the water samples to complement the SEC results using the procedures described in Section 5.2.3.

6.3. Results and Discussions

6.3.1. Effect of ozonation and biodegradation on formation potentials of halogenated DBPs produced by subsequent chlorination

6.3.1.1. Ozonation

Ozone is known to significantly alter NOM characteristics because of its reaction towards their electron-rich moieties which include activated aromatic systems, olefins, and non-protonated amines. These reactions favor the effectiveness of biofiltration if it follows ozone treatment and impact DBP formation by post-chlorination. The reactions of ozone with such moieties have been extensively studied in the literature (von Gunten 2003a, von Sonntag and von Gunten 2012) (see also Section 2.6.2). Briefly, ozone reacts with phenolic compounds (Figure 6.6a) via an ozone adduct which

proceeds primarily to ring cleavage, formation of muconic-type compounds, and eventually resulting in aliphatic aldehydes and ketones (Hammes et al. 2006, Ramseier and von Gunten 2009).

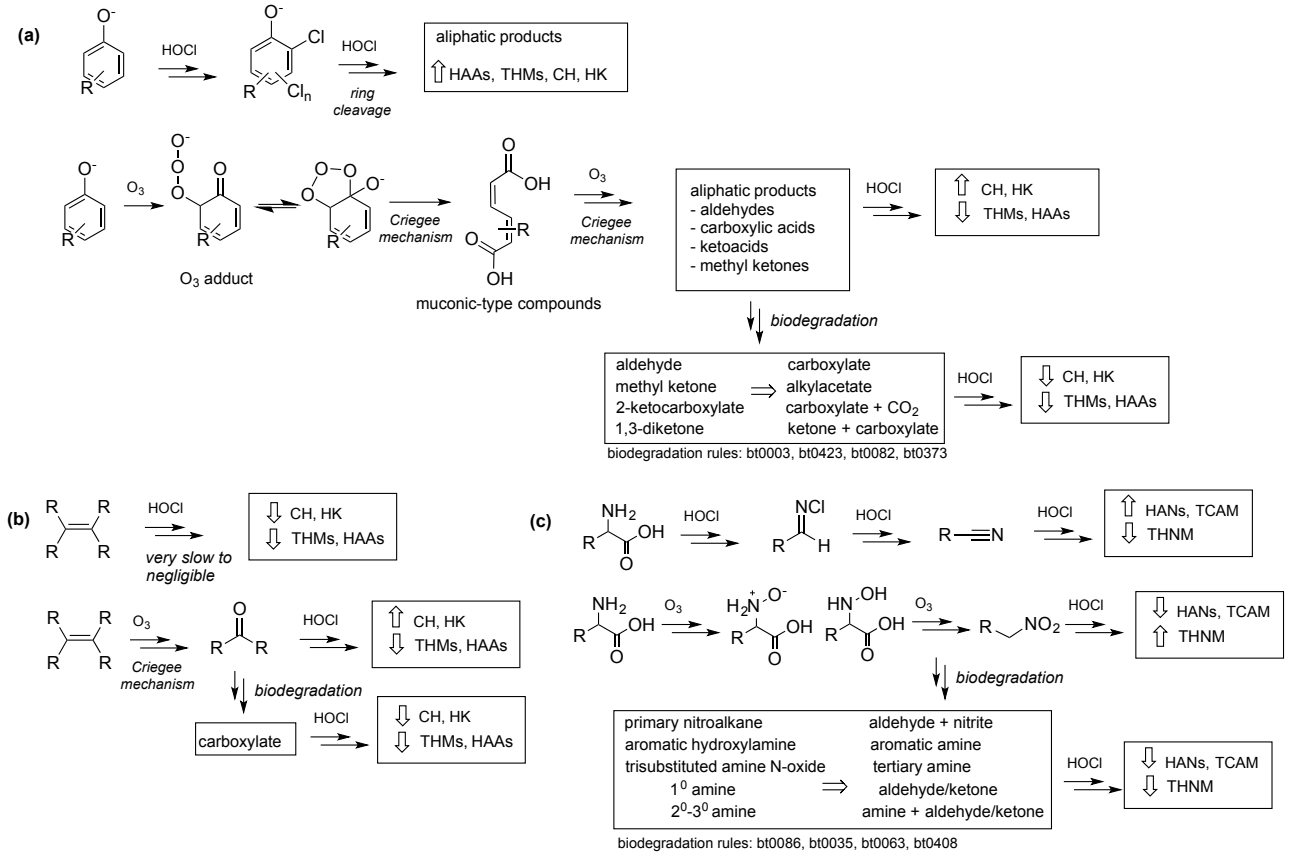

Figure 6.6. Impact of chlorination, ozonation, and biodegradation on DBP precursors: (a) phenolates, (b) olefins, and (c) amines. Biotransformation rules were taken from the University of Minnesota Biocatalysis/Biodegradation Database (https://umbbd.ethz.ch/) (Gao et al. 2010). THMs = trihalomethanes, HAAs = haloacetic acids, CH = chloral hydrate, HK = haloketones, HANs = haloacetonitriles, TCAM = trichloroacetamide, THNM = trihalonitromethanes. Reactions were based on the following references: Deborde and von Gunten (2008), Hubner et al. (2015), McCurry et al. (2016), Wenk et al. (2013), Ramseier and von Gunten (2009), von Sonntag and von Gunten (2012).

In our study, ozonation of the water sample (1 mgO_3/mgDOC) caused an 11% decrease in DOC and a 56% decrease in SUVA (Figure 6.7). These results were consistent with the typical degree of mineralization of NOM (~10% at 1 mgO_3/mgDOC) (Nöthe et al. 2009) resulting from decarboxylation reactions that occur during further oxidation of substantially oxidized NOM (von Sonntag and von Gunten 2012). The high decrease in SUVA supports the likelihood that the ring-opening mechanism shown in Figure 6.6a for phenolic compounds occurred in our reactions. These observations were in agreement with the SEC images that show significant removal of NOM (humics and building block region) by ozone with the UV_{254} detector (Figure 6.8a) but barely any with the organic carbon detector (Figure 6.8b; OCD). The results indicate that certain UV absorbing units of

NOM were partially oxidized and transformed to lower molecular weight compounds rather than being mineralized since the overall DOC was mostly unchanged. Minor pathways could generate products such as catechol, hydroquinone, and quinones (Ramseier and von Gunten 2009) especially at lower O_3 doses (Chon et al. 2015).

For olefins (Figure 6.6b), the ozone reaction occurs via a Criegee mechanism that involves cleavage of the C=C double bond and formation of carbonyl compounds (Criegee 1975). For amines (Figure 6.6c), an ozone adduct on the nitrogen atom leads to formation of *N*-oxide for tertiary amines and hydroxylamine for primary and secondary amines (von Gunten 2003a) (see also Chapter 4). A recent study also reported formation of nitromethane from ozonation of methylamine (McCurry et al. 2016). Amine radical cations can also be formed leading to dealkylated amines and ketones or aldehydes (von Sonntag and von Gunten 2012). These ozonation transformation products could be formed along with products from $^{\bullet}OH$ reactions since ozonation conditions at treatment plants do not scavenge for these radicals. Addition reactions are very common for $^{\bullet}OH$ since the radicals readily add to C-C and C-N bonds (von Sonntag and von Gunten 2012).

These transformation products can affect the subsequent DBP formation potentials during post-chlorination, as shown in this study. Consistent trends were observed for all the DBPs presented in the following sections. Results are presented as relative residual concentrations (C/C_0) to show the extent of the change in concentrations with respect to C_0 or the concentration resulting from chlorination alone (i.e., without prior ozonation and biodegradation). The average analyte concentrations are provided in Tables 6.2 – 6.5, and 6.7.

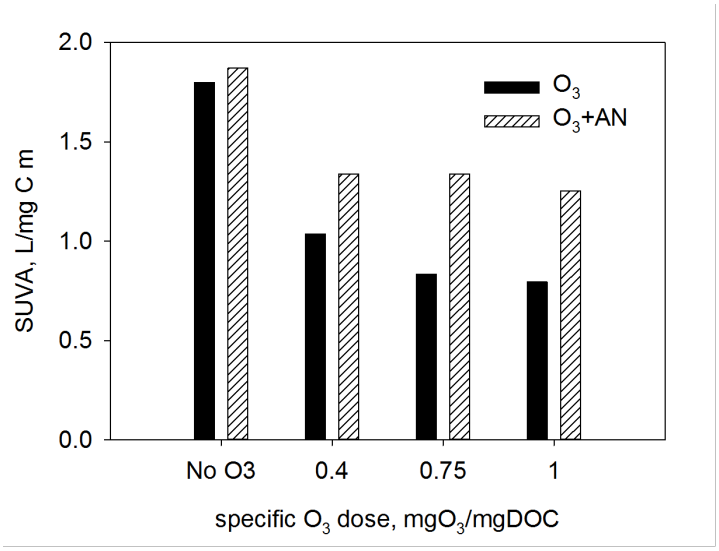

Figure 6.7. Changes in specific UV absorbance (SUVA) after ozonation and batch biodegradation. Conditions: specific ozone dose = 0.4–1 $mgO_3/mgDOC$; water sample/bioactive anthracite (AN; volume/mass) = 500 mL/170 g; contact time = 7 days; temperature = 22 ± 1 °C.

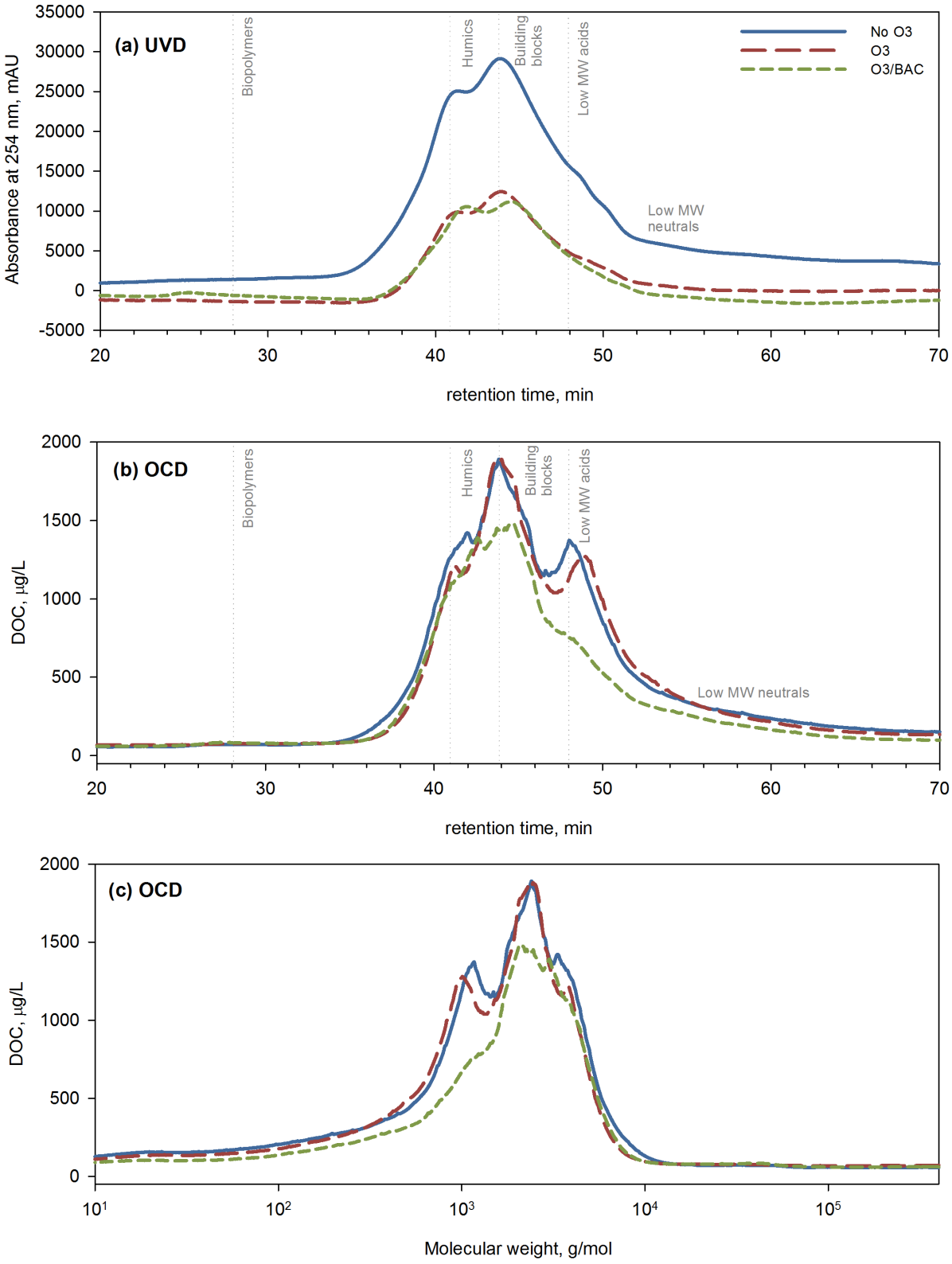

Figure 6.8. Size exclusion chromatogram of O_3/BAC treated water samples obtained with (a) UV detector (UVD) and (b-c) organic carbon detector (OCD). Conditions: DOC before treatment = 15.1 mg/L, specific O_3 dose = 1 mgO_3/mgDOC, BAC filtration EBCT = 15 min. Molecular weight was determined using polyethylene glycol standards.

The mechanisms of Figures 6.6a and 6.6b show example precursors for aliphatic aldehydes and ketones formed from ozone. In this study CH and HK2 were found to more than double in concentration at 1 $mgO_3/mgDOC$ that could have resulted from ring-opening of phenolic groups in NOM (see decrease in SUVA in Figure 6.7). THM4 and HAA8 decreased by about 30% and 10% respectively after ozonation at the same O_3 dose because reaction sites for chlorine such as those in activated aromatic systems, β-diketones and β-diketoacids will have already been oxidized by O_3. HAN4 and TCAM (Table 6.2, 1 $mgO_3/mgDOC$) also decreased in concentration (HAN4 = 0.13 to 0.11 μM; TCAM = 0.014 to 0.006 μM) most likely because of the oxidation of the precursor amino groups (Figure 6.6c), leading to pronounced formation of THNM2 especially with increasing O_3 dose (0.007 to 0.068 μM). Lower AOX (19.7 to 15.7 μM Cl^-, Table 6.3) was also observed which suggests the benefit of ozonation in decreasing formation potentials of other non-volatile DBPs that were not measured. Consistent with the previous chapter, after O_3/HOCl treatment, bromine-containing DBPs namely tribromomethane (TBM), dibromochloromethane (DBCM), dibromoacetic acid (DBAA), dibromoacetonitrile (DBAN), and tribromonitromethane (TBNM) also increased (Tables 6.2 and 6.3) because of the production of more hydrophilic NOM during ozonation which are more amenable to HOBr than HOCl reactions (Hua and Reckhow 2013, Westerhoff et al. 2004). HOBr, produced from oxidation of bromide during chlorination and ozonation, can react with NOM to form the previously mentioned bromo-organic DBPs (Gruchlik et al. 2014). Under the conditions used, no bromate was observed above the method reporting limit (10 μg/L).

6.3.1.2. Biodegradation

The impact of ozonation on biodegradability of the water samples was evaluated using (1) batch experiments with bioactive anthracite and (2) biofiltration columns containing either anthracite or BAC. The results of batch biodegradation experiments using bioactive anthracite (contact time = 7 days) are shown in Figure 6.9 while biofiltration experiments (EBCT = 11 min) are shown in Figure 6.10.

6.3.1.2.1. Biodegradation before ozonation

Biodegradation experiments without pre-ozonation ("No O_3" in Figures 6.9 and 6.10) yielded notably different results for anthracite batch and column filtration experiments, likely due to differences in contact time (i.e., 7 day exposure with anthracite for batch biodegradation and 11 min for column experiment). This longer contact time may explain the higher DOC removals (38%) and better reduction of formation potentials of THM4 (51%), CH (52%), and HK2 (76%) in Figures 6.9a – 6.9d (batch biodegradation) compared to their equivalents using the biofilter columns (Figures 6.10a –

6.10d; % removal: DOC = 12%, THM4 = 30%, CH = 34%, HK2 = 32%). After batch biodegradation, higher HAN4 formation potentials were observed which could have been caused by release of soluble microbial products (SMPs) (e.g., nucleic acids, proteins, amino acids) (Rittman et al. 1987) during long contact times.

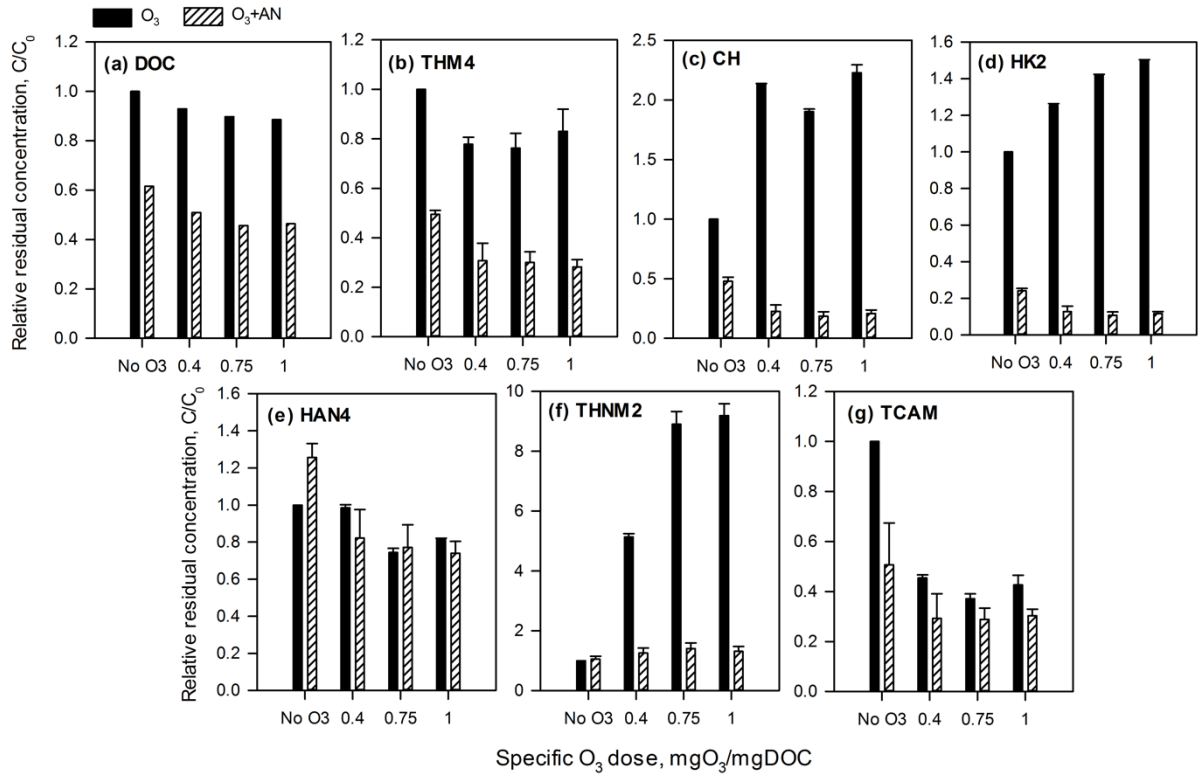

Figure 6.9. Effect of batch biodegradation (O_3+AN) on water samples ozonated (O_3) at different doses on (a) dissolved organic carbon (DOC) and formation potentials of (b) trihalomethanes (THM4), (c) chloral hydrate (CH), (d) haloketones (HK2), (e) haloacetonitriles (HAN4), (f) trihalonitromethanes (THNM2), and (g) trichloroacetamide (TCAM). Conditions: Sample/bioactive anthracite (volume/mass) = 500 mL/170g; empty bed contact time = 7 days; pH = 7; temperature = 22 ± 1 °C, chlorine residual = 3.4 ± 0.9 mg/L as Cl_2. "No O3" represents formation potentials of non-ozonated samples. Error bars depict mean absolute deviation obtained from experiment (n=1) with 2 DBP extractions per sample. C_0 = contaminant concentration before ozonation and biodegradation, C = contaminant concentration after treatment.

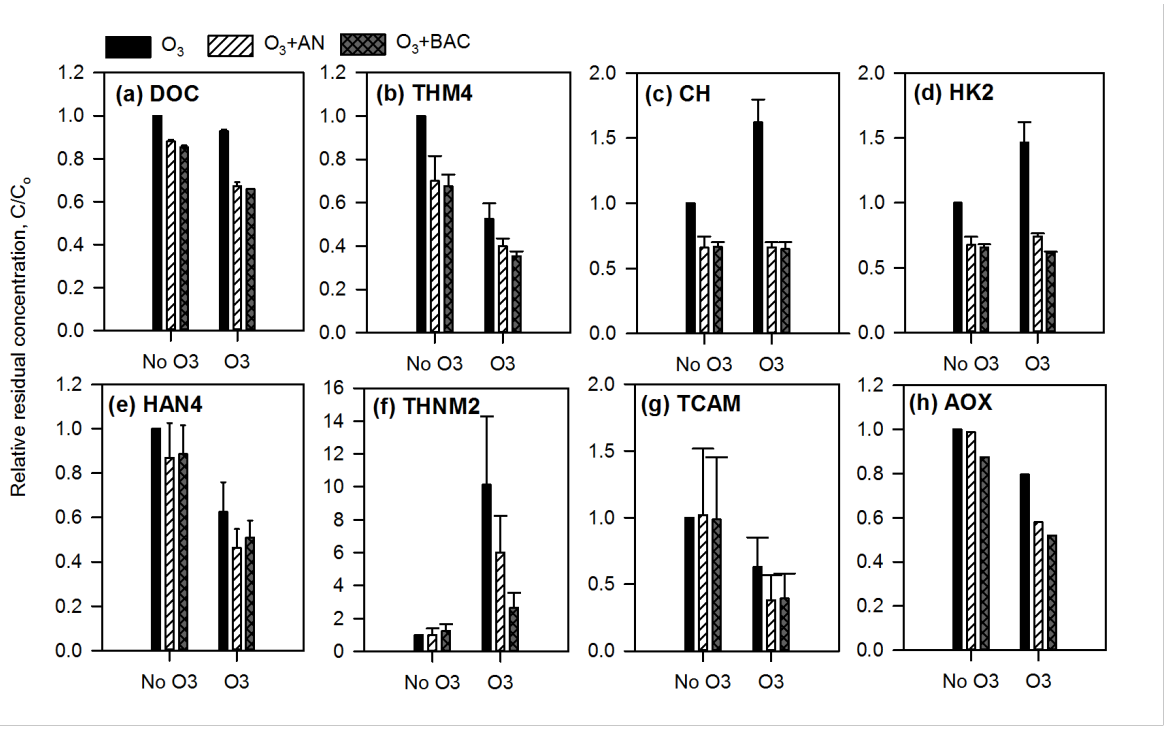

Figure 6.10. Effect of ozonation and biofiltration with anthracite (AN) and activated carbon (BAC) media on (a) dissolved organic carbon (DOC) and formation potentials of (b) trihalomethanes (THM4), (c) chloral hydrate (CH), (d) haloketones (HK2), (e) haloacetonitriles (HAN4), (f) trihalonitromethanes (THNM2), (g) trichloroacetamide (TCAM), and (h) adsorbable organic halogen (AOX). Conditions: specific O_3 dose = 1.2 $mgO_3/mgDOC$; bed volume = 7 mL; empty bed contact time = 11 min, pH = 7; temperature = 22 ± 1 °C; chlorine residual = 1.5 ± 0.6 mg/L as Cl_2. Error bars depict mean absolute deviation of duplicate experiments (n=2, with 2 DBP extractions per sample; for AOX, n=1). C_0 = contaminant concentration before ozonation and biodegradation, C = contaminant concentration after treatment.

THNM2 precursors (Figures 6.9f and 6.10f), which were present at very low concentrations (~0.01 µM) before ozonation, had low removals of less than 6% which suggests that non-ozonated THNM precursors were not readily biodegradable. This result was in agreement with the observations by Wadhawan et al. (2014) who demonstrated the importance of ozonation in increasing the concentrations of biodegradable DON. Biofiltration of non-ozonated samples did not change the resultant TCAM levels (Figure 6.10g) whereas at the longer contact times in batch biodegradation tests (Figure 6.9g), removals of 50% were achieved indicating the presence of TCAM precursors that biodegrade slowly. The relatively high error bars for TCAM are a result of its concentrations near the MRL. Because of the contrasting effects of TCAM and HAN4 in Figures 6.9e and 6.9g, it is likely that TCAM precursors are independent from HAN4 precursors in the biodegraded water sample. The SMP released during batch biodegradation could be a major contributor to HAN4 formation, while TCAM could predominantly come from humic substances of the water sample (Huang et al. 2012). For AOX, biofiltration of non-ozonated precursors only resulted in a 2 – 13% decrease in formation potentials.

6.3.1.2.2. Biodegradation after ozonation

Combining ozonation (1 $mgO_3/mgDOC$) with batch anthracite biodegradation resulted in an overall reduction of 54% of DOC (Figure 6.9a, Table 6.2: No O_3 = 9.8 mg/L DOC; No O_3 + AN = 6.0 mg/L DOC; O_3 only = 8.7 mg/L DOC; combined O_3 + AN = 4.5 mg/L DOC). The observed better DOC removal (O_3 + AN versus O_3 only) is most likely due to the formation of smaller, more hydrophilic, and readily biodegradable compounds following ozonation such as aldehydes, ketones, and carboxylic acids (Figure 6.6) (Hammes et al. 2006). For aromatic compounds, ring cleavage products have been estimated to be more biodegradable compared to their parent compounds (Hubner et al. 2015, Weinberg et al. 1993). These products are reported to be biodegraded via a pathway that leads to carboxylate as shown in the University of Minnesota biocatalysis/biodegradation database (Gao et al. 2010) (refer to Table 6.1 for a list of different biotransformation (bt) rules relevant to this study). No significant change in biodegradability was associated for possible aromatic hydroxylation products such as catechols (Hubner et al. 2015). These observations support the increase in SUVA after biodegradation (Figure 6.7) since compounds with low UV absorbance are consumed, decreasing the DOC and leaving behind other UV absorbing aromatic compounds (Figure 6.8). The improved biodegradability of NOM also translated to a decrease in THM4, CH, and HK2 formation during post chlorination (shown in Figures 6.9b, 6.9c, and 6.9d respectively) with the most notable effects on CH and HK2 because of the readily biodegradable aldehyde and ketone precursors.

Table 6.1. Biodegradation rules for selected compounds obtained from Gao et al. (2010)

Possible DBP precursors	Aerobic likelihood	Biodegradation rule
hydroquinone → cis,cis-4-hydroxymuconic semialdehyde	likely	Bt0297
catechol → cis,cis-muconate	likely	Bt0254
1,4-benzoquinone derivative →1,4-dihydroxybenzoid	likely	Bt0107
4,4-dimethyl-3-oxopentanoate → 3,3-dimethyl-2-butanone	neutral	Bt0051
1,3-diketone → ketone + carboxylate	neutral	Bt0373
2-ketocarboxylate → carboxylate + CO_2	neutral	Bt0082
methyl ketone → alkyl acetate	neutral	Bt0423
aldehyde → carboxylate	likely	Bt0003
tri-substituted amine N-oxide → tertiary amine	neutral	Bt0408
aromatic hydroxylamine → aromatic amine	likely	Bt0035
primary nitroalkane → aldehyde + nitrite	neutral	Bt0086
nitrile → carboxylate	neutral	Bt0030
nitroaromatic → aminoaromatic	neutral	Bt0080
primary amine → aldehyde or ketone	likely	Bt0063
secondary amine → amine + aldehyde or ketone	likely	Bt0063
tertiary amine → secondary amine + aldehyde or ketone	likely	Bt0063

Aerobic biodegradation of amine compounds is expected to form aldehydes and ketones through oxidative removal of an alkyl substituent from an amine using dehydrogenase enzymes (Gao et al. 2010). In this biodegradation pathway (biotransformation rule bt0063 of the biodegradation database shown in Table 6.1), aldehydes and ketones are produced if the leaving substituent is attached to a primary or secondary carbon, respectively. Other N-DBP precursors formed by ozone containing *N*-oxide, hydroxylamine, and nitromethane moieties can also be biodegraded accordingly (biotransformation rules bt0408, bt0035, bt0086). These transformations resulted in decreased HAN4, THNM2, and TCAM concentrations as shown in Figures 6.9e, 6.9f, and 6.9g, respectively. Precursors of THNM2 were observed to be very biodegradable with a decrease in formation potentials of up to 98%. This decrease was mostly caused by the removal of trichloronitromethane precursors. Although formed at low concentrations, total trihalonitromethanes was found to increase because of higher bromine substitution (Figure 6.11) with subsequent chlorination of biodegraded water samples. This was also observed for other brominated THMs and HANs confirming the known influence of the bromide to carbon ratio in DBP speciation. Since bromide was not consumed as DOC decreased during biodegradation, the bromide to carbon ratio increased leading to the formation of more available HOBr in relation to the reduced NOM concentration. Due to the higher electrophilicity of HOBr compared to HOCl (Heeb et al. 2014, Symons et al. 1993, Westerhoff et al. 2004), halogenation by HOBr is favored resulting in formation of more brominated DBPs. The apparent rate constants of bromine reactions (pH 7) were reported to be up to 3 orders of magnitude higher than those of chlorine reactions (Heeb et al. 2014) . In addition, better bromine substitution occurs especially for ozonated waters since hydrophilic organic materials (e.g., aliphatic products of ozone) were found to be more reactive to HOBr compared to hydrophobic fractions (Hua and Reckhow 2007a, Liang and Singer 2003).

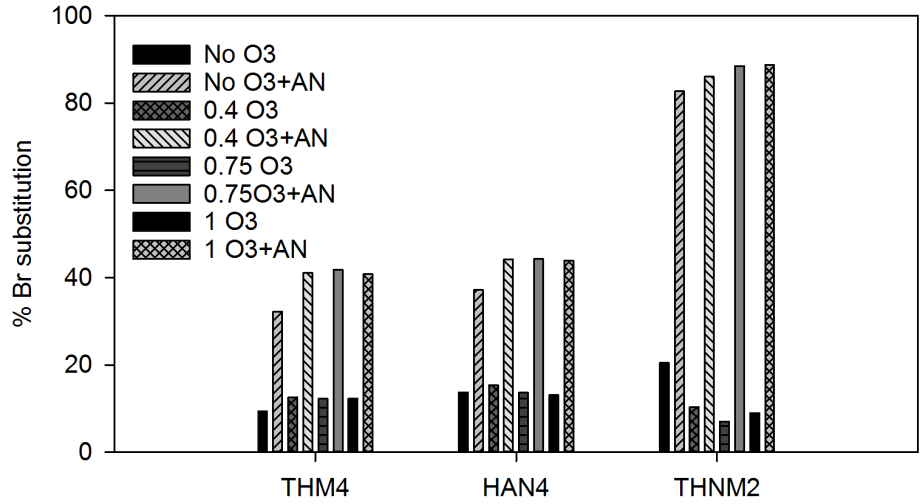

Figure 6.11. %Bromine substitution after batch biodegradation of water samples before and after ozonation. Conditions: specific ozone dose = 0.4 – 1 mgO_3/mgDOC; water sample/bioactive anthracite (AN) (volume/mass) = 500 mL/170 g; contact time = 7 days; pH = 7; temperature = 22 ± 1 °C.

To simulate conditions commonly encountered in actual water treatment conditions, the results of the batch biodegradation experiments were confirmed using bench-scale columns with anthracite and BAC (Figure 6.10, Table 6.3). The extent of DOC removal using both biofilters was similar (33–34 %) after an EBCT of 11 min, despite the filter media having different surface areas and possibly biological activity. The results of SEC with either a UV or organic carbon detector (Figure 6.8) showed that this DOC decrease was a result of removal of low molecular weight compounds (*ca.* 10^3 g/mol) consistent with their transport across cell membranes and attack by metabolic enzymes during biodegradation (Nishijima and Speitel 2004). Similar trends were observed for the DBP formation potentials suggesting that comparable enzymatic functions were responsible for biodegradation in both media. All DBPs, including those that increased after ozonation (e.g., CH, HK2, and THNM2), decreased compared to their initial DBP formation potential after biofiltration. For AOX, a reduction of about 45% compared to non-ozonated and non-biofiltered conditions was observed for samples treated with combined ozonation and biofiltration (Figure 6.10h).

Table 6.2. Effect of ozone dose on reduction of DBP formation potentials (μM) and DOC (mg C/L, n=1) during batch biodegradation. Conditions: specific ozone dose = 0.4-1 $mgO_3/mgDOC$; water sample/bioactive anthracite (AN) (volume/mass) = 500 mL/170 g; contact time = 7 days; pH = 7; temperature = 22 ± 1 ^0C; chlorine residual = 3.4 ± 0.9 mg/L; bromide = 0.19 mg/L. "No O_3" are formation potentials of non-ozonated samples. DBP values are average formation potentials (±mean absolute deviation) obtained from experiment (n=1) with two extractions per sample. Mean absolute deviation = $\frac{1}{n}\sum_{i=1}^{n}|x_i - \bar{x}|$.

DBP	No O_3	0.4 O_3	0.75 O_3	1 O_3	No O_3 + AN	0.4 O_3 + AN	0.75 O_3 + AN	1 O_3 + AN
TCM	2.28E+0 (2E-1)	1.62E+0 (1E-1)	1.59E+0 (1E-2)	1.74E+0 (6E-2)	5.16E-1 (6E-2)	2.24E-1 (4E-2)	2.20E-1 (1E-2)	2.10E-1 (4E-3)
BDCM	6.36E-1 (4E-2)	5.84E-1 (2E-2)	5.53E-1 (4E-3)	5.88E-1 (2E-3)	5.72E-1 (2E-2)	3.39E-1 (7E-2)	3.24E-1 (3E-2)	3.14E-1 (9E-3)
DBCM	9.80E-2 (4E-3)	1.34E-1 (2E-3)	1.31E-1 (1E-3)	1.49E-1 (3E-3)	3.40E-1 (1E-3)	2.63E-1 (3E-2)	2.58E-1 (2E-2)	2.42E-1 (1E-2)
TBM	4.74E-3 (3E-4)	1.01E-2 (6E-5)	9.29E-3 (3E-4)	8.98E-3 (1E-4)	6.32E-2 (6E-4)	8.58E-2 (6E-3)	9.39E-2 (1E-2)	7.81E-2 (1E-3)
TCAN	1.85E-3 (9E-5)	1.92E-3 (4E-5)	1.77E-3 (7E-5)	1.84E-3 (1E-4)	3.04E-3 (3E-4)	2.06E-3 (1E-4)	2.24E-3 (3E-5)	1.96E-3 (1E-4)
DCAN	9.79E-2 (1E-3)	9.50E-2 (1E-4)	7.44E-2 (2E-3)	8.31E-2 (1E-3)	7.29E-2 (4E-3)	3.99E-2 (1E-2)	3.73E-2 (7E-3)	3.61E-2 (3E-3)
BCAN	3.23E-2 (2E-4)	3.01E-2 (4E-4)	2.02E-2 (2E-4)	2.11E-2 (4E-4)	6.03E-2 (3E-3)	3.91E-2 (7E-3)	3.62E-2 (6E-3)	3.55E-2 (3E-3)
DBAN	2.27E-3 (2E-4)	5.30E-3 (1E-4)	3.50E-3 (6E-6)	3.85E-3 (4E-4)	3.25E-2 (2E-3)	2.92E-2 (2E-3)	2.77E-2 (2E-3)	2.58E-2 (2E-3)
CH	1.10E-1 (3E-3)	2.34E-1 (7E-3)	2.09E-1 (4E-3)	2.44E-1 (2E-4)	5.27E-2 (5E-3)	2.49E-2 (7E-3)	2.06E-2 (5E-3)	2.30E-2 (4E-3)
TCNM	5.92E-3 (4E-4)	3.42E-2 (1E-3)	6.14E-2 (4E-4)	6.21E-2 (4E-4)	1.35E-3 (6E-5)	1.30E-3 (1E-4)	1.19E-3 (2E-5)	1.10E-3 (1E-4)
TBNM	1.52E-3 (3E-5)	3.95E-3 (1E-4)	4.64E-3 (2E-4)	6.14E-3 (2E-4)	6.45E-3 (4E-4)	7.98E-3 (9E-4)	9.18E-3 (9E-4)	8.62E-3 (6E-4)
DCP	1.32E-2 (2E-3)	8.07E-3 (3E-5)	2.28E-2 (3E-3)	1.09E-2 (2E-4)	2.57E-3 (6E-4)	1.71E-3 (3E-5)	1.47E-3 (9E-5)	1.40E-3 (2E-4)
TCP	9.45E-2 (2E-3)	1.27E-1 (8E-4)	1.30E-1 (3E-3)	1.50E-1 (1E-3)	2.34E-2 (2E-3)	1.21E-2 (3E-3)	1.02E-2 (2E-3)	1.13E-2 (9E-4)
TCAM	1.44E-2 (2E-3)	6.51E-3 (5E-4)	5.31E-3 (3E-4)	6.07E-3 (1E-4)	7.55E-3 (3E-3)	4.36E-3 (2E-3)	4.22E-3 (1E-3)	4.40E-3 (9E-4)
THM4	3.02E+0 (3E-1)	2.34E+0 (1E-1)	2.29E+0 (2E-2)	2.49E+0 (5E-2)	1.49E+0 (8E-2)	9.12E-1 (1E-1)	8.96E-1 (5E-2)	8.44E-1 (2E-2)
HAN4	1.34E-1 (2E-3)	1.32E-1 (6E-4)	9.99E-2 (2E-3)	1.10E-1 (2E-3)	1.69E-1 (8E-3)	1.10E-1 (2E-2)	1.03E-1 (2E-2)	9.94E-2 (7E-3)
THNM2	7.44E-3 (4E-4)	3.81E-2 (1E-3)	6.61E-2 (2E-4)	6.82E-2 (6E-4)	7.80E-3 (3E-4)	9.28E-3 (8E-4)	1.04E-2 (9E-4)	9.72E-3 (7E-4)
HK2	1.08E-1 (2E-4)	1.35E-1 (8E-4)	1.53E-1 (7E-5)	1.61E-1 (1E-3)	2.60E-2 (1E-3)	1.38E-2 (3E-3)	1.16E-2 (2E-3)	1.27E-2 (1E-3)
DOC	9.79	9.10	8.79	8.67	6.03	4.98	4.47	4.55

Table 6.3. Effect of ozonation and column biofiltration with anthracite (AN) and activated carbon (BAC) media on DBP formation potentials (μM) and DOC (mg/L). Conditions: specific ozone dose = 1.2 mg O_3/mgDOC; empty bed contact time = 11 min, pH = 7; temperature = 22 ± 1 ^{0}C; chlorine residual = 1.5 ± 0.6 mg/L as Cl_2. DBP values are average formation potentials (±mean absolute deviation) obtained from experiments (n=2; n=1 for AOX) with two extractions per sample.

DBP	No O_3	O_3	No O_3 + AN	O_3 + AN	No O_3 + BAC	O_3 + BAC
TCM	1.91E+0 (1E-1)	8.36E-1 (1E-1)	1.28E+0 (2E-1)	6.13E-1 (4E-2)	1.18E+0 (7E-2)	4.92E-1 (7E-3)
BDCM	6.02E-1 (4E-2)	3.90E-1 (4E-2)	4.52E-1 (7E-2)	3.03E-1 (2E-2)	4.64E-1 (3E-2)	2.96E-1 (5E-3)
DBCM	9.62E-2 (8E-3)	1.28E-1 (1E-2)	9.06E-2 (1E-2)	1.09E-1 (1E-2)	1.04E-1 (9E-3)	1.19E-1 (1E-3)
TBM	4.12E-3 (2E-4)	9.63E-3 (1E-3)	5.22E-3 (6E-4)	1.45E-2 (2E-3)	7.03E-3 (8E-4)	1.64E-2 (8E-4)
TCAN	2.56E-3 (1E-4)	1.70E-3 (1E-4)	2.44E-3 (2E-4)	1.59E-3 (3E-5)	2.27E-3 (5E-5)	1.49E-3 (5E-6)
DCAN	1.07E-1 (1E-2)	6.48E-2 (7E-3)	8.63E-2 (5E-3)	3.89E-2 (3E-3)	8.59E-2 (6E-3)	4.06E-2 (2E-4)
BCAN	3.32E-2 (8E-3)	1.82E-2 (2E-3)	3.17E-2 (7E-3)	1.99E-2 (3E-3)	3.38E-2 (4E-3)	2.31E-2 (8E-4)
DBAN	3.15E-3 (1E-3)	4.62E-3 (7E-4)	4.11E-3 (1E-3)	5.97E-3 (1E-3)	5.07E-3 (1E-3)	7.82E-3 (5E-4)
CH	1.04E-1 (5E-3)	1.68E-1 (1E-2)	6.83E-2 (9E-3)	6.86E-2 (2E-3)	6.88E-2 (1E-3)	6.71E-2 (4E-3)
TCNM	4.77E-3 (6E-4)	5.08E-2 (5E-3)	3.81E-3 (8E-4)	2.25E-2 (3E-3)	4.69E-3 (5E-4)	6.96E-3 (3E-4)
TBNM	1.34E-3 (1E-3)	6.24E-3 (7E-4)	1.95E-3 (3E-4)	1.19E-2 (1E-3)	2.30E-3 (1E-4)	8.11E-3 (8E-5)
DCP	1.13E-2 (6E-3)	2.33E-2 (1E-2)	7.58E-3 (1E-3)	1.05E-2 (2E-3)	7.61E-3 (1E-4)	6.27E-3 (7E-4)
TCP	9.64E-2 (8E-3)	1.35E-1 (1E-2)	6.55E-2 (6E-3)	6.96E-2 (5E-4)	6.33E-2 (1E-3)	5.98E-2 (2E-3)
TCAM	1.21E-2 (5E-3)	5.44E-3 (4E-4)	1.08E-2 (2E-3)	4.04E-3 (8E-4)	1.05E-2 (4E-4)	4.19E-3 (2E-4)
THM4	2.61E+0 (1E-1)	1.36E+0 (1E-1)	1.82E+0 (3E-1)	1.04E+0 (8E-2)	1.76E+0 (1E-1)	9.22E-1 (1E-2)
HAN4	1.45E-1 (2E-2)	8.93E-2 (7E-3)	1.25E-1 (1E-2)	6.63E-2 (7E-3)	1.27E-1 (8E-4)	7.30E-2 (1E-3)
THNM2	6.11E-3 (2E-3)	5.71E-2 (5E-3)	5.76E-3 (1E-3)	3.43E-2 (5E-3)	6.99E-3 (6E-4)	1.51E-2 (3E-4)
HK2	1.08E-1 (2E-3)	1.58E-1 (2E-2)	7.30E-2 (5E-3)	8.01E-2 (3E-3)	7.09E-2 (1E-3)	6.61E-2 (9E-4)
AOX, as Cl^-	1.97E+1	1.57E+1	1.94E+1	1.14E+1	1.72E+1	1.02E+1
DOC	11.6	10.5	10.2	7.78	9.85	7.61

6.3.2. Process improvement

6.3.2.1. Ozonation: Use of O_3/H_2O_2 before biofiltration

Since DBP formation potentials can be affected differently by ozone and $^{\bullet}OH$ reactions as presented in Chapter 5 (de Vera et al. 2015), the effect of ozone exposure on the biodegradability of DBP precursors was investigated. This was achieved through batch experiments involving ozone with and without addition of H_2O_2 to the water samples. Although no $^{\bullet}OH$ concentration measurements were made in this study, it has been well-established that the presence of H_2O_2 accelerates O_3 decay through formation of $^{\bullet}OH$ and superoxide radical ($O_2^{\bullet-}$) which further reacts with O_3 (von Gunten 2003a, von Sonntag and von Gunten 2012). Thus, at conditions with higher H_2O_2 concentrations, O_3 would decay faster and be transformed more quickly to $^{\bullet}OH$.

Figure 6.12a shows the changes in DOC resulting from O_3/H_2O_2 and biofiltration treatment and the impact of these treatments on DBPs formed by subsequent chlorination. At all H_2O_2 doses, source DOC decreased by no more than 10% after ozonation, similar to the values obtained in Figures 6.9 and 6.10. After biofiltration of the ozonated waters using both anthracite and BAC, a ~30% DOC removal was achieved. The remaining ~6 mg/L DOC (Tables 6.4 and 6.5) represents the non-biodegradable fraction of NOM as classified by Yavich et al. (2004). While the DOC remained relatively unchanged at all H_2O_2 concentrations, a different behaviour was observed for DBPs (Figures 6.12b – 6.12i; Tables 6.4 and 6.5). Addition of H_2O_2 during ozonation confirmed the results of the previous chapter showing that $^{\bullet}OH$ reactions increased the DBP formation potentials of THM4, HAA8, CH, HK2, HAN4, TCAM, and AOX (de Vera et al. 2015) (Chapter 5). For THNM2, an opposite trend (i.e., lower formation potentials at higher H_2O_2 concentrations) was observed which shows that THNM2 precursors are predominantly formed through O_3 reactions (McCurry et al. 2016). When biofiltration was employed after the oxidation process, a dramatic drop in DBP formation potentials was observed in the column effluent especially for CH, HK2, and THNM2 suggesting the high biodegradability of their precursors. The slightly better removal of formation potentials of DBPs with BAC over AN may be attributed possibly to the different surface area and biological activity of each filter media.

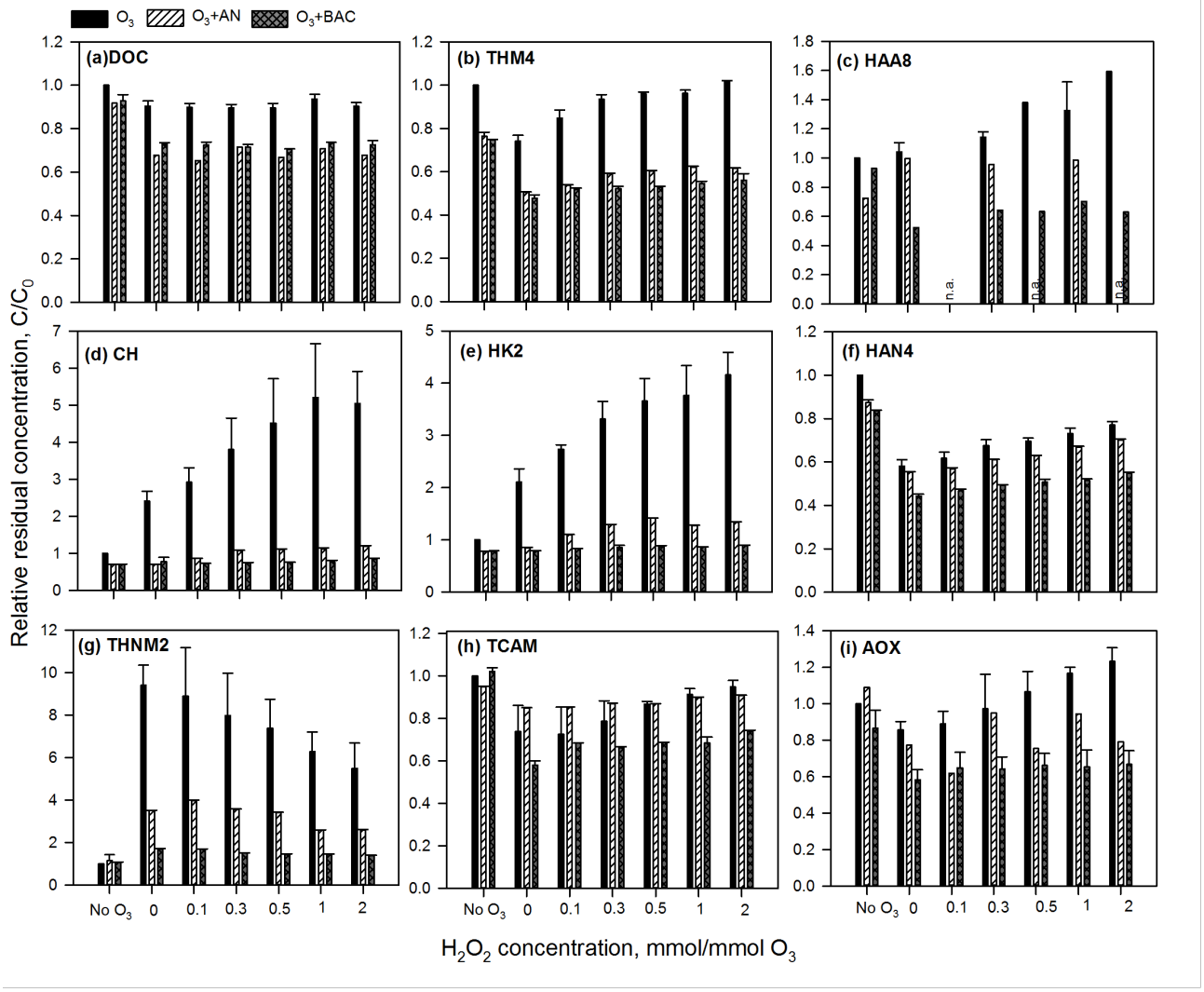

Figure 6.12. Changes in (a) dissolved organic carbon (DOC) and formation potentials post-chlorination of (b) trihalomethanes (THM4), (c) haloacetic acids (HAA8), (d) chloral hydrate (CH), (e) haloketones (HK2), (f) haloacetonitriles (HAN4), (g) trihalonitromethanes (THNM), (h) trichloroacetamide (TCAM), and (i) adsorbable organic halogen (AOX) as a result of O_3/H_2O_2 treatment and subsequent column biofiltration with anthracite (AN), and biological activated carbon (BAC). Conditions: specific ozone dose = 1 mgO_3/mg DOC mg/L; bed volume = 7 mL; empty bed contact time = 11 min, pH = 7; influent DO = 11.5 ± 0.7 mg/L; effluent DO = 6.6 ± 0.2 mg/L; temperature = 22 ± 1 °C; chlorine residual = 1 – 2.7 mg/L as Cl_2. "No O_3" at x-axis are formation potentials of non-ozonated samples. Error bars depict mean absolute deviation of experiments (BAC: n=2, AN: n=1, with 2 DBP extractions per sample; for HAA, n=1). n.a. = no test done at the specific experimental condition

Table 6.4. Effect of H_2O_2 addition on DBP formation potentials (μM) and DOC (mg C/L) on BAC filtration performance. Conditions: ozone dose = 10 mg/L; H_2O_2 = 0 – 2 mmol/mmol O_3; bed volume = 7 mL; flow rate = 0.67 ± 0.07 mL/min; empty bed contact time = 10.5 ± 1.1 min, pH = 7; temperature = 22 ± 1 ^{0}C; chlorine residual = 1.0 ± 0.3 mg/L as Cl_2. "No O_3" are formation potentials of non-ozonated samples; H_2O_2 was quenched with MnO_2 prior to BAC filtration; DBP values are average formation potentials (±mean absolute deviation) obtained from experiments (n=2; n=1 for HAAs) with two extractions per sample.

DBP	No O_3	O_3+ 0H_2O_2	O_3+ 0.1H_2O_2	O_3+ 0.3H_2O_2	O_3+ 0.5H_2O_2	O_3+ 1H_2O_2	O_3+ 2H_2O_2	No O_3 + BAC	O_3+ 0H_2O_2 +BAC	O_3+ 0.1H_2O_2 +BAC	O_3+ 0.3H_2O_2 +BAC	O_3+ 0.5H_2O_2 +BAC	O_3+ 1H_2O_2 +BAC	O_3+ 2H_2O_2 +BAC
TCM	1.86E+0 (1E-2)	1.28E+0 (3E-2)	1.43E+0 (5E-2)	1.63E+0 (3E-2)	1.72E+0 (2E-2)	1.72E+0 (2E-2)	1.85E+0	1.27E+0 (9E-3)	6.77E-1 (4E-2)	7.73E-1 (1E-2)	7.60E-1 (3E-2)	7.71E-1 (9E-3)	8.18E-1 (2E-2)	8.34E-1 (7E-2)
BDCM	5.10E-1 (5E-3)	4.35E-1 (2E-3)	4.86E-1 (2E-3)	5.22E-1 (2E-3)	5.28E-1 (7E-3)	5.12E-1 (6E-3)	5.39E-1	4.46E-1 (2E-3)	3.39E-1 (7E-3)	3.48E-1 (1E-3)	3.59E-1 (3E-3)	3.64E-1 (7E-5)	3.64E-1 (2E-3)	3.82E-1 (8E-3)
DBCM	1.20E-1 (6E-5)	1.59E-1 (1E-3)	1.48E-1 (8E-4)	1.44E-1 (5E-4)	1.41E-1 (5E-4)	1.38E-1 (1E-4)	1.42E-1	1.34E-1 (4E-4)	1.60E-1 (4E-4)	1.57E-1 (1E-3)	1.68E-1 (1E-3)	1.68E-1 (1E-4)	1.66E-1 (4E-4)	1.71E-1 (2E-3)
TBM	3.31E-3 (1E-5)	7.00E-3 (2E-4)	6.28E-3 (8E-5)	6.02E-3 (3E-5)	5.91E-3 (7E-5)	6.19E-3 (4E-4)	5.74E-3	4.62E-3 (1E-4)	1.27E-2 (6E-5)	1.11E-2 (2E-4)	1.21E-2 (2E-4)	1.22E-2 (2E-4)	1.19E-2 (3E-4)	1.15E-2 (1E-4)
TCAN	3.38E-3 (2E-5)	3.17E-3 (1E-5)	3.17E-3 (2E-5)	3.19E-3 (5E-6)	3.26E-3 (1E-5)	3.25E-3 (5E-5)	3.31E-3	3.60E-3 (7E-6)	3.14E-3 (7E-6)	3.18E-3 (3E-5)	3.16E-3 (2E-5)	3.19E-3 (4E-6)	3.20E-3 (1E-6)	3.23E-3 (7E-5)
DCAN	8.39E-2 (1E-3)	4.33E-2 (4E-4)	4.60E-2 (5E-4)	5.12E-2 (7E-4)	5.37E-2 (5E-4)	5.57E-2 (8E-4)	5.91E-2	6.52E-2 (1E-3)	2.63E-2 (4E-4)	2.94E-2 (2E-4)	3.05E-2 (3E-5)	3.13E-2 (3E-4)	3.22E-2 (2E-4)	3.48E-2 (8E-5)
BCAN	1.66E-2 (6E-4)	1.02E-2 (3E-4)	1.14E-2 (3E-4)	1.24E-2 (4E-4)	1.27E-2 (2E-4)	1.36E-2 (4E-4)	1.50E-2	1.69E-2 (3E-4)	1.19E-2 (2E-5)	1.19E-2 (8E-5)	1.30E-2 (3E-4)	1.35E-2 (2E-4)	1.35E-2 (1E-4)	1.44E-2 (3E-4)
DBAN	4.03E-3 (8E-5)	4.17E-3 (2E-4)	4.34E-3 (2E-4)	4.53E-3 (2E-4)	4.57E-3 (1E-4)	4.81E-3 (9E-5)	4.94E-3	4.43E-3 (1E-4)	6.49E-3 (2E-4)	6.06E-3 (2E-4)	6.60E-3 (3E-4)	6.80E-3 (5E-5)	6.68E-3 (1E-4)	6.79E-3 (2E-4)
CH	6.76E-2 (8E-5)	1.72E-1 (8E-3)	2.11E-1 (1E-2)	2.87E-1 (2E-2)	3.51E-1 (2E-2)	4.09E-1 (6E-3)	3.75E-1	4.75E-2 (3E-4)	5.25E-2 (8E-3)	4.86E-2 (5E-4)	4.95E-2 (1E-3)	5.09E-2 (4E-4)	5.16E-2 (3E-3)	5.66E-2 (2E-3)
TCNM	4.36E-3 (2E-6)	4.68E-2 (1E-4)	3.99E-2 (7E-4)	3.60E-2 (1E-3)	3.49E-2 (2E-3)	3.01E-2 (2E-3)	2.48E-2	4.57E-3 (1E-4)	6.45E-3 (3E-5)	6.83E-3 (5E-5)	5.96E-3 (1E-4)	5.52E-3 (1E-4)	5.61E-3 (1E-4)	5.38E-3 (2E-4)
TBNM	1.18E-3 (3E-5)	2.29E-3 (9E-5)	2.09E-3 (6E-5)	1.94E-3 (2E-5)	1.90E-3 (1E-4)	1.88E-3 (3E-5)	1.78E-3	1.39E-3 (3E-6)	2.95E-3 (1E-4)	2.51E-3 (3E-5)	2.43E-3 (5E-5)	2.44E-3 (1E-5)	2.34E-3 (1E-4)	2.27E-3 (6E-6)
DCP	8.89E-3 (1E-3)	1.34E-2 (6E-4)	1.39E-2 (2E-4)	1.56E-2 (1E-6)	1.55E-2 (4E-4)	1.49E-2 (2E-4)	1.26E-2	6.94E-3 (2E-4)	7.31E-3 (1E-4)	7.76E-3 (7E-5)	7.63E-3 (1E-4)	7.75E-3 (6E-5)	7.64E-3 (3E-4)	7.84E-3 (3E-4)
TCP	7.14E-2 (3E-3)	1.67E-1 (9E-3)	2.08E-1 (1E-2)	2.65E-1 (1E-2)	2.98E-1 (1E-2)	3.12E-1 (3E-2)	3.41E-1	5.54E-2 (1E-4)	5.51E-2 (5E-4)	5.91E-2 (1E-3)	6.06E-2 (2E-3)	6.19E-2 (5E-5)	6.15E-2 (2E-3)	6.40E-2 (2E-3)
TCAM	7.24E-3 (1E-4)	4.87E-3 (4E-4)	4.72E-3 (2E-4)	5.33E-3 (4E-4)	6.24E-3 (3E-5)	6.61E-3 (3E-4)	6.97E-3	7.38E-3 (2E-4)	4.20E-3 (2E-4)	4.94E-3 (8E-5)	4.78E-3 (3E-5)	4.97E-3 (7E-5)	4.95E-3 (3E-4)	5.37E-3 (1E-4)
MCAA	8.39E-2	1.57E-1	n.a.	1.68E-1	1.99E-1	1.89E-1	1.99E-1	6.29E-2	<5.00E-2	n.a.	6.29E-2	<5.00E-2	5.24E-2	<5.00E-2
MBAA	<4.00E-2	5.04E-2	n.a.	<4.00E-2	<4.00E-2	<4.00E-2	<4.00E-2	<4.00E-2	<4.00E-2	n.a.	<4.00E-2	<4.00E-2	<4.00E-2	<4.00E-2

DBP	No O_3	O_3+ 0H_2O_2	O_3+ 0.1H_2O_2	O_3+ 0.3H_2O_2	O_3+ 0.5H_2O_2	O_3+ 1H_2O_2	O_3+ 2H_2O_2	No O_3 + BAC	O_3+ 0H_2O_2 +BAC	O_3+ 0.1H_2O_2 +BAC	O_3+ 0.3H_2O_2 +BAC	O_3+ 0.5H_2O_2 +BAC	O_3+ 1H_2O_2 +BAC	O_3+ 2H_2O_2 +BAC
DCAA	4.81E-1	5.43E-1	n.a.	6.67E-1	7.68E-1	8.53E-1	8.53E-1	4.03E-1	2.25E-1	n.a.	2.56E-1	2.72E-1	2.95E-1	2.79E-1
TCAA	3.79E-1	2.88E-1	n.a.	3.00E-1	3.67E-1	4.10E-1	4.47E-1	4.04E-1	1.71E-1	n.a.	2.02E-1	2.20E-1	2.39E-1	2.20E-1
BCAA	1.27E-1	1.27E-1	n.a.	1.33E-1	1.56E-1	1.61E-1	1.67E-1	1.38E-1	1.10E-1	n.a.	1.15E-1	1.21E-1	1.27E-1	1.21E-1
BDCAA	1.15E-1	9.62E-2	n.a.	1.06E-1	1.20E-1	1.44E-1	1.73E-1	1.97E-1	1.30E-1	n.a.	1.54E-1	1.64E-1	1.59E-1	1.54E-1
DBAA	<2.00E-2	5.05E-2	n.a.	2.75E-2	2.75E-2	2.75E-2	2.75E-2	2.75E-2	4.13E-2	n.a.	4.13E-2	4.13E-2	4.13E-2	4.13E-2
CDBAA	<2.00E-2	<2.00E-2	n.a.	<2.00E-2	<2.00E-2	2.00E-2	2.38E-2	2.38E-2	3.17E-2	n.a.	3.96E-2	3.96E-2	3.96E-2	3.57E-2
THM4	2.49E+0 (5E-3)	1.88E+0 (2E-2)	2.07E+0 (5E-2)	2.31E+0 (4E-2)	2.40E+0 (2E-2)	2.37E+0 (2E-2)	2.54E+0	1.86E+0 (7E-3)	1.19E+0 (4E-2)	1.29E+0 (1E-2)	1.30E+0 (3E-2)	1.32E+0 (9E-3)	1.36E+0 (2E-2)	1.40E+0 (8E-2)
HAN4	1.08E-1 (2E-3)	6.08E-2 (8E-4)	6.49E-2 (1E-3)	7.13E-2 (1E-3)	7.42E-2 (8E-4)	7.73E-2 (1E-3)	8.24E-2	9.01E-2 (2E-3)	4.78E-2 (2E-4)	5.05E-2 (7E-6)	5.32E-2 (5E-4)	5.48E-2 (5E-4)	5.55E-2 (2E-6)	5.93E-2 (6E-4)
THNM2	5.54E-3 (3E-5)	4.91E-2 (3E-5)	4.20E-2 (6E-4)	3.79E-2 (1E-3)	3.68E-2 (2E-3)	3.20E-2 (2E-3)	2.66E-	5.96E-3 (1E-4)	9.40E-3 (9E-5)	9.34E-3 (8E-5)	8.39E-3 (8E-5)	7.96E-3 (1E-4)	7.95E-3 (2E-4)	7.65E-3 (2E-4)
HK2	8.03E-2 (2E-3)	1.81E-1 (8E-3)	2.22E-1 (1E-2)	2.81E-1 (1E-2)	3.13E-1 (1E-2)	3.27E-1 (3E-2)	3.53E-1	6.24E-2 (1E-5)	6.25E-2 (4E-4)	6.69E-2 (1E-3)	6.83E-2 (2E-3)	6.97E-2 (1E-4)	6.92E-2 (2E-3)	7.18E-2 (1E-3)
HAA8	1.19E+0	1.31E+0	n.a.	1.40E+0	1.64E+0	1.81E+0	1.89E+0	1.26E+0	7.09E-1	n.a.	8.71E-1	8.58E-1	9.53E-1	8.52E-1
AOX, as Cl^-	2.44E+1 (1E+0)	2.14E+1 (7E-1)	2.08E+1 (4E-1)	2.12E+1 (9E-1)	2.71E+1 (2E-1)	2.84E+1 (7E-1)	3.02E+1	2.10E+1 (1E+0)	1.41E+1 (6E-1)	1.57E+1 (1E+0)	1.55E+1 (8E-1)	1.60E+1 (8E-1)	1.58E+1 (1E+0)	1.62E+1 (9E-1)
DOC	8.30	7.62	7.47	7.39	7.54	7.81	7.49	7.71	6.05	6.02	5.94	5.85	6.08	6.02

n.a. = not available (not analysed for the specific condition)

Table 6.5. Effect of H_2O_2 addition on DBP formation potentials (μM) and DOC (mg C/L) on anthracite biofiltration performance. Conditions: ozone dose = 10 mg/L; H_2O_2 = 0 – 2 mmol/mmol O_3; bed volume = 7 mL; flow rate = 0.63 ± 0.04 mL/min; empty bed contact time = 11.2 ± 0.7 min; pH = 7; temperature = 22 ± 1 ^{0}C; chlorine residual = 2.7 ± 0.6 mg/L as Cl_2. "No O_3" are formation potentials of non-ozonated samples. DBP values are average formation potentials (±mean absolute deviation) obtained from experiment (n=1) with two extractions per sample.

DBP	No O_3	O_3+ 0H_2O_2	O_3+ 0.1H_2O_2	O_3+ 0.3H_2O_2	O_3+ 0.5H_2O_2	O_3+ 1H_2O_2	O_3+ 2H_2O_2	No O_3 + AN	O_3+ 0H_2O_2 +AN	O_3+ 0.1H_2O_2 + AN	O_3+ 0.3H_2O_2 + AN	O_3+ 0.5H_2O_2 + AN	O_3+ 1H_2O_2 + AN	O_3+ 2H_2O_2 + AN
TCM	1.36E+0 (4E-2)	8.75E-1 (1E-2)	1.13E+0 (3E-2)	1.24E+0 (4E-3)	1.24E+0 (6E-2)	1.29E+0 (2E-2)	1.36E+0 (1E-2)	9.81E-1 (2E-2)	5.66E-1 (1E-3)	6.04E-1 (2E-3)	6.90E-1 (3E-3)	7.06E-1 (2E-3)	7.16E-1 (4E-3)	6.98E-1 (2E-3)
BDCM	3.67E-1 (1E-2)	3.01E-1 (3E-3)	3.56E-1 (1E-2)	3.80E-1 (1E-3)	3.82E-1 (2E-2)	3.75E-1 (6E-3)	3.79E-1 (2E-3)	3.16E-1 (7E-3)	2.42E-1 (3E-4)	2.56E-1 (1E-3)	2.69E-1 (5E-4)	2.77E-1 (1E-3)	2.89E-1 (2E-3)	2.98E-1 (5E-4)
DBCM	6.90E-2 (1E-3)	9.82E-2 (5E-4)	9.78E-2 (2E-3)	9.20E-2 (4E-4)	9.05E-2 (4E-3)	9.23E-2 (1E-3)	9.00E-2 (5E-4)	7.61E-2 (1E-3)	9.44E-2 (2E-4)	9.88E-2 (6E-4)	9.73E-2 (2E-4)	9.75E-2 (5E-4)	1.05E-1 (8E-4)	1.06E-1 (5E-4)
TBM	1.74E-3 (3E-5)	5.00E-3 (6E-6)	4.20E-3 (8E-5)	4.03E-3 (8E-6)	3.92E-3 (2E-4)	4.12E-3 (6E-5)	3.82E-3 (3E-5)	2.54E-3 (5E-5)	8.36E-3 (2E-5)	8.53E-3 (6E-5)	7.61E-3 (3E-5)	6.97E-3 (5E-5)	8.28E-3 (6E-5)	7.16E-3 (3E-5)
TCAN	1.84E-3 (2E-5)	1.65E-3 (4E-6)	1.65E-3 (3E-5)	1.70E-3 (5E-5)	1.65E-3 (2E-5)	1.76E-3 (5E-6)	1.78E-3 (1E-6)	2.04E-3 (2E-5)	1.67E-3 (1E-5)	1.59E-3 (6E-7)	1.68E-3 (8E-6)	1.70E-3 (9E-6)	1.72E-3 (3E-6)	1.65E-3 (4E-5)
DCAN	7.57E-2 (1E-3)	4.21E-2 (2E-4)	4.55E-2 (6E-4)	4.95E-2 (3E-4)	4.99E-2 (2E-3)	5.19E-2 (6E-4)	5.42E-2 (3E-4)	6.05E-2 (9E-4)	3.09E-2 (2E-4)	3.18E-2 (2E-4)	3.58E-2 (3E-6)	3.78E-2 (1E-4)	3.87E-2 (2E-4)	4.10E-2 (2E-4)
BCAN	2.40E-2 (3E-4)	1.57E-2 (7E-5)	1.61E-2 (1E-4)	1.77E-2 (9E-6)	1.80E-2 (5E-4)	2.01E-2 (2E-4)	2.05E-2 (9E-5)	2.43E-2 (3E-4)	1.73E-2 (5E-5)	1.77E-2 (9E-5)	1.84E-2 (5E-5)	1.88E-2 (7E-5)	2.04E-2 (7E-5)	2.17E-2 (2E-4)
DBAN	4.85E-3 (3E-5)	6.18E-3 (1E-5)	6.03E-3 (2E-5)	6.36E-3 (1E-4)	6.32E-3 (1E-4)	7.11E-3 (3E-5)	6.89E-3 (3E-5)	6.21E-3 (5E-5)	9.10E-3 (4E-6)	9.57E-3 (1E-4)	9.25E-3 (3E-6)	8.68E-3 (4E-5)	1.03E-2 (9E-5)	1.04E-2 (8E-5)
CH	1.01E-1 (2E-3)	2.15E-1 (1E-2)	2.56E-1 (1E-3)	2.96E-1 (3E-3)	3.22E-1 (3E-3)	3.59E-1 (1E-2)	4.09E-1 (6E-3)	7.18E-2 (3E-4)	7.17E-2 (8E-4)	8.72E-2 (1E-3)	1.09E-1 (1E-3)	1.13E-1 (7E-4)	1.14E-1 (2E-3)	1.21E-1 (2E-3)
TCNM	2.80E-3 (7E-5)	3.74E-2 (4E-4)	4.16E-2 (1E-3)	3.70E-2 (6E-5)	3.20E-2 (1E-3)	2.59E-2 (4E-4)	2.45E-2 (1E-4)	2.21E-3 (4E-5)	9.67E-3 (2E-5)	1.14E-2 (6E-5)	1.07E-2 (6E-5)	1.05E-2 (4E-5)	7.52E-3 (4E-5)	7.63E-3 (4E-7)
TBNM	1.06E-3 (3E-5)	3.13E-3 (4E-5)	2.91E-3 (2E-5)	2.70E-3 (2E-6)	2.38E-3 (5E-5)	2.28E-3 (8E-6)	2.04E-3 (0E+0)	2.24E-3 (1E-3)	3.89E-3 (2E-5)	3.89E-3 (3E-5)	3.05E-3 (2E-5)	2.63E-3 (1E-5)	2.48E-3 (3E-5)	2.42E-3 (2E-5)
DCP	5.00E-3 (2E-4)	7.07E-3 (4E-4)	9.74E-3 (1E-4)	9.79E-3 (3E-4)	1.02E-2 (2E-4)	8.32E-3 (1E-4)	8.13E-3 (1E-4)	4.07E-3 (2E-5)	4.33E-3 (2E-5)	5.33E-3 (5E-5)	6.02E-3 (1E-4)	6.30E-3 (1E-4)	5.55E-3 (1E-4)	5.29E-3 (2E-5)
TCP	7.13E-2 (2E-3)	1.32E-1 (4E-4)	1.94E-1 (3E-3)	2.15E-1 (5E-4)	2.31E-1 (7E-3)	2.34E-1 (2E-3)	2.72E-1 (1E-3)	5.51E-2 (8E-4)	6.06E-2 (3E-4)	7.84E-2 (5E-4)	9.27E-2 (2E-5)	1.02E-1 (2E-4)	9.15E-2 (6E-4)	9.66E-2 (8E-4)
TCAM	1.98E-2 (4E-4)	1.73E-2 (2E-4)	1.72E-2 (7E-5)	1.76E-2 (3E-5)	1.74E-2 (1E-5)	1.81E-2 (4E-5)	1.82E-2 (7E-5)	1.88E-2 (5E-5)	1.68E-2 (2E-5)	1.69E-2 (3E-5)	1.72E-2 (4E-5)	1.72E-2 (4E-6)	1.78E-2 (7E-5)	1.79E-2 (7E-5)
MCAA	8.39E-2	2.31E-1	n.a.	1.68E-1	n.a.	1.26E-1	n.a.	1.05E-1	7.34E-2	n.a.	9.43E-2	n.a.	7.34E-2	n.a.
MBAA	<4.00E-2	5.04E-2	n.a.	3.60E-2	n.a.	<4.00E-2	n.a.	<4.00E-2	<4.00E-2	n.a.	<4.00E-2	n.a.	<4.00E-2	n.a.

DBP	No O_3	O_3+ 0H_2O_2	O_3+ 0.1H_2O_2	O_3+ 0.3H_2O_2	O_3+ 0.5H_2O_2	O_3+ 1H_2O_2	O_3+ 2H_2O_2	No O_3 + AN	O_3+ 0H_2O_2 +AN	O_3+ 0.1H_2O_2 + AN	O_3+ 0.3H_2O_2 + AN	O_3+ 0.5H_2O_2 + AN	O_3+ 1H_2O_2 + AN	O_3+ 2H_2O_2 + AN
DCAA	5.82E-1	5.66E-1	n.a.	7.29E-1	n.a.	7.45E-1	n.a.	3.41E-1	4.58E-1	n.a.	5.12E-1	n.a.	5.28E-1	n.a.
TCAA	5.14E-1	3.18E-1	n.a.	3.92E-1	n.a.	4.59E-1	n.a.	2.20E-1	4.59E-1	n.a.	3.06E-1	n.a.	3.24E-1	n.a.
BCAA	1.44E-1	1.27E-1	n.a.	1.56E-1	n.a.	1.50E-1	n.a.	1.10E-1	1.27E-1	n.a.	1.38E-1	n.a.	1.44E-1	n.a.
BDCAA	1.49E-1	1.20E-1	n.a.	1.35E-1	n.a.	1.78E-1	n.a.	1.30E-1	1.78E-1	n.a.	1.54E-1	n.a.	1.73E-1	n.a.
DBAA	2.75E-2	5.51E-2	n.a.	4.13E-2	n.a.	3.21E-2)	n.a.	4.13E-2	2.75E-2	n.a.	4.59E-2	n.a.	4.59E-2	n.a.
CDBAA	1.98E-2	2.38E-2	n.a.	2.38E-2	n.a.	3.17E-2	n.a.	3.57E-2	2.77E-2	n.a.	4.36E-2	n.a.	4.76E-2	n.a.
THM4	1.80E+0 (5E-2)	1.28E+0 (2E-2)	1.59E+0 (5E-2)	1.72E+0 (2E-3)	1.71E+0 (8E-2)	1.76E+0 (3E-2)	1.83E+0 (1E-2)	1.38E+0 (3E-2)	9.10E-1 (6E-4)	9.67E-1 (4E-3)	1.06E+0 (4E-3)	1.09E+0 (4E-3)	1.12E+0 (7E-3)	1.11E+0 (1E-3)
HAN4	1.06E-1 (2E-3)	6.56E-2 (3E-4)	6.92E-2 (8E-4)	7.53E-2 (3E-4)	7.58E-2 (2E-3)	8.09E-2 (9E-4)	8.34E-2 (4E-4)	9.30E-2 (1E-3)	5.90E-2 (2E-4)	6.06E-2 (4E-4)	6.51E-2 (5E-5)	6.70E-2 (3E-4)	7.12E-2 (4E-4)	7.47E-2 (4E-4)
THNM2	3.86E-3 (9E-5)	4.05E-2 (4E-4)	4.45E-2 (1E-3)	3.97E-2 (6E-5)	3.44E-2 (1E-3)	2.82E-2 (4E-4)	2.65E-2 (1E-4)	4.45E-3 (1E-3)	1.36E-2 (5E-5)	1.53E-2 (8E-5)	1.37E-2 (8E-5)	1.32E-2 (5E-5)	1.00E-2 (7E-5)	1.01E-2 (2E-5)
HK2	7.64E-2 (2E-3)	1.39E-1 (7E-4)	2.04E-1 (3E-3)	2.25E-1 (8E-4)	2.41E-1 (7E-3)	2.43E-1 (3E-3)	2.80E-1 (9E-4)	5.92E-2 (8E-4)	6.49E-2 (3E-4)	8.38E-2 (5E-4)	9.87E-2 (2E-4)	1.08E-1 (4E-4)	9.70E-2 (7E-4)	1.02E-1 (8E-4)
HAA8	1.52E+0	1.49E+0	n.a.	1.68E+0	n.a.	1.72E+0	n.a.	9.83E-1	1.35E+0	n.a.	1.29E+0	n.a.	1.34E+0	n.a.
AOX, as Cl-	1.95E+1	1.57E+1	1.87E+1	2.28E+1	1.89E+1	2.27E+1	2.26E+1	2.13E+1	1.51E+1	1.21E+1	1.85E+1	1.47E+1	1.84E+1	1.54E+1
DOC	8.47	7.43	7.60	7.69	7.38	7.88	7.68	7.77	5.74	5.53	6.06	5.66	5.99	5.74

n.a. = not available (not analysed for the specific condition)

6.3.2.2. Biofiltration: Variation of empty bed contact time (EBCT)

To optimize biofiltration, column experiments using BAC were performed at different EBCTs (3 – 55 min). Bioactivity of the columns was confirmed from the increase in oxygen consumption and nitrate concentration with increasing EBCT (Figure 6.5). BAC filtration resulted in about 30% decrease in DOC as shown in Figure 6.14a, which is within the range of removal efficiencies reported in the literature (Juhna and Melin 2006). This decrease mostly happened within the first 20 min, with the largest decrease happening within the first three minutes. Such observation supports previous studies (Black and Berube 2014, Carlson and Amy 1998, Yavich et al. 2004) where a characteristic initial period of fast DOC decrease followed by a period of slow decrease was observed. The remaining DOC corresponds to the slowly biodegradable to non-biodegradable DOC. A similar trend was also observed for the formation potentials of all the DBPs studied (Figures 6.14b – 6.14i). These results followed first-order reaction kinetics, with biofilm being in excess compared to the influent biodegradable DOC or DBP precursor (Black and Berube 2014, Huck et al. 1994), and can be modelled using equation 6.1:

$$P_t = P_{biodeg}e^{-kt} + P_f \qquad \text{(eq. 6.1)}$$

where t is the EBCT (min), k is the specific first-order rate constant (min^{-1}), P_t is the concentration at time t (μM), P_{biodeg} is the biodegradable concentration (μM), and P_f is the minimum contaminant concentration or DBP formation potential (μM) after a certain EBCT. The parameters shown in equation 6.1 are illustrated in Figure 6.13.

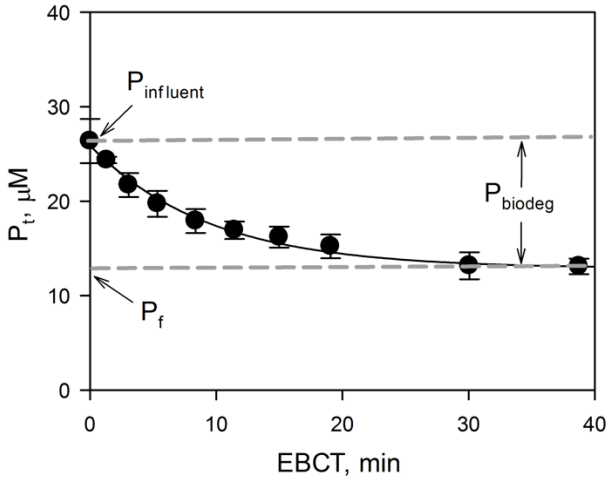

Figure 6.13. Model parameters used in the decay kinetics of contaminant (DOC or DBP precursor) during BAC filtration at different EBCT

The model fit (single exponential decay to P_f) for DOC and DBP formation potentials was carried out using the software SigmaPlot, version 13.0 (Systat Software, Inc.) and resulted in the kinetic parameters (± standard error) summarized in Table 6.6. Residuals from the model fit showed a normal distribution (P values > 0.05, Shapiro-Wilk test). It should be noted that the kinetic parameters reported in this study could be site-specific due to differences in water quality, type of filter media, and nature of bacterial community as previously described by others (Huck et al. 1994, Melin and Odegaard 2000). All measured formation potentials at different EBCTs are presented in Table 6.7.

Following ozonation, THM4 formation potential was reduced by 46% after a BAC EBCT of 15 min (i.e., 2.70 μM down to 1.47 μM) and remained at almost the same level up to 55 min. This indicates that THM precursors, mostly for TCM and BDCM, were not completely degraded even at extended EBCTs. In terms of speciation, the decrease in TCM and BDCM was also accompanied by an increase in the more brominated THM species, namely DBCM and TBM. TBM formation potentials increased from 0.003 ± 0.001 to 0.022 ± 0.002 μM in 15 min and continued to increase to 0.031 ± 0.001 μM in 55 min, while DBCM started to slightly increase at 15 min (i.e., 0.20 ± 0.02 μM to 0.24 ± 0.01 μM in 55 min). These observations can be understood as a result of increased HOBr availability relative to DOC during chlorination since the bromide to DOC ratio increases with increasing EBCT (Figure 6.15). The increase in brominated DBPs (between 0 to 55 min EBCT) was also observed with other DBP groups such as DBAN (0.010 to 0.018 μM), TBNM (0.010 to 0.016 μM) and CDBAA (0.028 to 0.050 μM). Hence, an increase in the levels of bromine-containing DBPs with O_3/BAC treatment may occur, especially in source waters containing high bromide concentrations.

The concentrations of other non-bromine-containing DBPs such as HK2 and CH were reduced significantly after biofiltration at 10 min EBCT. While their formation potentials increased after O_3/HOCl treatment (i.e., by 73% for HK2 and 111% for CH), their BAC effluent formation potentials of about 0.06 μM for both CH and HK2 appeared to be the lowest attainable during biofiltration. These concentrations were lower than those obtained without ozonation (i.e., HK2 = 0.14 μM and CH = 0.17 μM) which confirms the benefit of combined O_3/BAC in reducing formation potentials of these DBPs. The calculated rate constants for these C-DBPs (after ozone/BAC treatment) were 0.50 ± 0.07 min^{-1} for HK2 and 0.58 ± 0.07 min^{-1} for CH, which were highest among the rate constants determined for other DBP groups suggesting the high biodegradability of CH and HK2 precursors.

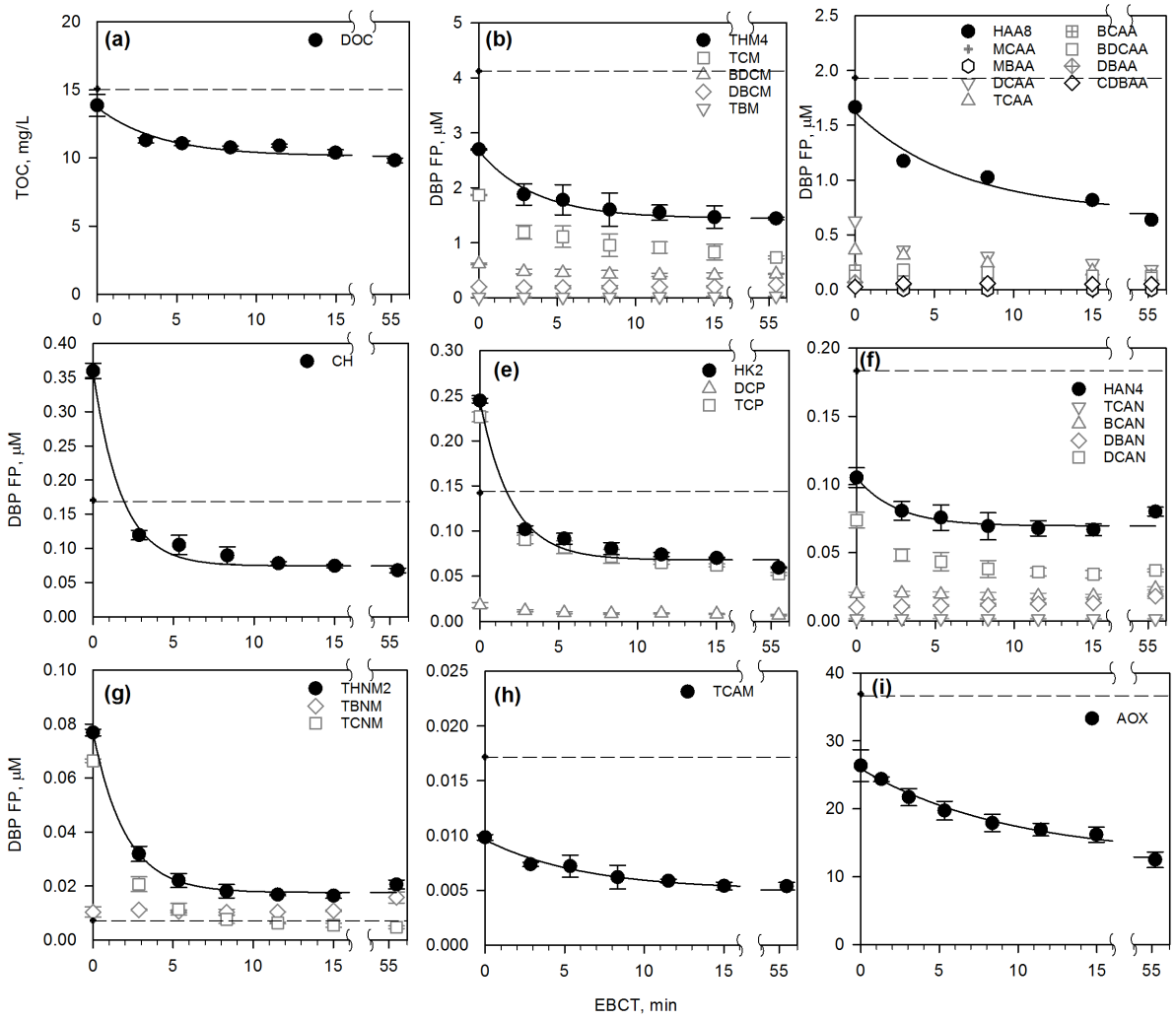

Figure 6.14. Effect of biofiltration EBCT on changes in (a) DOC and formation potentials of (b) trihalomethanes (THM4), (c) haloacetic acids (HAA8), (d) chloral hydrate (CH), (e) haloketones (HK2), (f) haloacetonitriles (HAN4), (g) trihalonitromethanes (THNM2), (h) trichloroacetamide (TCAM), and (i) adsorbable organic halogen (AOX) of ozonated water sample. Conditions: specific ozone dose = 1 mgO_3/mg DOC, DOC = 15 mg/L, bromide = 300 µg/L, bed volume = 12 mL, media = BAC, pH = 6.9, temperature = 22 ± 1 °C, chlorine residual = 3.1 ± 0.8 mg/L as Cl_2. The symbols are the experimental data, broken lines correspond to formation potentials measured without ozonation, and solid lines present model fits (single exponential decay to P_f). Residuals from the model fit shows a normal distribution (P values > 0.05, Shapiro-Wilk test, excluding the last point for THNM2 and HAN4). Error bars depict standard deviation of 3 replicate experiments (with 2 DBP extractions per sample).

Table 6.6. Model parameters for reduction in DBP formation potentials after BAC filtration of ozonated water samples[a]

DBP	P_f[b], µM	P_{biodeg}[c], µM	k[d], min^{-1}	R^2[e]	$S_{y|x}$[f]	n[g]
THM4	1.45 ± 0.04	1.22 ± 0.09	0.28 ± 0.05	0.9657	0.0840	10
HAA8	0.69 ± 0.06	0.93 ± 0.10	0.15 ± 0.04	0.9688	0.0860	6
CH	0.074 ± 0.004	0.284 ± 0.012	0.58 ± 0.07	0.9877	0.0113	10
HK2	0.068 ± 0.003	0.176 ± 0.009	0.50 ± 0.07	0.9808	0.0087	10
HAN4	0.068 ± 0.001	0.037 ± 0.002	0.33 ± 0.04	0.9844	0.0018	9
THNM2	0.0171 ± 0.0002	0.0597 ± 0.0006	0.48 ± 0.01	0.9993	0.0006	9
TCAM	0.0050 ± 0.0002	0.0046 ± 0.0004	0.16 ± 0.03	0.9561	0.0004	10
AOX	12.86 ± 0.34	13.03 ± 0.46	0.11 ± 0.01	0.9904	0.5113	11
DOC	10.14 ± 0.17[h]	3.57 ± 0.38[h]	0.26 ± 0.06	0.9268	0.3646	10
Cl_2 demand	3.77 ± 0.13[h]	3.03 ± 0.23[h]	0.13 ± 0.02	0.9621	0.2272	10

[a]obtained from non-linear regression, ± depicts the standard error (SigmaPlot 13.0); [b]P_f = final steady state concentration (EBCT > 20 min); [c]P_{biodeg}= DBP formation potential from influent - P_f; [d]k = specific first-order rate constant; [e]R^2 = coefficient of determination; [f]$S_{y|x}$ (standard error of the estimate) = $(SS/df)^{1/2}$ where SS is the sum-of-squares of the distance of the linear regression from the data points and df is the degrees of freedom (i.e. n-2); [g]n = number of data points (each data point is the average of 3 replicate experiments); [h]units = mg/L as C for DOC and as Cl_2 for chlorine demand.

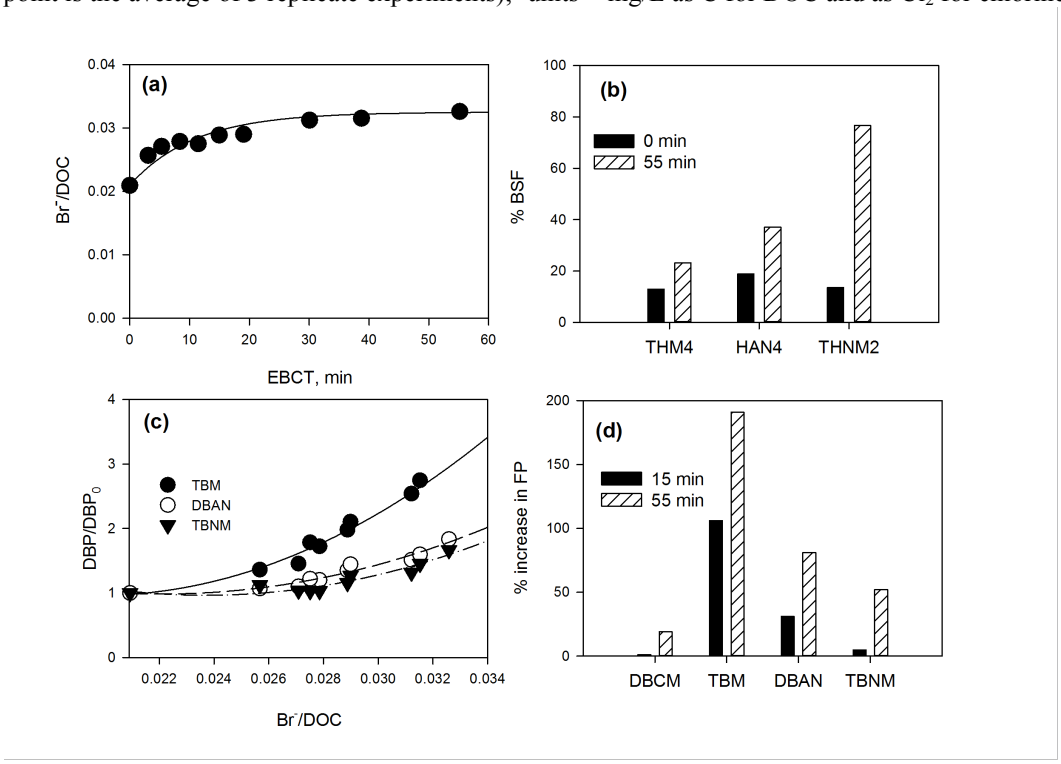

Figure 6.15. Influence of bromide on DBP formation after biofiltration and subsequent chlorination. (a) change in bromide to carbon ratio, (b) change in bromine substitution factor before and after BAC filtration at 55 min EBCT, (c) relative residual formation potentials of brominated DBPs as a function of Br^-/DOC ratio, and (d) increase in formation potentials (FP) of brominated DBPs after biofiltration at EBCTs of 15 and 55 min.

In terms of the HAA species, dihaloacetic acid (DHAA) precursors were removed faster (k = 0.18 ± 0.05 min^{-1}) than those of trihaloacetic acids (THAA) (k = 0.06 ± 0.02 min^{-1}) (Figure 6.16). At the highest EBCT (55 min) there was a reduction of 58% in DHAA and 47% in THAA in the chlorinated column effluent. The slightly better removal of DHAA than THAA may suggest having more biodegradable precursors (i.e., hydrophilic, low molecular weight) consistent with the findings of Hua and Reckhow (2007a).

Similar features to those presented for other DBPs were observed for HAN4, with DCAN being the most dominant HAN produced during chlorination. Low TCAN concentrations were observed due to this compound's low stability (Glezer et al. 1999). Despite HAN4 having the lowest reduction in formation potential (24%, compared to formation potentials after ozonation) after biofiltration at 55 min EBCT, they had a higher k value (0.33 ± 0.04 min^{-1}) than THM4 which had a higher removal (47%) at the same EBCT. This suggests that the biodegradable HAN4 precursors (e.g., aliphatic dissolved organic nitrogen) can be removed faster than their THM4 counterparts.

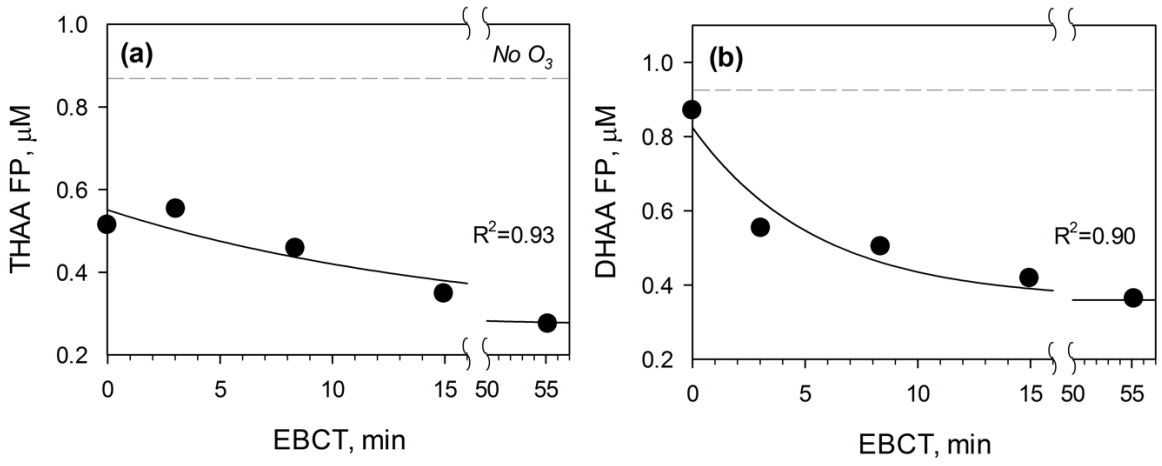

Figure 6.16. Changes in (a) trihaloacetic acid (THAA) and (b) dihaloacetic acid (DHAA) formation potentials after biofiltartion at different EBCTs. Conditions: ozone dose = 15 mg/L, DOC = 15 mg/L, bromide = 300 µg/L, bed volume = 12 mL, media = BAC, pH = 6.9, temperature = 22 ± 1 ºC, chlorine residual = 1–2 mg/L Cl_2. Broken lines correspond to conditions without ozonation and solid lines present model fits.

TCNM formation potentials were found to decrease after BAC filtration confirming results from previous studies (Krasner 2009, Lyon et al. 2014a). Lowest total concentrations were already achieved at 12 min EBCT and were almost equal to the levels before ozonation. At this EBCT, about 90% of the TCNM formation potential present after ozonation was removed. While good TCNM removals were observed, an increase in TBNM formation potentials became apparent after 5 min EBCT. A similar increase in TBNM formation potentials was observed by Lyon et al. (2014a) in full-scale plants in SEQ that utilized O_3/BAC. At the highest EBCT tested in the current study, TBNM increased by 52% relative to its formation potential before biofiltration. Despite the contrasting trends of TCNM and TBNM, the sum of their concentrations (THNM2) could still be modelled with a $k = 0.48 \pm 0.01$ min^{-1}, where TBNM accounted for 77% of the remaining P_f.

TCAM formation potentials also decreased with first-order kinetics ($k = 0.16 \pm 0.03$ min^{-1}) although at a rate that was lower than for HAN4 and THNM2, suggesting differences in biodegradability of their precursors. Based on the calculated rate constant, THNM2 precursors were more readily biodegradable than those of HAN4 and TCAM. This supports the results of Mitch et al. (2009) who showed a higher removal of TCNM compared to DHANs after sequential ozonation, biofiltration, and chlorination. In their study, the median reduction of TCNM formation potentials was 48% while for DHAN it was only 3%.

The change in effluent AOX formation potential and chlorine demand followed the trends discussed above. Their first-order reaction kinetics were relatively close (between 0.11 and 0.13 min^{-1} (Table 6.7)). This similarity confirms the intuitive direct relationship of AOX and chlorine demand (slope = 0.17 mg AOX/mg Cl_2 demand, R = 0.99, $P=1.2x10^{-9}$) as shown in Figure 6.17a. AOX formation was also found to correlate well with DOC (Figure 6.17a, slope = 0.15 mg AOX/mg DOC, R = 0.98, $P=3.7x10^{-7}$) which was in agreement with previous studies (Farré et al. 2016b) . The x-intercept of the AOX versus DOC plot gives a DOC (6.4 mg/L) which is equivalent to 42% of the DOC before ozonation and represents the non-reactive NOM fraction of the water sample.

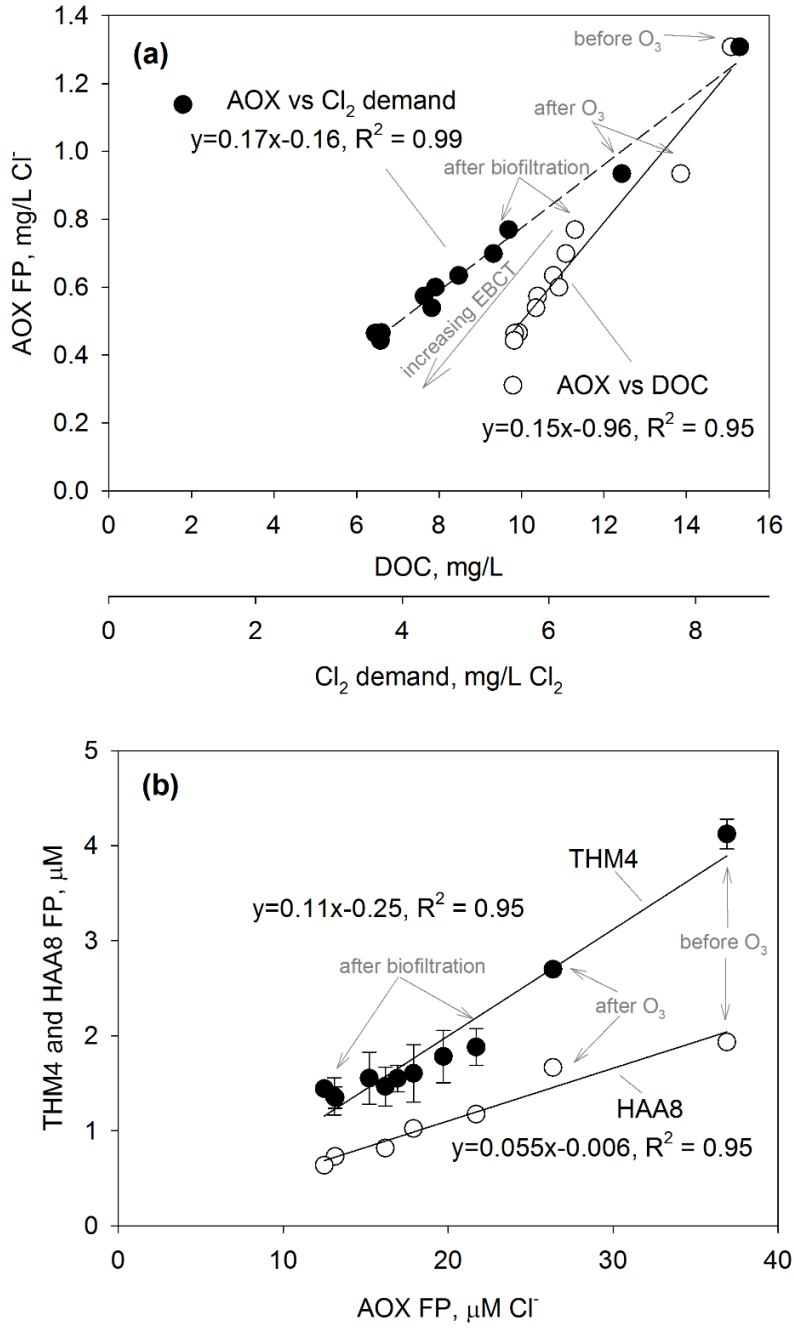

Figure 6.17. Correlations involving AOX formation potentials (FP). (a) AOX FP as a function of DOC and chlorine demand. (b) Relationship of THM4 and HAA8 FP with AOX FP. Conditions: ozone dose = 15 mg/L; bed volume = 12 mL; pH = 7; temperature = 22 ± 1 °C; chlorine residual = 3.1 ± 0.8 mg/L as Cl_2

Following biofiltration, AOX in the chlorinated water decreased from 21.7 µM (3 min EBCT) to 12.5 µM (55 min EBCT). At all conditions (i.e., before and after O_3 addition, and after biofiltration from 3 – 55 min EBCTs), the percentage of known and unknown AOX remained relatively constant as depicted in Figure 6.18a. Unknown AOX was calculated by subtracting AOX equivalents accounted for by the individually measured DBPs from the measured AOX. In this study, while AOX formation potentials decreased with ozonation and increasing biofiltration EBCTs, the percentage of known AOX remained at 48 ± 4% and the unknown AOX at 52 ± 4 %. These results were comparable to many other studies that reported unknown AOX concentrations of about 50% during chlorination (Reckhow and Singer 1984, Richardson 2003, Singer et al. 1995). As shown in Figure 6.18b, the measured AOX in the current study was largely attributed to THM4 (30 ± 3%) and HAA8 (13 ± 0.8%) at all applied experimental conditions. These findings are similar to those in a study by Hua and Reckhow (2007b) where they found 25.2% of the total AOX attributed to THMs and 14.4% attributed to HAAs after ozonation (1mgO_3/mgDOC) and subsequent chlorination of a raw water sample. Other DBP groups only had minor contribution. In the current study, THNM2, HAN4, HK2, CH, and TCAM could only explain 0.4%, 0.9%, 1.5%, 2.1%, and 0.1%, respectively, of the measured AOX. As the AOX attributed to both THM4 and HAA8 remained relatively constant despite differences in the measured AOX concentrations, formation potentials of these two DBP groups were in a linear relationship (i.e., $R = 0.98$, $P < 1.5 \times 10^{-4}$) with AOX formation potentials (Figure 6.17b). In addition to THM4 and HAA8, the AOX values were also strongly correlated with HAN4 ($R=0.92$, $P=6.2 \times 10^{-5}$) and TCAM ($R=0.98$, $P=3.7 \times 10^{-7}$). The relation of CH and HK2 with AOX was not markedly significant ($R=0.65 – 0.71$, $P = 0.01 – 0.03$) since their formation potentials increased after ozonation. THNM2 had no significant relationship ($R=0.21$, $P = 0.541$) with AOX which is also a result of its increase after ozonation. Such correlations might be useful predictors of AOX formation in chlorinated biofilter effluents of water treatment plants.

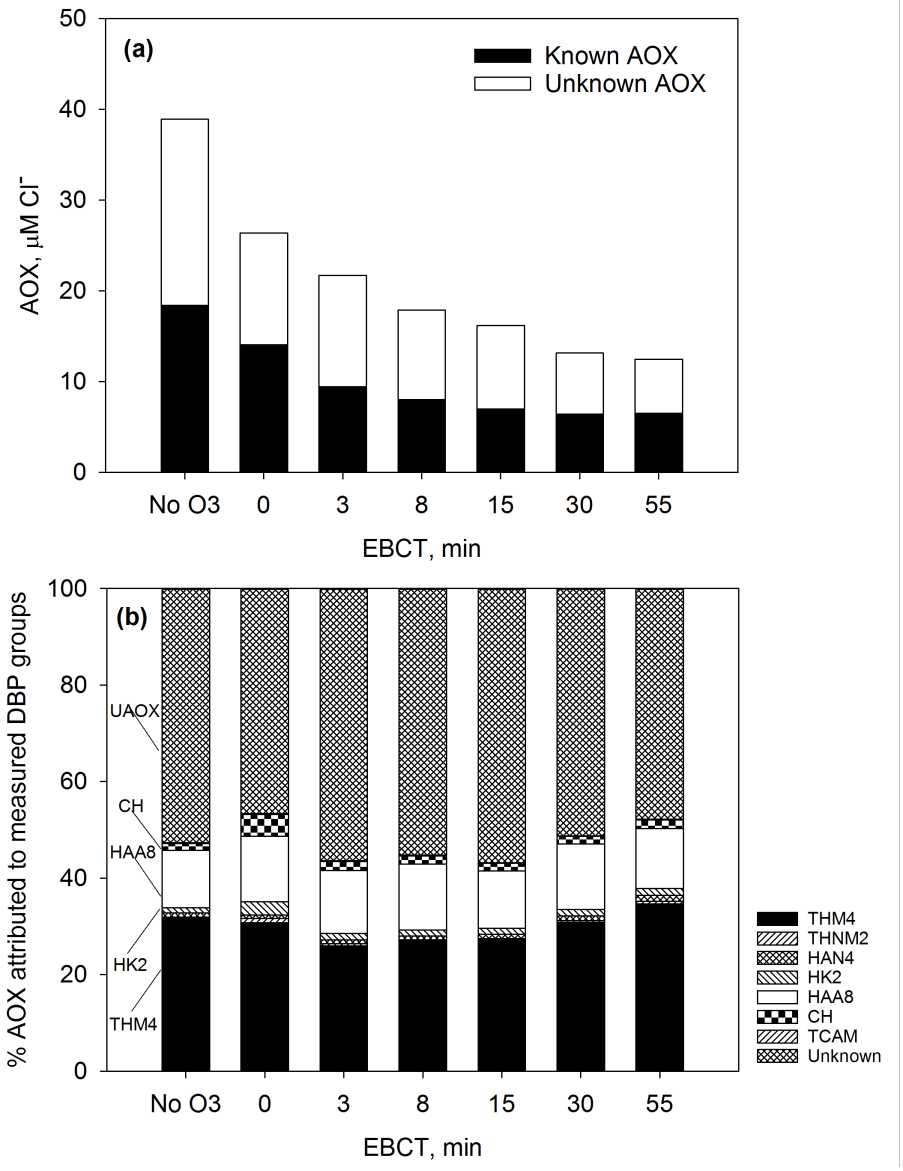

Figure 6.18. AOX formation after BAC filtration at different EBCTs and subsequent chlorination. (a) Sum of known and unknown AOX as a function of EBCT. (b) % AOX attributed to each measured DBP group. Conditions: ozone dose = 15 mg/L; bed volume = 12 mL; pH = 7; temperature = 22 ± 1 °C; chlorine residual = 3.1 ± 0.8 mg/L as Cl_2.

Table 6.7. Effect of different empty bed contact time (EBCT) on DOC (mg C/L) and DBP formation potentials (μM) during BAC filtration[a]. Conditions: ozone dose = 15 mg/L; bed volume = 12 mL; pH = 7; temperature = 22 ± 1 ^{0}C; chlorine residual = 3.1 ± 0.8 mg/L as Cl_2; DBP values are average formation potentials (±standard deviation (n=3) for all DBPs except HAAs (n=2, ±mean absolute deviation)) obtained from experiments (n=3 for THMs, HANs, CH, THNMs, HKs, TCAM, AOX; n=2 for HAAs at 3-55 min EBCT; n=1 for HAAs before and after ozonation) with two extractions per sample.

DBP	No O_3	0 min	3 min	5 min	8 min	12 min	15 min	19 min	30 min	39 min	55 min
TCM	3.21E+0 (1E-1)	1.87E+0 (9E-3)	1.19E+0 (1E-1)	1.11E+0 (2E-1)	9.58E-1 (2E-1)	9.15E-1 (1E-1)	8.32E-1 (1E-1)	8.78E-1 (2E-1)	7.09E-1 (6E-2)	7.11E-1 (1E-1)	7.37E-1 (3E-2)
BDCM	7.83E-1 (2E-2)	6.19E-1 (1E-2)	4.79E-1 (4E-2)	4.59E-1 (6E-2)	4.28E-1 (7E-2)	4.18E-1 (3E-2)	4.10E-1 (5E-2)	4.35E-1 (6E-2)	3.96E-1 (4E-2)	3.98E-1 (5E-2)	4.36E-1 (6E-3)
DBCM	1.26E-1 (6E-4)	2.01E-1 (7E-3)	1.91E-1 (2E-2)	1.95E-1 (3E-2)	1.99E-1 (3E-2)	1.97E-1 (7E-3)	2.03E-1 (2E-2)	2.17E-1 (2E-2)	2.16E-1 (2E-2)	2.20E-1 (2E-2)	2.38E-1 (7E-3)
TBM	3.05E-3 (4E-6)	1.08E-2 (5E-4)	1.51E-2 (1E-3)	1.64E-2 (1E-3)	1.89E-2 (2E-3)	2.06E-2 (7E-4)	2.23E-2 (2E-3)	2.32E-2 (2E-3)	2.82E-2 (3E-3)	3.10E-2 (2E-3)	3.14E-2 (1E-3)
TCAN	2.18E-3 (4E-5)	1.50E-3 (7E-5)	1.65E-3 (5E-5)	1.60E-3 (8E-5)	1.50E-3 (8E-5)	1.48E-3 (5E-5)	1.40E-3 (8E-5)	1.40E-3 (1E-4)	1.34E-3 (2E-5)	1.36E-3 (8E-5)	1.49E-3 (6E-5)
DCAN	1.42E-1 (9E-4)	7.38E-2 (6E-3)	4.82E-2 (5E-3)	4.35E-2 (7E-3)	3.80E-2 (6E-3)	3.57E-2 (3E-3)	3.41E-2 (3E-3)	3.59E-2 (5E-3)	3.06E-2 (3E-3)	3.11E-2 (4E-3)	3.69E-2 (1E-3)
BCAN	3.26E-2 (5E-4)	1.98E-2 (1E-3)	2.01E-2 (2E-3)	1.94E-2 (2E-3)	1.82E-2 (3E-3)	1.81E-2 (2E-3)	1.82E-2 (1E-3)	1.94E-2 (2E-3)	1.86E-2 (2E-3)	1.92E-2 (2E-3)	2.36E-2 (1E-3)
DBAN	6.28E-3 (7E-5)	9.96E-3 (4E-4)	1.06E-2 (8E-4)	1.12E-2 (6E-4)	1.17E-2 (1E-3)	1.24E-2 (8E-4)	1.30E-2 (3E-4)	1.38E-2 (1E-3)	1.49E-2 (1E-3)	1.59E-2 (8E-4)	1.80E-2 (2E-3)
CH	1.70E-1 (4E-3)	3.60E-1 (1E-2)	1.19E-1 (7E-3)	1.05E-1 (1E-2)	8.94E-2 (1E-2)	7.79E-2 (3E-3)	7.41E-2 (2E-3)	7.80E-2 (1E-2)	6.25E-2 (4E-3)	6.36E-2 (8E-3)	6.76E-2 (3E-3)
TCNM	5.15E-3 (1E-4)	6.64E-2 (7E-4)	2.07E-2 (3E-3)	1.15E-2 (2E-3)	7.69E-3 (1E-3)	6.37E-3 (3E-4)	5.51E-3 (8E-4)	5.62E-3 (8E-4)	4.44E-3 (7E-4)	4.35E-3 (5E-4)	4.79E-3 (5E-4)
TBNM	2.15E-3 (1E-4)	1.04E-2 (2E-3)	1.12E-2 (3E-4)	1.06E-2 (5E-4)	1.04E-2 (1E-3)	1.04E-2 (8E-5)	1.09E-2 (3E-4)	1.17E-2 (8E-4)	1.25E-2 (6E-4)	1.37E-2 (2E-3)	1.58E-2 (2E-3)
DCP	1.19E-2 (9E-5)	1.79E-2 (3E-3)	1.16E-2 (1E-3)	9.46E-3 (1E-3)	8.45E-3 (1E-3)	8.72E-3 (4E-4)	8.08E-3 (7E-4)	7.40E-3 (9E-4)	7.33E-3 (5E-4)	7.18E-3 (1E-3)	6.95E-3 (9E-4)
TCP	1.31E-1 (2E-3)	2.27E-1 (5E-3)	9.03E-2 (5E-3)	8.19E-2 (7E-3)	7.19E-2 (8E-3)	6.51E-2 (2E-3)	6.20E-2 (2E-3)	6.45E-2 (4E-3)	5.32E-2 (5E-3)	5.25E-2 (6E-3)	5.23E-2 (2E-3)
TCAM	1.72E-2 (2E-4)	9.84E-3 (3E-4)	7.37E-3 (2E-4)	7.21E-3 (1E-3)	6.21E-3 (1E-3)	5.87E-3 (2E-4)	5.41E-3 (4E-4)	5.64E-3 (6E-4)	4.68E-3 (3E-4)	4.70E-3 (6E-4)	5.38E-3 (4E-4)
MCAA	1.36E-1	2.10E-1	6.81E-2 (5E-3)	n.a.	6.29E-2 (0E+0)	n.a.	5.24E-2 (0E+0)	n.a.	<5.00E-2	n.a.	<5.00E-2
MBAA	<4.00E-2	7.19E-2	<4.00E-2	n.a.	<4.00E-2	n.a.	<4.00E-2	n.a.	<4.00E-2	n.a.	<4.00E-2
DCAA	7.21E-1	6.28E-1	3.61E-1 (4E-3)	n.a.	3.06E-1 (1E-2)	n.a.	2.40E-1 (8E-3)	n.a.	2.21E-1 (1E-2)	n.a.	1.86E-1 (2E-2)
TCAA	6.73E-1	3.61E-1	3.15E-1 (9E-3)	n.a.	2.42E-1 (9E-3)	n.a.	1.71E-1 (0E+0)	n.a.	1.44E-1 (9E-3)	n.a.	1.19E-1 (3E-3)

DBP	No O_3	0 min	3 min	5 min	8 min	12 min	15 min	19 min	30 min	39 min	55 min
BCAA	1.79E-1	1.73E-1	1.44E-1 (0E+0)	n.a.	1.44E-1 (0E+0)	n.a.	1.27E-1 (0E+0)	n.a.	1.33E-1 (6E-3)	n.a.	1.24E-1 (3E-3)
BDCAA	1.68E-1	1.25E-1	1.80E-1 (7E-3)	n.a.	1.59E-1 (5E-3)	n.a.	1.25E-1 (5E-3)	n.a.	1.18E-1 (2E-3)	n.a.	1.06E-1 (1E-2)
DBAA	2.75E-2	6.88E-2	4.82E-2 (2E-3)	n.a.	5.28E-2 (2E-3)	n.a.	5.05E-2 (0E+0)	n.a.	5.74E-2 (2E-3)	n.a.	5.28E-2 (2E-3)
CDBAA	2.77E-2	2.77E-2	5.75E-2 (2E-3)	n.a.	5.75E-2 (2E-3)	n.a.	5.15E-2 (4E-3)	n.a.	5.75E-2 (2E-3)	n.a.	4.95E-2 (6E-3)
THM4	4.12E+0 (2E-1)	2.70E+0 (1E-2)	1.88E+0 (2E-1)	1.78E+0 (3E-1)	1.60E+0 (3E-1)	1.55E+0 (1E-1)	1.47E+0 (2E-1)	1.55E+0 (3E-1)	1.35E+0 (1E-1)	1.36E+0 (2E-1)	1.44E+0 (3E-2)
HAN4	1.83E-1 (1E-3)	1.05E-1 (7E-3)	8.05E-2 (7E-3)	7.56E-2 (9E-3)	6.93E-2 (1E-2)	6.77E-2 (6E-3)	6.67E-2 (4E-3)	7.05E-2 (8E-3)	6.55E-2 (6E-3)	6.76E-2 (8E-3)	8.00E-2 (3E-3)
THNM2	7.30E-3 (2E-5)	7.68E-2 (1E-3)	3.19E-2 (3E-3)	2.21E-2 (3E-3)	1.81E-2 (2E-3)	1.68E-2 (3E-4)	1.64E-2 (1E-3)	1.74E-2 (1E-3)	1.70E-2 (1E-3)	1.80E-2 (2E-3)	2.06E-2 (2E-3)
HK2	1.42E-1 (2E-3)	2.45E-1 (3E-3)	1.02E-1 (4E-3)	9.14E-2 (6E-3)	8.04E-2 (7E-3)	7.38E-2 (2E-3)	7.01E-2 (9E-4)	7.19E-2 (3E-3)	6.05E-2 (5E-3)	5.97E-2 (5E-3)	5.93E-2 (1E-3)
HAA8	1.93E+0	1.67E+0	1.17E+0 (7E-3)	n.a.	1.02E+0 (3E-2)	n.a.	8.18E-1 (3E-2)	n.a.	7.30E-1 (3E-2)	n.a.	6.38E-1 (4E-2)
AOX, as Cl-	3.69E+1 (0E+0)	2.64E+1 (2E+0)	2.17E+1 (1E+0)	1.97E+1 (1E+0)	1.79E+1 (1E+0)	1.69E+1 (9E-1)	1.62E+1 (1E+0)	1.52E+1 (1E+0)	1.31E+1 (1E+0)	1.31E+1 (8E-1)	1.25E+1 (1E+0)
DOC	15.1	13.9	11.3	11.1	10.8	10.9	10.4	10.4	9.90	9.80	9.80

n.a. = not available (not analysed for the specific condition)

6.4. Conclusions

Coupling ozonation with biological treatment was found to be beneficial for DBP control. In this study, we investigated the biodegradability of DBP precursors using batch biodegradation experiments with bioactive anthracite and column experiments with bioactive anthracite and BAC. The following conclusions from this study confirm previously published literature:

- Ozonation decreased the formation potentials of THM4, HAA8, HAN4, TCAM and increased formation potentials of THNM2, CH, and HK2 with subsequent chlorination.
- Compared to conditions that favor $^{\bullet}OH$ reactions (i.e., high H_2O_2 concentrations), O_3 reactions resulting from the lowest H_2O_2 concentrations led to lower formation potentials of the following DBPs: THM4, HAA8, CH, HK2, HAN4, TCAM, and AOX. The opposite was observed for THNM2.

The following novel conclusions can be drawn from this study:

- For the water sample tested, the increase in formation potentials of CH, HK2, and THNM2 after ozonation was effectively offset by biodegradation at typical contact times regardless of the initial concentration of precursors in the influent.
- The dynamics of removal of DOC and DBP formation potentials by biofiltration at different EBCTs followed first-order reaction kinetics with a plateau of residual biorecalcitrant concentration attained after approximately 10 – 20 min of EBCT. This study highlighted the importance of EBCT as a key design parameter for biofiltration. The experimentally determined rate constants may be useful in prediction of DBP formation potential reductions and determine the EBCT required to attain a target DBP concentration in the treated drinking water.
- The reduction in DBP formation potentials varied with respect to species, indicating the influence of DBP precursor structure and reactivity on biodegradability. The measured rate constants of DBP formation potential before reaching the steady-state concentration followed this order: CH > HK2 ≈ THNM2 > HAN4 > THM4> TCAM > HAA8.
- Due to the increase in bromide to DOC ratio after ozonation and biofiltration, the concentrations of bromine-containing DBPs (e.g., TBM, DBAN, TBNM) increased after these sequential treatments followed by chlorination. Thus, conditions promoting strong DOC removal such as longer EBCTs (e.g., > 20 min) can promote the formation of bromine-containing DBPs in bromide-containing waters. Treatment engineers should take this risk into account on a case-by-case basis.

Chapter 7

General Conclusions

This doctoral thesis aimed to develop an improved understanding of the fundamental processes that govern the fate of natural organic matter (NOM) as it undergoes ozonation (Chapter 4), ozonation with chlorination (Chapter 5), and ozonation/biofiltration with subsequent chlorination (Chapter 6). These processes were investigated successively (Figure 7.1) to determine the effect of ozone on each treatment step to provide useful insights for water treatment plants in improving their ozonation process. Dissolved organic nitrogen (DON) was also highlighted as it acts as precursor of potentially more toxic nitrogenous disinfection byproducts (N-DBPs) (e.g., halonitromethanes, haloacetonitriles, haloacetamides) compared to carbon-based DBP (C-DBPs). The N-DBP results were reported in conjunction with other DBP families including trihalomethanes, haloacetic acids, chloral hydrate, and haloketones. Several DBP groups were used to understand the impact of ozonation, biofiltration, and chlorination on a wide array of pollutants, with an ultimate aim of identifying critical points in water treatment that can be exploited for better DBP control. The following sections provide the conclusions, potential applications of results in water utilities, and other opportunities for future research.

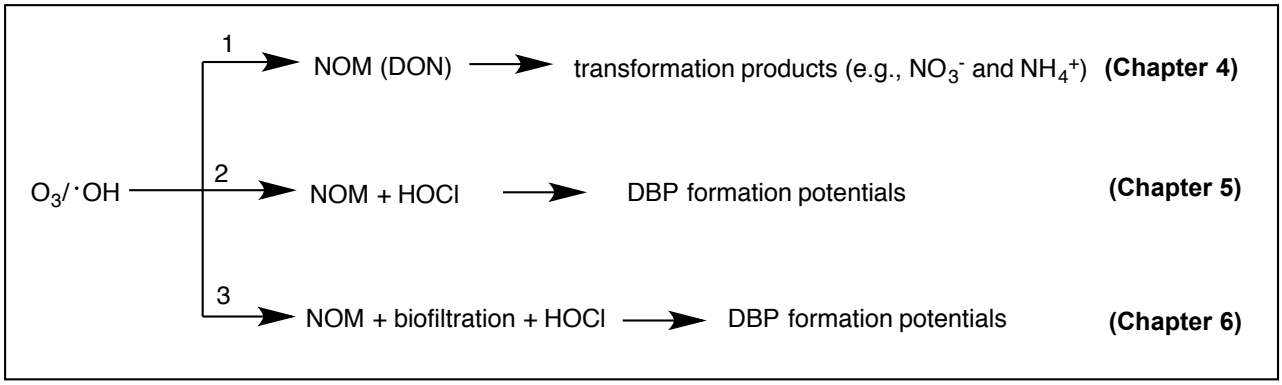

Figure 7.1. Processes investigated in this study

7.1. Conclusions and overall findings

Several conclusions about the reaction of ozone with NOM and subsequent DBP formation can be drawn from this study:

First, a fundamental understanding of the reaction of ozone with DON was achieved through experiments with real water samples, standard NOM sources, and model DON solutions (e.g., glycine). Ozonation of DON moieties showed formation of nitrate (NO_3^-) and ammonium (NH_4^+),

which are parameters that are quite easily accessible to water treatment operators for characterization of the ozonation process. It was observed that the formation of these inorganic nitrogen species is greatly influenced by the ozonation conditions, i.e., more NO_3^- and less NH_4^+ was formed when higher ozone doses were applied. Based on O_3 dosage experiments, kinetic studies, and hydroxyl radical ($^{\bullet}OH$) yield determinations (25%), this study provides evidence that NO_3^- is formed via amine nitrogen oxidation from oxygen transfer and NH_4^+ via electron-transfer reactions involving ozone. O_3 exposure also showed good correlation with NO_3^- formation, which could be essential in monitoring contributions of ozone and $^{\bullet}OH$ in oxidation reactions.

Second, treatment conditions that favor oxidation by ozone reactions (i.e., high ozone exposure) were found to be advantageous for DBP control. Modifying treatment conditions to promote O_3 decay consistently increased formation of all studied DBPs (e.g., trihalomethanes, haloacetic acids, haloacetonitriles, chloral hydrate, haloketones, trihaloacetamides, and bromate) except trihalonitromethanes. The results for AOX also followed the trend for the measured known DBPs. However, a higher percentage of unknown AOX was observed. Using *in vitro* bioassays, the associated toxic effects of the treated water samples were not very prominent.

Third, the combination of ozonation and biodegradation was effective in minimizing DBP formation potentials. Ozonated DBP precursors were reduced well during biofiltration, regardless of the ozonation conditions favoring either O_3 or $^{\bullet}OH$ reactions. The efficiently removed DBP precursors include those for trihalonitromethanes, chloral hydrate, and haloketones, all of which increased after ozonation. The reduction of DBP formation potentials was also found to follow first-order kinetics with respect to EBCT reaching a plateau of residual biorecalcitrant DBP precursors at 10 – 20 mins EBCT, depending on the DBP species. Highest rate of reduction was observed for trihalonitromethanes, chloral hydrate and haloketones, suggesting the high biodegradability of their precursors. The formation of bromine-containing DBPs, however, increased with increasing EBCT, most likely due to an increase in Br^-/DOC ratio.

To summarize, Table 7.1 presents the research highlights of this PhD thesis. The impacts and implications of these research findings on drinking water treatment plant operations are further discussed below.

Table 7.1. Research highlights of the PhD thesis

Chapter (system)	Research Highlights
Chapter 4 (DON + O_3)	• Ozonation of dissolved organic nitrogen forms NO_3^- and NH_4^+ • NO_3^- concentrations correlate with O_3 exposures • Lower O_3 doses cause higher NH_4^+ concentrations • Amine-N oxidation from oxygen transfer induces NO_3^- formation • NH_4^+ formation is induced from electron-transfer reactions involving ozone
Chapter 5 (NOM + O_3 + chlorine)	• Compared to $^{\bullet}OH$, oxidation by O_3 led to less C-DBPs and AOX formation potential • Haloacetonitriles and haloacetamides showed opposite trends to halonitromethane formation when modifying $O_3/^{\bullet}OH$ ratio • 4 bioassay tests showed low differences in toxicity between different $O_3/^{\bullet}OH$ exposures
Chapter 6 (NOM + O_3 + biofilter + chlorine)	• Biofiltration reduces DBP FP with 1st-order dependence on filter contact time • NOM removal by biofiltration increases Br substitution in subsequent disinfection • Combined O_3 + biofiltration (EBCT: 10 – 20 min) effectively controlled DBP formation • DBP precursor removal by BAC was highest for CH, THNM2, and HK2 • Biofiltration attenuates effects of varying O_3 exposures on DBP formation

7.2. Revisiting the research hypotheses

1. *The transformation products that give rise from the reaction of ozone with the DON fraction of NOM can be used to characterize the ozonation process.*

It was clearly demonstrated in Chapter 4 that ozonation of DON resulted in formation of inorganic nitrogen, NO_3^- and NH_4^+, which are easily measurable in water treatment plants. The NO_3^- formation was found to be sensitive to changes in ozonation conditions for every water sample investigated including surface, wastewater effluent, and model NOM solutions. For all the applied conditions, it was consistently observed that NO_3^- increases with increasing O_3 doses and exposures ($R^2 \geq 0.82$). Formation of NH_4^+, on the other hand, was found to decrease with higher ozone doses. These relationships could be used to characterize the ozonation process and to predict the desired O_3 exposure required for a target disinfection credit or removal of DBP precursors.

2. *Oxidation of NOM by ozone and/or hydroxyl radicals during ozonation will have different effects on NOM properties and subsequent reactivity with chlorine and DBP formation.*

The reaction of ozone and $^{\bullet}OH$ resulted in different effects on NOM properties and DBP formation potentials (Chapter 5). Lower specific UV absorbance and fluorescence intensities at the humic/fulvic acid-like regions were observed at conditions of higher ozone exposures. Compared to $^{\bullet}OH$, ozone-dominated reactions resulted in lower DBP formation potentials of trihalomethanes, haloacetic acids, chloral hydrate, haloketones, haloacetonitriles, haloacetamides, and AOX which proves that $^{\bullet}OH$-transformed organic matter is more susceptible to halogen incorporation. The opposite trend for trihalonitromethanes was observed indicating that intermediates from ozone reactions (not $^{\bullet}OH$ reactions) promote halonitromethane formation.

3. *Variations in ozone and hydroxyl radical exposure will impact the performance of biological filtration and thereby the final water quality. Provided that a target water quality is defined, it will be possible to optimize the oxidation process and biological filtration towards that outcome.*

The variations in ozone and $^{\bullet}OH$ exposure were found to be significant when followed directly by post-chlorination (i.e., higher DBP formation potentials formed with $^{\bullet}OH$-dominated reactions). However, different oxidant exposures seemed not to cause substantial impact on biodegradability of DBP precursors. In this study, it was shown that DBP formation potentials can be reduced well (even the DBPs that increased after ozonation like trihalonitromethanes, chloral hydrate, and haloketones) regardless of the effect of O_3 and $^{\bullet}OH$ reactions as long as biofiltration uses sufficient EBCT (~ 10 – 20 min) (Chapter 6). The biofiltration process can also be optimized by manipulating the EBCT, which was highlighted as a key design parameter for biofiltration. Since the reduction of DBP

formation potentials in the biofilters showed a first-order dependence on EBCT, it could be possible to predict the removal of DBP precursors based on the kinetic results.

7.3. Practical applications and recommendations to drinking water utilities

The research outcomes of this PhD thesis provide significant contributions to the field of drinking water treatment, particularly in controlling formation of chlorination DBPs using ozonation and biofiltration. The results could have potential applications at different points (shown in arrows) in drinking water treatment plants (Figure 7.2).

Ozone exposures can be adjusted at Points 1 and 2 of Figure 7.2. Point 1 refers to pH adjustment which could be by addition of lime, CO_2, or NaOH and Point 2 is where ozone is added for oxidation purposes. Since the results from Chapter 5 showed that minimal DBP formation could be at conditions that favor ozone reactions (except for halonitromethanes), these points can be exploited to adjust the ozone exposure by varying the pH and the specific O_3 dose. Lowering the pH at Point 1 in tandem with the pH effects during coagulation may result in better reductions of DBP formation potentials compared to conditions at higher pH. However, a drawback of this approach would be addition of more reagents prior to distribution to bring the pH back to neutral. Carbonate alkalinity could also be increased at Point 1 to have a higher ozone exposure, although this may be disadvantageous for bromide-rich waters because of bromate formation (Figure 5.11). These tradeoffs can be site-specific and can therefore be addressed with prior source water characterization.

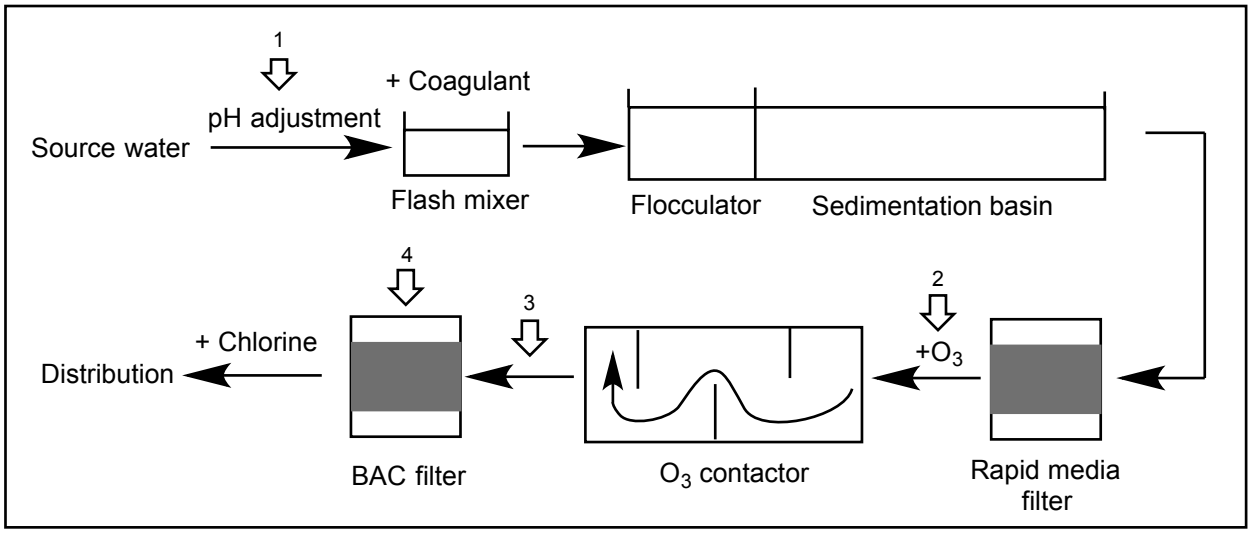

Figure 7.2. Engineering schematic of a drinking water treatment plant and points of potential applications of the thesis results

It was also shown that increasing ozone doses resulted in a mixture of effects caused by O_3 and $^{\bullet}OH$ reactions. DBP formation potentials first decreased at the initial O_3 dose (0.4 mg O_3/mg DOC) but increased at higher doses due to the contribution of $^{\bullet}OH$ in organic matter oxidation. From these results, together with those observed at different ozonation pH, the study showed that ozonation at lower doses and pH may be necessary for better control of formation of C-DBPs, N-DBPs, AOX, and bromate in ozonation plants. These operational adjustments should be made while maintaining a target CT to ensure that disinfection will not be compromised.

Ozone exposures, which are not only relevant for DBP control (Chapter 5) but also for assessment of disinfection efficiency, could be constantly monitored by measuring inorganic nitrogen (NO_3^- and NH_4^+). Since a strong correlation was found between NO_3^- and O_3 exposure (Chapter 4), water utilities could monitor NO_3^- concentrations at Point 3 (Figure 7.2) to verify the prevalent reaction mechanisms taking place in ozone contactors and to evaluate if their treatment plant achieves the required O_3 exposure for disinfection or oxidation of micropollutants and DBP precursors. This can be attained by initial calibrations of the ozone exposure with NO_3^- formation (see Figure 4.9). This approach might be applicable to a wide range of conditions as the direct correlation of NO_3^- with O_3 exposures shows for various types of water samples and treatment conditions (R_{ct}s = 10^{-10}–10^{-7}). Thus, NO_3^- could be a valuable parameter to signal water treatment operators of possible water quality changes occurring at the source water (e.g., varying DON concentrations). For example, waters showing a decrease in NO_3^- concentration despite having the same ozonation conditions could indicate having lower O_3 exposures and that higher ozone doses might be needed to reach the target disinfection credit. Thus, NO_3^- measurements after the ozone contactor may be useful to complement the monitoring tools currently applied in water treatment to assess O_3 exposure. However, this new concept has some limitations related to the analytical determination of the formation of NO_3^- and/or NH_4^+. Prior source water characterization is also needed before applying this approach as monitoring formation of inorganic nitrogen is a challenge with waters having very high background inorganic nitrogen or very low DON concentrations.

Following ozonation would be biofiltration (Point 4, Figure 7.2). To improve biofiltration, EBCT could be optimized by water treatment operators. For the experimental conditions used, an EBCT of 10 – 20 min following ozonation ensured near maximum possible removal of DBP precursors in biofilters including those for regulated DBPs such as trihalomethanes and those that increased after ozonation (e.g., chloral hydrate, haloketones, trihalonitromethanes). However, it was also observed that brominated DBPs, which are relatively more toxic than chlorinated DBPs, increased after biofiltration, with a much higher increase at longer EBCTs. Thus, treatment engineers should take this into account especially when dealing with waters containing high bromide concentrations. In

addition, the observed first-order removal kinetics of DBP precursors before reaching a plateau of residual biorecalcitrant concentration could also be used to predict reductions in DBP formation potentials and determine the EBCT required to attain low DBP concentrations in the treated water. The needed EBCT for DBP precursor removal, however, should also be considered along with the cost associated with increasing the EBCT (e.g., larger filters). Shorter EBCTs may potentially be used when biofiltration is combined with enhanced pretreatment processes. For example, if coagulation is performed to sufficiently remove DBP precursors, biofilter contact time could be shortened since bulk of the precursors is already removed during this pretreatment. Optimization of the filter characteristics versus NOM/DBP precursor removal requirement is therefore necessary to arrive at cost-effective solutions involving biofiltration.

7.4. Opportunities for future research

The results of this thesis also gave rise to a number of opportunities for future studies. These include the following:

1. *NO_3^- measurement as surrogate parameter for disinfection efficiency and micropollutant removal during ozonation*

It was demonstrated in Chapter 4 that NO_3^- formation has a direct correlation with O_3 exposure. In a follow-up test using a South East Queensland water, it was observed that the NO_3^- formation in lab-scale studies was relatively close to those measured before and after full-scale drinking water ozonation (Table 7.2). Consistent with the thesis results, NO_3^- levels in the full-scale plant also increased after ozonation. This shows that NO_3^- monitoring might be feasible in this water treatment plant. In applying this concept, however, it is important to know the properties of the source water (i.e., in terms of DON and background NO_3^-) to determine whether NO_3^- formation can be reliably measured. As O_3 exposure (CT value) in water treatment plants is constantly measured to assess inactivation of microorganisms (e.g., *C. parvum* oocysts), it would be worth exploring if NO_3^- concentrations would be an appropriate surrogate parameter for log removals of microorganisms. This approach may also be useful in predicting the abatement of micropollutants. Previous studies have shown that micropollutant elimination could be predicted from the R_{ct} of an ozonation process (Elovitz and von Gunten 1999). For water samples whose R_{ct}s are mainly dominated by changes in O_3 exposure (e.g., at relatively constant $^{\bullet}OH$ exposure), it would be possible to relate the changes in NO_3^- concentrations with the R_{ct}.

Table 7.2. Comparison of NO_3^- concentrations measured before and after pre- and intermediate-ozonation in full-scale plant and lab-scale experiment. *Conditions: pre-ozone dose = 2.1 mg/L, pH=7.4, intermediate ozone dose = 0.5 mg/L, pH = 6.8, DOC = 4.5 mg/L, DON = 0.2 mg/L*[*]

Sampling points	NO_3^--N, µg/L	
	Laboratory	Full-scale
Before pre-O_3	Same as full-scale	13.5 ± 0.5
After pre-O_3	23.7 ± 0.7	24.9 ± 0.6
Before inter-O_3	Same as full-scale	69.9 ± 0.5
After inter-O_3	73.4 ± 0.9	77.4± 0.1

[*] *± standard deviation of 3 measurements*

2. Understanding the reactions of DON intermediates during ozonation

In the kinetic simulations of glycine ozonation (Section 4.3.8), the rate constant of the reaction of *N*-centered radicals and ozone was assumed based on the experimental NO_3^- and NH_4^+ concentrations. Thus, further investigations are necessary to confirm the assigned rate constants along with verification of intermediates formed during ozonation of DON. In addition, about 25% $^{\bullet}OH$ yield was determined for the reaction of glycine and ozone, but data on $^{\bullet}OH$ yields for other aliphatic amines are lacking in the literature. These rate constants and $^{\bullet}OH$ yields are essential for a better understanding of electron-transfer reactions during ozonation of amines. Moreover, with oxygen transfer reactions, intermediates such as hydroxylamines are formed which could be essential for the formation of N-DBPs like halonitromethanes. Evaluating NO_3^- concentrations might provide useful insights in the formation of halonitromethanes as well as removal of haloacetonitriles.

3. Surrogate measurements for NOM reactivity and DBP formation

This study also highlighted that DBP formation varies depending on the reactivity of NOM. For example, lower DBP formation was found after pre-ozonation, and chlorine demand was higher for waters treated at conditions favoring O_3 decay. It is worth studying if the reactivity of the water samples towards oxidants can be predicted. On-going work is being conducted for rapid measurement of NOM reactivity in terms of its electron donating capacity (EDC) using an electrochemical approach developed by Aeschbacher et al. (2010). In this study, model compounds namely resorcinol, tannic acid, vanillin, and cysteine were used to represent the reactive moieties of complex DOM mixtures. The EDC was determined by mediated electrochemical oxidation (MEO) which involves the use of 2,2′-azino-bis(3-ethylbenzthiazoline-6-sulfonic acid) (ABTS) as an electron shuttle. The

Cl_2 demand of these readily oxidizable compounds (resorcinol, tannic acid, vanillin, and cysteine) was found to correlate well with EDC (R^2 = 0.98) which could potentially be used in predicting chlorine demand of water samples (Figure 7.3a) (de Vera et al. 2017). After ozonation (Figure 7.3b), the UV absorbance, EDC, and chlorine demand of resorcinol and tannic acid also decreased at a relatively the same extent due to ring opening mechanisms of the phenolic groups.

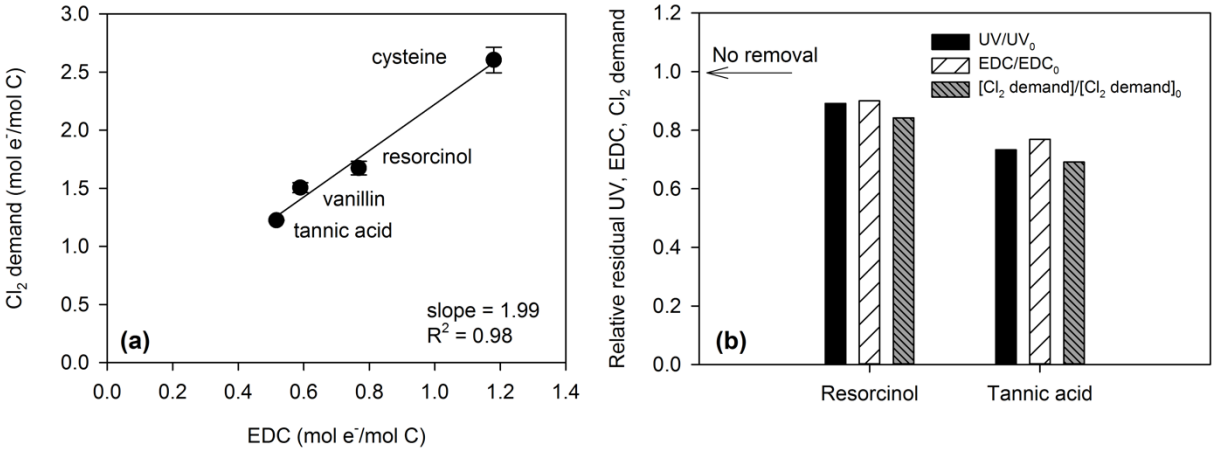

Figure 7.3. (a) Linear relationship of chlorine demand with electron-donating capacity (EDC) of tannic acid, vanillin, resorcinol, and cysteine (b) Relative residual UV absorbance (at 220 nm for recorcinol, 278 nm for tannic acid), EDC, and chlorine demand of resorcinol and tannic acid (3.2 mM DOC) after ozonation (0.1 mol O_3/mol DOC) at pH 7 (de Vera et al. 2017).

4. Measures to prevent brominated DBP formation during O_3/BAC

As demonstrated in this study, one of the drawbacks of ozone and BAC treatment is the increase in brominated DBP formation potentials (e.g., bromoform, tribromonitromethane, dibromoacetonitrile, chlorodibromoacetic acid) which are potentially more toxic than chlorinated DBPs (Section 2.4). For ozonation, this is due to the formation of hydrophilic NOM fractions which are more amenable for bromine reactions, while for biofiltration, this is due to the increase in bromide/DOC ratio. Further toxicity tests would therefore be of interest to assess the impact of Br-DBP increase in the overall effect of O_3/BAC treatment. More importantly, measures to minimize bromide prior to oxidation should be investigated. Previous studies reported the use of ion exchange resins, membranes, silver-impregnated activated carbon and aerogels, electrochemical processes (e.g., electrodialysis reversal), among others, to remove halide ions in drinking water sources (Watson et al. 2012). Thus, these processes could be further optimized and developed (e.g. into hybrid/combined systems) for efficient removal of bromide, and consequently Br-DBPs.

5. DBP precursor removal through the GAC-BAC filter lifetime

In this study, the filter media used for biofiltration have been in operation for more than 2 years, minimizing the role of adsorption in DBP precursor removal. Water treatment plants, however, occasionally replace portions of their BAC filters with new GAC, while some retrofits their existing processes to incorporate a GAC filter. These changes make adsorption an important NOM removal mechanism. It is worth exploring to differentiate the effects of adsorption and biodegradation on the removal of DBP precursors from GAC, to saturation of adsorption sites, until the filter becomes biological (Simpson 2008). Preliminary results in our group shows that biodegradation constantly removes about 40% of THM precursors, and adsorption provides an additional 40% removal (i.e., only at the beginning of GAC operation) (Doederer et al. 2016). Since DBP precursors have different physicochemical properties (e.g., aromaticity, functional groups, size, solubility, charge), precursor removal by adsorption of other DBPs could also be different.

In addition, during extended BAC filtration periods, leaching of soluble microbial products (SMPs) containing N-DBP precursors is possible. This could be due to detachment of dead bacteria from the biofilm matrix and/or degradation of extracellular polymeric substances (EPS) over time. These SMPs were thought to have contributed in haloacetonitrile formation in batch biodegradations tests in Section 6.3.1.2. Future studies are needed to identify the factors affecting biofilm integrity, EPS formation, as well as SMP release, and determine how these factors affect DBP formation during effluent chlorination. Such studies may involve examining the interplay of substrate utilization rate, accumulated biomass (e.g., concentration, thickness, composition), and hydraulic action (e.g., backwashing regimes), among others. Media type and surface characteristics as well as influent water quality (e.g., nutrient (C/N/P) content) may also play a significant part in the release of potential SMP-derived DBP precursors.

References

Abramovitch, S. and Rabani, J. (1976) Pulse radiolytic investigations of peroxyl radicals in aqueous solutions of acetate and glycine. J. Phys. Chem. 80(14), 1562-1565.

Acero, J.L. and von Gunten, U. (2001) Characterization of oxidation processes: Ozonation and the AOP O_3/H_2O_2. J. Am. Water Works Assoc. 93(10), 90-100.

ACS (2017) Key statistics for bladder cancer. American Cancer Society. Available at http://www.cancer.org/cancer/bladder-cancer/about/key-statistics.html.

Aeschbacher, M., Graf, C., Schwarzenbach, R.P. and Sander, M. (2012) Antioxidant properties of humic substances. Environ. Sci. Technol. 46(9), 4916-4925.

Aeschbacher, M., Sander, M. and Schwarzenbach, R.P. (2010) Novel electrochemical approach to assess the redox properties of humic substances. Environ. Sci. Technol. 44(1), 87-93.

Ahmad, R., Amirtharajah, A., Al-Shawwa, A. and Huck, P.M. (1998) Effects of backwashing on biological filters. J. Am. Water Works Assoc. 90(12), 62-73.

Akcay, M.U., Avdan, Z.Y. and Inan, H. (2015) Effect of biofiltration process on the control of THMs and HAAs in drinking water. Desalin. Water Treat. 57(6), 2546-2554.

Aktas, O. and Cecen, F. (2007) Bioregeneration of activated carbon: A review. Int. Biodeter. Biodegr. 59(4), 257-272.

Allard, S., Nottle, C.E., Chan, A., Joll, C. and von Gunten, U. (2013) Ozonation of iodide-containing waters: selective oxidation of iodide to iodate with simultaneous minimization of bromate and I-THMs. Water Res. 47(6), 1953-1960.

Allard, S., Tan, J., Joll, C.A. and von Gunten, U. (2015) Mechanistic study on the formation of Cl-/Br-/I-trihalomethanes during chlorination/chloramination combined with a theoretical cytotoxicity evaluation. Environ. Sci. Technol. 49(18), 11105-11114.

Allpike, B.P., Heitz, A., Joll, C.A., Kagi, R.I., Abbt-Braun, G., Frimmel, F.H., Brinkmann, T., Her, N. and Amy, G. (2005) Size exclusion chromatography to characterize DOC removal in drinking water treatment. Environ. Sci. Technol. 39(7), 2334-2342.

APHA, AWWA and WEF (1999) Standard methods for the examination of water and wastewater.

Aslam, Z., Chow, C.W.K., Murshed, F., van Leeuwen, J.A., Drikas, M. and Wang, D. (2013) Variation in character and treatability of organics in river water: An assessment by HPAC and alum coagulation. Sep. Purif. Technol. 120, 162-171.

Ates, N., Kitis, M. and Yetis, U. (2007) Formation of chlorination by-products in waters with low SUVA-correlations with SUVA and differential UV spectroscopy. Water Res. 41(18), 4139-4148.

Bader, H. and Hoigné, J. (1981) Determination of ozone in water by the indigo method. Water Res. 15(4), 449-456.

Bader, H., Sturzengger, V. and Hoigné, J. (1988) Photometric method for the determination of low concentrations of hydrogen peroxide by the peroxidase catalyzed oxidation of N,N-diethyl-p-phenylenediamine (DPD). Water Res. 22(9), 1109-1115.

Baghoth, S.A., Sharma, S.K. and Amy, G.L. (2011) Tracking natural organic matter (NOM) in a drinking water treatment plant using fluorescence excitation-emission matrices and PARAFAC. Water Res 45(2), 797-809.

Bell, K., LeChevallier, M., Abbaszadegan, M., Amy, G., Sinha, S., Benjamin, M. and Ibrahim, E. (1998) Enhanced and optimized coagulation for particulate and microbial removal. AWWA Research Foundation, American Water Works Association, CO, U.S.A.

Benner, J. and Ternes, T.A. (2009) Ozonation of propranolol: formation of oxidation products. Environ. Sci. Technol. 43(13), 5086-5093.

Berger, P., Karpel Vel Leitner, N., Dore, M. and Legube, B. (1999) Ozone and hydroxyl radicals induced oxidation of glycine. Water Res. 33(2), 433-441.

Bichsel, Y. and von Gunten, U. (2000) Formation of iodo-trihalomethanes during disinfection and oxidation of iodide-containing waters. Environ. Sci. Technol. 34(13), 2784-2791.

Bieroza, M.Z., Bridgeman, J. and Baker, A. (2010) Fluorescence spectroscopy as a tool for determination of organic matter removal efficiency at water treatment works. Drink. Water Eng. Sci. 3(1), 63-70.

Black, K.E. and Berube, P.R. (2014) Rate and extent NOM removal during oxidation and biofiltration. Water Res. 52, 40-50.

Bond, T., Goslan, E.H., Jefferson, B., Roddick, F., Fan, L. and Parsons, S.A. (2009a) Chemical and biological oxidation of NOM surrogates and effect on HAA formation. Water Res. 43(10), 2615-2622.

Bond, T., Goslan, E.H., Parsons, S.A. and Jefferson, B. (2012) A critical review of trihalomethane and haloacetic acid formation from natural organic matter surrogates. Environ. Technol. Rev. 1(1), 93-113.

Bond, T., Goslan, E.H., Parsons, S.A. and Jefferson, B. (2011a) Treatment of disinfection by-product precursors. Environ. Technol. 32(1-2), 1-25.

Bond, T., Henriet, O., Goslan, E.H., Parsons, S.A. and Jefferson, B. (2009b) Disinfection byproduct formation and fractionation behavior of natural organic matter surrogates. Environ. Sci. Technol. 43(15), 5982-5989.

Bond, T., Huang, J., Templeton, M.R. and Graham, N. (2011b) Occurrence and control of nitrogenous disinfection by-products in drinking water--a review. Water Res. 45(15), 4341-4354.

Bond, T., Templeton, M.R., Rifai, O., Ali, H. and Graham, N.J. (2014) Chlorinated and nitrogenous disinfection by-product formation from ozonation and post-chlorination of natural organic matter surrogates. Chemosphere 111, 218-224.

Bonifacic, M., Stefanic, I., Hug, G.L., Armstrong, D.A. and Asmus, K.-D. (1998) Glycine decarboxylation: the free radical mechanism. J. Am. Chem. Soc. 120(38), 9930-9940.

Bove, G.E., Jr., Rogerson, P.A. and Vena, J.E. (2007a) Case control study of the geographic variability of exposure to disinfectant byproducts and risk for rectal cancer. Int. J. Health Geogr. 6(18), 18.

Bove, G.E., Rogerson, P.A. and Vena, J.E. (2007b) Case-control study of the effects of trihalomethanes on urinary bladder cancer risk. Arch. Environ. Occup. Health 62(1), 39-47.

Boyer, T.H., Singer, P.C. and Aiken, G.R. (2008) Removal of dissolved organic matter by anion exchange: effect of dissolved organic matter properties. Environ. Sci. Technol. 42(19), 7431-7437.

Buffle, M.O., Schumacher, J., Salhi, E., Jekel, M. and von Gunten, U. (2006) Measurement of the initial phase of ozone decomposition in water and wastewater by means of a continuous quench-flow system: application to disinfection and pharmaceutical oxidation. Water Res. 40(9), 1884-1894.

Buxton, G.V., Greenstock, C.L., Helman, W.P. and Ross, A.B. (1988) Critical review of rate constants for reactions of hydrated electrons, hydrogen atoms, and hydroxyl radicals (•OH/•O$^-$) in aqueous solution. J. Phys. Chem. Ref. Data 17(2), 513-886.

Cantor, K.P. (2010) Carcinogens in drinking water: The epidemiologic evidence. Rev. Environ. Health 25(1), 9-16.

Cantor, K.P., Villanueva, C., Garcia-Closas, M., Silverman, D., Real, F.X., Dosemeci, M., Malats, N., Yeager, M., Welch, R., Chanock, S., Tardon, A., Garcia-Closas, R., Serra, C., Carrato, A., Castano-Vinyals, G., Samanic, C., Rothman, N. and Kogevinas, M. (2006) Bladder cancer, disinfection byproducts, and markers of genetic susceptibility in a case–control study from Spain. Epidemiology 17((6) Suppl), S150.

Carlson, K.H. and Amy, G.L. (1998) BOM removal during biofiltration. J. Am. Water Works Assoc. 90(12), 42-52.

Chaiket, T., Singer, P.C., Miles, A., Moran, M. and Pallotta, C. (2002) Effectiveness of coagulation, ozonation, and biofiltration in controlling DBPs. J. Am. Water Works Assoc. 94(12), 81-95.

Chen, C., Zhang, X., He, W., Lu, W. and Han, H. (2007) Comparison of seven kinds of drinking water treatment processes to enhance organic material removal: a pilot test. Sci. Total Environ. 382(1), 93-102.

Chen, K.-C., Wang, Y.-H. and Chang, Y.-H. (2009) Using catalytic ozonation and biofiltration to decrease the formation of disinfection by-products. Desalination 249(3), 929-935.

Chen, Q., Westerhoff, P., Leenheer, J.A. and Booksh, K. (2003) Fluorescence excitation-emission matrix regional integration to quantify spectra for dissolved organic matter. Environ. Sci. Technol. 37(24), 5701-5710.

Cho, M., Kim, J., Kim, J.Y., Yoon, J. and Kim, J.H. (2010) Mechanisms of Escherichia coli inactivation by several disinfectants. Water Res. 44(11), 3410-3418.

Cho, M., Kim, J.H. and Yoon, J. (2006) Investigating synergism during sequential inactivation of *Bacillus subtilis* spores with several disinfectants. Water Res. 40(15), 2911-2920.

Chon, K., Lee, Y., Traber, J. and von Gunten, U. (2013) Quantification and characterization of dissolved organic nitrogen in wastewater effluents by electrodialysis treatment followed by size-exclusion chromatography with nitrogen detection. Water Res. 47(14), 5381-5391.

Chon, K., Salhi, E. and von Gunten, U. (2015) Combination of UV absorbance and electron donating capacity to assess degradation of micropollutants and formation of bromate during ozonation of wastewater effluents. Water Res. 81, 388-397.

Chu, W., Gao, N., Yin, D., Deng, Y. and Templeton, M.R. (2012) Ozone-biological activated carbon integrated treatment for removal of precursors of halogenated nitrogenous disinfection by-products. Chemosphere 86(11), 1087-1091.

Criegee, R. (1975) Mechanism of ozonolysis. Angew Chem 14(11), 745-752.

Croué, J.P., Korshin, G.V. and Benjamin, M. (2000) Characterization of natural organic matter in drinking water. AWWA Research Foundation, CO, USA. ISBN: 1-58321-015-6.

de Vera, G.A., Gernjak, W. and Radjenovic, J. (2017) Predicting reactivity of model DOM compounds towards chlorine with mediated electrochemical oxidation. Water Res. 114, 113-121.

de Vera, G.A., Stalter, D., Gernjak, W., Weinberg, H.S., Keller, J. and Farre, M.J. (2015) Towards reducing DBP formation potential of drinking water by favouring direct ozone over hydroxyl radical reactions during ozonation. Water Res. 87, 49-58.

Deborde, M. and von Gunten, U. (2008) Reactions of chlorine with inorganic and organic compounds during water treatment-Kinetics and mechanisms: a critical review. Water Res. 42(1-2), 13-51.

Delpla, I., Jung, A.V., Baures, E., Clement, M. and Thomas, O. (2009) Impacts of climate change on surface water quality in relation to drinking water production. Environ. Int. 35(8), 1225-1233.

Dickenson, E.R., Summers, R.S., Croué, J.P. and Gallard, H. (2008) Haloacetic acid and trihalomethane formation from the chlorination and bromination of aliphatic B-dicarbonyl acid model compounds. Environ. Sci. Technol. 42(9), 3226-3233.

Diehl, A.C., Speitel, G.E., Symons, J.M., Krasner, S.W., Hwang, C.J. and Barrett, S.E. (2000) DBP formation during chloramination. J. Am. Water Works Ass. 92(6), 76-90.

DiGiano, F.A., Singer, P.C., Parameswar, C. and Lecourt, T. (2001) Biodegradation kinetics of ozonated NOM and aldehydes. J. Am. Water Works Assoc. 93(8), 92-104.

Dodds, L., King, W., Allen, A.C., Armson, B.A., Fell, D.B. and Nimrod, C. (2004) Trihalomethanes in public water supplies and risk of stillbirth. Epidemiology 15(2), 179-186.

Doederer, K., de Vera, G.A., Espino, M.P.B. and Keller, J. (2016) Evaluation of BAC life extension during biofiltration of ozonated waters. Manuscript in preparation for submission.

Doederer, K., Gernjak, W., Weinberg, H.S. and Farre, M.J. (2014) Factors affecting the formation of disinfection by-products during chlorination and chloramination of secondary effluent for the production of high quality recycled water. Water Res. 48, 218-228.

Domino, M.M., Pepich, B.V., Munch, D.J., Fair, P.S. and Xie, Y. (2003) US EPA Method 552.3. Determination of haloacetic acids and dalapon in drinking water by liquid-liquid microextraction, derivatization, and gas chromatography with electron capture detection. EPA 815-B-03-002. US EPA, Cincinnati, OH, USA.

Doyle, T.J., Zheng, W., Cerhan, J.R., Hong, C.-P., Sellers, T.A., Kushi, L.H. and Folsom, A.R. (1997) The association of drinking water source and chlorination by-products with cancer incidence among postmenopausal women in Iowa: A prospective cohort study. Am. J. Public Health 87(7), 1168-1176.

Edzwald, J.K. (1993) Coagulation in drinking water treatment: particles, organics and coagulants. Water Sci. Technol. 27(11), 21-35.

Edzwald, J.K. (2010) Water quality and treatment - A handbook on drinking water, 6th ed. American Water Works Association, McGraw-Hill, CO, U.S.A.

Edzwald, J.K., Becker, W.C. and Wattier, K.L. (1985) Surrogate parameters for monitoring organic matter and THM precursors. J. Am. Water Works Assoc. 77(4), 122-132.

Elmghari-Tabib, M., Laplanche, A., Venien, F. and Martin, G. (1982) Ozonation of amines in aqueous solutions. Water Res. 16(2), 223-229.

Elovitz, M.S. and von Gunten, U. (1999) Hydroxyl radical/ozone ratios during ozonation processes. I. the Rct concept. Ozone Sci. Eng. 21(3), 239-260.

Elovitz, M.S., von Gunten, U. and Kaiser, H.-P. (2000a) Hydroxyl radical/ozone ratios during ozonation processes. II. the effect of temperature, pH, alkalinity, and DOM properties. Ozone Sci. Eng. 22(2), 123-150.

Elovitz, M.S., von Gunten, U. and Kaiser, H.-P. (2000b) The influence of dissolved organic matter character on ozone decomposition rates and Rct. In Natural Organic Matter and Disinfection By-Products; Barrett, S., et al.; ACS Symposium Series; American Chemical Society: Washignton, DC., 248-269.

Emelko, M.B., Huck, P.M., Coffey, B.M. and Smith, E.F. (2006) Effects of meia, backwash, and temperature on full-scale biological filtration. J. Am. Water Works Assoc. 98(12), 61-73.

Escher, B.I., Dutt, M., Maylin, E., Tang, J.Y., Toze, S., Wolf, C.R. and Lang, M. (2012) Water quality assessment using the AREc32 reporter gene assay indicative of the oxidative stress response pathway. J. Environ. Monit. 14(11), 2877-2885.

Escobar, I.C. and Randall, A.A. (2001) Assimilable organic carbon (AOC) and biodegradable dissolved organic carbon (BDOC): complementary measurements. Water Res 35(18), 4444-4454.

Evans, P.J., Smith, J.L., LeChevallier, M.W., Schneider, O.D., Weinrich, L.A. and Jjemba, P.K. (2013) Biological filtration monitoring and control toolbox: Guidance manual. Water Research Foundation, CO, USA.

Farré, M.J., Day, S., Neale, P.A., Stalter, D., Tang, J.Y. and Escher, B.I. (2013) Bioanalytical and chemical assessment of the disinfection by-product formation potential: role of organic matter. Water Res. 47(14), 5409-5421.

Farré, M.J., de Vera, G.A., Lyon, B.A., Doederer, K., Weinberg, H.S., Gernjak, W. and Keller, J. (2016a) Engineering solutions to minimize nitrogen-containing DBPs. Water Research Foundation, CO, USA. Available at http://www.waterrf.org/Pages/Projects.aspx?PID=4484.

Farré, M.J. and Knight, N. (2012) Assessment of regulated and emerging disinfection by-products in South East Queensland drinking water. Urban Water Security Research Alliance Technical Report No. 90.

Farré, M.J., Lyon, B., de Vera, G.A., Stalter, D. and Gernjak, W. (2016b) Assessing adsorbable organic halogen formation and precursor removal during drinking water production. J. Environ. Eng.-ASCE 142(3), 04015087.

Farré, M.J., Reungoat, J., Argaud, F.X., Rattier, M., Keller, J. and Gernjak, W. (2011) Fate of N-nitrosodimethylamine, trihalomethane and haloacetic acid precursors in tertiary treatment including biofiltration. Water Res. 45(17), 5695-5704.

Flyunt, R., Leitzke, A., Mark, G., Mvula, E., Reisz, E., Schick, R. and von Sonntag, C. (2003) Determination of $^{\bullet}OH$, $O_2^{\bullet-}$, and hydroperoxide yields in ozone reactions in aqueous solution. J. Phys. Chem. B 107(30), 7242-7253.

Gagnon, G.A., Booth, S.D.J., Peldszus, S., Mutti, D., Smith, F. and Huck, P.M. (1997) Carboxylic acids: formation and removal in full-scale plants. J. Am. Water Works Assoc. 89(8), 88-97.

Gagnon, G.A. and Huck, P.M. (2001) Removal of easily biodegradable organic compounds by drinking water biofilms: analysis of kinetics and mass transfer. Water Res. 35(10), 2254-2564.

Gallard, H. and von Gunten, U. (2002) Chlorination of natural organic matter: kinetics of chlorination and of THM formation. Water Res. 36(1), 65-74.

Gao, J., Ellis, L.B.M. and Wacket, L.P. (2010) The University of Minnesota biocatalysis/biodegradation database: improving public access. Nucleic Acids Res. 38(Database issue), D488-D491.

Gillogly, T., Najm, I., Minear, R., Marinas, B., Urban, M., Kim, J.H., Echigo, S., Amy, G., Douville, C., Daw, B., Andrews, R., Hofmann, R. and Croué, J.-P. (2001) Bromate formation and control during ozonation of low bromide waters. AWWA Research Foundation, CO, USA. ISBN: 1-58321-155-1.

Gjessing, E.T., Egeberg, P.K. and Hakedal, J. (1999) Natural organicmatter in drinking water - the "NOM-typing project", background and basic characteristics of original water samples and NOM isolates. Environ. Int. 25(2/3), 145-159.

Glezer, V., Harris, B., Tal, N., Iosefvon, B. and Lev, O. (1999) Hydrolysis of haloacetonitriles: Linear free energy relationship, kinetics and products. Water Res. 33(8), 1938-1948.

Goel, S., Hozalski, R.M. and Bouwer, E.J. (1995) Biodegradation of NOM: effect of NOM source and ozone dose. J. Am. Water Works Assoc. 87(1), 90-105.

Gone, D.L., Seidel, J.L., Batiot, C., Bamory, K., Ligban, R. and Biemi, J. (2009) Using fluorescence spectroscopy EEM to evaluate the efficiency of organic matter removal during coagulation-flocculation of a tropical surface water (Agbo reservoir). J. Hazard. Mater. 172(2-3), 693-699.

Graeber, D., Boechat, I.G., Encina-Montoya, F., Esse, C., Gelbrecht, J., Goyenola, G., Gucker, B., Heinz, M., Kronvang, B., Meerhoff, M., Nimptsch, J., Pusch, M.T., Silva, R.C., von Schiller, D. and

Zwirnmann, E. (2015) Global effects of agriculture on fluvial dissolved organic matter. Sci. Rep. 5(16328), 1-8.

Grazuleviciene, R., Kapustinskiene, V., Vencloviene, J., Buinauskiene, J. and Nieuwenhuijsen, M.J. (2013) Risk of congenital anomalies in relation to the uptake of trihalomethane from drinking water during pregnancy. Occup. Environ. Med. 70(4), 274-282.

Gruchlik, Y., Heitz, A., Tan, J., Sebastien, A., Bowman, M., Halliwell, D., von Gunten, U., J., C. and Joll, C. (2014) Impact of bromide and iodide during drinking water disinfection and potential treatment processes for their removal or mitigation. Water J. Aust. Water Assoc. 41(8), 38-43.

Hammes, F., Salhi, E., Koster, O., Kaiser, H.P., Egli, T. and von Gunten, U. (2006) Mechanistic and kinetic evaluation of organic disinfection by-product and assimilable organic carbon (AOC) formation during the ozonation of drinking water. Water Res. 40(12), 2275-2286.

Heeb, M.B., Criquet, J., Zimmermann-Steffens, S.G. and von Gunten, U. (2014) Oxidative treatment of bromide-containing waters: formation of bromine and its reactions with inorganic and organic compounds - a critical review. Water Res. 48, 15-42.

Her, N., Amy, G., Foss, D., Cho, J., Yoon, Y. and Kosenka, P. (2002) Optimization of method for detecting and characterizing NOM by HPLC-size exclusion chormatography with UV and on-line DOC detection. Environ. Sci. Technol. 36(5), 1069-1076.

Hildesheim, M.E., Cantor, K.P., Lynch, C.F., Dosemeci, M., Lubin, J., Alavanja, M. and Craun, G. (1998) Drinking water source and chlornation byproducts II. Risk of colon and rectal cancer. Epidemiology 9(1), 29-35.

Hoigné, J. and Bader, H. (1988) The formation of trichloronitromethane (chloropicrin) and chloroform in a combined ozonation/chlorination treatment of drinking water. Water Res. 22(3), 313-319.

Hoigné, J. and Bader, H. (1983) Rate constants of reactions of ozone with organic and inorganic compounds in water II. Dissociating organic compounds. Water Res. 17(2), 185-194.

Hoigné, J., Bader, H., Haag, W.R. and Staehelin, J. (1985) Rate constants of reactions of ozone with organic and inorganic compounds in water - III. Inorganic compounds and radicals. Water Res. 19(8), 993-1004.

Hong, S. and Elimelech, M. (1997) Chemical and physical aspects of natural organic matter (NOM) fouling of nanofiltration membranes. J. Membrane Sci. 132(2), 159-181.

Hozalski, R.M. and Bouwer, E.J. (2001) Non-steady state simulation of BOM removal in drinking water biofilters: Model development. Water Res. 35(1), 198-210.

Hrudey, S.E. (2009) Chlorination disinfection by-products, public health risk tradeoffs and me. Water Res 43(8), 2057-2092.

Hrudey, S.E., Backer, L.C., Humpage, A.R., Krasner, S.W., Michaud, D.S., Moore, L.E., Singer, P.C. and Stanford, B.D. (2015) Evaluating evidence for association of human bladder cancer with drinking-water chlorination disinfection by-products. J. Toxicol. Environ. Health B Crit. Rev. 18(5), 213-241.

Hrudey, S.E. and Fawell, J. (2015) 40 years on: what do we know about drinking water disinfection by-products (DBPs) and human health? Water Sci. Technol. Water Supply 15(4), 667-674.

Hua, G. (2006) Characterization of total organic halogen produced by chlorine, chloramines, and chlorine dioxide. *Doctoral dissertation available from Proquest*. Paper AAI3242358. http://scholarworks.umass.edu/dissertations/AAI3242358.

Hua, G. and Reckhow, D.A. (2007a) Characterization of disinfection byproduct precursors based on hydrophobicity and molecular size. Environ. Sci. Technol. 41(9), 3309-3315.

Hua, G. and Reckhow, D.A. (2007b) Comparison of disinfection byproduct formation from chlorine and alternative disinfectants. Water Res. 41(8), 1667-1678.

Hua, G. and Reckhow, D.A. (2008) DBP formation during chlorination and chloramination: Effect of reaction time, pH, dosage, and temperature. J. Am. Water Works Assoc. 100(8), 82-95.

Hua, G. and Reckhow, D.A. (2013) Effect of pre-ozonation on the formation and speciation of DBPs. Water Res. 47(13), 4322-4330.

Hua, G., Reckhow, D.A. and Abusallout, I. (2015) Correlation between SUVA and DBP formation during chlorination and chloramination of NOM fractions from different sources. Chemosphere 130, 82-89.

Hua, G., Reckhow, D.A. and Kim, J. (2006) Effect of bromide and iodide ions on the formation and speciation of disinfection byproducts during chlorination. Environ. Sci. Technol. 40(9), 3050-3056.

Huang, H., Wu, Q.Y., Hu, H.Y. and Mitch, W.A. (2012) Dichloroacetonitrile and dichloroacetamide can form independently during chlorination and chloramination of drinking waters, model organic matters, and wastewater effluents. Environ. Sci. Technol. 46(19), 10624-10631.

Huber, S.A., Balz, A., Abert, M. and Pronk, W. (2011) Characterisation of aquatic humic and non-humic matter with size-exclusion chromatography--organic carbon detection--organic nitrogen detection (LC-OCD-OND). Water Res. 45(2), 879-885.

Hubner, U., von Gunten, U. and Jekel, M. (2015) Evaluation of the persistence of transformation products from ozonation of trace organic compounds - a critical review. Water Res. 68, 150-170.

Huck, P.M. and Sozanski, M.M. (2008) Biological filtration for membrane pre-treatment and other applications: towards the development of a practically-oriented performance parameter. J. Water Supply Res. T. 57(4), 203-224.

Huck, P.M., Zhang, S. and Price, M.L. (1994) BOM removal during biological treatment: a first-order model. J. Am. Water Works Assoc. 86(6), 61-71.

Hudson, N., Baker, A. and Reynolds, D. (2007) Fluorescence analysis of dissolved organic matter in natural, waste and polluted waters—a review. River Res. Applic. 23(6), 631-649.

Ianni, J.C. (2003) A comparison of the Bader-Deuflhard and the Cash-Karp Runge-Kutta integrators for the GRI-MECH 3.0 model based on the chemical kinetics code Kintecus. In: Bathe, K.J. (Ed.), Computational Fluid and Solid Mechanics. Elsevier, Amsterdam, pp. 1368–1372.

IHSS (2016) Elemental compositions and stable isotopic ratios of IHSS samples. Available at http://www.humicsubstances.org/elements.html.

Jayson, G.G., Scholes, G. and Weiss, J. (1955) Chemical action of ionising radiations in solution. Part XIV. The action of X-rays (200 kv) on some aliphatic amines in aqueous solution with particular reference to the formation of oximes. J. Chem Soc., 2594-2600.

Joo, S.H. and Mitch, W.A. (2007) Nitrile, aldehyde, and halonitroalkane formation during chlorination/chloramination of primary amines. Environ. Sci. Technol. 41(4), 1288-1296.

Juhna, T. and Melin, E. (2006) Ozonation and biofiltration in water treatment - Operational status and optimization issues. Techneau WP5.3 Operation of water treatment facilities - Optimization efforts

and modelling of unit processes. Available at http://www.techneau.org/fileadmin/files/Publications/Publications/Deliverables/D5.3.1B-OBF.pdf. .

Karpel Vel Leitner, N., Berger, P. and Legube, B. (2002) Oxidation of amino groups by hydroxyl radicals in relation to the oxidation degree of the a-carbon. Environ. Sci. Technol. 36(14), 3083-3089.

Kim, H.C. and Yu, M.J. (2005) Characterization of natural organic matter in conventional water treatment processes for selection of treatment process focused on DBPs control. Water Res. 39(19), 4779-4789.

King, W.D., Dodds, L., Allen, A.C., Armson, B.A., Fell, D. and Nimrod, C. (2005) Haloacetic acids in drinking water and risk for stillbirth. Occup. Environ. Med. 62(2), 124-127.

King, W.D., Marrett, L.D. and Woolcott, C.G. (2000) Case-control study of colon and rectal cancers and chlorination by-products in treated water. Cancer Epidemiol. Biomarkers Prev. 9(8), 813-818.

Kitis, M., Karanfil, T., Kilduff, J.E. and Wigton, A. (2001) The reactivity of natural organic matter to disinfection by-products formation and its rejection to specific ultraviolet absorbance. Water Sci. Technol. 43(2), 9-16.

Kitis, M., Karanfil, T., Wigton, A. and Kilduff, J.E. (2002) Probing reactivity of dissolved organic matter for disinfection by-product using XAD-8 resin adsorption and ultrafiltration fractionation. Water Res. 36(15), 3834-3848.

Kleiser, G. and Frimmel, F.H. (2000) Removal of precursors for disinfection by-products (DBPs) - differences between ozone- and OH-radical-induced oxidation. Sci. Total Environ. 256(1), 1-9.

Koffskey, W.E. and Lykins, B.W. (1999) Disinfection/disinfectant by-product optimisation with ozone, biological filtration and chloramines. J. Water Supply Res. T. 48(3), 92-105.

Konya, K.G., Paul, T., Lin, S., Lusztyk, J. and Ingold, K.U. (2000) Laser flash photolysis studies on the first superoxide thermal source. First direct measurements of the rates of solvent-assisted 1,2-hydrogen atom shift and a proposed new mechanism for this unusual rearrangement. J. Am. Chem. Soc. 122(31), 7518-7527.

Krasner, S.W. (2009) The formation and control of emerging disinfection by-products of health concern. Philos. Trans. A Math. Phys. Eng. Sci. 367(1904), 4077-4095.

Krasner, S.W., Mitch, W.A., McCurry, D.L., Hanigan, D. and Westerhoff, P. (2013) Formation, precursors, control, and occurrence of nitrosamines in drinking water: a review. Water Res. 47(13), 4433-4450.

Krasner, S.W., Sclimenti, M.J. and Coffey, B.M. (1993) Testing biologically active filters for removing aldehydes formed during ozonation. J. Am. Water Works Assoc. 85(5), 62-71.

Krasner, S.W., Sclimenti, M.J. and Means, E.G. (1994) Quality degradation: implication for DBP formation. J. Am. Water Works Assoc. 86(4), 34-47.

Krasner, S.W., Weinberg, H.S., Richardson, S.D., Pastor, S.J., Chinn, R., Sclimenti, M.J., Onstad, G.D. and Thruston, A.D. (2006) Occurrence of a new generation of disinfection byproducts. Environ. Sci. Technol. 40(23), 7175-7185.

Krasner, S.W., Westerhoff, P., Chen, B., Rittmann, B.E., Nam, S.-N. and Amy, G. (2009) Impact of wastewater treatment processes on organic carbon, organic nitrogen, and DBP precursors in effluent organic matter. Environ. Sci. Technol. 43(8), 2911-2918.

Lange, F., Cornelissen, S., Kubac, D., Sein, M.M., von Sonntag, J., Hannich, C.B., Golloch, A., Heipieper, H.J., Moder, M. and von Sonntag, C. (2006) Degradation of macrolide antibiotics by ozone: A mechanistic case study with clarithromycin. Chemosphere 65(1), 17-23.

Langlais, B., Reckhow, D.A. and Brink, D.A. (1991) Ozone in water treatment: Application and engineering. Cooperative Research Report. AWWA Research Foundation, Campagnie Generale Eaux. ISBN: 0-87371-474-1.

Lauderdale, C., Chadik, P., Kirisits, M.J. and Brown, J. (2012) Engineered biofiltration: Enhanced biofilter performance through nutrient and peroxide addition. J. Am. Water Works Assoc. 104(5), E298-E309.

Laurent, P., Prevost, M., Cigana, J., Niquette, P. and Servais, P. (1999) Biodegradable organic matter removal in biological filters: evaluation of the CHABROL model. Water Res. 33(6), 1387-1398.

Le Lacheur, R.M. and Glaze, W.H. (1996) Reactions of ozone and hydroxyl radicals with serine. Environ. Sci. Technol. 30(4), 1072-1080.

Lee, Y., Gerrity, D., Lee, M., Bogeat, A.E., Salhi, E., Gamage, S., Trenholm, R.A., Wert, E.C., Snyder, S.A. and von Gunten, U. (2013) Prediction of micropollutant elimination during ozonation

of municipal wastewater effluents: use of kinetic and water specific information. Environ. Sci. Technol. 47(11), 5872-5881.

Lee, Y. and von Gunten, U. (2016) Advances in predicting organic contaminant abatement during ozonation of municipal wastewater effluent: reaction kinetics, transformation products, and changes of biological effects. Environ. Sci.: Water Res. Technol. 2(3), 421-442.

Lee, Y. and von Gunten, U. (2010) Oxidative transformation of micropollutants during municipal wastewater treatment: comparison of kinetic aspects of selective (chlorine, chlorine dioxide, ferrate VI, and ozone) and non-selective oxidants (hydroxyl radical). Water Res. 44(2), 555-566.

Leenheer, J.A. and Croué, J.-P. (2003) Characterizing dissolved aquatic organic matter. Environ. Sci. Technol. 37(1), 18A-26A.

Levallois, P., Gingras, S., Marcoux, S., Legay, C., Catto, C., Rodriguez, M. and Tardif, R. (2012) Maternal exposure to drinking-water chlorination by-products and small-for-gestational-age neonates. Epidemiology 23(2), 267-276.

Leverenz, H.L., Tchobanoglous, G. and Asano, T. (2011) Direct potable reuse: a future imperative. J. Water Reuse Desal. 1(1), 2-10.

Liang, L. and Singer, P.C. (2003) Factors influencing the formation and relative distribution of haloacetic acids and trihalomethanes in drinking water. Environ. Sci. Technol. 37(13), 2920-2928.

Liao, X., Zou, R., Chen, C., Yuan, B., Zhou, Z., Ma, H. and Zhang, X. (2016) Biomass development in GAC columns receiving influents with different levels of nutrients. Water Sci. Technol. Water Supply 16(4), 1024-1032.

Linden, K.G., Shin, G.A., Faubert, G., Cairns, W. and Sobsey, M.D. (2002) UV disinfection of *Giardia lamblia* cysts in water. Environ. Sci. Technol. 36(11), 2519-2522.

Liu, W., Andrews, S.A., Stefan, M.I. and Bolton, J.R. (2003) Optimal methods for quenching H_2O_2 residuals prior to UFC testing. Water Res. 37(15), 3697-3703.

Lyon, B.A., Farré, M.J., de Vera, G.A., Keller, J., Roux, A., Weinberg, H.S. and Gernjak, W. (2014a) Organic matter removal and disinfection byproduct management in South East Queensland's drinking water. Water Sci. Technol. Water Supply 14(4), 681-689.

Lyon, B.A., Milsk, R.Y., DeAngelo, A.B., Simmons, J.E., Moyer, M.P. and Weinberg, H.S. (2014b) Integrated chemical and toxicological investigation of UV-chlorine/chloramine drinking water treatment. Environ. Sci. Technol. 48(12), 6743-6753.

Magdeburg, A., Stalter, D., Schlusener, M., Ternes, T. and Oehlmann, J. (2014) Evaluating the efficiency of advanced wastewater treatment: target analysis of organic contaminants and (geno-) toxicity assessment tell a different story. Water Res. 50, 35-47.

Maillard, B., Ingold, K.U. and Scaiano, J.C. (1983) Rate constants for the reaction of free radicals with oxygen in solution. J. Am. Chem. Soc. 105(15), 5095-5099.

Markechova, D., Tomkova, M. and Sadecka, J. (2013) Fluorescence excitation-emission matrix spectroscopy and parallel factor analysis in drinking water treatment: A review. J. Environ. Stud. 22(5), 1289-1295.

Matilainen, A., Gjessing, E.T., Lahtinen, T., Hed, L., Bhatnagar, A. and Sillanpaa, M. (2011) An overview of the methods used in the characterisation of natural organic matter (NOM) in relation to drinking water treatment. Chemosphere 83(11), 1431-1442.

Matilainen, A., Lindqvist, N., Korhonen, S. and Tuhkanen, T. (2002) Removal of NOM in different stages of the water treatment process. Environ. Int. 28(6), 457-465.

Matilainen, A., Vepsalainen, M. and Sillanpaa, M. (2010) Natural organic matter removal by coagulation during drinking water treatment: a review. Adv. Colloid Interface Sci. 159(2), 189-197.

McCurry, D.L., Quay, A.N. and Mitch, W.A. (2016) Ozone Promotes Chloropicrin Formation by Oxidizing Amines to Nitro Compounds. Environ. Sci. Technol. 50(3), 1209-1217.

McDonald, S., Bishop, A.G., Prenzler, P.D. and Robards, K. (2004) Analytical chemistry of freshwater humic substances. Anal. Chim. Acta 527(2), 105-124.

Melin, E.S. and Odegaard, H. (2000) The effect of biofilter loading rate on the removal of organic ozonation by-products. Water Res. 34(18), 4464-4476.

Merényi, G., Lind, J., Naumov, S. and von Sonntag, C. (2010) Reaction of ozone with hydrogen peroxide (peroxone process): a revision of current mechanistic concepts based on thermokinetic and quantum-chemical considerations. Environ. Sci. Technol. 44(9), 3505-3507.

Michaud, D.S., Kogevinas, M., Cantor, K.P., Villanueva, C.M., Garcia-Closas, M., Rothman, N., Malats, N., Real, F.X., Serra, C., Garcia-Closas, R., Tardon, A., Carrato, A., Dosemeci, M. and Silverman, D.T. (2007) Total fluid and water consumption and the joint effect of exposure to disinfection by-products on risk of bladder cancer. Environ Health Perspect 115(11), 1569-1572.

Mitch, W.A., Krasner, S.W., Westerhoff, P. and Dotson, A. (2009) Occurrence and formation of nitrogenous disinfection by-products. Water Research Foundation, CO, USA. ISBN: 978-1-60573-053-0.

Molnar, J., Agbaba, J., Dalmacija, B., Roncevic, S., Prica, M. and Tubic, A. (2012a) Influence of pH and ozone dose on the content and structure of haloacetic acid precursors in groundwater. Environ. Sci. Pollut. Res. Int. 19(8), 3079-3086.

Molnar, J.J., Agbaba, J.R., Dalmacija, B.D., Klasnja, M.T., Dalmacija, M.B. and Kragulj, M.M. (2012b) A comparative study of the effects of ozonation and TiO_2-catalyzed ozonation on the selected chlorine disinfection by-product precursor content and structure. Sci. Total Environ. 425, 169-175.

Munch, J.W., Munch, D.J. and Winslow, S.D. (1998) Method 556: Determination of crabonyl compounds in drinking water by pentafluorobenzylhydroxylamine derivatization and capillary gas chromatography with electron capture detection. US EPA, Cincinnati, OH, USA.

Muñoz, F., Mvula, E., Braslavsky, S.E. and von Sonntag, C. (2001) Singlet dioxygen formation in ozone reactions in aqueous solution. J. Chem. Soc., Perkin Trans. 2 (7), 1109-1116.

Muñoz, F. and von Sonntag, C. (2000) The reactions of ozone with tertiary amines including the complexing agents nitrilotriacetic acid (NTA) and ethylenediaminetetraacetic acid (EDTA) in aqueous solution. J. Chem. Soc., Perkin Trans. 2 (10), 2029-2033.

Narotsky, M.G., Klinefelter, G.R., Goldman, J.M., DeAngelo, A.B., Best, D.S., McDonald, A., Strader, L.F., Murr, A.S., Suarez, J.D., George, M.H., Hunter, E.S. and Simmons, J.E. (2015) Reproductive toxicity of a mixture of regulated drinking-water disinfection by-products in a multigenerational rat bioassay. Environ. Health Perspect. 123(6), 564-570.

NATA (2013) Technical note 17-Guidelines for validation and verification of quantitative and qualitative test methods. Available at: http://www.nata.com.au/nata/phocadownload/publications/Guidance_information/tech-notes-information-papers/technical_note_17.pdf.

Naumov, S. and von Sonntag, C. (2011) Standard Gibbs free energies of reactions of ozone with free radicals in aqueous solution: quantum-chemical calculations. Environ. Sci. Technol. 45(21), 9195-9204.

Neale, P.A., Antony, A., Bartkow, M.E., Farre, M.J., Heitz, A., Kristiana, I., Tang, J.Y. and Escher, B.I. (2012) Bioanalytical assessment of the formation of disinfection byproducts in a drinking water treatment plant. Environ. Sci. Technol. 46(18), 10317-10325.

Neta, P., Huie, R.E. and Ross, A.B. (1988) Rate constants for reactions of inorganic radicals in aqueous solution. J. Phys. Chem. Ref. Data 17(3), 1027-1284.

Neta, P., Huie, R.E. and Ross, A.B. (1990) Rate constants for reactions of peroxyl radicals in fluid solutions. J. Phys. Chem. Ref. Data 19(2), 413-513.

NHMRC and NRMMC (2011) Australian Drinking Water Guidelines Paper 6 National Water Quality Management Strategy. National Health and Medical Research Council, National Resource Management Ministerial Council, Commonwealth of Australia, Canberra.

Nilson, J.A. and DiGiano, F.A. (1996) Influence of NOM composition on nanofiltration. J. Am. Water Works Assoc. 88(5), 53-66.

Nishijima, W. and Speitel, G.E. (2004) Fate of biodegradable dissolved organic carbon produced by ozonation on biological activated carbon. Chemosphere 56(2), 113-119.

Nkambule, T.I., Krause, R.W.M., Mamba, B.B. and Haarhoff, J. (2009) Characterisation of natural organic matter (NOM) and its removal using cyclodextrin polyurethanes. Water SA 35(2), 200-203.

Nogueira, R.F., Oliveira, M.C. and Paterlini, W.C. (2005) Simple and fast spectrophotometric determination of H_2O_2 in photo-Fenton reactions using metavanadate. Talanta 66(1), 86-91.

Nöthe, T., Fahlenkamp, H. and von Sonntag, C. (2009) Ozonation of wastewater: rate of ozone consumption and hydroxyl radical yield. Environ. Sci. Technol. 43(15), 5990-5995.

Odom, R., Regli, S., Messner, M., Cromwell, J. and Javdan, M. (1999) Benefit-cost analysis of the Stage 1D/DBP rule. J. Am .Water Works Ass. 91(4), 137-147.

Persson, F., Heinicke, G., Hedberg, T., Hermansson, M. and Uhl, W. (2007) Removal of geosmin and MIB by biofiltration--an investigation discriminating between adsorption and biodegradation. Environ. Technol. 28(1), 95-104.

Petala, M., Samaras, P., Zouboulis, A., Kungolos, A. and Sakellaropoulos, G.P. (2008) Influence of ozonation on the in vitro mutagenic and toxic potential of secondary effluents. Water Res. 42(20), 4929-4940.

Pipe-Martin, C. (2008) Dissolved organic carbon removal by biological treatment. WIT Transactions on Ecology and the Environment 111, 445-452. www.witpress.com, ISSN 1743-3541 (on-line).

Plewa, M.J. and Wagner, E.D. (2015) Charting a new path to resolve the adverse health effects of DBPs. Karanfil et al.; Recent Advances in Disinfection By-Products. ACS Symposium Series. American Chemical Society. Washington, DC, USA. Available at: http://pubs.acs.org/doi/pdf/10.1021/bk-2015-1190.ch001.

Plewa, M.J., Wagner, E.D., Muellner, M.G., Hsu, K.-M. and Richardson, S.D. (2008) Comparative mammalian cell toxicity of N-DBPs and C-DBPs. Symposium Series 995. In: Karanfil T., Krasner S., Westerhoff P., Xie Y. (Eds.), Disinfection by-products in drinking water: Occurrence, formation, health effect, and control. Washington, District of Columbia, US, American Chemical Society, pp. 36–50.

Pocostales, J.P., Sein, M.M., Knolle, W., von Sonntag, C. and Schmidt, T.C. (2010) Degradation of ozone-refractory organic phosphates in wastewater by ozone and ozone/hydrogen peroxide (peroxone): The role of ozone consumption by dissolved organic matter. Environ. Sci. Technol. 44(21), 8248-8253.

Rahman, M.B., Cowie, C., Driscoll, T., Summerhayes, R., Armstrong, B.K. and Clements, M.S. (2014) Colon and rectal cancer incidence and water trihalomethane concentrations in New South Wales, Australia. BMC Cancer 14(445), 1-9.

Ramseier, M.K., Peter, A., Traber, J. and von Gunten, U. (2011) Formation of assimilable organic carbon during oxidation of natural waters with ozone, chlorine dioxide, chlorine, permanganate, and ferrate. Water Res. 45(5), 2002-2010.

Ramseier, M.K. and von Gunten, U. (2009) Mechanisms of phenol ozonation—Kinetics of formation of primary and secondary reaction products. Ozone Sci. Eng. 31(3), 201-215.

Ratpukdi, T., Siripattanakul, S. and Khan, E. (2010) Mineralization and biodegradability enhancement of natural organic matter by ozone-VUV in comparison with ozone, VUV, ozone-UV, and UV: effects of pH and ozone dose. Water Res. 44(11), 3531-3543.

Rattier, M. (2013) Understanding of micropollutant removal during biological activated carbon filtration. PhD Thesis, School of Chemical Engineering, The University of Queensland.

Rattier, M., Reungoat, J., Keller, J. and Gernjak, W. (2014) Removal of micropollutants during tertiary wastewater treatment by biofiltration: Role of nitrifiers and removal mechanisms. Water Res. 54, 89-99.

Reckhow, D.A., Platt, T.L., MacNeill, A.L. and McClellan, J.N. (2001) Formation and degradation of dichloroacetonitrile in drinking waters. J. Water Supply Res. T. 50.1, 1-13.

Reckhow, D.A. and Singer, P.C. (1984) The removal of organic halide precursors by preozonation and alum coagulation. J. Am. Water Works Assoc. 76(4), 151-157.

Reckhow, D.A., Singer, P.C. and Malcolm, R.L. (1990) Chlorination of humic materials: Byproduct formation and chemical interpretations. Environ. Sci. Technol. 24(11), 1655-1664.

Reifferscheid, G., Heil, J., Oda, Y. and Zahn, R.K. (1991) A microplate version of the SOS/umu-test for rapid detection of genotoxins and genotoxic potentials of environmental samples. Mutat. Res. 253(3), 215-222.

Reisz, E., Fischbacher, A., Naumov, S., von Sonntag, C. and Schmidt, T.C. (2014) Hydride transfer: a dominating reaction of ozone with tertiary butanol and formate ion in aqueous solution. Ozone Sci. Eng. 36(6), 532-539.

Rennecker, J.L., Driedger, A.M., Rubin, S.A. and Marinas, B.J. (2000) Synergy in sequential inactivation of *Cryptosporidium parvum* with ozone/free chlorine and ozone/monochloramine. Water Res. 34(17), 4121-4130.

Reungoat, J., Macova, M., Escher, B.I., Carswell, S., Mueller, J.F. and Keller, J. (2010) Removal of micropollutants and reduction of biological activity in a full scale reclamation plant using ozonation and activated carbon filtration. Water Res. 44(2), 625-637.

Richardson, S.D. (2003) Disinfection by-products and other emerging contaminants in drinking water. TrAC-Trend Anal. Chem. 22(10), 666-684.

Richardson, S.D., Plewa, M.J., Wagner, E.D., Schoeny, R. and Demarini, D.M. (2007) Occurrence, genotoxicity, and carcinogenicity of regulated and emerging disinfection by-products in drinking water: a review and roadmap for research. Mutat. Res. 636(1-3), 178-242.

Rittman, B.E. (1995) Transformation of organic micropollutants by biological processes. Water Pollution. The Handbook of Environmental Chemistry, Volume 5/5B, J. Hrubec (ed.). Springer-Verlag Berlin Heidelberg. DOI: 10.1007/978-3-540-48468-4_3.

Rittman, B.E., Bae, W., Namkung, E. and Lu, C.-J. (1987) A critical evaluation of microbial product formation in biological processes. Water Sci. Technol. 19(3-4), 517-528.

Rittmann, B.E. (1990) Analyzing biofilm processes used in biological filtration. J. Am. Water Works Assoc. 82(12), 62-66.

Rodriguez, C., Van Buynder, P., Lugg, R., Blair, P., Devine, B., Cook, A. and Weinstein, P. (2009) Indirect potable reuse: a sustainable water supply alternative. Int. J. Environ. Res. Public Health 6(3), 1174-1203.

Rook, J.J. (1977) Chlorination reactions of fulvic acids in natural waters. Environ. Sci. Technol. 11(5), 478-482.

Rook, J.J. (1974) Formation of haloforms during chlorination of natural waters. Water Treat. Exam. 23(2), 234-243.

Sarathy, S.R. (2004) Effects of UV/H_2O_2 advanced oxidation on physical and chemical characteristics of natural organic matter in raw drinking water sources. PhD thesis. University of British Columbia, Vancouver, Canada.

Sedlak, D.L. and von Gunten, U. (2011) The chlorine dilemma. Science 331(6013), 42-43.

Seidel, A. and Elimelech, M. (2002) Coupling between chemical and physical interactions in natural organic matter (NOM) fouling of nanofiltration membranes: implications for fouling control. J. Membrane Sci. 203(1-2), 245-255.

Servais, P., Anzil, A. and Ventresque, C. (1989) Simple method for determination of biodegradable dissolved organic carbon in water. Appl. Environ. Microbiol. 55(10), 2732-2734.

Servais, P., Billen, G. and Boillot, P. (1994) Biological colonization of granular activated carbon filters in drinking-water treatment. J. Environ. Eng. 120(4), 888-899.

Shah, A.D. and Mitch, W.A. (2012) Halonitroalkanes, halonitriles, haloamides, and N-nitrosamines: a critical review of nitrogenous disinfection byproduct formation pathways. Environ. Sci. Technol. 46(1), 119-131.

Shan, J., Hu, J., Kaplan-Bekaroglu, S.S., Song, H. and Karanfil, T. (2012) The effects of pH, bromide and nitrite on halonitromethane and trihalomethane formation from amino acids and amino sugars. Chemosphere 86(4), 323-328.

Sharma, V.K. and Graham, N.J.D. (2010) Oxidation of amino acids, peptides and proteins by ozone: a review. Ozone Sci. Eng. 32(2), 81-90.

Sharp, E.L., Jarvis, P., Parsons, S.A. and Jefferson, B. (2006) Impact of fractional character on the coagulation of NOM. Colloids Surf. A 286(1-3), 104-111.

Shin, J., Hidayat, Z.R. and Lee, Y. (2015) Influence of seasonal variation of water temperature and dissolved organic matter on ozone and OH radical reaction kinetics during ozonation of a lake water. Ozone Sci. Eng. 38(2), 100-114.

Siddiqui, M.S., Amy, G.L. and Murphy, B.D. (1997) Ozone enhanced removal of natural organic matter from drinking water sources. Water Res. 31(12), 3098-3106.

Simpson, D.R. (2008) Biofilm processes in biologically active carbon water purification. Water Res. 42(12), 2839-2848.

Singer, P.C. and Bilyk, K. (2002) Enhanced coagulation using a magnetic ion exchange resin. Water Res. 36(16), 4009-4022.

Singer, P.C., Harrington, G.W., Cowman, G.A., Smith, M.E., Schechther, D.S. and Harrington, L.J. (1999) Impacts of ozonation on the formation of chlorination and chloramination by-products, AWWA Research Foundation, CO. ISBNO-89867-994-X., USA.

Singer, P.C., Obolensky, A. and Greiner, A. (1995) DBPs in chlorinated North Carolina drinking waters. J. Am. Water Works Assoc. 87(10), 83-92.

Sohn, J., Amy, G. and Yoon, Y. (2007) Process-train profiles of NOM through a drinking water treatment plant. J. Am. Water Works Assoc. 99(6), 145-153.

Speitel, G.E.J., Symons, J.M., Diehl, A.C., Sorensen, H.W. and Cipparone, L.A. (1993) Effect of ozone dosage and subsequent biodegradation on removal of DBP precursors. J. Am. Water Works Assoc. 85(5), 86-95.

Stalter, D., Magdeburg, A. and Oehlmann, J. (2010) Comparative toxicity assessment of ozone and activated carbon treated sewage effluents using an in vivo test battery. Water Res. 44(8), 2610-2620.

Stalter, D., O'Malley, E., von Gunten, U. and Escher, B.I. (2016a) Fingerprinting the reactive toxicity pathways of 50 drinking water disinfection by-products. Water Res. 91, 19-30.

Stalter, D., Peters, L., O'Malley, E., Tang, J.Y., Revalor, M., Farre, M.J., Watson, K., von Gunten, U. and Escher, B.I. (2016b) Sample enrichment for bioanalytical assessment of disinfected drinking water: concentrating the polar, the volatiles, the unknowns. Environ. Sci. Technol. 50(12), 6495-6505.

Sun, L., Perdue, E.M. and McCarthy, J.F. (1995) Using reverse osmosis to obtain organic matter from surface and ground waters. Water Res. 29(6), 1471-1477.

Symons, J.M., Krasner, S.W., Simms, L.A. and Sclimenti, M. (1993) Measurement of THM and precursor concentrations revisited: The effect of bromide ion. J. Am. Water Works Assoc. 85(1), 51-62.

Tang, J.Y., McCarty, S., Glenn, E., Neale, P.A., Warne, M.S. and Escher, B.I. (2013) Mixture effects of organic micropollutants present in water: towards the development of effect-based water quality trigger values for baseline toxicity. Water Res. 47(10), 3300-3314.

Teixeira, M.R. and Nunes, L.M. (2011) The impact of natural organic matter seasonal variations in drinking water quality. Desalin. Water Treat. 36(1-3), 344-353.

Tekle-Rottering, A., Jewell, K.S., Reisz, E., Lutze, H.V., Ternes, T.A., Schmidt, W. and Schmidt, T.C. (2016) Ozonation of piperidine, piperazine and morpholine: Kinetics, stoichiometry, product formation and mechanistic considerations. Water Res. 88, 960-971.

Thurman, E.M. and Malcolm, R.L. (1981) Preparative isolation of aquatic humic substances. Environ. Sci. Technol. 15(4), 463-466.

Tretyakova, N.Y., Lebedev, A.T. and Petrosyan, V.S. (1994) Degradative pathways for aqueous chlorination of orcinol. Environ. Sci. Technol. 28(4), 606-613.

Urfer, D. and Huck, P.M. (1997) Effects of hydrogen peroxide residuals on biologically active filters. Ozone Sci. Eng. 19(4), 371-386.

Urfer, D. and Huck, P.M. (2000) A study of the impacts of periodic ozone residuals on biologically active filters. Ozone Sci. Eng. 22(1), 77-97.

Urfer, D., Huck, P.M., Booth, S.D.J. and Coffey, B.M. (1997) Biological filtration for BOM and particle removal: a critical review. J. Am. Water Works Assoc. 18(12), 83-98.

USEPA (2010) 40 CFR Appendix B to part 136 - Definition and procedure for determination of the method detection limit - revision 1.11. Available at: https://www.gpo.gov/fdsys/pkg/CFR-2012-title40-vol24/pdf/CFR-2012-title40-vol24-part136-appB.pdf.

USGS (2014) Dissolved oxygen solubility tables. Available at: http://water.usgs.gov/software/DOTABLES/.

van der Kooij, D., Hijnen, W.A.M. and Kruithof, J.C. (1989) The effects of ozonation, biological filtration and distribution on the concentration of easily assimilable organic carbon (AOC) in drinking water. Ozone Sci. Eng. 11(3), 297-311.

Villanueva, C.M., Cantor, K.P., Cordier, S., Jaakkola, J.J.K., King, W.D., Lynch, C.F., Porru, S. and Kogevinas, M. (2004) Disinfection byproducts and bladder cancer: A pooled analysis. Epidemiology 15(3), 357-367.

Villanueva, C.M., Cantor, K.P., Grimalt, J.O., Malats, N., Silverman, D., Tardon, A., Garcia-Closas, R., Serra, C., Carrato, A., Castano-Vinyals, G., Marcos, R., Rothman, N., Real, F.X., Dosemeci, M. and Kogevinas, M. (2007) Bladder cancer and exposure to water disinfection by-products through ingestion, bathing, showering, and swimming in pools. Am. J. Epidemiol. 165(2), 148-156.

von Gunten, U. (2007) The basics of oxidants in water treatment. Part B: ozone reactions. Water Sci. Technol. Water Supply 55(12), 25-29.

von Gunten, U. (2003a) Ozonation of drinking water: Part I. Oxidation kinetics and product formation. Water Res. 37(7), 1443-1467.

von Gunten, U. (2003b) Ozonation of drinking water: Part II. Disinfection and by-product formation in presence of bromide, iodide or chlorine. Water Res. 37(7), 1469-1487.

von Gunten, U. and Hoigné, J. (1994) Bromate formation during ozonation of bromide-containing waters: Interaction of ozone and hydroxyl radical reactions. Environ. Sci. Technol. 28(7), 1234-1242.

von Gunten, U. and Oliveras, Y. (1998) Advanced oxidation of bromide-containing waters; bromate formation mechanism. Environ. Sci. Technol. 32(1), 63-70.

von Gunten, U. and Ramseier, M.K. (2010) Critical review of literature for rate constants for reaction of chemical oxidants with inorganic and organic pollutants. Techneau D 2.4.2.7. Available at http://www.techneau.org/fileadmin/files/Publications/Publications/Deliverables/D2.4.2.7.pdf.

von Sonntag, C. (2006) Free-radical-induced DNA damage and its repair: a chemical perspective. Springer-Verlag Berlin Heidelberg, Germany. eISBN: 978-3-540-30592-7.

von Sonntag, C. and Schuchmann, H.-P. (1991) The elucidation of peroxyl radical reactions in aqueous solution with help of radiation-chemical methods. Angew. Chem. Int. Ed. Engl. 30(10), 1229-1253.

von Sonntag, C. and von Gunten, U. (2012) Chemistry of ozone in water and wastewater treatment - from basic principles to applications. IWA Publishing, London, UK. eISBN: 9781780400839.

Wadhawan, T., Simsek, H., Kasi, M., Knutson, K., Prubeta, B., McEvoy, J. and Khan, E. (2014) Dissolved organic nitrogen and its biodegradable portion in a water treatment plant with ozone oxidation. Water Res. 54, 318-326.

Watson, K., Farre, M.J. and Knight, N. (2012) Strategies for the removal of halides from drinking water sources, and their applicability in disinfection by-product minimisation: a critical review. J. Environ. Manage. 110, 276-298.

Weinberg, H.S. (1999) Disinfection byproducts in drinking water: The analytical challenge. A call for analytical techniques to determine unidentified disinfection byproducts in drinking water. Anal. Chemi. 71(23), 801A-808A.

Weinberg, H.S. (2001) Formation and stability of ozonation by-products in drinking water, US EPA http://cfpub.epa.gov/ncer_abstracts/index.cfm/fuseaction/display.abstractDetail/abstract/202/report/F.

Weinberg, H.S. (2009) Modern approaches to the analysis of disinfection by-products in drinking water. Phil. Trans. R. Soc. A 367, 4097-4118.

Weinberg, H.S., Glaze, W.H., Krasner, S.W. and Sclimenti, M.J. (1993) Formation and removal of aldehydes in plants that use ozonation. J. Am. Water Works Assoc. 85(5), 72-85.

Weishaar, J.L., Aiken, G.R., Bergamaschi, B.A., Fram, M.S., Fujii, R. and Mopper, K. (2003) Evaluation of specific ultraviolet absorbance as an indicator of the chemical composition and reactivity of dissolved organic carbon. Environ. Sci. Technol. 37(20), 4702-4708.

Wenk, J., Aeschbacher, M., Salhi, E., Canonica, S., von Gunten, U. and Sander, M. (2013) Chemical oxidation of dissolved organic matter by chlorine dioxide, chlorine, and ozone: effects on its optical and antioxidant properties. Environ. Sci. Technol. 47(19), 11147-11156.

Westerhoff, P., Aiken, G., Amy, G. and Derboux, J. (1999) Relationships between the structure of natural organic matter and its reactivity towards molecular ozone and hydroxyl radicals. Water Res. 33(10), 2265-2276.

Westerhoff, P., Chao, P. and Mash, H. (2004) Reactivity of natural organic matter with aqueous chlorine and bromine. Water Res. 38(6), 1502-1513.

Westerhoff, P. and Mash, H. (2002) Dissolved organic nitrogen in drinking water supplies: a review. J. Water Supply Res. T. 51(8), 415-448.

White, M.C., Thompson, J.D., Harrington, G.W. and Singer, P.C. (1997) Evaluating criteria for enhanced coagulation compliance. J. Am. Water Works Assoc. 89(5), 64-77.

WHO (2006) Guidelines for Drinking Water Quality, World Health Organization, Geneva, Switzerland.

Wobma, P., Pernitsky, D., Bellamy, B., Kjartanson, K. and Sears, K. (2000) Biological filtration for ozone and chlorine DBP removal. Ozone Sci. Eng. 22(4), 393-413.

Xie, Y. (2004) Disinfection byproducts in drinking water: formation, analysis, and control. CRC Press LLC, FL, U.S.A., ISBN 1-56676-974-4.

Xie, Y., Rashid, I., Zhou, H. and Gammie, L. (2002) Acidic methanol methylation for HAA analysis: limitations and possible solutions. J. Am. Water Works Assoc. 94(11), 115-122.

Yang, X., Peng, J., Chen, B., Guo, W., Liang, Y., Liu, W. and Liu, L. (2012a) Effects of ozone and ozone/peroxide pretreatments on disinfection byproduct formation during subsequent chlorination and chloramination. J. Hazard. Mater. 239-240, 348-354.

Yang, X., Shang, C., Shen, Q., Chen, B., Westerhoff, P., Peng, J. and Guo, W. (2012b) Nitrogen origins and the role of ozonation in the formation of haloacetonitriles and halonitromethanes in chlorine water treatment. Environ. Sci. Technol. 46(23), 12832-12838.

Yavich, A.A., Lee, K.H., Chen, K.C., Pape, L. and Masten, S.J. (2004) Evaluation of biodegradability of NOM after ozonation. Water Res. 38(12), 2839-2846.

Yeh, R.Y., Farre, M.J., Stalter, D., Tang, J.Y., Molendijk, J. and Escher, B.I. (2014) Bioanalytical and chemical evaluation of disinfection by-products in swimming pool water. Water Res. 59, 172-184.

Yu, Z., Zhang, Q., Kraus, T.E.C., Dahlgren, R.A., Anastasio, C. and Zasoski, R.J. (2002) Contribution of amino compounds to dissolved organic nitrogen in forest soils. Biogeochemistry 61(2), 173-198.

Zevin, A.S., Nam, T., Rittmann, B. and Krajmalnik-Brown, R. (2015) Effects of phosphate limitation on soluble microbial products and microbial community structure in semi-continuous Synechocystis-based photobioreactors. Biotechnol. Bioeng. 112(9), 1761-1769.

Zhang, P. and Jian, L. (2006) Ozone-enhanced photocatalytic degradation of natural organic matter in water. Water Sci. Technol. Water Supply 6(3), 53-61.

Zhang, Z., Wang, L. and Shao, L. (2010) Study on relationship between characteristics of DOC and removal performance by BAC filter. 2010 4th International Conference on Bioinformatics and Biomedical Engineering (iCBBE). IEEE. DOI: 10.1109/ICBBE.2010.5516234.

Zimmermann, S.G., Schmukat, A., Schulz, M., Benner, J., von Gunten, U. and Ternes, T.A. (2012) Kinetic and mechanistic investigations of the oxidation of tramadol by ferrate and ozone. Environ. Sci. Technol. 46(2), 876-884.